Morphology and Mucin Histochemistry of the Gastrointestinal Tracts of Three Insectivorous Mammals: *Acomys spinosissimus*, *Crocidura cyanea and Amblysomus hottentotus*

by

Julia Boonzaier

Thesis presented in partial fulfilment of the requirements for the degree of Master of Medical Science in the Faculty of Health Sciences at Stellenbosch University.

Supervisor: Dr. Sanet H. Kotzé

Department of Biomedical Sciences

Faculty of Health Sciences

University of Stellenbosch

Co-supervisor: Dr. Elizabeth L. van der Merwe

Department of Human Biology

Faculty of Health Sciences

University of Cape Town

March 2012

DECLARATION

By submitting this thesis electronically, I declare that the entirety of the work contained therein is my own, original work, that I am the sole author thereof, that reproduction and publication thereof by Stellenbosch University will not infringe any third party rights and that I have not previously in its entirety or in part submitted it for obtaining any qualification.

Date: 08 December 2011

ABSTRACT

The gastrointestinal morphology and the distribution of the different types of mucin secreting goblet cells were investigated in three mammalian insectivorous species, namely *A. spinosissimus*, *C. cyanea* and *A. hottentotus*. The aim of the study was to provide a comprehensive morphological comparison between the different species. Another aim was to illustrate and compare the distribution of mucins (neutral, sulfo- and sialomucins) in the gastrointestinal tracts (GITs) of these species, in order to better understand the quality of the biofilm in the GIT. Mucins secreted onto the surface of the GIT have an effect on the colonisation of microflora in the mucosal layer, constructing a biofilm which protects the GIT surface from opportunistic pathogens.

The shape, proportional length, and proportional surface areas of the different gastrointestinal regions were recorded and compared in the three species. Histochemical staining methods were used to detect and to distinguish between neutral, sulfo- and sialomucins. The number of goblet cells in the GIT containing each of the above mucins in the epithelium lining the surface or crypts was quantified, and the data expressed as the number of neutral, sulfo- or sialomucin containing goblet cells per mm^2 of the surface or crypt epithelium.

In all three species the stomach was uncompartmentalised. The internal aspect of the stomach in *A. spinosissimus* was hemi-glandular, containing stratified squamous epithelium in the fundus, with glandular epithelium in the body and pyloric region. However, *C. cyanea* and *A. hottentotus* had wholly glandular stomachs. *A. spinosissimus* was the only species studied that had a caecum which demonstrated transverse mucosal folds and V-shaped mucosal folds in the proximal colon. Both *C. cyanea* and *A. hottentotus* had villi up to the distal part of the GIT. Longitudinal mucosal folds were present in the distal colon. The GITs of both *C. cyanea* and *A. hottentotus* showed little morphological differentiation namely a simple, glandular stomach and the lack of a caecum.

Mixed (neutral and acid) mucins and mixed acid (sulfo- and sialomucins) mucin secreting goblet cells were prominent mucin cell types in all three mammalian insectivorous species. Despite these general similarities, marked differences were observed in the qualitative expression and distribution of the three types of mucins throughout the GIT. The overall similarity between the three insectivores and other distantly related mammalian species suggests that mixed mucin secreting goblet cell types are prominent contributors to the

maintenance of the intestinal biofilm in the majority of mammals, irrespective of their diet or taxonomy.

OPSOMMING

Die bestudering van die morfologie van die spysverteringskanaal (SVK) en die verspreiding van die verskillende musien produserende bekerselle was in drie insek-etende soogdier spesies uitgevoer, naamlik in *A. spinosissimus*, *C. cyanea* en *A. hottentotus*. Die doel van die studie was om ‘n omvattende morfologiese vergelyking te maak tussen die drie spesies, sowel as om die verspreiding van die verskillende musiene te beskryf in die SVK. Kennis van die verspreiding van die verskillende tipes musiene (neutral, sulfaat en nie-sulfaat bevattende musiene) kan moontlik inligting verskaf aangaande die kwaliteit van die biofilm in the SVK. Die laasgenoemde musiene wat gesekreteer word op die oppervlak van die SVK, bepaal die kolonisasie van die mikroflora in die mukosale laag wat ‘n biofilm vorm en die SVK beskerm teen patogene.

Die vorm, proportionele lengte en proportionele oppervlaks areas van die verskillende SVK gebiede is opgeteken, waarna dit vergelyk is tussen die drie insektivore spesies. Histochemiese kleurings tegnieke is gebruik om die musiene waar te neem en om te onderskei tussen die neutraal, sulfaat en nie-sulfaat bevattende musiene. Die aantal beker selle wat elk van die bogenoemde musiene bevat het, is getel in die oppervlaks epiteel- en kript areas van die SVK. Hierdie data is weergegee as die aantal neutraal, sulfaat en nie-sulfaat bevattende beker selle per oppervlaks epiteel- of kript area (mm^2).

Die vorm van die maag in al drie spesies was eenvoudig en nie gekompartementaliseer nie. Die interne aspek van die maag in *A. spinosissimus* het meerlagige plaveisel epiteel in die fundus gehad en klieragtige epiteel in die liggaam en pilorus gedeeltes. Daarbenewens het *C. cyanea* en *A. hottentotus* slegs klieragtige epiteel in die maag gehad. *A. spinosissimus* was die enigste spesie in hierdie studie wat ‘n sekum gehad het met dwars voue, asook V-vormige mukosale voue in die proksimale kolon. Beide *C. cyanea* en *A. hottentotus* het villi tot in die distale gedeelte van die SVK gehad. Longitudinale mukosale voue was teenwoordig in die distale gedeelte van die kolon. Die SVK van beide *C. cyanea* en *A. hottentotus* het min morfologiese differensiasie getoon deurdat die spesies ‘n eenvoudige, klieragtige maag gehad het en geen sekum nie.

Gemenge (neutral en suur) musiene asook gemengde suur (sulfaat en nie-sulfaat bevattende) musiene was die dominante musien tipes in the SVK van al drie insek-etende soogdier spesies. Ten spyte van die algemene ooreenkomste, was daar merkwaardige verskille in die getalle en verspreiding van die verskillende musiene in die SVK. Die algemene ooreenkomste tussen die drie insektivore soogdier spesies met soogdiere van

ander families, stel voor dat die gemende musien sekreterende beker selle ‘n prominente bydrae maak tot die onderhoud van die biofilm in the SVK in die meerderheid van soogdiere, ongeag van hul dieet of spesie klassifikasie.

AKNOWLEDGEMENTS

This report would not have been possible without the essential and gracious support of many individuals. A special thanks to my supervisors, Dr. S. H. Kotzé and Dr. E. L. van der Merwe for all their effort and support during the writing of this document. Your patience, kindness, as well as your academic experience has been invaluable to me.

I would like to thank Prof. Nigel Bennett for donating the specimens that were used in this study to the Division of Anatomy and Histology. Thank you for all your time and effort in the capturing of the animals and ensuring that the specimens were handled correctly.

I am extremely grateful to Prof. Martin Kidd for the statistical analysis of all the data, and also for assistance in the interpretation and understanding thereof.

Thank you to Mr Reggie Williams and Miss Zandré Fourie, at the University of Stellenbosch and Morea Petersen at the University of Cape Town for technical support with the histochemical techniques.

Thank you to the Division of Anatomy and Histology (Department of Biomedical Sciences, Faculty of Health Sciences), and the University of Stellenbosch for financial assistance and for the opportunity to attend the ASSA conference. Thank you to the Harry Crossley Foundation for funding this project. Without this financial support this project would not have been possible.

I would also like to acknowledge the following authors for the use of their photographs and illustrations in my thesis: Mills & Hess (1997); Stevens & Hume (1998); Shirazi et al. (2000); Kierszenbaum (2002); Young et al. (2006); Brockhausen et al. (2009) and McGuckin et al. (2009).

I am grateful to my surrogate family (Frik Fourie, Erika Fourie, Elmarie Fourie), Pieter Fourie, and all of my friends and everyone at Anatomy and Histology for their help and moral support. I would especially like to thank Elsje-Marie Geldenhuys, Mandi Alblas and Linda Greyling for their support.

Finally, I am forever indebted to my parents for their understanding, endless patience and encouragement when it was most required.

TABLE OF CONTENTS

LIST OF FIGURES

LIST OF TABLES

LIST OF ABBREVIATIONS

AB	Alcian Blue
AF	Aldehyde Fuchsin
Ala	Alanine
ANOVA	Analysis of Variance
BR	Basic Research
BW	Bodyweight
C. I.	Colour Index
Cat. No.	Catalogue number
Cys	Cysteine
D-domains	Cysteine rich domains
GI	Gastrointestinal
GIT/s	Gastrointestinal tract/s
Gly	Glycine
H&E	Haematoxylin & Eosin
HID	High Iron Diamine
IBD	Inflammatory bowel disease
Int.	Intestine
L.	Length
Ltd.	Limited
Mu	Mucin
MUC	Mucin Genes
N	Number
O-GalNAc	α-linked N-acetylgalactosamine
O-glycans	O-linked oligosaccharides

PAS	Periodic Acid Schiff
RSA	Republic of South Africa
RER	Rough Endoplasmic Reticulum
Pro	Proline
Prod.	Product
SA	Surface Area
Ser	Serine
SI+LI	Small intestine plus large intestine
Sm. Int.	Small Intestine
St.	Stomach
St. Len.	Stomach Length
Std. Dev.	Standard Deviation
SVK	Spysverteringskanaal
Thr	Threonine
UP	University of Pretoria
US	University of Stellenbosch
VNTR	Variable Number of Tandem Repeats

CHAPTER 1

INTRODUCTION

1.1 Introduction

Acomys spinosissimus (Southern African Spiny Mouse), *Amblysomus hottentotus* (Hottentot Golden Mole) and *Crocidura cyanea* (Reddish-grey Musk Shrew) are insectivorous mammals, which are widely distributed throughout Southern Africa (Mills & Hes, 1997). The latter species ingests a wide variety of insects (Kingdon, 1974a, b; Perrin & Curtis, 1980; Dickman, 1995). Small amounts of plant material and seeds are also consumed by *A. spinosissimus* and *C. cyanea*. Although all three species are insectivorous mammals, they belong to three different superorders viz. Euarchontoglires, Afrotheria and Laurasiatheria respectively (Wilson & Reeder, 2005). Even though it is well known that most insectivorous species have a simple GIT (Stevens & Hume, 1995), without a caecum, little is known about their intestinal morphology (Kurohmaru et al., 1980). Several morphological studies have been performed to relate the variations in gastrointestinal structures to different feeding habits (Chivers & Hladik, 1980; Perrin & Curtis, 1980; Langer, 2002). The insectivorous diets of *A. spinosissimus*, *C. cyanea* and *A. hottentotus* may therefore provide insights into the distribution and functions of the different mucins (neutral, sulfo- and sialomucins) in the GIT. The different types of mucins are implemented in the colonisation of bacteria in the mucosal layer which protects the internal aspect of the GIT against pathogens (Deplancke & Gaskins, 2001).

Mucins are high molecular weight (>200 kDa) glycoproteins, with large numbers of carbohydrate side chains attached to a protein core (Devine & McKenzie, 1992; Hattrup & Gendler, 2008). Mucins are classified according to their ability to form a gel, namely gel-forming (secreted) or non-gel-forming (membrane bound) mucins (Devine & McKenzie, 1992). In addition, mucins are also classified into neutral or acid mucins according to the net charge of the molecule. Acid mucins are further differentiated based on their histochemical properties into sulfate-containing mucins (sulfomucins) and sialic-acid-containing mucins (sialomucins) (Filipe, 1979).

In the GIT mucin granules are synthesised and secreted by specialised goblet cells (Sharma & Schumacher, 1995; Kierszenbaum, 2002; Young et al., 2006). When the mucin granules are released via exocytosis into the lumen and combined with water, it forms a viscous, gel-like mucus layer (Bansil & Turner, 2006; Young et al., 2006; Pavelka & Roth, 2010). The mucus layer of the digestive tract have several functions such as, lubrication, digestion, absorption, hosting intestinal microflora and protecting the GIT against toxins and pathogens (Laux et al., 2005; Bansil & Turner, 2006; Rose & Voynow, 2006).

The distribution of the various types of mucins has been determined histochemically in several mammalian (Filipe, 1979; Sheahan & Jervis, 1976; Kotzé & Coetzee, 1994) and fish species (Tibbetts, 1997; Cao & Wang, 2009). Thus, it is well known that the number and distribution of mucins can differ according to cell type, anatomical region, pathological condition and species (Scillitani et al., 2007). However, there is still a need for the better understanding of the distribution of mucins in normal tissues, particularly the examination of different types of mucins in a variety of tissues (Hattrup & Gendler, 2008). Knowledge of the distribution of the different types of mucins can indirectly provide insights about the quality of the mucus gel and biofilm which protects the internal surface of the GIT against pathogens (Deplancke & Gaskins, 2001; Pearson & Brownlee, 2005). Therefore, knowledge of the variations in mucin composition and distribution along the GIT is of importance to help explain functional, pathological and even taxonomic problems (Scillitani et al., 2007).

The present study was undertaken to describe the morphology and histology of the GITs of *A. spinosissimus* and the hitherto unknown gastrointestinal morphology of *C. cyanea* and *A. hottentotus*. In addition, histochemical methods were used to detect and determine the distribution of the different types of mucins along the GITs of the latter insectivorous species. Subsequently this study will provide a basis for further investigations into the histochemical structure of mucins via lectin histochemistry.

1.2 Aims

Since limited morphological and histological studies have been performed *on A. spinosissimus*, *C. cyanea* and *A. hottentotus*, the aim of this study was to do an in-depth/detailed morphological and morphometric analysis of the GIT of these species. This was in order to provide a valuable contribution to the field of comparative anatomy and to broaden our knowledge of the GIT of species from a wider range of taxonomical groups.

It was envisaged that the findings of this study could provide insights into the functional significance for the distribution of the different mucin secreting goblet cells in the GITs of the three insectivorous species. In addition, another aim was to provide baseline data on the distribution of the mucous/mucin secreting goblet cells in the intestinal tract. Knowledge of this cell distribution will indirectly give information about the quality of the protective mucus layer which is inhabited by bacterial populations, also known as biofilm. The biofilm protects the intestinal surface from pathogens. Therefore, it is important to understand the mucin composition of the mucus gel and the normal microbiome of the GIT in various species, as well as to better understand the role of normal gut flora which is important for the maintenance of a healthy intestinal tract.

1.3 Objectives

- To describe the anatomy of the gastrointestinal tract of *A. spinosissimus*, *A. hottentotus*, and *C. cyanea*.
- To describe the histology of the gastrointestinal tract of *A. spinosissimus, A. hottentotus*, and *C. cyanea*.
- To use histochemical techniques to identify the neutral, sulfo- and sialomucin producing goblet cells in the GIT of *A. spinosissimus*, *A. hottentotus*, and *C. cyanea*.
- To quantify the number of different mucin cell types in the GIT of these species and to determine their distribution throughout the GIT.
- To compare the distribution of the different types of mucin secreting goblet cells found in the intestinal tract of the three insectivorous species with each other, and with species from different dietary types.

CHAPTER 2

LITERATURE REVIEW

2.1 History of the Order Insectivora and New Views of Placental Phylogeny

Of all the mammalian orders, Insectivora has been one of the most difficult orders to classify (Symonds, 2005). The difficulty and uncertainty stemmed from the lack of clearly defined mutual characteristics – apart from being small and mostly insectivorous. Butler (1972) described the insectivores as being "eutherians which do not belong to any of the more clearly defined orders". Time and again terms such as 'scrap-basket' (Simpson, 1945) or 'waste-basket' (Butler, 1972) was used to refer to this group.

Butler (1972) provided a background history of the insectivore classification, starting from Linnaeus (1758). The latter author placed the three families of hedgehogs, shrews and moles into the order Bestiae. This order also included armadillos, opossums and pigs and they were united based on their elongated snouts. St. Geoffroy and Cuvier (1795) grouped the insectivore families with the carnivores, because of their plantigrade feet (walking with feet on the ground). Furthermore in 1811, Illiger placed the hedgehogs, shrews, moles, desmans, tenrecs and golden moles into a separate group; namely the family Subterranea (order Faculata) (Illiger, 1811). De Blainville (1816) renamed the latter family to 'insectivore' and Bowdich (1821) latinised the name to Insectivora.

Following this, Wagner (1855) included the two genera of tree shrews, three genera of elephant-shrews and the flying lemur into the order Insectivora. Thus, at this stage the order Insectivora consisted of 10 distinct families, namely: Erinaceidae (hedgehogs), Soricidae (shrews), Talpidae (moles), Solenodontidae (solenodons), the recently extinct Nesophontidae (West Indian shrews), Tenrecidae (tenrecs), Macroscelidae (elephant shrews), Tupaiidae (tree shrews), Chrysochloridae (golden moles), and Cynocephalidae (flying lemurs). In 1864 Peters remarked on the absence of a caecum in the 'traditional' insectivores (Peters, 1864). Consequently, Haeckel (1866) used this observation to divide the order Insectivora into two suborders, namely Menotyphla for species that possess a caecum (tree shrews, elephant-shrews and flying lemurs) and Lipotyphla for species without a caecum (hedgehogs, shrews, moles, solenodons, West Indian shrews, tenrecs and golden moles).

Evidence argued against Menotyphla and the three species within this suborder were eventually placed in their own consecutive orders (Douady & Douzery, 2009). The flying lemurs was removed from the former grouping by Gill (1872) and Leche (1885), and elevated to ordinal status, order Dermoptera. Further in 1910, Gregory separated Lipotyphla and Menotyphla completely, moving each to ordinal level and relating

Lipotyphla to the Carnivora and Menotyphla to the Primates (Gregory, 1910). Robert Broom (1915; 1916), the African evolutionary biologist, questioned the placing of the golden moles within Insectivora, and suggested that they should be moved to a separate ordinal status, namely the Chrysochlorida. The classification of golden moles caused many of the difficulties in establishing insectivore phylogeny (Symonds, 2005).

Although the species within Menotyphla shared some characteristics, such as skull features (Butler, 1956), they were simple. Similar characteristics were found in other mammals as well. In addition, the tree shrews and elephant-shrews were very different from one another and Butler (1972) separated the two species and promoted each to ordinal level as Scandentia and Macroscelidae, respectively. Butler (1972), also envisioned an order of Insectivora which comprised of four suborders, called; Erinaceomorpha, Soricomorpha, Tenrecomorpha, and Chrysochlorida. However, the issues surrounding the order Insectivora and the golden moles (Chrysochlorida) was still not resolved.

In 1993, MacPhee and Novacek removed the Chrysochloridae from the other insectivores and placed them in a suborder called Chrysochloromorpha (MacPhee & Novacek, 1993). Springer et al. (1997) analysed the nucleotide sequences of mitochondrial genes, nuclear genes and an adrenergic receptor gene, and concluded that golden moles are not related to other insectivores. Instead, these animals were part of a clade (named Afrotheria) of endemic African mammals, which includes hyraxes, elephants, elephant-shrews, sirenians and aardvarks. A subsequent analysis done by Stanhope et al. (1998), proposed that tenrecs are also members of the Afrotherian clade.

The relationships among the orders of the placental mammals have been the subject of debate for more than a century (Springer & Murphy, 2007). Recently, a well-resolved view of the placental phylogeny was obtained with the use of sophisticated analyses of sequenced molecular data (Springer et al., 2004; 2005; Beck et al., 2006). The phylogenetic analyses of data were based on nuclear and mitochondrial DNA, together with rare genomic changes (Springer & Murphy, 2007). Consequently the remaining lipotyphlans (hedgehogs, shrews, moles and solenodons) was split into Eulipotyphla and Afrosoricida (Stanhope et al., 1998; Waddell et al., 1999) (Wilson & Reeder, 2005). At interordinal level, the molecular data divided the extant placental groups into four superorders viz. Afrotheria, Xenarthra, Laurasiatheria and Euarchontoglires, of which only

the superorders relevant to this study is listed in Table 2.1 (Beck et al., 2006; Asher et al., 2009).

According to Madsen et al. (2001), Afrotheria and Xenarthra are Gondwanan clades originating in Africa and South America respectively. In addition, Euarchontoglires and Laurasiatheria are Laurasian in origin, and together they form a clade named Boreoeutheria, which reflects its northern hemisphere ancestry (Springer and De Jong, 2001). Table 2.1 lists the species relevant to this study and their classification into the respective superorders. The species in bold represent those of interest for the present study.

Table 2.1: The superorders, supraordinal clades and orders that are currently supported by the molecular consensus view of placental phylogeny (Springer et al., 2004; 2005; Wilson & Reeder, 2005; Beck et al., 2006).

Superorders	Supraordinal Clades	Orders	Common Names & Species of Interest
Afrotheria	Afroinsectiphilia	Afrosoricida	African 'insectivores' (tenrecs, and golden moles) ***Amblysomus hottentotus***
Euarchontoglires	Glires	Rodentia	Rodents ***Acomys spinosissimus***
Laurasiatheria		Eulipotyphla	True 'insectivores' (hedgehogs, shrews, true moles and Solenondon) ***Crocidura cyanea***

2.2 Superorder: Euarchontoglires

2.2.1 Family Muridae

Acomys (spiny mice) belongs to the family Muridae in the order Rodentia (Wilson & Reeder, 2005). The order Rodentia, by comparison with all living mammals, are the most numerous and successful group of mammals (Mills & Hes, 1997). Of all the other species present in the family Muridae, the Southern African Spiny Mouse is the only species of interest for this study, and will be further discussed in the following section.

The spiny mice consist of four species and several sub-species (Kingdon, 1974b). Generally, they are characterised by the thick spiny hair that grows on their back. They mostly inhabit the drier parts of Africa, but are also found in the Middle East and North

West India (Kingdon, 1974b). These animals find shelter in rocky crevices, cracked soil, or burrows of other rodents. Spiny mice eat a variety of plant material and animal matter, and can even survive on coarse dry plants.

According to Kingdon (1974b) spiny mice are primarily nocturnal, but some species are active early morning as well. They are social animals and, apart from their adaptation to arid regions and their thick spiny hair, they resemble the genus *Mus* (mice). Dieterlen (1962), found that *Acomys* breed continuously in captivity and that their gestational period (5-6 weeks) is longer than that of most other mice (18-21 days) (cited in Kingdon, 1974b).

2.2.2 *Acomys spinosissimus* (Southern African Spiny Mouse)

In southern Africa, *A. spinosissimus* is found in north-eastern Botswana, north-eastern South Africa, Mozambique and Zimbabwe (Figure 2.1) (Mills & Hes, 1997). Further afield, this species is also found in Zambia, Zaïre and Tanzania. The spiny mouse is nocturnal and terrestrial, and may occur either singly or in small groups. This species feeds on grass and seeds and will also eat insects. Vesey-FitzGerald (1966) discovered that *Acomys spinosissimus selousi* ate beetles, ants, bugs, termites, millipedes, small snails, spiders and seeds.

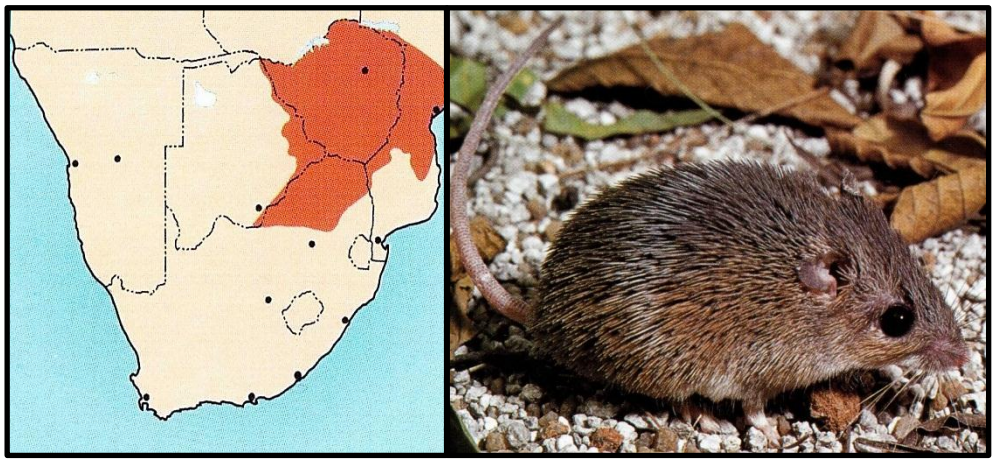

Figure 2.1: The distribution of *A. spinosissimus* in southern Africa and its morphological characteristics (Mills & Hes, 1997, p. 138).

The brown shaded area in the left-sided image demonstrates the distribution of *A. spinosissimus*, which is located predominantly in the north of South Africa, most of Zimbabwe, and in strips along the west and eastern borders of Botswana, and Mozambique respectively. The image on the right shows the outward morphological characteristics of this species.

A. spinosissimus has a dark, brownish back and the sides of the head and body are a reddish colour (Kingdon, 1974b; Mills & Hes, 1997). The head to body length is between

85-109 mm, tail length between 80-100 mm, and long-nosed nasals of over 9.8 mm. This species is found in the dry woodlands at rocky sites.

2.3 Superorder: Laurasiatheria

2.3.1 Family Soricidae (Shrews)

Hedgehogs, shrews, solenodons and moles form the order Eulipotyphla (Douady & Douzery, 2009). Currently, there are 452 species recognized by Wilson and Reeder (2005) in the latter order, which belongs to four living families, namely: Erinaceidae (hedgehogs), Soricidae (shrews), Talpidae (moles) Solenodontidae (solenodons), as well as the recently extinct Nesophontidae (West Indian shrews). These species share morphological characteristics such as a simple hindgut without a caecum, long narrow snouts and poorly developed or absent eyes (Douady & Douzery, 2009). The primitive characteristics of the latter species have led many zoologists to believe that these species resemble the basic stock which gave rise to most eutherian (placental mammals plus all extinct mammals) lineages.

Southern African shrews all belong to the primarily Afro-oriental subfamily of white-toothed shrews, the Crocidurinae (Mills & Hes, 1997). Uniquely, they all share the behavioural trait of caravanning where the young attach themselves to each other and to the female. This usually occurs for two to three weeks before weaning.

There are four different shrew families in southern Africa: the forest shrews (genus *Myosorex)*; the musk shrews (genus *Crocidura)*; a climbing shrew (genus *Sylvisorex)*; and the dwarf shrews (genus *Suncus)* (Mills & Hes, 1997). Apart from *Mysorex* and *Sylvisorex*, the other shrew families are not easily distinguishable in the field.

2.3.2 *Crocidura cyanea* (Reddish-grey Musk Shrew)

This species is small and primarily grey to grey-brown in colour. It was first described in 1838 near Citrusdal in the Western Cape (Mills & Hes, 1997). It weighs about 9 g, with a head and body length of about 76 mm, and the tail measures 69% of the head and body length.

Crocidura cyanea is widely distributed in southern Africa (East Central and East Africa) but is absent from the north-central Karoo to northern Botswana (Figure 2.2) (Mills & Hes, 1997). This species inhabits a wide diversity of environments, occurring in savannahs,

grasslands, marshlands, dense shrubs, rocky outcrops, and montane forests (Stuart and Stuart, 2001; Kingdon, 1974a).

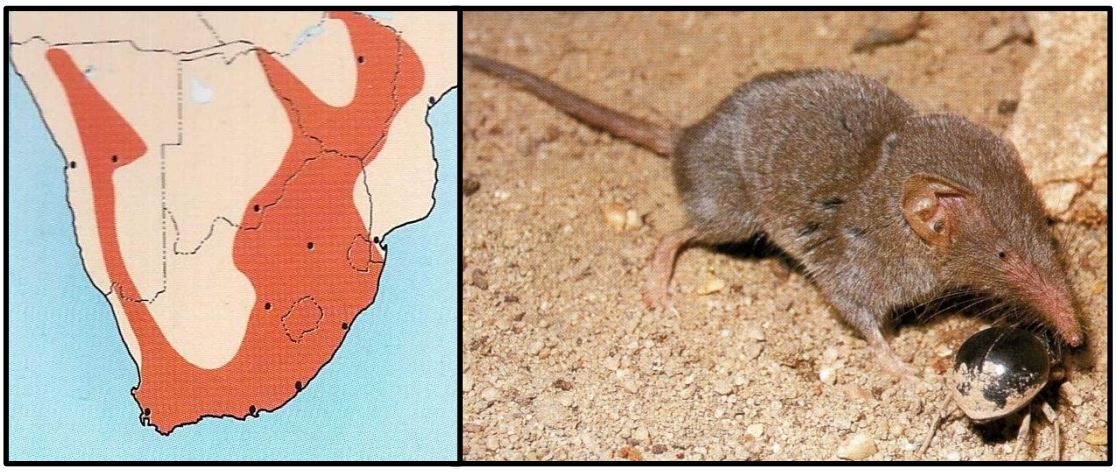

Figure 2.2: The distribution of *C. cyanea* in southern Africa and its morphological characteristics (Mills & Hes, 1997, p. 50).

The brown shaded area in the left-sided image demonstrates the distribution of *C. cyanea* which is located predominantly in South Africa, except in the north central Karoo to northern Botswana. They are also found in Namibia, Zimbabwe and along the western border of Mozambique. The image on the right shows the outward morphological characteristics of this species.

In Namibia, a cave-dwelling population of this species was found to thrive on invertebrates, such as beetles, crickets, and pseudoscorpions (Mills & Hes, 1997). These shrews are predominantly nocturnal, solitary, terrestrial, and insectivorous. In addition, Dickman (1995) examined the diets and habitat preferences of three crocidurine shrews. All three species, *Crocidura cyanea*, *Crocidura fuscomurina* and *Crocidura hirta*, were primarily insectivorous. Isoptera (termites), Chilopoda (centipedes), Araneida (spiders) and insect larvae were consumed consistently by all three species. The latter taxa are mostly soft-bodied and have a high ratio of body water to energy content (Churchfield, 1990), which may be preferred in water scarce environments. Although beetles were also prominent in the diets of the other two crocidurine species, *C. cyanea* avoided these heavily-chitinized beetles. Dickman (1995) suggested that these beetles may be unpalatable to *C. cyanea*.

2.4 Superorder: Afrotheria

2.4.1 Family Chrysochloridae (Golden Moles)

The family Chrysochloridae belongs to the order Afrosoricida, in the superorder or supercohort of Afrotheria (Skinner & Chimimba, 2005; Wilson & Reeder, 2005). A diverse number of golden moles belonging to the family Chrysochloridae are endemic to Sub-Saharan Africa, of which 18 species are endemic to the southern African sub-region

(Bronner, 1995). These animals occur in a wide range of environments and habitats, ranging from forests, deserts and temperate grasslands (Mills & Hess, 1997; Stuart & Stuart, 2001).

Species within the family Chrysochloridae differ noticeably from each other in terms of size, fur colour and texture (Mills & Hes, 1997). All golden moles have fusiform bodies, lacking a tail and external ear pinnae, which are adaptations for underground living (Mills & Hes, 1997; Stuart & Stuart, 2001). Most golden moles are solitary and subterrestrial. The forequarters are well developed to power the strong, pick-shaped claws of the forefeet. As an adaptation for excavating loose soil from the burrows, their hind feet are webbed. Golden moles are completely blind, because of a degenerate optic nerve (Mills & Hes, 1997). Their fur colour varies from jet black through various shades of honey to orange and brown to yellow, despite the colloquial name ‘golden mole’. The term ‘golden mole’ and ‘Chrysochloridae’ refers to the distinct bronze, silver, violet or green opalescence of the fur, which is unmistakable in all species (Skinner & Chimimba, 2005). In addition, these animals are opportunistic insectivores and feed primarily on termites, millipedes and earthworms (Mills & Hes, 1997).

2.4.2 *Amblysomus hottentotus* (Hottentot Golden Mole)

The Hottentot Golden Mole is the most widespread golden mole species in southern Africa (Skinner & Smithers, 1990; Mills & Hes, 1997). They are specifically widespread and common in the moist, eastern parts of South Africa; from Stellenbosch in the Western Cape to Graskop in Mpumalanga, and inland to the Drakensberg Mountains (Figure 2.3). In addition, the Hottentot Golden Mole is also found in the north-eastern Free State, the Highveld of Mpumalanga, and the adjacent parts of eastern Swaziland. Consequently, this species also inhabits a wide spectrum of subterrestrial environments such as coastal forests, temperate grasslands, montane marshlands and savannah woodlands, but not the dry bushveld (Kuyper, 1985; Skinner & Smithers, 1990; Mills & Hes, 1997). They are associated with sandy soils, but can also occur in clay or loamy soils (Stuart & Stuart, 2001).

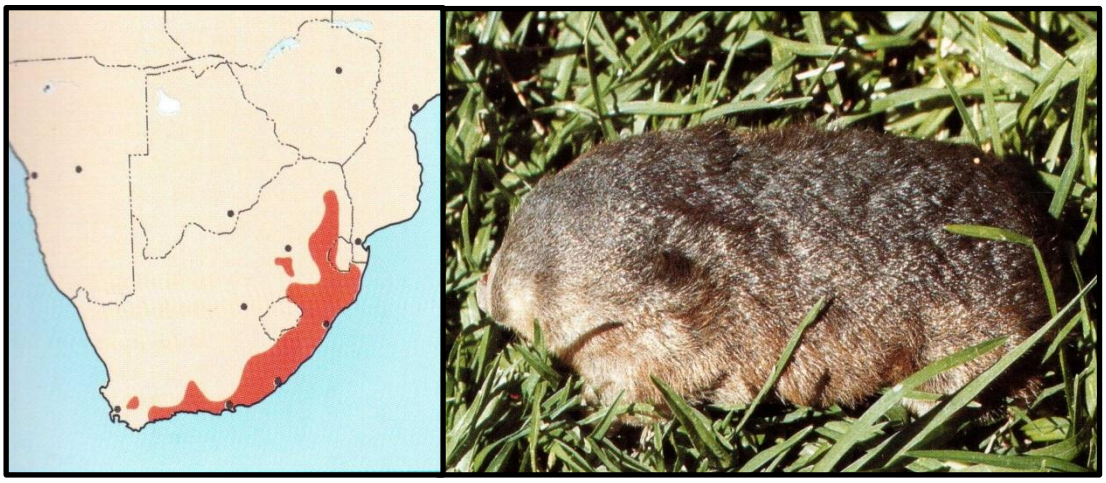

Figure 2.3: The distribution of *A. hottentotus* in southern Africa and its morphological characteristics (Mills & Hes, 1997, p. 61).

The left image indicates a brown shaded area, demonstrating the distribution of *A. hottentotus* which is located primarily along the east coast of South Africa, the north-eastern Free State, the Highveld of Mpumalanga and the adjacent parts of eastern Swaziland. The image on the right shows the outward morphological characteristics of this species.

This species has extensive burrow systems, reaching lengths of up to 200 m, which are extended daily in search of food (Mills & Hes, 1997). Even though the Hottentot Golden Mole vigorously defends its burrows against other moles of the same species, it peacefully coexists with the common mole-rat (*Cryptomus hottentotus*) and sometimes both species live together in the same burrow system. These two species have a symbiotic relationship, as they do not compete for food. *Cryptomus hottentotus*, the common mole-rat, is herbivorous and mainly feeds on geophytes (plants with underground storage organs) (Spinks, Bennett, & Jarvis, 2000), whereas *A. hottentotus* is insectivorous. By using each other's burrows, the energy involved in excavating burrows is substantially reduced. Burrowing activity occurs occasionally during the day, with peaks at sunset, midnight and sunrise (Cizek & Myers, 2000).

The size and colour of these animals vary geographically and within populations (Mills & Hes, 1997)**.** Their length and weight varies between 110-140 mm and 40-70 g respectively. The Hottentot Golden Mole in the Ingwavuma district of KwaZulu-Natal is noticeably smaller; about 90 mm in length and weighs between 30-35 g. The males are larger than the females. Communication between animals takes place via head knocking and the use of vibrations (Cizek and Myers, 2000; Mason, 2003; Mills and Hes, 1997).

The back of the Hottentot Golden Mole is generally blackish to reddish-brown, with a copper-green or violet iridescence; the ventral part and flanks are pale (Mills & Hes, 1997; Stuart & Stuart, 2001). *A. hottentotus* is insectivorous and feeds mainly on earth worms; it

also consumes crickets, snails, slugs, insect larvae, spiders and occasionally bulbs and garlic. The moist environment and dew provide these animals with the amount of water that is needed (Skinner and Smithers, 1990).

Although *A. spinosissimus*, *C. cyanea* and *A. hottentotus* are all insectivorous mammals, with similar dietary preferences, they belong to three different clades. Therefore, the morphology of their GITs and mucin histochemistry are of great interest as their insectivorous diet may shed some light on the functions of specific mucins in the intestinal tract. The following sections present firstly, and overview of the general gastrointestinal morphology; secondly describes and discusses the differences in the gastrointestinal morphology between different dietary types; and finally, the mucin structure and function in the GIT.

2.5 Introduction to the Mammalian Gastrointestinal Tract

The main function of the GIT is to provide for the assimilation of nutrients that is required for energy, maintenance, growth and reproduction (Stevens & Hume, 1995). Digestion involves a number of physical and chemical processes. When food is ingested, it is broken down into small particles, macerated, and mixed with digestive enzymes, while it is being propelled through the digestive tract. Several secretions of the digestive tract either provide protection of the digestive tract, or aids in the hydrolysis of carbohydrates, proteins and lipids. Protection and lubrication of the intestinal tract is provided by salivary, gastric, pancreatic, biliary and mucous secretions. In addition, digestive enzymes at the optimal pH allows for the breakdown of food. Indigenous micro-organisms of the digestive tract also allows for further breakdown of carbohydrates, proteins and lipids so that it can be suitable for absorption.

According to Langer (1988), the digestive tract of mammals evolved following two different strategies. The GIT either evolved as an ‘autoenzymatic’ or ‘alloenzymatic’ digestion device of food. An autoenzymatic type of digestion entails the digestion of food with the mammals’ own digestive enzymes (Langer, 1988). On the other hand, alloenzymatic type of digestion comprises of micro-organisms that contribute to microbial degradation of plant-based diets. Mammals using the latter type of digestion can have a highly differentiated large intestine and/or stomach. This means that multi-chambered stomachs or the enlargement of the caecum and colon appears to be a common trend in mammals hosting microbial biota (Langer, 1991).

Variations occurring in the digestive system of vertebrates can be related to the animals' nutritional requirements (Stevens & Hume, 1995). The nutritional niche can be explained according to two parameters viz. the energy and nutrients the animal needs and how the animal harvests and extracts what is needed from its nutritional environment.

2.6 Overview of the Macroscopic Anatomy of the GIT of Vertebrates

Vertebrates share many of the structural and functional characteristics of their digestive system (Stevens & Hume, 1995). Variations of the GIT between species have resulted from adaptations to diet or the environment. This was either due to divergence or convergence from a common or more primitive form. Although all vertebrates have a digestive tract and accessory digestive glands, the different parts of the GIT vary greatly between species. Thus, various parts of the digestive system are not necessarily homologous, comparable, or present in all species. Therefore, the vertebrate digestive system will be broadly divided into the headgut, foregut, pancreas and biliary system, midgut and the hindgut (Stevens & Hume, 1998). The latter digestive divisions are not the same as the embryonic origins.

The headgut (cranial portion of the GIT) consists of the oral (buccal cavity) and the throat (pharynx) (Stevens & Hume, 1995). The foregut comprises the oesophagus and stomach. The midgut (small intestine) comprises the duodenum, jejunum and ileum. Embryonically, the pancreas and liver parenchyma are derived from the foregut epithelium and these structures contribute to the digestion processes on this segment of the tract. In addition, the hindgut refers to the entire large intestine.

The morphology of the GIT differs greatly between diverse dietary types. The following section will provide a comparative overview of the GITs of carnivores, herbivores, omnivores and insectivores.

2.6.1 The GIT of Carnivores

Carnivores are primarily flesh eaters (Stevens & Hume, 1995). Most carnivores have a relatively short and simple GIT compared to herbivores (Stevens & Hume, 1998). The stomach is usually a unilateral dilation of the digestive tract (Figure 2.4, image of the dog) (Stevens & Hume, 1998). Exceptions to the latter statements are the Cetaceans (dolphins, whales and porpoises) with large multi-compartmental stomachs and the vampire bats which have convoluted stomachs. The anatomical structure of the stomach of Cetaceans is thought to be preserved from herbivorous ancestors (Milinkovitch, Guillermo, & Meyer,

1993). A distinct hindgut is absent in some Carnivora. The hindgut is generally short and without haustrations. A caecum may be present in some species of Carnivora.

2.6.2 The GIT of Herbivores

Evidence suggests that the earliest mammals were carnivores, but currently the majority of the mammalian orders consist of herbivorous species (Stevens & Hume, 1995). A high body temperature and high rates of microbial activity is partly what lead to the success of the mammalian herbivores. The diet of herbivores consists largely of the fibrous portions of plants (leaves, petioles, stems). Most of the mammalian herbivores obtain a large portion of their nutrients via retention and microbial fermentation of plant materials in a voluminous caecum, colon or fore-stomach (Stevens & Hume, 1995, 1998).

A characteristic in small herbivorous animals is a big caecum that serves as the main site of microbial fermentation (Stevens & Hume, 1995). Large herbivorous mammals (perissodactyls, elephants, wombats, sirenians, orangutans, and gorillas) have an enlarged colon which serves as the principle site for digesta retention and microbial fermentation (Figure 2.4, image of the sheep). Digesta are retained with the help of haustra, as well as compartmentalisation in perissodactyls and elephants. Haustrations in the wombat species are extended over the caecum and over the entire length of the colon. For the remainder of the large herbivores (most artiodactyls, sloths, macropods marsupials, colobus- and langur monkeys) a large compartmentalised or haustrated stomach is the main site for microbial fermentation.

2.6.2.1 Foregut Fermenters

Foregut fermenters (artiodactyls, kangaroos, monkeys, colobus) possess complex stomachs with multiple compartments and cellulose digesting micro-organisms (White, 2007). Advanced ruminants have a highly compartmentalised stomach which consists of a fore stomach (reticulum, rumen and omasum) and a glandular stomach (abomasums) (Stevens & Hume, 1995). After food is obtained by grazing or cropping, it passes into the rumen, where it is moistened and mixed with micro-organisms. Large food particles pass from the rumen to the reticulum. Fermentation takes place in both the rumen and reticulum where the absorption of short-chained fatty acids occurs. When the animal is at rest, the softened mass of food is regurgitated, allowing the animal to re-masticate. The food is re-swallowed and enters the omasum for further processing. The final chamber is the true stomach (abomasum). Digestive enzymes are secreted in the latter region and protein

digestion is completed. The digested material passes into the small intestine where further digestion and absorption occurs.

2.6.2.2 Hindgut Fermenters

The hindgut (large intestine) functions as the final site for storage of digesta and to retrieve dietary or endogenous electrolytes and water (Stevens & Hume, 1995). It is also the main site of microbial fermentation in herbivorous reptiles, most herbivorous birds and herbivorous mammals. Cell walls containing cellulose and lignin in plant material are difficult to digest (Vaughan et al., 2000). Micro-organisms in the digestive tract can synthesise cellulytic enzymes which can break down plant material, but microbial fermentation is a slow process.

Hindgut fermenters masticate food as they eat, initiating digestion with salivary enzymes (White, 2007). Digestion occurs by enzymatic activity within the simple stomach. Hindgut fermenters do not regurgitate food. Food passes from the small intestine into the caecum. Large food particles move through to the large intestine. Micro-organisms ferment the ingested cellulose in the caecum and large intestine.

Mass-specific energy requirements of homeothermic animals are high and related to body mass, i.e. the smaller the animal the greater its energy need per unit of body mass (Björnhag, 1994). Thus, small animals that feed on plant material with low energy density cannot only rely on microbial fermentation because the process is too slow to produce sufficient amounts of energy. Small herbivorous animals combine autoenzymatic digestion in the foregut with microbial fermentation in the large intestine. These small herbivorous animals are hindgut fermenters.

2.6.3 The GIT of Omnivores

Omnivores feed on plants, plant concentrates (seeds, nectar, roots, fruit) and animals (Stevens & Hume,1998). They have simple, single chambered stomachs, except for some rodents, nectivorous and frugivorous bats. The total length of the intestine varies in terms of the relative length of the mid- and hindgut, as well as a function of the body length. For example, bears have a very long intestine and a short, ill-defined hindgut. However, the intestine of the opossum is nearly equally divided between a small- and large intestine. The entire length of the colon in humans, pigs (Figure 2.4Figure 2.4, image of the pig), and other primates (monkey, chimpanzee) is haustrated (Stevens & Hume, 1995).

Derting and Noakes (1995) conducted a study on two rodent species with diets of different types. They concluded that because of their high quality and non-fibrous diet, omnivorous and granivorous species do not depend on post-gastric fermentation chambers to store digesta and to extract nutrients. Protein and easily digestible carbohydrates can be processed and the nutrients absorbed in the foregut. The hindgut is more important in herbivorous than in omnivorous animals (Wang et al., 2003).

2.6.4 The GIT of Insectivores

As discussed previously, the order Insectivora no longer exists. This order was eventually split into Eulipotyphla (true insectivores) and Afrosoricida (African insectivores) (Stanhope, et al., 1998). The 'true insectivores' (hedgehogs, true moles, shrews, Solenodon) refer to insectivores originally grouped in the order Insectivora, and the 'African insectivores' (tenrecs and golden moles) refers to insectivores found in Africa.

The GIT of insectivores varies among different species (Stevens and Hume, 1995). They usually have a simple hindgut which lacks a caecum (Figure 2.4, image of the mole). Members of the Soricidae (shrew) family have a rounder stomach than that of other insectivores; its cardiac inlet and pyloric outlet are close to one another. A very short intestine is present, which is only three to four times the length of the shrew's body. Tenrecs, indigenous to Madagascar, feed primarily on worms (Flower, 1872). Their intestines showed no indication of any division into small and large bowel, other than a slight enlargement of the terminal straight segment.

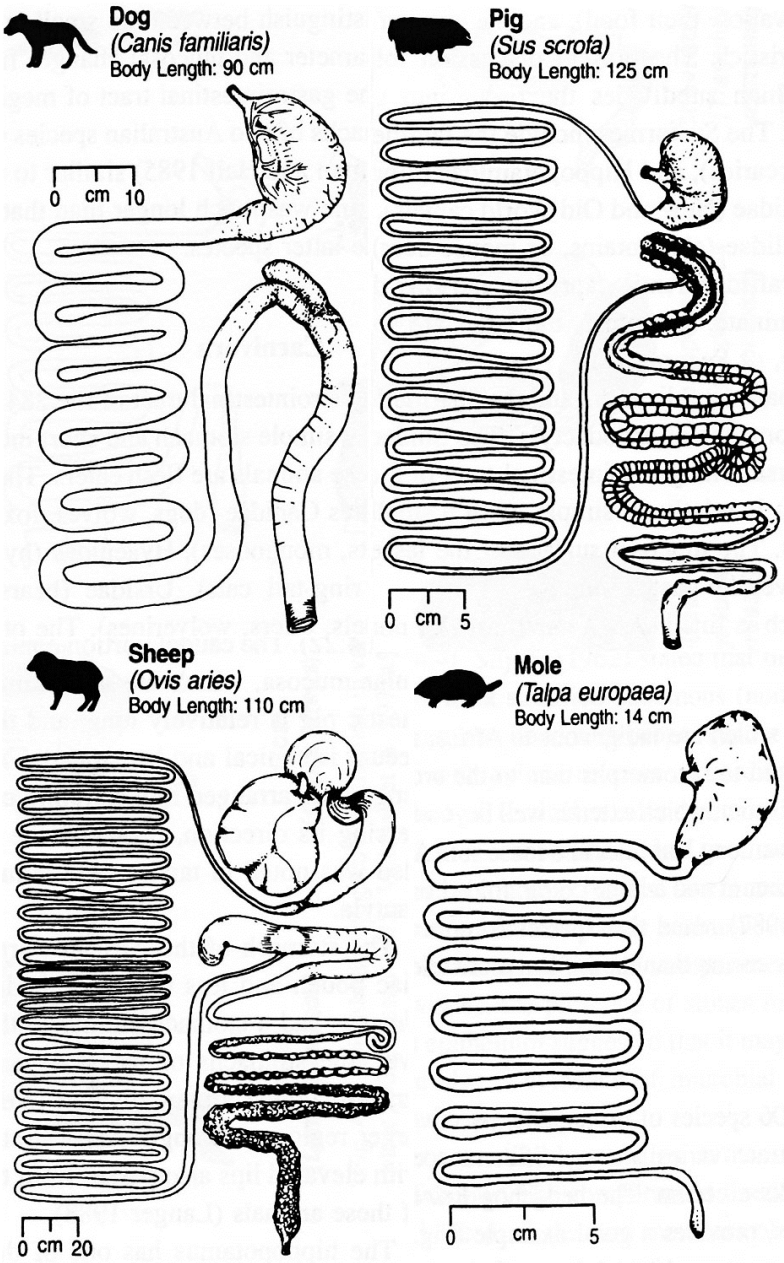

Figure 2.4: Comparison of the gastrointestinal tracts of a carnivore (dog), herbivore (sheep), omnivore (pig), and insectivore (mole) (Stevens & Hume, 1998, pp. 399, 400, 402).

2.7 Introduction to the Histology of the Gastrointestinal Tract

The GIT conforms to a general structure that is noticeable from the oesophagus to the anus (Young et al., 2006). Essentially, it is a muscular tube lined by a mucous membrane. In the different regions of the GIT, minor variations are evident in the muscular component, but most strikingly is the underlying changes in structure and function of the mucosa in the different regions (Figure 2.5). The GIT has four functionally distinguishable layers, namely: mucosa, submucosa, muscularis propria and adventitia.

The mucosa consists of an epithelial lining, an underlying lamina propria of vascularised loose connective tissue, and a thin smooth muscle layer (the muscularis mucosae) (Kierszenbaum, 2002; Young et al., 2006). Furthermore, the mucosa undergoes sudden changes during the transition from one region of the GIT to another. This occurs at the gastro-oesophageal junction, the gastro-duodenal junction, the ileo-caecal junction, and also at the recto-anal junction.

The submucosa supports the mucosa and consists of loose fibrous connective tissue, blood vessels, lymphatics and nerves (Kierszenbaum, 2002; Young et al., 2006). The muscularis propria, usually consisting of smooth muscle, is generally arranged as an inner circular- and outer longitudinal layer, which is responsible for peristaltic contraction (Young et al., 2006). Only in the stomach is there a third muscle layer, namely the inner oblique muscle layer. The adventitia is an outer layer of loose supporting tissue and it conducts major blood vessels, nerves and adipose tissue. Where the GIT lies within the peritoneal cavity, the adventitia (outermost connective tissue layer) is referred to as the serosa and it is lined by mesothelium.

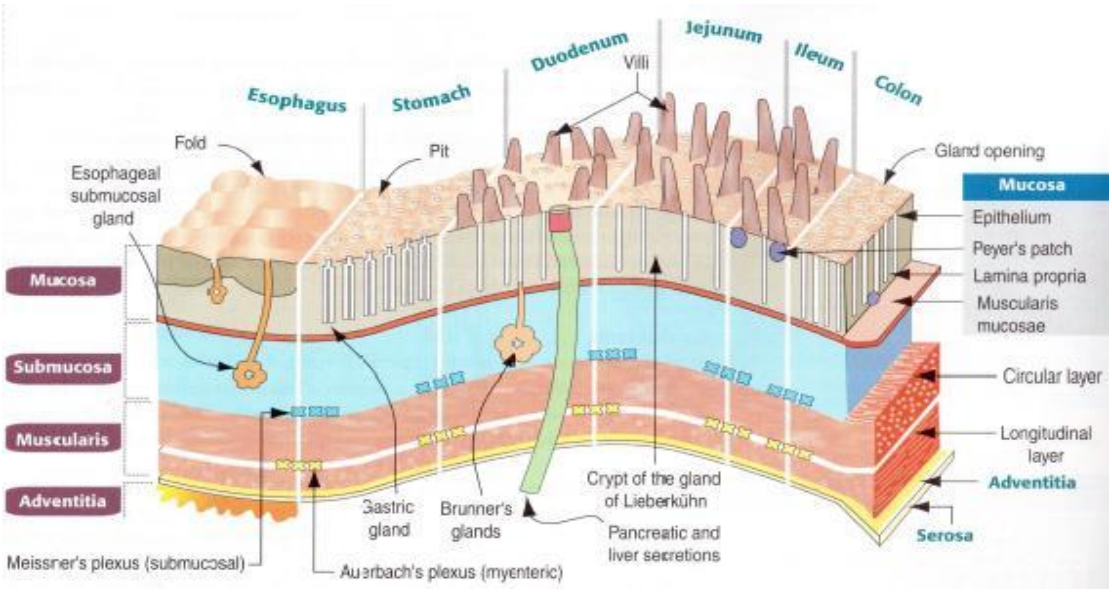

Figure 2.5: An overall histological representation of the gastrointestinal tract (Kierszenbaum, 2002).

2.8 Mucosal Surfaces and Mucous Secreting Cells

Mucosal surfaces of the body (gastrointestinal-, respiratory- and urinogenital tracts) are those areas where the absorption and excretion of substances occur (Pearson & Brownlee, 2005). As a consequence, these surfaces are exposed to the potentially harmful external environment, but the cells in the mucosa, along with their mucous secretions, create a protective barrier (mucus layer) which protects the pathogen-free internal

environment of the body. Evidently, the mucosal surfaces are the primary areas of attack by micro-organisms. The mucosal surfaces, in response to microbes, secrete many defensive compounds into the mucus layer. These include compounds such as: antibodies, mucins, protegrins, defensins, collectins, cathlecidins, histatins, lysozyme, and nitric oxide (Linden et al., 2008). In the present study, the mucosal surface and the mucous secreting cells of the GIT are of great interest.

The mucosal surface of the intestinal tract is covered with a viscoelastic and lubricant layer of mucus (Forstner & Forstner, 1994). Even though mucus is a constantly changing mixture of many secretions and exfoliated epithelial cells, the main determinants of the functional and physical properties of mucous secretions are highly glycosylated, high molecular weight proteins, named mucins. Mucin granules are synthesised and secreted by specialised epithelial cells (goblet cells) in the GIT that is located on the mucosal surface and also in the invaginated epithelial lining of the crypts.

Mucus has a number of functions in the GIT (Kierszenbaum, 2002; Young et al., 2006). In the cranial part of the GIT, mucus lubricates the oral cavity, the surface epithelium of the oesophagus, protects the intestinal lining of the stomach from auto-digestion, and in the caudal part it lubricates the passage of faeces. Apart from lubrication, the mucus layer of the GIT also protects the underlying cells from mechanical damage and prevents bacterial invasion (Montagne et al., 2004; Pavelka & Roth, 2010).

2.8.1 Mucous Cells in the Stomach

The stomach mucosa is protected from auto-digestion by a thick surface mucus layer. The pH of this mucus layer is alkaline and thus counters the effect of the gastric acid juices through the secretion of bicarbonate ions via the gastric surface of the mucous cells (Kierszenbaum, 2002; Young et al., 2006). Two types of mucous cells are found in the stomach: surface mucous cells and neck mucous cells. The surface mucous cells secrete mucin granules, which forms a protective mucus layer when it is combined with water. These cells line the luminal surface of the stomach and partially line the gastric pits. Surface mucous cells have short surface microvilli, and secrete the protective bicarbonate ions directly into the deeper levels of the surface mucus layer.

2.8.2 Mucous Secreting Cells in the Intestinal Tract

2.8.2.1 Brunner's Glands

In the duodenum, Brunner's glands mostly occur in the submucosa, but a small component thereof may also be found in the lamina propria, where the duct of the gland empties into the base of the crypt (Young et al., 2006). Brunner's glands are only present in mammals (Takehana et al., 2000), and can be described as coiled tubules that are lined by epithelial cells that contain mucous substances (Young et al., 2006). Furthermore, Brunner's glands have a slightly alkaline (pH 8.2 to 9.3) mucoid secretion, which protects the duodenal mucosa from autodigestion by the acidic stomach contents (Takehana et al., 2000; Young et al., 2006). Histochemical studies done on several species have confirmed that Brunner's glands primarily consist of neutral carbohydrates (Takehana et al., 2000).

2.8.2.2 Goblet Cells

Goblet cells are specialised columnar epithelial cells with the important function of synthesising and secreting mucus. They are found in the respiratory tract and throughout the GIT (Fahy, 2002; Young et al., 2006). The 'stem' of the goblet cell attaches to the basal lamina and is occupied by a condensed, basal nucleus and rough endoplasmic reticulum, which produces the protein portion of mucus. The Golgi apparatus, situated above the nucleus, adds oligosaccharide groups to mucus (Paulus et al.,1993).

In the small intestine the goblet cells are arranged in between the absorptive cells (Figure 2.6Figure 2.6) (Goralski, Sawicki, & Blaton, 1975), gradually increasing in number towards the large intestine (Trier, 1968). According to unpublished observations of Neutra, as cited in Forstner (1978, p. 235), the number of goblet cells in the descending colon and rectum of humans comprises one eighth of the entire epithelial cell population. Furthermore, Cheng et al. (1984) reported that approximately 10% of the duodenal epithelium and 24% of the total epithelial cell population in the distal colon is comprised of goblet cells. Their secretions form a crucial physiological barrier between the intestinal mucosa and the luminal environment.

Goblet cells migrate from the crypts to the villus over a period of 3-5 days (Radwan, Oliver, & Specian, 1990) while undergoing maturation, during which lysosomes decrease, Golgi membranes are enhanced, rough endoplasmic reticulum (RER) becomes more abundant, and there is an increase in number of mucin-filled secretory vesicles (Freeman, 1966). As the goblet cell reaches maturity, its most prominent feature is the wine goblet appearance

(Figure 2.6), which is due to the abundance of mucin droplets in the apical portion of the cell. Mucin granules or droplets within the apical cytoplasm of goblet cells are released during exocytosis and, when combined with water, forms the viscid secretion called mucus (Young et al., 2006; Pavelka & Roth, 2010). Goblet cells secrete mucin granules at a constant basal rate, but upon stimulation by local irritation (Table 2.2) their entire mucin content may be released. Table 2.2 indicates several classes of agents that regulate mucin secretion.

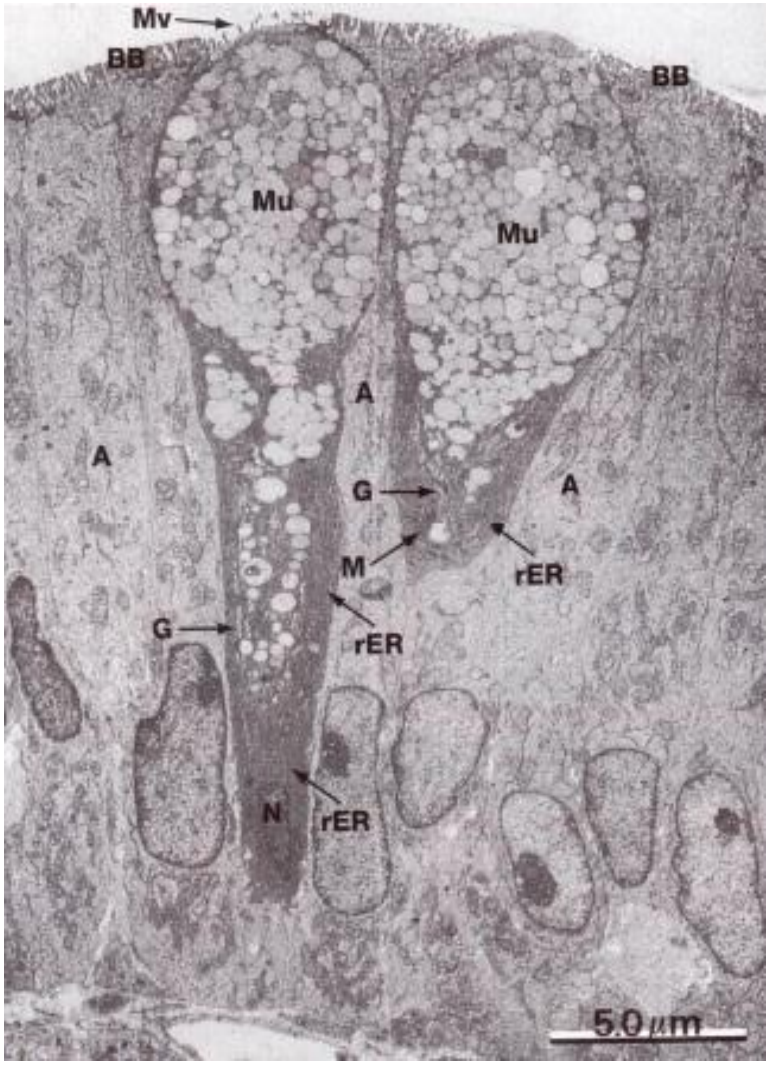

Figure 2.6: An electron microscope image of goblet cells, positioned between absorptive columnar cells (A), filled with mucin (Mu) granules (Young et al., 2006, p. 94).

Table 2.2: *Agents that affect the production and secretion of mucins.

Agent	Example	Proposed action on mucins
Irritants	Triglycerides, mustard oil	Stimulate secretion
Metabolic substrates and inhibitors	Puromycin, anti-inflammatory drugs, cycloheximide	Inhibits production
Hormones	Secretin, Serotonin , Parathyroid hormone	Stimulate secretion
Neurotransmitters	Isoproterenol Acetylcholine	Stimulate production Stimulate secretion
Vitamins	Vitamin A	Stimulate production
Drugs	Carbenoxolone	Stimulate production
Metals	Copper	Stimulate secretion
Micro-tubular agents	Colchicine	Inhibits secretion
Bacterial toxins	Cholera toxins and E. coli	Stimulate secretion

*Modified from Forstner, 1978

2.9 Mucins

In 1865 E. Eichwald, a Russian physician that worked in Germany, delivered the first chemical evidence that mucins are proteins bound to carbohydrates (Brockhausen, Schachter, & Stanley, 2009). Mucins are highly O-glycosylated, glycoproteins with a high molecular weight (larger than 200 kDA) (Devine & McKenzie, 1992). Some mucins are small with only a hundred amino acid residues, yet others can contain more than a thousand residues (Perez-Villar & Hill, 1999). Generally, mucins can be divided into two main categories: (i) membrane associated and (ii) secreted mucins (Montagne, Piel, & Lallès, 2004). The secreted mucins characteristically have a very high molecular weight and size with many O-linked oligosaccharides to form viscoelastic gels. Membrane-associated mucins have similar structural properties as the secreted mucins, but they have different functional properties because they are active membrane-bound components (Montagne, Piel, & Lallès, 2004).

2.9.1 Mucin Structure

Each mucin glycoprotein consists of a central protein backbone with numerous oligosaccharides attached to it (Allen & Pearson, 1993). The protein backbone has a central domain that contains high levels of threonine (Thr), serine (Ser), proline (Pro), alanine (Ala), and glycine (Gly), and low levels of sulphur and aromatic containing amino acids (Devine & McKenzie, 1992; Montagne et al., 2004). The central domain can also be referred to as the "variable number of tandem repeat" (VNTR) region (Figure 2.7) (Brockhausen, Schachter, & Stanley, 2009). This region has a repetitive amino acid sequence (rich in Thr, Ser and Pro) that can be repeated a variable number of times and is unique to each mucin gene (Pearson & Brownlee, 2005). These VNTR regions are rich in Ser and Thr O-linked oligosaccharide acceptor sites and have a large number of mucin O-linked oligosaccharides attached to it (Brockhausen, Schachter, & Stanley, 2009). About 80% of the weight of these molecules consists of oligosaccharides, also referred to as carbohydrates (Pearson & Brownlee, 2005).

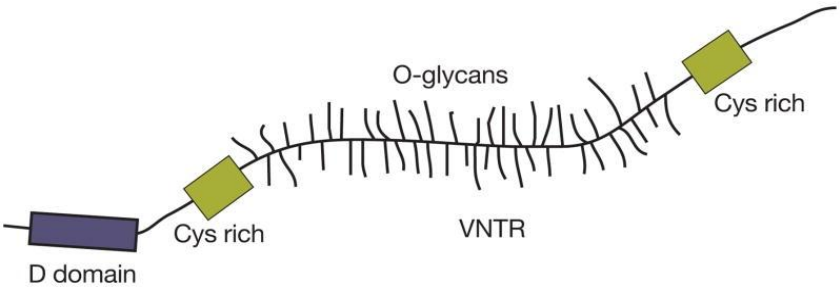

Figure 2.7: A structural model of a large secreted mucin (Brockhausen, Schachter & Stanley, 2009, p. 117).

The VNTR region and the central domain have numerous serine, threonine, and proline residues, which are highly O-glycosylated, giving the mucin a 'bottle brush' confirmation. Many O-GalNac glycans with different structures attaches to the VNTR domain. The cysteine (Cys) rich domains are involved in disulphide bonding to form large polymers. D domains are similar to von Willebrand factor and are also involved in polymerisation.

These mucin O-linked oligosaccharides (O-glycan) start with a α-linked N-acetylgalactosamine (GalNAc) residue that is linked to a hydroxyl group of Thr or Ser (Brockhausen et al., 2009; Varki & Sharon, 2009). The GalNAc can be extended with several sugars which include galactose, fucose, N-acetylglucosamine, or sialic acid, but not glucose, mannose, or xylose residues. These monosaccharides attach to the O-glycans, which attach to the VNTR region, allowing for a further classification of the mucins into neutral and acidic groups (Montagne, Piel, & Lallès, 2004). The latter group is at the same time further divided into non-sulfated (sialomucin) and sulfated (sulfomucin) mucins.

O-acetylation (adding of sialic acid) and O-sulfation (adding of galactose and N-acetylglucosamine) are important modifications that occur within the mucin O-glycans.

The Pro residues within the VNTR region appear to facilitate O-GalNAc glycosylation. Glycosylation is the enzymatic process by which glycans (monosaccharides or oligosaccharides) are attached to proteins (The Free Dictionary, 2004). The numerous O-GalNAc glycans attaching to the VNTR region gives the mucin glycoproteins a “bottle brush” appearance (Figure 2.7) (Brockhausen, Schachter, & Stanley, 2009). Despite the O-linked glycan chains, mucins also contain potential N-glycosylation sites with an amino acid sequence of asparagine-X-serine/threonine (X = any amino acid, except proline) (Pearson & Brownlee, 2005). Similar to the O-glycan chains, the N-linked glycan chains bind to the central domain (VNTR) via N-acetylgalactosamine, but the N-glycans contain mannose and other sugars similar to those on O-glycans on their chains.

Secreted gel-forming mucins contain cysteine rich domains outside the VNTR region (Pearson & Brownlee, 2005). The cysteine-rich domains are also known as D-domains which are homologous to the D-domains of von Willebrand factor (vWF), a blood clotting factor (Figure 2.7). Theses mucin subunits bind together end-to-end via these D-domains by disulphide bridges (Figure 2.8) to form large, hydrated and flexible polymers that form the components of a viscous solution (Montagne, Piel, & Lallès, 2004). Furthermore, mucins produce recognition molecules similar to the epithelial cell surface, thus preventing the bacteria from attaching to the true epithelial cell surface (Pearson & Brownlee, 2005). Consequently, one of the major functions of mucins is to misguide bacteria.

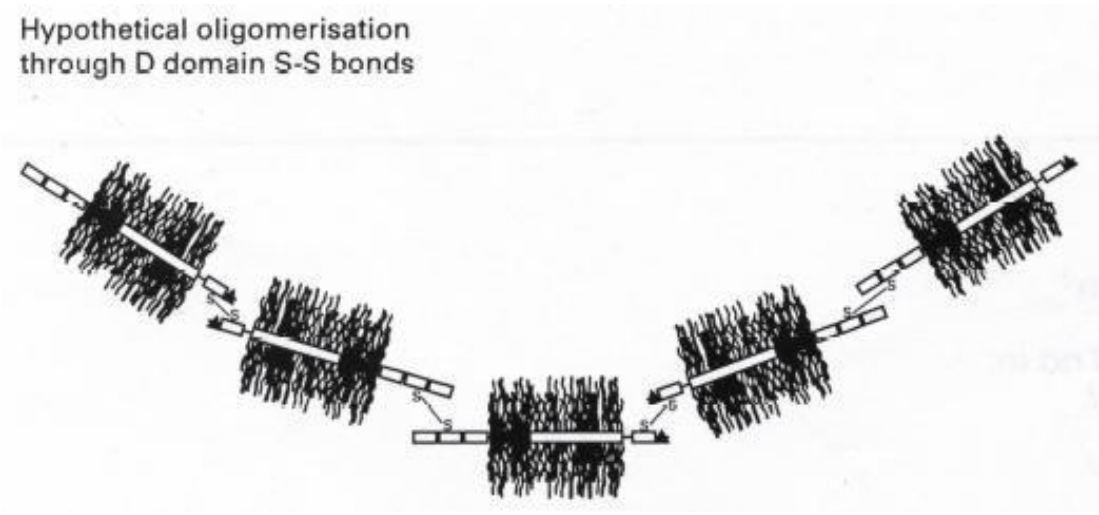

Figure 2.8: Cysteine rich domains (D-domains) bind together via disulphide bonds to form large polymers (Shirazi et al., 2000, p. 473).

Although all mucins have a VNTR region, the structure outside of the VNTR region differs greatly between the secreted gel-forming mucins and the membrane associated mucins (Pearson & Brownlee, 2005). Membrane-tethered mucins have a highly glycosylated extracellular domain (the VNTR region) (Figure 2.9) that carries O-GalNAc glycan chains (Brockhausen, Schachter, & Stanley, 2009), a transmembrane domain and also a short cytoplasmic tail, which might contain potential serine/tyrosine phosphorylation sites (Figure 2.9). Mucins that are membrane-bound (Figure 2.9) are involved in signal transduction, mediating cell-to-cell adhesion and have an anti-adhesive function.

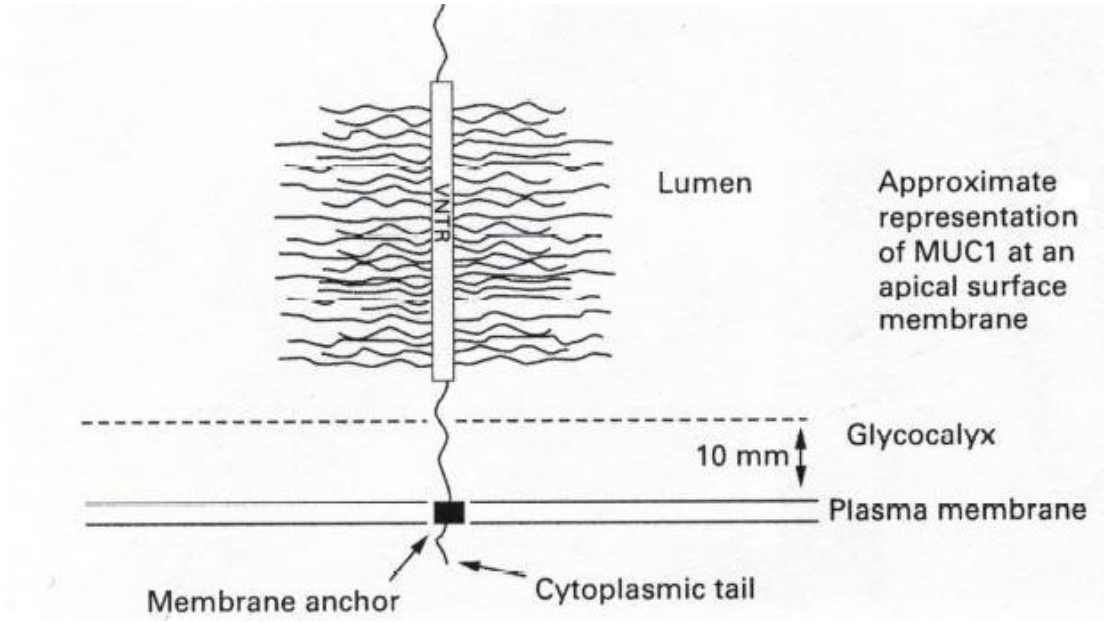

Figure 2.9: A representation of MUC1 at a surface membrane (Shirazi et al., 2000, p. 474).

The membrane associated mucin attaches to the plasma membrane via a membrane anchor. The protein backbone (VNTR region) with its attached oligosaccharide chains are in contact with the gastrointestinal lumen.

2.9.2 MUC Genes

Table 2.3 lists about 20 different human mucin genes (MUC genes) which have been identified in the different regions of the GIT (Pearson & Brownlee, 2005; Brockhausen Schachter, & Stanley, 2009). The different MUC genes are expressed in different areas of the body which suggests these genes have specific functions related to specific regions. The GIT shows the highest and most diverse expression of the MUC genes (Linden et al., 2008).

MUC7 is a secreted mucin, uninvolved in gel-forming, which binds bacteria in saliva. Consequently, the expression of both membrane-associated and gel-forming mucins forms two lines of pre-epithelial defence (Pearson & Brownlee, 2005). The secreted gel overlies

the membrane associated mucins, which forms part of the glycocalyx on the apical surface of the epithelial cells.

Table 2.3: The locations of the MUC gene products in the different regions of the body and their positions on the chromosomes (Dekker et al., 2002; Pearson et al., 2004; Pearson & Brownlee, 2005; Linden et al., 2008). ***Modified from Pearson & Brownlee, 2005 and Linden et al., 2008.***

Classification	MUC Gene	Location of Gene Product in the Body	Chromosome
Membrane	**MUC 1**	(All epithelia) Stomach, duodenum, small intestine, colon	1q21
Secreted	**MUC 2**	Small intestine, colon	11p15.5
Membrane	**MUC 3A**	Small intestine, colon	#
Membrane	**MUC 3B**	Small intestine, colon	7q22
Membrane	**MUC 4**	Stomach, small intestine, colon	3q29
Secreted	**MUC 5AC**	Stomach	11p15.5
Secreted	**MUC 6**	Stomach, duodenum	11p15.5
Secreted	**MUC 7**	Salivary glands	4q13-21
Membrane	**MUC 11**	Colon	7q22
Membrane	**MUC 12**	Stomach, small intestine, colon	7q22
Membrane	**MUC 13**	Stomach, and the rest of the GIT (goblet & columnar cells)	3q13.3
Membrane	**MUC 15**	Small intestine	11p14.3
Membrane	**MUC 17**	Membrane associated; stomach, duodenum, small intestine, colon	7q22
Secreted	**MUC 19**	Salivary glands	12
Membrane	**MUC 20**	Colon	#

#Chromosomal position still needs to be determined.

2.10 The Functions of Mucus and Mucins

2.10.1 Functions of Mucins

Mucins display the tendency to aggregate and form gels (Taylor et al., 2003). Therefore, the secreted gel-forming mucins of the respiratory, gastrointestinal, and genitourinary tracts, as well as the eyes, are protected by the ability of the O-GalNAc glycans of the mucus glycoproteins to lubricate and protect their epithelial surfaces (Brockhausen, Schachter, & Stanley, 2009).

These O-glycans are usually negatively charged and hydrophilic, which allows for the binding of water and salt (Brockhausen, Schachter, & Stanley, 2009). In addition, these characteristics contribute to the viscosity and adhesiveness of mucus, forming the physical barrier between the external environment and the epithelium. An important physiological process is the removal of particles and micro-organisms that are trapped in mucus via peristaltic movements.

The functions of all mucins depend mainly on their O-glycosylated state (Van Klinken et al., 1995), which are responsible for their filamentous conformation. The advantage of this extended filamentous and often negatively charged structure causes the mucin to act as a barrier that protects the cell. Secreted and cell surface mucins express many oligosaccharide structures that are found on the cell surface and can therefore probably function as decoys for adhesins that have been evolved by pathogens to attach to the cell surface (Linden et al., 2008). Some mucins can effectively clump viral agents together and exogenous mucins can inhibit viral infection. Viruses such as influenza, reo-, adeno-, and entero-virusses, bind to the sialic acid residues on mucins and can be removed from the GIT when the mucus layer is sloughed off.

Mucins have direct and indirect roles in defence from infections (Linden et al., 2008). The mucin oligosaccharides can bind microbes and, in some cases, they either have direct antimicrobial activity or carry other antimicrobial molecules. For example, a mucin oligosaccharide expressed by gastric mucins, directly interferes with the synthesis of *H. pylori* cell wall components (Kawakubo et al., 2004). Cell-surface membrane associated mucins initiate intracellular signalling in response to bacteria, which suggests that they have both a barrier and reporting function on the apical surface of all mucosal epithelial cells. It is hypothesized that one of the main functions of cell-surface mucins is to act as

releasable decoy ligands for microbes attempting to anchor themselves to the glycocalyx (Kawakubo et al., 2004).

2.10.2 Functions and Structure of Mucus

Mucus consists primarily of water (~95%), but also contain fatty acids, salts, cholesterol (Allen, 1981), phospholipids, defensive proteins such as immunoglobins, defensins, lysozyme trefoil factors and growth factors (Bansil & Turner, 2006). The main component of mucus, however, is the glycoprotein mucin, which are responsible for the viscous and gel-like properties.

The secreted mucous barrier in the GIT consists of two layers, which are most prominent in the stomach and colon (Figure 2.10) (Pearson & Brownlee, 2005). This was discovered when experiments done on rats demonstrated that the mucus barrier in the stomach and colon of the rat consisted of a bilayer (Strugala et al., 2003). During further experiments (Taylor et al., 2003), it became clear that the mucus bilayer has the following important properties: (1) the mucus gels can reform after disruption; and (2) the non-adherent or 'sloppy' mucus layer can more easily be removed than the firm, adherent mucus layer. Thus, the non-adherent mucus layer has a lower resistance to flow than the adherent mucus layer. Furthermore, the non-adherent mucus layer predominantly acts as a lubricant gel, whereas the adherent layer functions as the in vivo mucus barrier. This mucus bilayer is therefore valuable to the host, because micro-organisms trapped in the non-adherent mucus layer, can easily be removed (Pearson & Brownlee, 2005). Another key function of mucus is to maintain a high concentration of antimicrobial molecules in the surroundings close to the epithelium (McGuckin et al., 2009).

Micro-organisms can, to a certain extent, modulate the mucus layers (Pearson & Brownlee, 2005). Goblet cells in the GITs and airways are activated by bacterial signals (Hecht, 1999). In reaction to these bacterial signals, goblet cells produce mucus to enhance the removal of micro-organisms trapped in the mucus layer. Mucous and mucin secretion is stimulated by micro-organisms, several cytokines, chemokines, and lipopolysaccharides (see Table 2.2) (Enss et al., 1996).

The newly secreted mucus, released upon stimulation, can bind *Escherichia coli* and clear it from the intestines. The release of cytokines and chemokines is part of the inflammatory response which attracts other immune cells such as macrophages and natural killer cells to remove microbes (Pearson & Brownlee, 2005). Furthermore, mucins in the intestines

prevent bacterial adherence and inhibit viral replication (Mack et al., 2003). The probiotic *Lactobacillus*, however, is an exception to the rule. *Lactobacillus* can adhere to intestinal cells and stimulate mucin production, and it can also reduce the binding of pathogens to intestinal cells (Crawley et al., 1999; Mack et al., 2003). The mucosal barrier is not degraded by the *Lactobacillus* strains (Ruselervanembden et al., 1995).

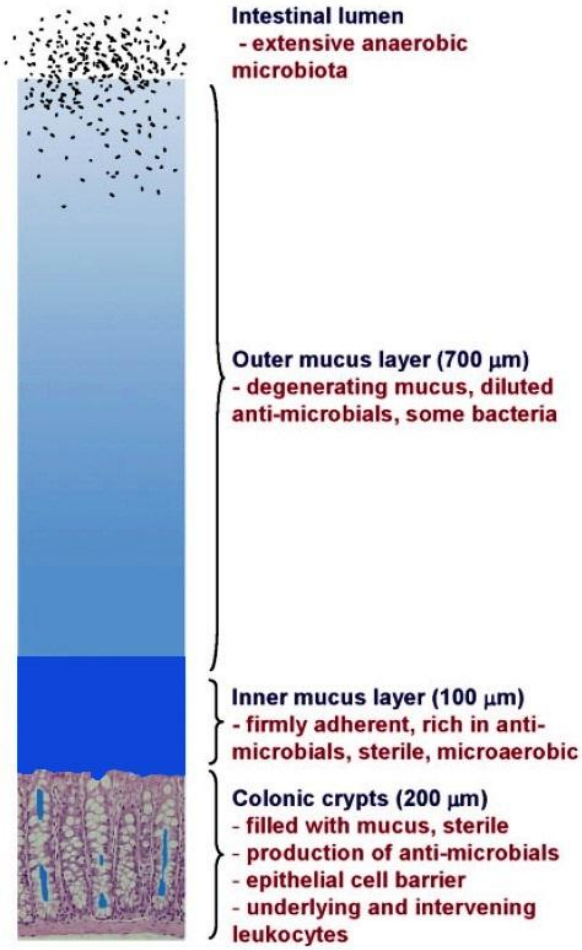

Figure 2.10: An illustration of the mucosal barrier in the mouse colon (McGuckin et al., 2009, p. 101).

The relative thicknesses of the secreted mucous barrier and the luminal micro-bacteria and the epithelium are illustrated.

The mucus layer and mucins have very important roles in terms of gut physiology and gut health (Montagne, Piel, & Lallès, 2004). Although the mucus layer and the mucins are equipped to successfully protect the GIT from pathogens and infections, it is not always possible. Alteration of the mucus barrier or of the mucins makes the host susceptible to infection and disease.

2.11 The Gastrointestinal Mucosal Surface and Disease

Interactions between a mammalian host and micro-organisms that are present in the environment usually occur at mucosal surfaces (Laux, Cohen, & Conway, 2005). Because of these interactions, mucosal surfaces have evolved a number of defensive and adaptive mechanisms to prevent bacterial colonisation. However, many bacterial species, namely the normal microflora, are very successful in colonising mucosal surfaces, while pathogen colonisation might only be long enough to cause disease. The mucosal surfaces are covered by a secreted mucous layer, which allows for colonisation of bacteria.

This surface mucus layer is exposed to physical, microbial and chemical challenges, which are intensified in the GIT by the presence of food and the symbiotic microflora (McGuckin et al., 2009). New evidence suggests that the cell surface or membrane associated mucins present in the glycocalyx of all the mucosal epithelial cells may be vital determinants of infection. It has been demonstrated in mice that when certain MUC genes are altered, these animals are more susceptible to infection by certain gastrointestinal pathogens (McAuley et al., 2007; McGuckin et al., 2007).

Gastrointestinal diseases such as Crohn's disease, ulcerative colitis and inflammatory bowel diseases are associated with defective MUC genes and an altered mucosal barrier. Distresses in the mucosal barrier associated with intestinal bowel diseases include an increased permeability, reduced mucosal and antimicrobial secretions, decreased number of secretory cells, disabled tight junctions in areas where ulceration occurs, and total loss of the epithelium (McGuckin et al., 2009). Work done by Pullen et al. (1994), has shown that there is also a difference in the thickness of the mucus layer between disease groups. The mucus layer is thicker than normal in Crohn's disease and thinner than normal in ulcerative colitis. The reduction of the mucus layer in ulcerative colitis is associated with the depletion of goblet cells which is associated with this disease, whereas in Crohn's disease there is retention of the goblet cells. In all other cases where there is acute inflammation of the colon, there is a decrease in the number of goblet cells (Rhodes, 1997).

There are still many unanswered questions concerning intestinal bowel diseases, especially in the mechanisms causing the diseases. Therefore, further research is needed to determine the interactions between the components of mucus and how it operates in barrier function in health and disease (Hattrup & Gendler, 2008). In addition, the

distribution and detailed description of mucins and other elements of the mucosal barrier and their interactions during health and disease is also of great importance.

Glycobiology has emerged as a leading field in biology over the last ten years. The detection of mucins in both the clinical and research environment is very important (McGuckin & Thornton, 2000). Mucins can be detected histologically and biochemically. Because mucins are such large molecules and the fact that the secreted mucins have the ability to form gels, biochemical detection of mucins had traditionally been quite difficult (McGuckin & Thornton, 2000). Therefore, it is important that the researcher must be familiar with the behaviour of mucin molecules in solution before attempting biochemical detection methods (Walsh & Jass, 2000).

2.12 Mucin Detection

2.12.1 Histological techniques used for the detection of mucins

Histochemical studies on the morphological aspects of mucins are very informative (Walsh & Jass, 2000). The latter studies are able to show the relationship between the structural characteristics of the mucins at the site of synthesis and secretion. Two principal matters need to be considered in order to increase the potential value of morphologically based methods: (i) nature and restrictions of the techniques, and (ii) interpretation and assessment of mucin staining.

i. The methods used to fix tissue influences the staining of mucin (Walsh & Jass, 2000). When using light microscopy, tissues are generally fixed in formalin, which fails to preserve the mucus layer that lines the epithelial surface of the GIT.
ii. For the interpretation and assessment of mucin stains, specific measures have to be in place in order to make correct conclusions. For example, know the restrictions of the staining methods used and make sure to use a fixed classification system to identify the different types of mucins.

2.12.1.1 Periodic acid Schiff (PAS) technique

Mucicarmine was the first specific stain used to identify mucin (Southgate, 1927), but this method has now been replaced by methods that are based on strict histochemical approaches (Walsh & Jass, 2000). Periodic acid-Schiff (PAS) is the essential mucin histochemical technique (Hotchkiss, 1948). Periodic acid (HIO_4) is an oxidizing agent used to detect mucosubstances (Pearce, 1968). Periodic acid breaks (oxidizes) the C-C bonds

in various structures, converting 1:2-glycol groups (CHOH-CHOH) into dialdehydes (CHO-CHO). Consequently, these oxidized dialdehyde groups cannot be further oxidized by Periodic acid and this allows for the binding of Schiff's reagent to the molecules and give it a red colour (Pearce, 1968). The O-C bond of the aldehyde groups oxidizes when it attaches to Schiff's reagent. The binding of Schiff's reagent to aldehyde groups produces a red/magenta colour, which is intensified by washing in running tap water.

The PAS positive mucins will stain a deep magenta colour and will represent neutral mucins. Acid mucins are demonstrated with cationic dyes, such as Alcian blue (AB). The AB attaches to the carboxyl group of sialic acid or to sugars with a sulfate substitution. AB is also used in combination with PAS. The combined stain of AB with PAS clearly separates the acid and neutral mucins from one another (Bancroft & Stevens, 1990).

2.12.1.2 Alcian blue technique

The AB-stain can be used on its own or in combination with other stains (PAS, Aldehyde Fuchsin, and High Iron Diamine) to detect acid mucin (Bancroft & Stevens, 1990). AB dye is positively charged and binds to the acid groups found on mucopolysaccharides and stains them blue (Pearce, 1968). At a pH of 2.5, AB reacts with the sulfated (sulfomucins) and carboxylated (sialomucins) mucopolysaccharides. However, at a pH of 1, it specifically reacts with sulfated mucopolysaccharides only.

2.12.1.3 Aldehyde Fuchsin technique

Aldehyde Fuchsin was firstly introduced as an elastic stain (Pearce, 1968). However, it was soon observed to stain a variety of acid mucosubstances, in addition with preference for sulfomucins. Spectrophotometric studies indicated that the active dye molecule in Aldehyde Fuchsin solution was pararosaniline (Pearce, 1968). These studies also confirmed that Aldehyde fuchsin is not a stable product. Staining was a result of the combination of carboxyl groups (COOH) with an intermediate meta-stable (highly energetic molecule) species formed in the Aldehyde Fuchsin dye. It was suggested that Aldehyde Fuchsin should be used in a combined staining procedure with AB, rather than on its own. Sulfated mucins and elastic tissues are strongly stained with Aldehyde Fuchsin, whereas lesser mucosubstances stain too weakly and only moderately.

2.12.1.4 High Iron Diamine technique

High Iron Diamine (HID) is specific for sulfomucins. HID combined with AB, is specific for both sulfo- and sialomucins (Bancroft & Stevens, 1990). Sections treated with the cationic solution of diamine salts (N, N-dimethyl-meta-phenylenediamine dihydrochloride; N, N-dimethyl-para-phenylenediamine dihydrochloride) and ferric chloride ($FeCl_3$), stain the acid (sulfated) mucopolysaccharides black (Pearce, 1968). The nature of the cationic (basic) dyes produced by oxidation of the diamine salts with ferric chloride is unknown.

It has been noted by Walsh and Jass (2000) that in the HID combined with AB technique, there is ionic competition between HID and AB. Therefore, if the latter technique gives a brown/black reaction it does not necessarily indicate the absence of sialic acid mucins, nor does a blue reaction indicate the absence of sulfate mucins. However, despite the requirement for care during the interpretation of results, and while using the carcinogenic diamine compounds, the HID/AB technique is the best method to stain acid mucins (Walsh & Jass, 2000).

2.12.1.5 Lectin Histochemistry

Lectins can be described as a diverse group of glycoproteins or proteins, which are mainly found in plant seeds, as well as in the fleshy parts of certain plants and invertebrates (Walsh & Jass, 2000). These lectins bind to sugars that consist of oligosaccharide chains of glycoproteins and glycolipids that are associated with cell membranes, and also bind to secretory glycoproteins (mucins). Lectins have been broadly used in the study of specific glycolipids and glycoproteins.

According to Scillitani et al. (2007), lectin-binding studies are valuable for disease diagnostics and for comparative purposes, because the lectins can detect variations between normal and pathologic conditions of the given tissues. In addition, it can detect variations between different regions in the same organ, and also between homologous regions in specimens of different sex, age or species. Lectin-binding studies have been successfully performed in the GITs of several mammals (Scillitani, Zizza, Liquori, & Ferri, 2007).

CHAPTER 3

MATERIALS & METHODS

MATERIALS

3.1 Tissue samples of the three insectivorous species

All specimens used in this study were obtained from Prof. Nigel Bennett at the University of Pretoria (UP), who used these animals for other aspects of study. Prof. Bennett donated the specimens to the Anatomy Department, specifically Biomedical Sciences, at the University of Stellenbosch for further research. Partially dissected carcasses and intact GITs of *Amblysomus hottentotus* (n = 4) and *Crocidura cyanea* (n = 5), as well as only intact GITs of *Acomys spinosissimus* (n = 5) were made available. The first batch of GITs of *A. hottentotus* could not be used in this study, because too much autolysis has occurred. Therefore, only four GITs of *A. hottentotus* were available to study, as it was difficult to locate and catch these animals. All specimens were fixed in 4% paraformaldehyde upon receipt. Ethical clearance for the studies of Prof. Bennett was obtained from the UP as well as Nature Conservation clearance for the study on wild animals. Ethical clearance for the present study was granted by the University of Stellenbosch (US). The details of all the ethical clearance numbers are listed in table 3.1.

Table 3.1: List of species used in the present study, including their common names, sample size, origin of preserved material and ethical clearance information.

SCIENTIFIC AND COMMON NAMES OF THE SPECIES	NUMBER OF ANIMALS	ORIGIN	UP ETHICAL CLEARANCE NUMBER	NATURE CONSERVATION PERMIT NUMBER	US ETHICAL CLEARANCE NUMBER
Acomys spinosissimus (Southern African Spiny Mouse)	5	UP	EC028-07	CPM-333-00002 Limpopo Nature Conservation	P09/03/013
Crocidura cyanea (Reddish-grey Musk Shrew)	5	UP	EC015-08	CPM001953 Limpopo Nature Conservation	P09/03/013
Amblysomus hottentotus (Hottentot Golden Mole)	4	UP	EC05-0222-006	1731/2005 Ezemvelo Nature Conservation KwaZulu Natal WRO 23/05WR private land Eastern Cape Province	P09/03/013

UP: Department of Zoology and Entomology, University of Pretoria

US: University of Stellenbosch

3.2 Reagents

- **Alcian Blue** (8GX, Colour Index (C. I.) 74240, Product 34089, Gurr Microscopy Materials, BDH Chemicals Ltd., Poole, England)
- **Charcoal Activated Powder** (SAARCHEM, UniTEK 159110, Muldersdrift, RSA)
- **DPX Mountant** (SAAR1935000KF, UN1307, uniLAB®, Merck (Pty.) Ltd.)
- **Eosin Yellowish** (SAAR2186000DC, Merck Chemicals (Pty.) Ltd., Gauteng, RSA)
- **Ferric Chloride Hexahydrate** (SAAR2340530EM, UN2582, Merck Chemicals (Pty.) Ltd., Gauteng, RSA)
- **Haematoxylin (Mayer's solution)** (SAAR2822001LC; Merck Chemicals (Pty.) Ltd., Gauteng, RSA)
- **Hydrochloric Acid 37% (HCℓ)** (SAAR3063054LCA, UN1789, univAR®, Merck Chemicals (Pty.) Ltd., Gauteng, RSA)
- **Neutral Red** (Vital & Fluorchrome, 15622, Gurr Ltd. London, England)
- **N, N-dimethyl-meta-phenylenediamine dihydrochloride** (21922-5G, 13614 TE, Sigma-Aldrich, Switzerland)
- **N, N-dimethyl-para-phenylenediamine dihydrochloride** (GA 21629, D4139 10g, Sigma-Aldrich, Switzerland)
- **Paraldehyde** (Art. 818255, Merck-Schuehardt, München)
- **Pararosaniline (Chlorid)** (C. I. 42500, Merck Chemicals, Darmstadt, Germany)
- **Periodic Acid** (SAARCHEM 4946180, UNIVAR, Muldersdrift, RSA)
- **Poly-L-Lysine Solution** (Catalog (Cat.) Number. P8920-100mℓ, Sigma Aldrich, Steinheim, Germany)
- **Potassium Meta-bisulphite**

3.3 Equipment

- **Oven** (Model: M53C, Serial Number 9513249)
- **Automated Stainer** (Leica Auto Stainer XL; Manufacturer & Model: Leica St 5010; Serial Number 1732/07.2007)
- **Digital Camera (**Sony, Model Number DSC-H7, Zeiss, 15X Optical Zoom, 8.1 Mega Pixels)
- **Embedding Table** (Leica EG1160, Cat. No. 038630528)
- **Incubator** (Model IH-150; Gallenkamp)

- **Magnetic Stirrer and Hotplate** (IKAMAG® RH: Janke & Kunkel GMBH & Co. IKA-WERK, Staufen)
- **Microscope** (Zeis Axioskop2, Ser. no. 801452)
- **Microtome** (Leica RM2125RT, SMM Instruments, Cat. No. 045737987)
- **Stereomicroscope** (Leica MZ6)
- **Tissue Processor** (Duplex processer, Shandon Elliott; Supplied by OptoLaboratory (Pty.) Ltd. Cape Town, Serial Nr. 3550)
- **Water bath** (Electrothermal, Cat. No. MH 8501)

3.4 Software packages

- **Axio Vision (AxioVs40),** Version 4.7.2.0 (Carl Zeiss Microscopy)
- **Hugin,** Version 2011.0.0.0fd3e119979c (SourceForge Inc.)
- **Leica Application Suite (LAS),** Version 3.3.0 (Leica Microsystems)
- **Microsoft Excel,** Version 7 (Microsoft Corporation)
- **NIS-Elements Basic Research,** Version 3.1 (Nikon Instruments Inc.)
- **Statistica,** Version 7 (StatSoft Southern Africa – Research (Pty.) Ltd.)

METHODOLOGY

3.5 Dissection of the carcasses of *C. cyanea* and *A. hottentotus*

All specimens received from the Zoology Department at the University of Pretoria were fixed. The carcasses had a midline abdominal incision and the heads were removed, but the GITs of *C. cyanea* were still *in situ*. Unfortunately, the GITs of *A. hottentotus* were situated outside the abdominal cavity and could not be used for topography. The anterior abdominal wall of *C. cyanea* was removed through dissection to reveal the abdominal intestinal topography, which was noted and photographed. The GITs of *C. cyanea* were not dissected from the carcasses, because there were already enough GITs available for this study. The GITs of *A. hottentotus* were removed from the carcasses by dissecting the oesophagus cranial to the gastro-oesophageal junction and by severing its attachments to the dorsal abdominal wall. The descending colon was dissected just before entering the pelvic cavity. The GITs were then preserved in 4% paraformaldehyde.

The GITs of *A. spinosissimus* had previously been removed and fixed in 4% paraformaldehyde. Therefore, the abdominal intestinal topography of the latter species is also not included in the present study.

3.6 Descriptive anatomy and measurements of the gastrointestinal tract

Before measuring the GITs of the various species, the weight of each GIT was recorded with the mesentery still attached. The respective GITs were photographed before and after the removal of the mesentery, and interspecies variations were documented. Throughout the measuring process the tissue was handled with care and as little as possible to prevent damage and desiccation.

All measurements were repeated for each specimen. The GIT lengths of all species were measured using a pliable, non-stretchable cord. Length measurements were performed on the anti-mesenteric border of the GIT, where after the various gastrointestinal regions were identified (stomach, small intestine, caecum, and colon). The different parts of the GIT were measured as well to determine their lengths relative to the total GIT length.

Furthermore, circumference measurements were also performed on the various sections of the GIT (Figure 3.1 diagrams A and B). Circumference measurements for *A. spinosissimus* were recorded at two locations for both the stomach and caecum, and three

measurements for the small- and large intestines (Figure 3.1 diagram A). For *C. cyanea* and *A. hottentotus* two circumference measurements were performed at the stomach and, because these animals lack caeca, four circumference measurements were recorded for the rest of the intestinal tract (Figure 3.1 diagram B). Measurements for the latter species were recorded at the duodenum, middle of the intestine, distal small intestine (1 cm above the GIT ending), and the colon (ending of the GIT). Extra information regarding the GIT length, circumference measurements, the body weight, GIT weight and sex of the animals are included in appendices 1-3.

In addition, the GITs were opened with scissors along the anti-mesenteric border and the contents were gently rinsed out. The cut GITs were pinned open and photographed with a digital camera (Sony DSC-H7) and a stereomicroscope (Leica MZ6) with a fixed camera. After the completion of all photography and measurements, the tissue was harvested for further processing and analysis.

3.7 Gastrointestinal tissue harvested for histology

For *A. spinosissimus*, tissue segments were harvested from the corpus (body) of the stomach, duodenum, middle of the small intestine, distal part of the ileum, caecum and the proximal colon (Figure 3.1 diagram C). *C. cyanea* and *A. hottentotus* have a simple GIT, therefore tissue segments were harvested from the duodenum, middle of the intestine, and the caudal part of the intestine which represents the colon. Tissue was removed from the distal small intestine (1 cm proximal to the GIT ending) and the colon (distal end of the GIT). The harvested tissue segments were fixed in 4% paraformaldehyde before processing.

3.8 Fixation and tissue processing

Fixation is a series of chemical events which is used to preserve tissue as close as possible to its living state (Bancroft & Stevens, 1990). Before tissue is processed and embedded in paraffin wax, the tissue must be completely fixed, dehydrated and cleared. The term ‘tissue processing’ refers to the treatment of tissue whereby it is necessary to impregnate it with a solid medium, namely paraffin wax, facilitating the production of microscopy sections.

The harvested tissue segments were placed into a fresh fixative (4% paraformaldehyde) for 12 to 24 hours prior to processing. Some tissue segments were fixed with contents, as mucosal damage occurred during the handling of the tissue. In some instances it was

possible to remove the contents through gentle rinsing with sterilized water. All tissue samples were processed in the Shandon Elliot Duplex Processor (Optolabor (Pty.)) through a series of increasing the concentrations of ethanol (see Appendix 4), followed by clearing in xylene and impregnation in paraffin wax.

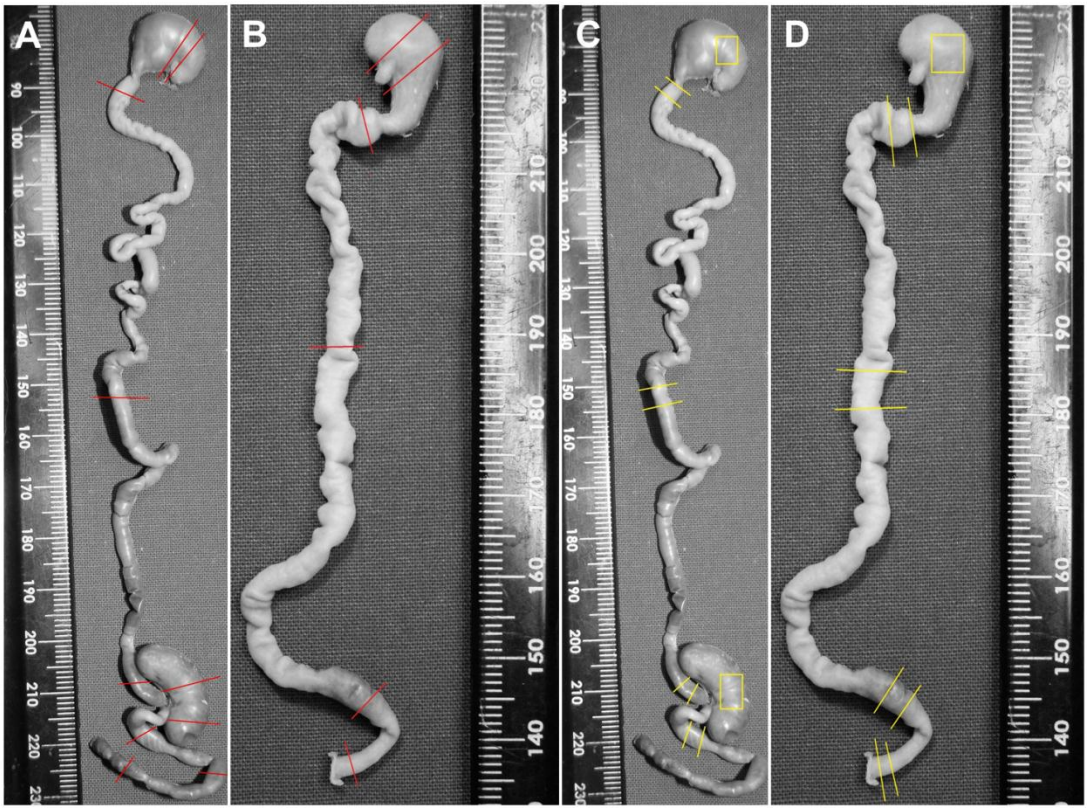

Figure 3.1: Site of measurements and tissue harvesting from the GIT of *A. spinosissimus* and *C. cyanea*.

The locations of circumference measurements are indicated by the red lines in diagrams A and B, and the locations of where tissue were harvested for histology and mucin histochemical staining are shown in yellow in diagrams C and D. (A & B) *A. spinosissimus*; (B & D) *C. cyanea*. Sites for *A. hottentotus* were identical to that shown for *C. cyanea*.

3.9 Embedding

After processing, the tissues samples were embedded into paraffin wax. Before the embedding of the tissue samples, the paraffin wax, metal moulds, and forceps were pre-heated to 60°C in a Leica EG 1160 Embedder (SMM Instruments).

A small amount of molten wax was inserted into the prewarmed mould, followed by the insertion of the tissue into the wax. The heated forceps were used to gently orientate the tissue so that the intended cutting edge faced the base of the mould. When the tissue was aligned, the mould was filled with molten wax and fitted with a plastic cassette. The moulds were placed on a frosted surface, allowing the wax to set. After ± 30 minutes, the wax

block was separated from the metal mould while attached to the plastic cassette. Thus, for each region of interest of the GIT, there was one block of embedded tissue.

During the embedding process certain safety measures were followed: (1) in order to ensure that a fine microcrystalline structure of wax is obtained, no clearing agent was present in the wax, and (2) immediately after tissue embedding, the wax was cooled rapidly to reduce the wax crystal size.

3.10 Sectioning

After the removal of the wax blocks from the moulds, the blocks were further cooled in a freezer for one to two hours before sectioning. Firstly, using a Leica RM 2125 RT microtome (SMM Instruments), all blocks were trimmed to the level of the tissue, followed by the serial sectioning of the blocks. Secondly, the tissue sections were placed in a water bath to stretch out, there after the sections were picked up with a glass microscope slide and placed into an oven. The oven heated the slides up and melted the paraffin surrounding the tissue, which allowed the section to dry before it was stained.

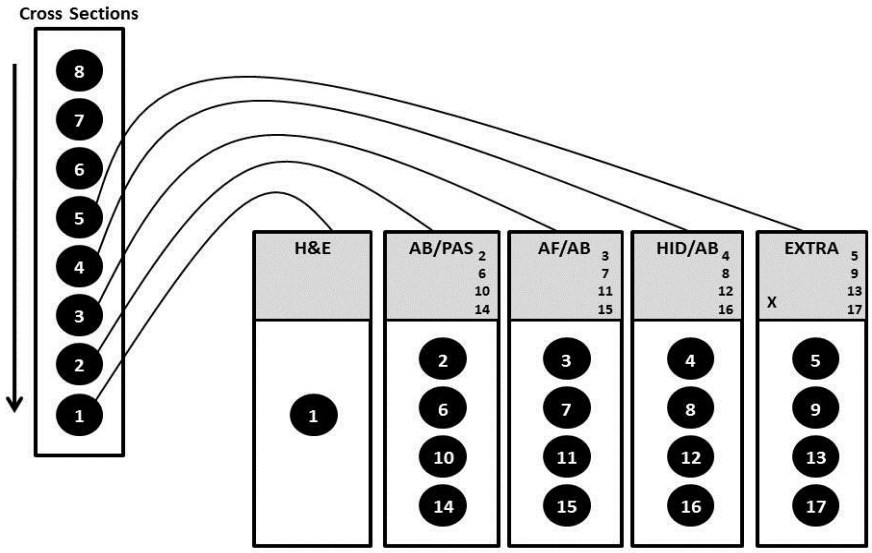

Figure 3.2: Organisation of wax sections: The sequence of the slides and the grouping of the tissue sections.

The strip on the left-hand side represents a string of cut tissue sections (black dots), and the arrow next to it indicates the direction of the tissue movement, while the block is being cut. The number 1 tissue section goes onto the H&E, the number 2 goes onto the AB/PAS slide, the number 3 goes onto the AF/AB slide and so forth.

The tissue blocks were sectioned at a thickness of 4 µm, for slides stained by Haematoxylin and Eosin (H&E), the combined Alcian blue-Periodic Acid Schiff (AB/PAS)

and the combined Aldehyde Fuchsin-Alcian blue (AF/AB) techniques. The tissue stained by the combined High Iron Diamine-Alcian blue (HID/AB) technique was sectioned at 8 µm.

For each block of tissue there were five slides (Figure 3.2). The first slide was used to do an H&E stain, containing only one section of tissue to determine whether the tissue was suitable for histology. A further three slides were used for each of the special stains and an extra slide for a spare if needed. Each of the former slides contained four non-adjacent tissue sections, each 16 µm apart. The sequence of the slides indicated is shown in Figure 3.2.

3.11 Staining

After the sectioning of the tissue, slides were stained with H&E, as well as with special histochemistry methods for the detection of mucin secreting goblet cells.

3.11.1 Haematoxylin and eosin (H&E) stain

H&E is the most common histological stain used (Bancroft and Gamble 2008). The stain gained popularity due to its comparative simplicity and the ability to clearly distinguish between many different tissue structures when used. The haematoxylin component stains the cell nuclei blue-black, whereas the eosin stains the cytoplasm and connective tissue fibres different shades and intensities of pink, red and orange.

In the present study, the H&E stain was mainly used to determine the condition of the tissue, because autolysis was detected in some of the first tissue samples. An automated staining instrument, Leica Auto Stainer XL, was used to perform the H&E staining (Appendix 5).

3.12 Histochemistry: Detection of mucins

3.12.1 Combined Alcian Blue-Periodic Acid Schiff (PAS) technique (Mowry, 1956)

The combined stain of AB with PAS clearly separates the acid and neutral mucins from one another (see Appendix 6) (Bancroft and Stevens 1990). To begin with, the tissue sections were stained with AB to detect all the acid mucins and mainly to prevent the acid mucins, which are also PAS positive, to react with the subsequent PAS. This left only the neutral mucins to react with the PAS solution. Consequently, a clear colour distinction was

made between the neutral and acid mucins. Neutral mucins appeared magenta, the acid mucins appeared blue and the mixed (neutral and acid) mucins appeared blue/purple.

3.12.2 Combined Aldehyde Fuchsin/Alcian Blue technique (Spicer and Meyer, 1960)

This staining technique is used to distinguish between sulfated and sialomucins (Appendix 7) (Bancroft and Stevens 1990). Sections were firstly stained in Aldehyde Fuchsin which has a greater affinity for sulfated mucins, followed secondly by staining in AB which stained the sialomucins. Sulfated mucins were stained purple and sialomucins stained blue. Other variations in colours were categorized accordingly: the strong acidic sulfomucins stained deep purple and weak acidic sulfomucins light purple (Bancroft & Gamble, 2008). A mixture of the sulfo- and sialomucins stained a blue/purple or blue/pink colour.

Although both the Aldehyde Fuchsin and HID staining techniques distinguish between sulfo- and sialomucins, the Aldehyde Fuchsin technique is more specific for sulfated mucins. The HID stain can identify sulfomucins, but the Aldehyde Fuchsin can distinguish between strong (deep purple) and weak (light purple) sulfomucins (Bancroft & Gamble, 2008).

3.12.3 Combined High Iron Diamine (HID)/Alcian Blue technique (Spicer, 1965)

The HID staining method is also specific for sulfated and sialomucins (Appendix 8) (Bancroft and Stevens 1990). The preparation of the HID solution requires the mixture of diamine salts which is oxidised by ferric chloride to form a black cationic chromogen, which in turn will bond with sulfate ester groups. The tissue sections were firstly stained with the HID solution, followed secondly by the AB counterstain – which will only stain the sialomucins. Finally, a clear colour distinction can be made between the two main groups of acidic mucins. Sulfated mucins stain black/brown and sialomucins stain blue. A mixture of the two acid mucins will stain a blue/green or black/blue colour.

3.13 Quantification of goblet cells and image analysis

The different staining methods were used to identify the different types of mucin secreting goblet cells in the GIT. In order to determine the relative proportions and distribution of the different types of mucin secreting goblet cells (neutral, acid, sulfo- & sialomucins), the goblet cells in each region of the GIT were quantified.

On each of the slides two tissue sections were examined; usually the first and third sections on the slide, which was approximately 24 µm apart. However, if some of the tissue sections washed off during the staining process, either two of the remaining sections on the slide were used. This meant that the sections analysed for each special stain were between 16-32 µm apart.

Each stained slide was examined using a Zeiss Axioxskop2 light microscope with a digital camera. Of the two sections of tissue per slide selected for examination, photographs were taken of the entire tissue section using the 2.5X magnification objective lens (Figure 3.3). Multiple photographs were used to create composite images and were taken in such a manner so that each photograph overlapped the previous photograph by approximately 10%-30% so that the software could align the images before merging them. Stitching software, Hugin (Version 2011.0.0.0fd3e119979c), was used to merge images. With the use of imaging software, NIS Elements Basic Research (BR) (Version 3.10), images were calibrated and the length of the tissue section was measured (Figure 3.3).

Furthermore, each selected tissue section was also examined and photographed at 200X magnification (eyepieces 10X magnification, objective 20X magnification). Starting at one region of the tissue section, a field of view was photographed and the adjacent field of view was skipped, followed by another field of view which was photographed (Figure 3.4). This was done for the entire length of the tissue section, which produced numerous photographed areas of the section. In most cases, it was necessary to take more than one photo per field of view, which was also stitched together using Hugin. These stitched images were then the final product which was used to count the goblet cells and measure the crypt and surface epithelial areas.

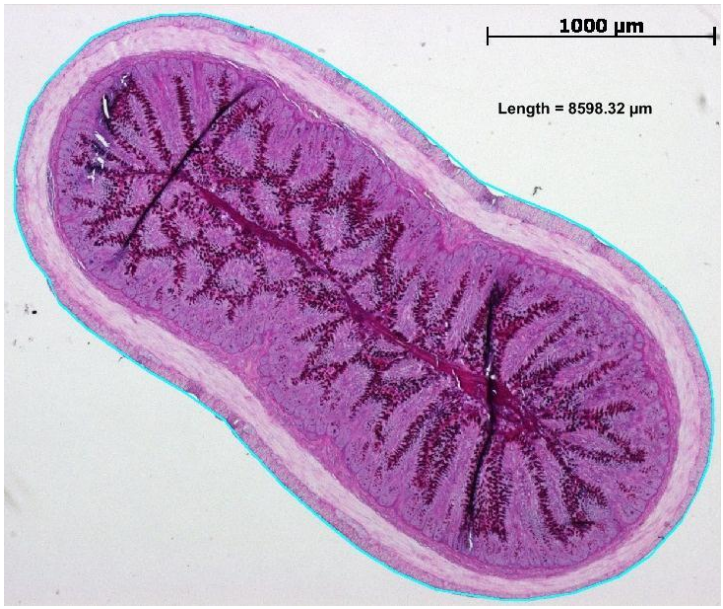

Figure 3.3: Method for the circumference length measurement of the tissue sections.

This is a distal small intestinal cross section, stained with AB/PAS. The entire tissue section is photographed and the circumference length of the tissue is measured. The total circumference length (blue line) measurement in this image is a total of 8598.32 µm.

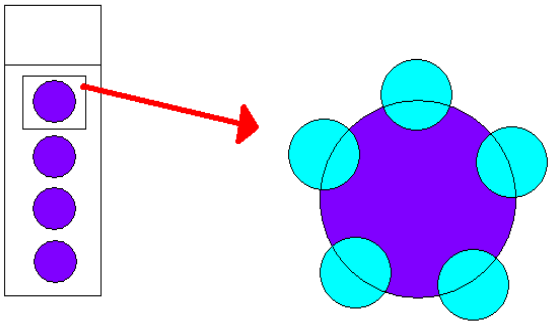

Figure 3.4: Method of photographing selected areas for goblet cell quantification.

This image illustrates how the different regions on a single section of tissue is selected and photographed. Each purple circle on the left represents a tissue section. On the enlarged purple section, the blue areas indicate the selected areas for quantification which are photographed, and the areas in-between are the skipped fields of view.

The NIS Elements BR program was used to measure the length of the tissue, as well as to measure the surface epithelial and crypt areas (Figure 3.5) on each photograph. The total length of the entire tissue section (Figure 3.3), and the length measurements of the tissue on each photograph (which represents a field of view) (Figure 3.4), were measured to quantify at least 50% of each tissue section. This would ensure adequate coverage of the distribution of the different types of mucin secreting goblet cells. The epithelium lining the surface and that lining the crypts of Lieberkühn/intestinal glands was demarcated as shown by the yellow and red lines respectively (see Figure 3.5), and the area within each of these boundaries was calculated. Within each demarcated area, the number of goblet

cells containing the specific mucins was counted and their numbers expressed per unit area of epithelium in either the surface or crypt zones (i.e. 2000 of goblet cells containing neutral mucins per mm^2 of surface epithelium).

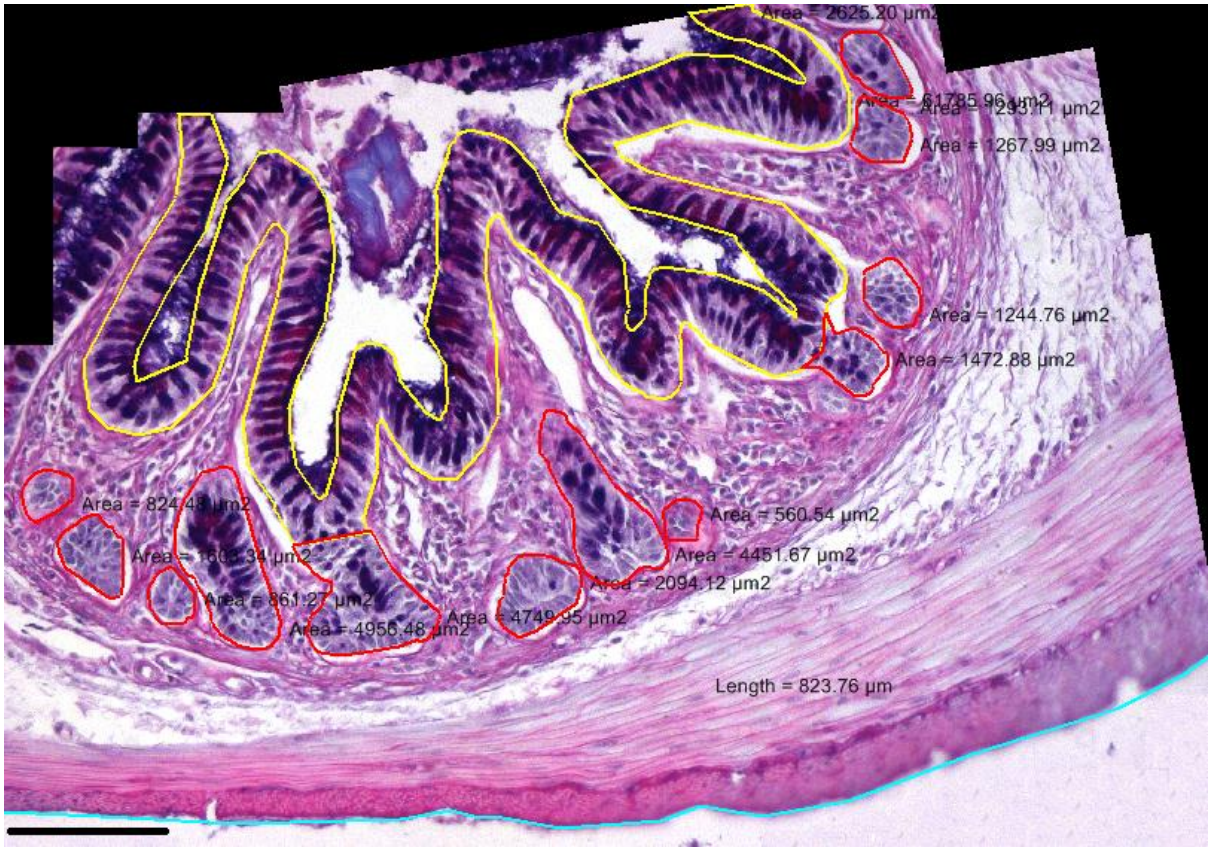

Figure 3.5: The measurements of the surface epithelial and crypt areas.

This is a composite image of the colon in *C. cyanea* stained with the AB/PAS technique. The yellow line indicates the surface epithelium measurement and the red lines represent the measurements of the crypt areas. The blue line shows the length measurement of the tissue. Bar = 100 µm.

The different types of mucin secreting goblet cells were also counted using NIS Elements BR software (Figure 3.6). Because the shades of colours of mixed and partitioned mucins were close, counting and identification of the different types of mucin secreting goblet cells was not always an easy task.

Figure 3.6: The quantification of the goblet cells in the measured surface epithelial and crypt areas.

This composite image is the same as the image used in Figure 3.5 (AB/PAS stained colon of *C. cyanea*). The image illustrates how the goblet cells are counted with the aid of crosses. The white crosses show the mixed mucin secreting goblet cells (composition of neutral and acid mucin granules in a single goblet cell). Whereas the pink crosses indicate the neutral mucin secreting goblet cells. Each cross represents one goblet cell. Bar = 100 µm.

For each stain there were fixed colours and categories into which the mucins were classified (Table 3.2). The classification system in table 3.2 was used to identify and count the different mucin secreting goblet cells, along with the help of a colour wheel and control sections of each stain (Figure 3.7). All data, the measured and counted areas, were exported by the NIS Elements BR program into Microsoft Excel sheets and used for statistical analysis.

Table 3.2: The classification of mucin types based on colour differentiation for each special stain.

MUCIN CLASSIFICATION	AB/PAS	AF/AB	HID/AB
Acid	Blue	-	-
Neutral	Magenta	-	-
Mixed	Blue/Purple	Blue/Pink	Blue/Brown
Sialylated	-	Blue	Blue
Sulfated	-	Strongly sulfated = Deep purple Weakly sulfated = Purple	Black/Brown

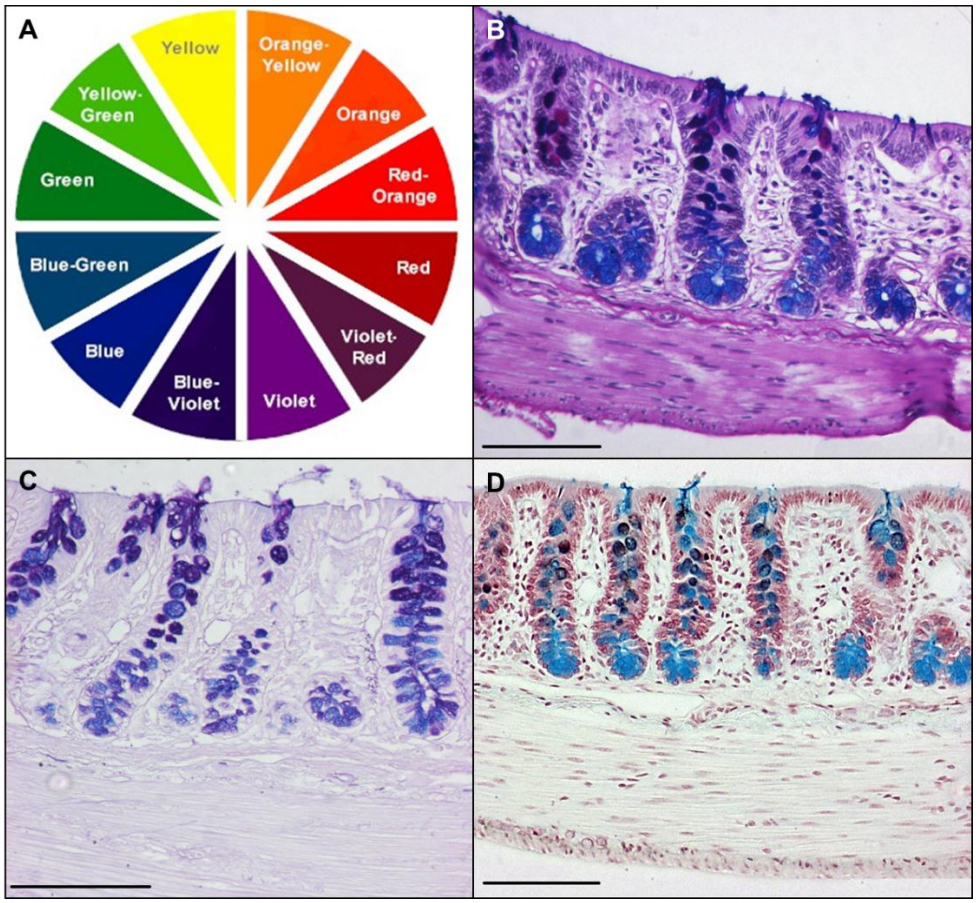

Figure 3.7: The colour wheel and control sections (for each special stain) used to identify the different mucin secreting goblet cells.

(A) Colour wheel used to identify the difference between closely related colours. Images B to D are rat colon control images each representing a specific stain. Bar = 100 µm.

(B) AB/PAS

(C) AF/AB

(D) HID/ AB

3.14 Statistical Data Analysis

A biostatistician was consulted to determine which methods should be used to statistically analyze the data of this study. Microsoft Excel and Statistica (version 10) software were used for statistical analysis. All the accumulated data were organised in Microsoft Excel for both the macroscopic and microscopic measurements, while Statistica was used for all the relevant statistical analysis.

The surface epithelial and crypt areas measured in the photographs (section 3.13) were initially measured in square micrometers (μm^2), which was converted to square millimeters (mm^2) to simplify the necessary data processing (1 μm^2 = 1 x 10^{-6} mm^2). The number of mucin secreting goblet cells was expressed as the number of cells per area measured (mm^2). For each region of the GIT the surface epithelial and crypt areas were measured (Figure 3.5) and the goblet cells were counted in those regions (Figure 3.6), as described in section 3.13. The data were arranged according to each GIT region and expressed as the total number of cells per total area measured (epithelial plus crypt area in mm^2), whereas the different types of mucin secreting goblet cells were expressed as the number of cells per epithelial or crypt area (mm^2).

To begin with, the macroscopic and microscopic results were analyzed with a normal probability test. Normal probability was done to assess whether or not the data were normally distributed (Keller, 2005). The data were plotted against a theoretical normal distribution and was estimated to form an approximate straight line. If some of the data deviates from the straight line, it means that those values differed from the norm and were classified as outshoot values or outliers. Outshoot values can sometimes be mistaken as an error in the data. Thereafter, descriptive statistics (mean, standard deviation and standard error) was done for all of the data, which was used to produce the graphs. Each of the descriptive statistics is defined as follows:

- Mean: The mean is also referred to as the arithmetic mean or the average. It is used to describe the center of a data set (Keller, 2005). The mean is calculated by using the sum of the observations and dividing it by the number of observations.
- Standard Deviation: The standard deviation is a measure of variability (Keller, 2005). It gives an indication of how much variation there is from the mean/average. For example, if the standard deviation value is low, it indicates that the data points are close to the mean. However, if the standard deviation value is high, the data points are far from the mean.

- Standard Error: The standard error is the standard deviation of the sampling distribution (Keller, 2005). It is used to determine the quality of the mean. The standard error can also be referred to as the standard deviation of the mean.

The macroscopic data were mainly analyzed by the F-test, Mann Whitney U and Kruskal-Wallis tests, which were used to calculate the p-values. The F- and Mann Whitney U tests were used to compare the macroscopic data of *C. cyanea* and *A. hottentotus*. Whereas the F- and Kruskal Wallis tests were used to compare the macroscopic measurements of all three insectivorous species (*A. spinosissimus*, *A. hottentotus*, and *C. cyanea*) with one another.

The analysis of variance (ANOVA) is built around a hypothesis test that is called the F-test (Keller, 2005). The F-test is designed to test if two population variances are equal by the comparison of the ratio of two variances. The Mann-Whitney test is a non-parametric test which is used to compare two independent groups of sampled data (Statsoft, 2011). In addition, the Kruskal-Wallis test is an extension of the Mann-Whitney U test which was used to compare three independent groups of sampled data. However, the p-value determined by the F-test is the only p-value that will be considered, because for the present study it has been found to be more suitable than the p-value of the Mann-Whitney U and Kruskal-Wallis tests. The F-test is more sensitive to non-normality than the Mann-Whitney U and Kruskal Wallis tests. The p-value can be defined as follows:

- The p-value is a number between zero and one which attempts to provide a measure of strength of the results of a test (Keller, 2005). If the p-value is less than 0.01 the test is highly significant. A p-value between 0.01 and 0.05 illustrates significance, but if the p-value exceeds 0.05 the result is not statistically significant.

The Levene's test was done to determine whether samples had equal variance (Levene, 1960). When the variances across samples are equal, it is called homogeneity of variance. ANOVA, for example, assumes that variances are equal across samples, and the Levene's test is used to verify this assumption. If the Levene's test is statistically significant, then the hypothesis of homogeneous variances should be rejected (Statsoft, 2011).

Furthermore, the F-test was also used to calculate p-values for the number of mucin secreting goblet cells per specific gastrointestinal region. Mean goblet cell counts and log transformed values were used to generate graphs for the entire GIT. These mean or log

transformed values indicated the differences in the number of cells per area for each gastrointestinal region, and also the differences between the three insectivorous species. If the mean value goblet cell counts did not show a satisfactory normal distribution of the data, the log transformed values were used as an alternative to represent the goblet cell counts. The log transformed values are not so sensitive to outshoot values, therefore better probability plots are observed when the data are transformed to log.

In the following section, the macroscopic, microscopic and quantification results were specified. Where possible, the macroscopic and microscopic data of all three insectivorous species were compared with one another. However, the number of mucin secreting goblet cells per gastrointestinal region and/or tract was statistically only compared between two species, namely *C. cyanea* and *A. hottentotus*. The latter species do not have caeca and therefore not easily distinguishable gastrointestinal regions opposed to *A. spinosissimus* with a caecum and clearly distinguishable gastrointestinal regions. Therefore, it was too difficult to compare the goblet cell quantification results of all three species statistically. The quantification results of *A. spinosissimus* would nevertheless be compared to *C. cyanea* and *A. hottentotus* through referral.

CHAPTER 4

RESULTS

4.1 Results

In the present study, the morphology and mucin histochemistry of the GITs of the three insectivorous species were examined. *Acomys spinosissimus* is the only species that has a caecum; therefore it will not be compared to *Amblysomus hottentotus* and *Crocidura cyanea* on all aspects of the different regions of the GIT, seeing as the latter two species lack a caecum. Consequently, the comparison of the morphology and mucin histochemistry of the GIT of all three species will be done where possible, otherwise only the two species without a caecum will be compared with one another. The mean gastrointestinal weight and body weight (BW), including the standard deviations (Std. Dev.) of the animals used for this study, is listed in table 4.1.

Table 4.1: List of the species used in the present study, including the origin of the preserved material, sample size, and mean gastrointestinal and body weights (± Std. Dev.)

Species	Origin	*n*	Mean GIT Weight (g)	Mean BW (g)
Acomys spinosissimus	UP	5	4.37 (±0.7)	21.11 (±6)
Crocidura cyanea	UP	5	1.73 (±0.4)	14.94 (±4)
Amblysomus hottentotus	UP	4	4.89 (±1.4)	60.5 (±10)

UP: Department of Zoology and Entomology, University of Pretoria.

The mean BWs ranged from 14.94-60.5 grams (Table 4.1). In some instances, there were large interspecies variations in the BW due to the fact that all animals were caught in the wild.

4.2 Topography of *Crocidura cyanea*

Only two fixed intact *C. cyanea* specimens were available for a topographical study. The topographical anatomy of *C. cyanea* (Figure 4.1) shows the abdominal intestinal tract *in situ*. In both specimens the left sided stomach was completely covered by the liver; both these structures were situated against the ventral abdominal wall. In specimen one (Figure 4.1 diagram A), the first loop of the intestinal tract crossed the abdominal cavity, whereas the rest of the intestinal tract was folded into several smaller loops. The caudal part of the intestinal tract descended on the left lateral side of the abdominal wall.

In the second specimen (Figure 4.1 diagram B), the loops of the GIT appeared different than the first specimen. The first loop did not cross the abdominal cavity, but rather folded on itself. The rest of the intestine was arranged into several loops and the caudal part descended on the medial aspect of the abdominal wall.

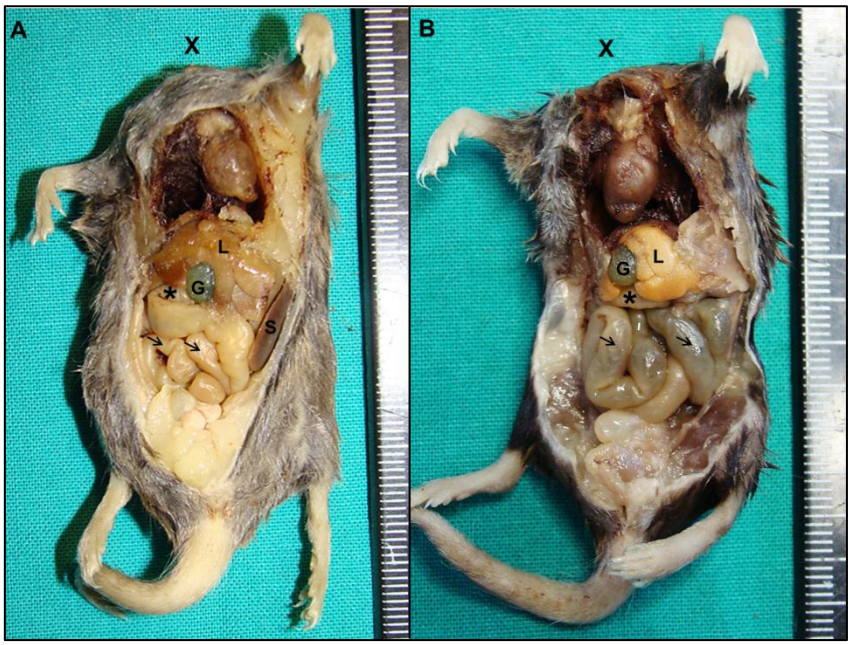

Figure 4.1: The topographical anatomy of the *in situ* abdominal intestinal tracts of two *C. cyanea* specimens of which the heads are removed.

The loops of the intestinal tracts are indicated with short arrows.

(A) *C. cyanea* specimen no. 1

(B) *C. cyanea* specimen no. 2. (*), duodenum; L, liver; G, gallbladder; S, spleen; X, position of the head.

4.3 The morphology and histology of the GITs of *A. spinosissimus*, *C. cyanea* and *A. hottentotus*

All of the histological images used to describe the morphology of the GIT were stained with the AB/PAS technique. The AB/PAS stain distinguishes the morphological structures better than the other special stains used in this study.

4.3.1 The morphology and histology of the stomach

The shape of the stomach was quite different between the three insectivorous species. The stomach of *A. spinosissimus* was U-shaped with well-developed greater and lesser curvatures and a spacious corpus region (Figure 4.2 diagrams A and B). The angular incision of the stomach was sharp, which caused the fornix- and pyloric regions to be close to one another. Consequently, these areas were also positioned higher than the cardia.

For *C. cyanea*, the shape of the stomach was subjected to interspecies variations. In some animals J-shaped stomachs were observed (Figure 4.2 diagram C), with a broad fornix region and a narrow, elongated pyloric region. Further, in some of the animals, there was a sharp cardial notch and angular incisure which positioned the fornix- and pyloric regions

opposite to one another (Figure 4.2 diagram D), but not as prominent as seen in *A. spinosissimus*. In one specimen the stomach was almost completely tubular, without a prominent cardial notch and a wide angular incisure, similar to the stomach of *A. hottentotus* in figure 4.2 diagram E.

The stomach of *A. hottentotus* had a noticeable elongation of the pyloric portion, due to a wide angular incisure (Figure 4.2 diagram E). This gave the stomach a tube-like appearance. In one of the animals examined a sharp cardial notch was observed, positioning the fornix parallel with the oesophagus (Figure 4.2 diagram F). The pyloric portion was also elongated but it had a dilated pyloric antrum compared to the other animals of this species. Overall, the external surface of the stomachs in all three species were simple (unilocular) and uncompartmentalised, with a clear transition from the stomach to the duodenum.

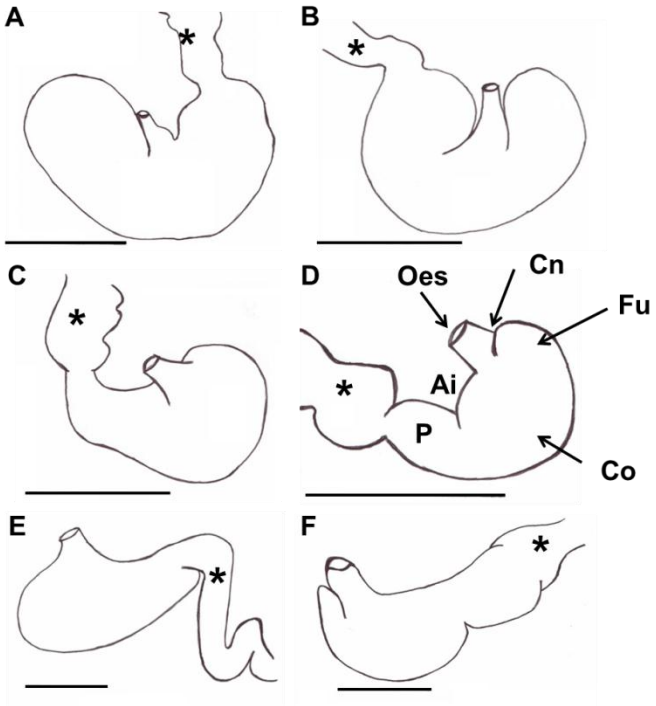

Figure 4.2: The shapes of the stomachs of the *A. spinosissimus*, *C. cyanea* and *A. hottentotus*.

A. spinosissimus (A, B), *C. cyanea* (C, D), and *A. hottentotus* (E, F). The asterisk indicates the position of the duodenum. The different stomach regions are indicated in image D and can be applied to all the other stomach images. Ai, Angular incisure; Cn, Cardiac notch; Co, Corpus; Fu, Fundus/Fornix; Oes, Oesophagus; P, Pyloric Antrum. Bar = 1 cm.

On the internal aspect of the stomach of *A. spinosissimus* (Figure 4.3 diagram A), the fundus is lined with microscopically visible stratified squamous epithelium around the oesophageal entrance. The fundus is demarcated from the glandular gastric epithelium by a clear line (limiting ridge/line). The limiting ridge/line crossed the lesser curvature at the

angular incisure and the greater curvature at a point opposite the angular incisure. Folds (rugae) were also observed in the fundic regions.

In *C. cyanea* and *A. hottentotus* a difference in the epithelium lining the oesophagus and the stomach could be observed macroscopically. Extensive rugae were present in the fundus and corpus of the stomach. No rugae were observed in the pyloric region.

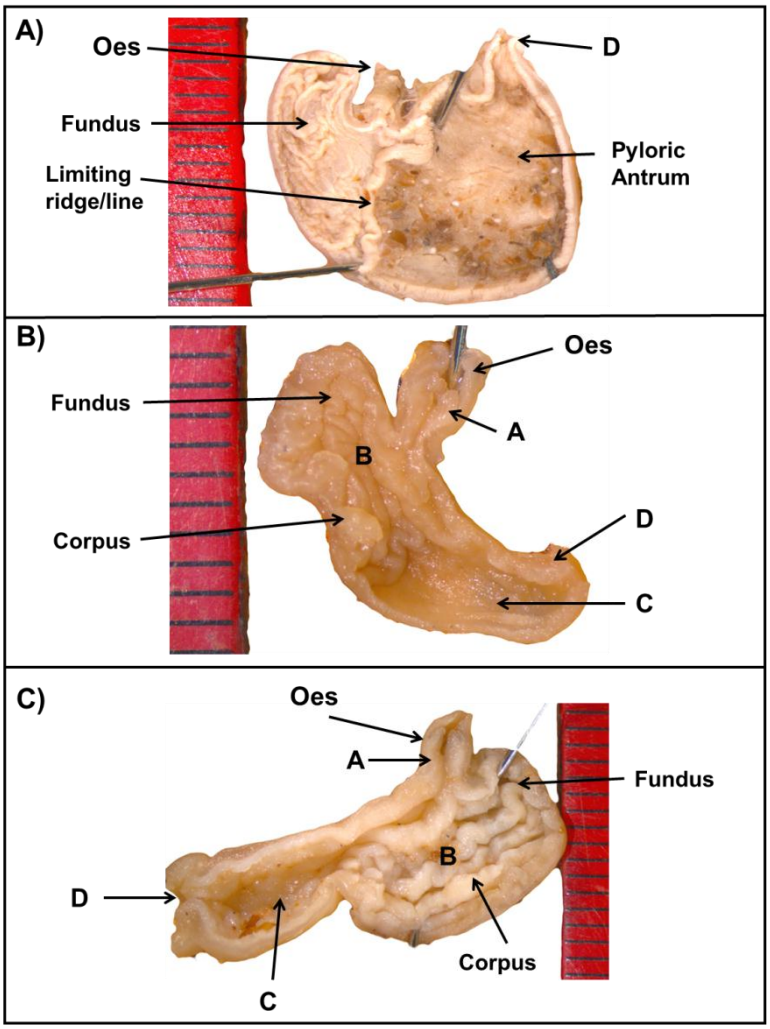

Figure 4.3: Macroscopic images of the internal aspect of the stomachs of *A. spinosissimus*, *C. cyanea* and *A. hottentotus*.

(A) The stomach of *A. spinosissimus*, with a bordering fold and rugae in the fundus.

(B) The stomach of *C. cyanea* has extensive rugae in the fundus and corpus.

(C) The stomach of *A. hottentotus* with extensive rugae in the fundus and corpus. Oes, oesophagus; A, cardiac glands; B, fundic glands; C, pylorus; D, position of the duodenum. The bars in the diagrams are measured in mm.

For the stomach histology of all three specimens, tissue was harvested from the corpus (body) of the stomach. In *A. spinosissimus*, the gastric glands of the stomach appeared tubular (Figure 4.4 diagrams A and B). Numerous parietal cells (triangular shaped) were present in the isthmus and neck of the glands, as well as several peptic cells at the base of the gland. With the AB/PAS staining technique, the surface mucous cells that lined the gastric pits stained a deep magenta (Figure 4.4 diagram B), which indicated the presence of neutral mucin granules within the mucous cells. The neck mucous cells stained a lighter magenta than the surface mucous cells. Some of the mucous neck cells stained purple with the AB/PAS technique, indicating both neutral and acid mucins in these cells. It was confirmed with the HID/AB and AF/AB stains that the latter cells were only slightly positive

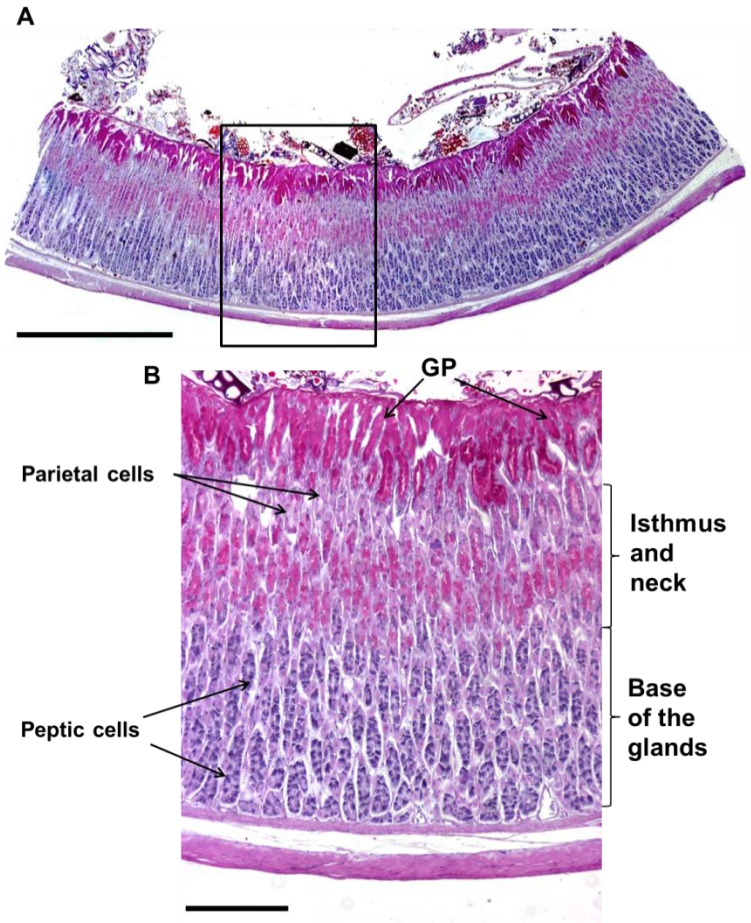

Figure 4.4: The corpus region of the stomach of *A. spinosissimus* stained with the AB/PAS technique.

(A) A low magnification image of the corpus region of the stomach, Bar = 1000 µm.

(B) This is an enlarged composite image of the boxed area in image A. The glands in the corpus region were tubular and the surface mucous cells lining the gastric pits (GP) stained a deep magenta. The mucous cells in the neck of the gastric glands stained a lighter magenta. The parietal cells were most prominent in the isthmus and neck regions of the gastric glands and stained a light pink. However the chief/peptic cells were located in the base of the gastric glands and stained dark purple. Bar = 200 µm.

for either sulfo- or sialomucins. However, few of these cells were observed in the corpus of the stomach of *A. spinosissimus*.

The corpus of the stomach in *C. cyanea* had very extensive rugae (Figure 4.5 diagram A) with tubular gastric glands. With the AB/PAS technique, the surface and neck mucous cells stained a deep magenta (Figure 4.5 diagram B). Parietal cells were the most

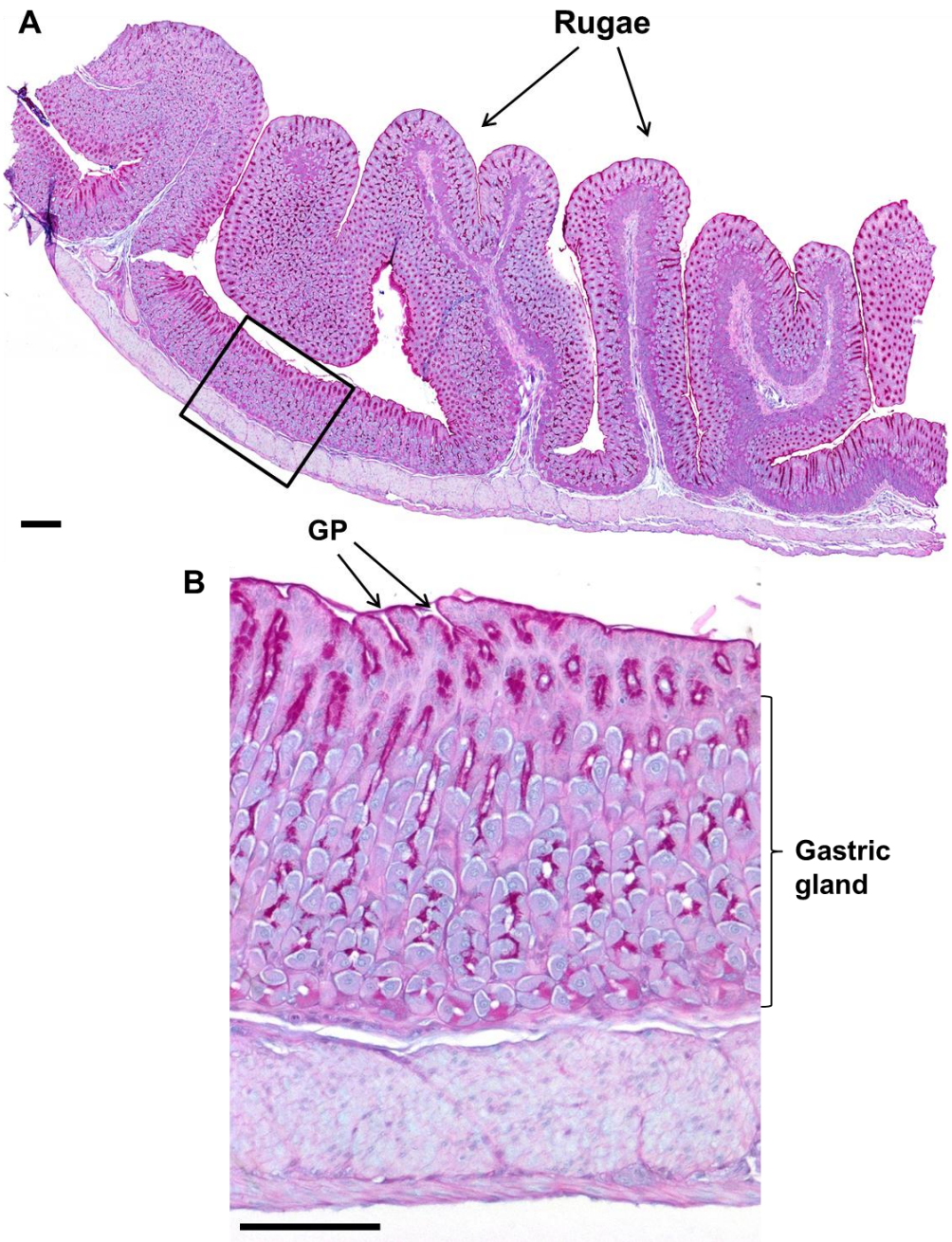

Figure 4.5: The corpus region of the stomach of *C. cyanea* stained with the AB/PAS technique.

(A) A composite image of the corpus region of the stomach with very prominent rugae. Bar = 100 µm.

(B) This is an enlargement of the boxed area in image A, which shows the tubular gastric glands. The surface mucous cells and the mucous neck cells stained deep magenta. Parietal cells were the most prominent cell type observed in the gastric glands. Bar = 100 µm.

prominent cell type observed in the gastric glands. No peptic cells were observed. It appeared that there were only neutral mucins in the corpus region of the stomach of *C. cyanea*. The HID/AB and AF/AB techniques did not detect any acid mucins in the mucous cells.

Similar to *C. cyanea*, in the stomach of *A. hottentotus*, the mucosa was thrown into prominent folds or rugae (Figure 4.6 diagram A) and consisted of tubular gastric glands (Figure 4.6 diagrams B and C) that extended from the muscularis mucosae to open into the stomach lumen via the gastric pits.

With the AB/PAS technique, the surface mucous cells in the corpus region of the stomach stained dark purple (Figure 4.6 diagrams B and C). This indicated the presence of both neutral and acid mucin granules within the gastric mucous cells of *A. hottentotus*. The neck mucous cells stained purple and dark blue, and the neck mucous cells close to the base of the gastric glands stained magenta. Sialomucin was the only type of acid mucin observed in the corpus region of the stomach. Both the HID/AB and AF/AB techniques stained the surface mucous cells and the mucous neck cells of the stomach blue. Parietal cells were prominent in the gastric glands, however, no peptic cells were observed. Three muscle layers could be distinguished in the stomachs of the three insectivorous species.

4.3.2 The morphology and histology of the small- and large intestines

All three species in the present study have primitive intestinal characteristics. *A. spinosissimus* has a simple GIT with a caecum, whereas the other two species lack caeca. Thus, for *C. cyanea* and *A. hottentotus* there is macroscopically no clear indication of a division between the small- and large intestines.

4.3.3 Duodenum

The villi in all three species were straight finger-like or broad leaf-like projections interspersed with short glands known as the crypts of Lieberkühn, which extended down to the muscularis mucosae (Figure 4.7 diagrams A-C). The mucosa was lined with tall columnar enterocytes and goblet cells. Brunner's glands (mucous secreting glands) were observed in all three species and were positioned in the submucosa beneath the mucosa. In addition, the Brunner's glands predominantly stained magenta with the AB/PAS technique, thus the mucous glands primarily contained neutral mucin granules. However, in *A. hottentotus* on the borders of the Brunner's gland ducts (Figure 4.7 diagram B), the mucous cells stained purple, therefore containing both neutral and acid mucin granules.

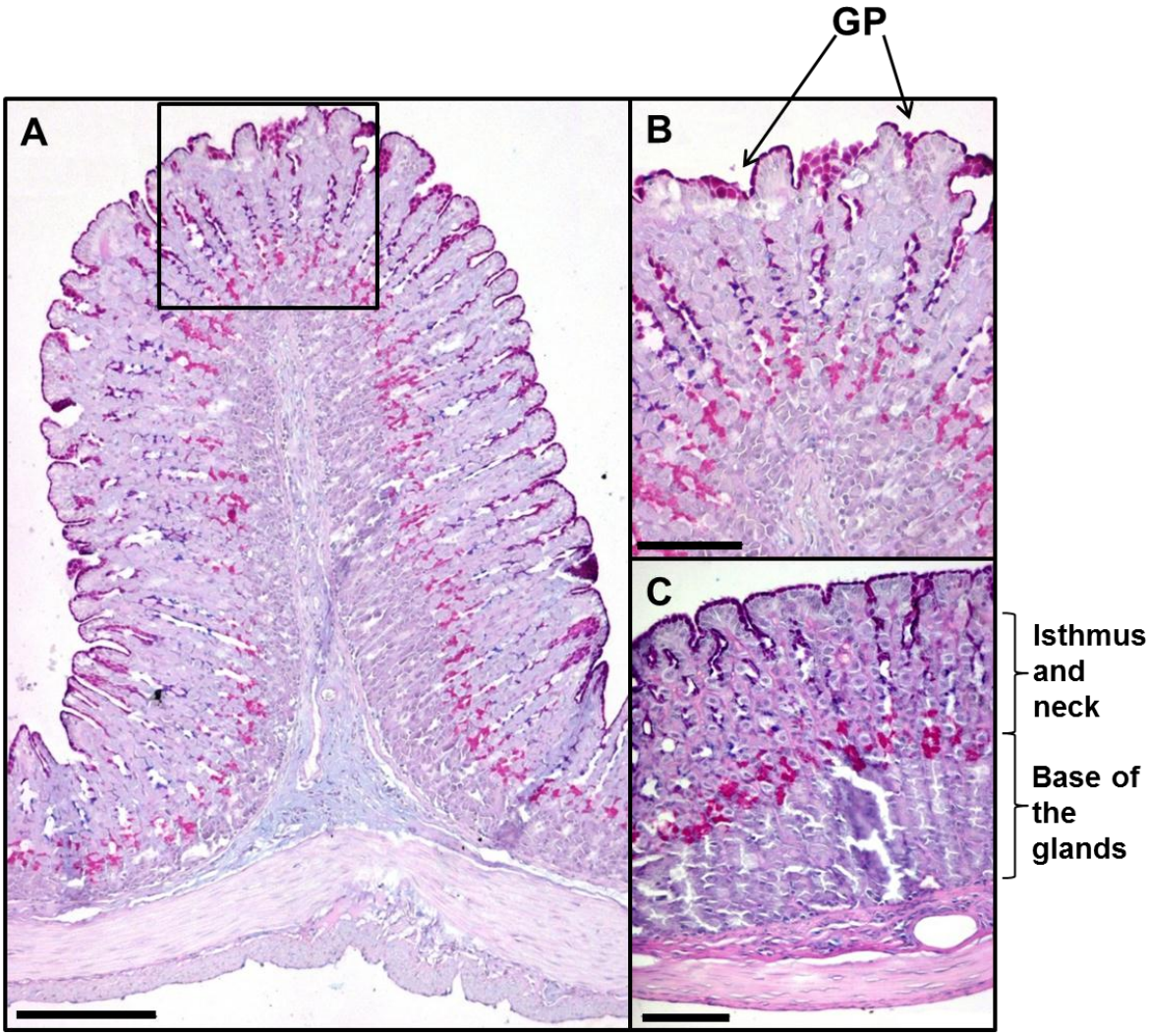

Figure 4.6: The corpus region of the stomach of *A. hottentotus* stained with the AB/PAS technique.

(A) A composite image of the prominent rugae in the corpus region of stomach, Bar = 200 µm.

(B) This is an enlargement of the boxed area in image A, which clearly indicated the differently stained mucous cells in the gastric pits (GP) and in the distal regions of the glands, Bar = 100 µm.

(C) This image illustrates the tubular glands in the corpus of the stomach, Bar = 100 µm.

The HID/AB and AF/AB staining techniques indicated that sialomucin was the only type of acid mucin present in the latter region. The ducts of the Brunner's glands opened into the base of the crypts of Lieberkühn and, in regions where no glands were present, subtle submucosal folds were observed.

The muscularis propria consisting of the inner circular (CM) and outer longitudinal (LM) smooth muscular layers, was observed in all three insectivorous species. In *A. spinosissimus* (Figure 4.7 diagram A), these layers appeared much thinner and more compressed as seen in *C. cyanea* (Figure 4.7 diagram B) and *A. hottentotus* (Figure 4.7 diagram C). In the latter two species the two smooth muscle layers was easily distinguishable.

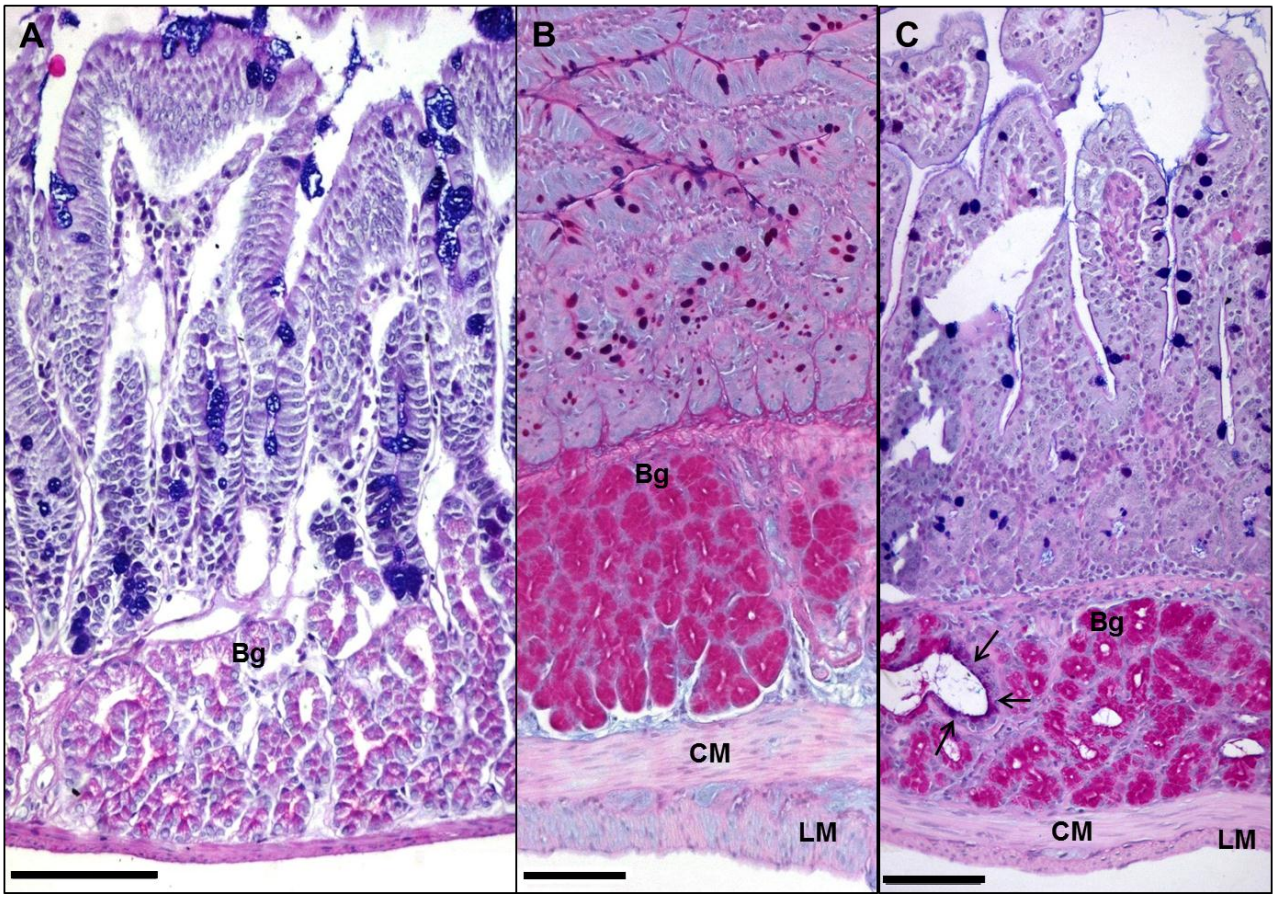

Figure 4.7: Composite images of the duodenums with Brunner's glands (Bg) that stained magenta with the AB/PAS technique in *A. spinosissimus*, *C. cyanea* and *A. hottentotus*.

(A) The duodenum of *A. spinosissimus* with Bg in the submucosa.

(B) The duodenum of *C. cyanea* with Bg in the submucosa.

(B) The duodenum of *A. hottentotus* with Bg in the submucosa; a few of the mucous cells in the ducts of Brunner's glands stained purple (short arrows). The purple mucous cells contain a mixture of both neutral and acid (sialomucin) mucins. CM, inner circular muscularis layer; LM, outer longitudinal muscularis layer; Bar = 100 µm.

4.3.4 Middle small intestine

In the middle of the small intestine of all species used here, the villi were lined with tall columnar enterocytes and goblet cells, and interspersed between the villi were the crypts of Lieberkühn. Other cell types, such as Paneth and endocrine cells, were observed in the crypts of *A. spinosissimus*. Endocrine cells were also observed in the crypts of *C. cyanea* and *A. hottentotus*, but no Paneth cells were present.

The villi in the middle small intestine of *A. spinosissimus* were broad and leaf-like (Figure 4.8 diagram A), with less goblet cells in the surface epithelial layer when compared to *C. cyanea* and *A. hottentotus*. In *C. cyanea* the villi in the middle of the small intestine looked like finger-like projections (Figure 4.8 diagram B). The villi in the latter region did not seem

to be much shorter than observed in the duodenum, but it was not as closely packed as in the duodenum. However, the villi in *A. hottentotus* appeared to be either finger-like (Figure 4.8 diagram C) or leaf-like projections (Figure 4.8 diagram D), which were shorter than seen in the duodenum. Both the circular and longitudinal muscle layers were also observed in the middle of the small intestine of the three insectivorous species.

The villi in the ileum of *A. spinosissimus*, compared to the villi in the duodenum and middle small intestine, were remarkably shorter. The number of goblet cells in the crypts also appeared to be more numerous, than in the duodenum and the middle small intestine.

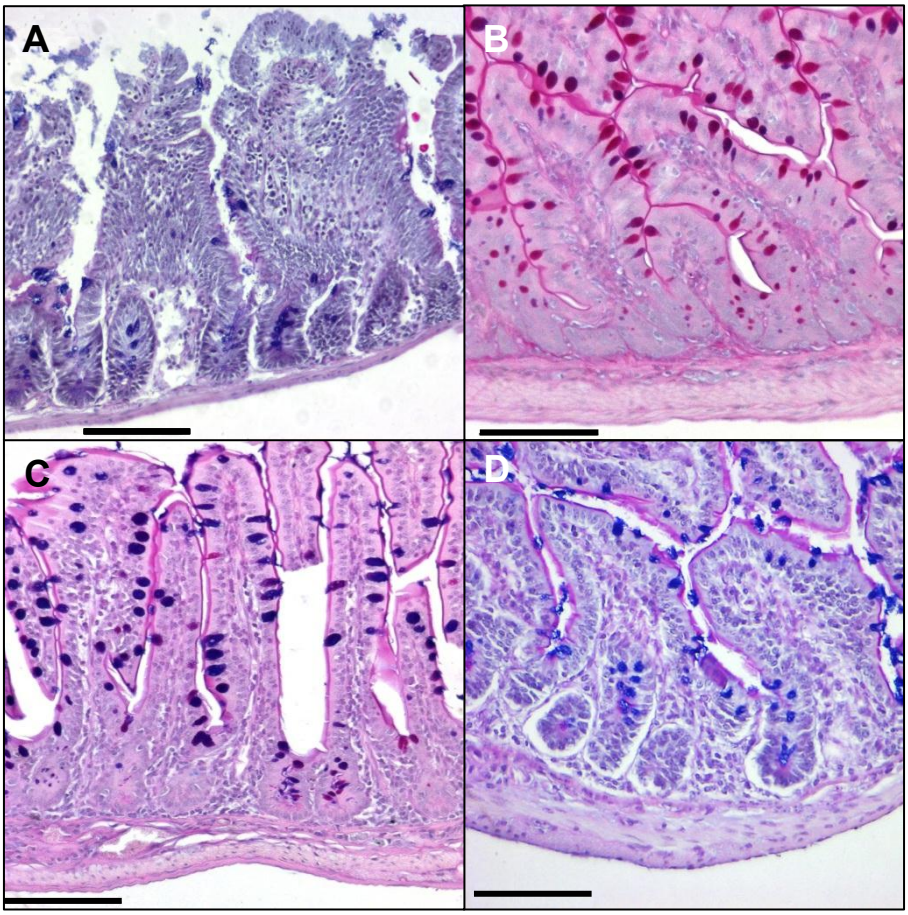

Figure 4.8: The finger-like and broad leaf-like projections of the villi in the middle of the small intestines of *A. spinosissimus* (A), *C. cyanea* (B), *A. hottentotus* (C, D).

The AB/PAS technique was used in all of these images. Bar = 100 µm.

4.3.5 Distal small intestine of *C. cyanea* and *A. hottentotus*

C. cyanea and A. hottentotus do not have caeca, therefore their distal small intestinal region will be described. The distal small intestine of *C. cyanea* (Figure 4.9 diagrams A and B) and *A. hottentotus* (Figure 4.9 diagrams C and D) consisted of villi interspersed with the crypts of Lieberkühn. The villi in *C. cyanea* varied between intermediate (Figure

4.9Figure 4.9 diagram A) and short villi (Figure 4.9 diagram B) that was densely packed together with a numerous amount of goblet cells in the surface epithelial layer. In *A. hottentotus*, the shape of the villi varied between thin finger-like and broad leaf-like projections (Figure 4.9 diagrams C and D) that were not as densely arranged as in *C. cyanea*. Prominent plicae circulares (folds of the mucosa and the underlying submucosa) with short villi were also observed in the distal small intestine of *A. hottentotus*. An occasional cluster of lymphoid tissue (Peyers patches) was present in the submucosa.

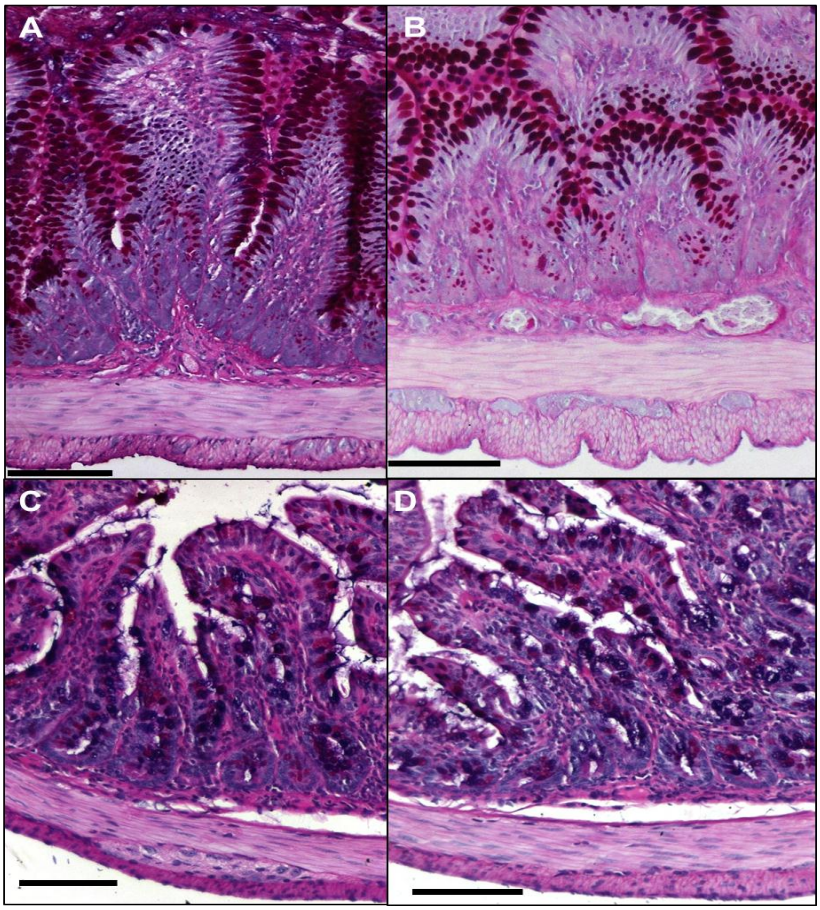

Figure 4.9: The distal small intestinal regions of *C. cyanea* (A, B) and *A. hottentotus* (C, D), stained with AB/PAS.

Bar = 100 µm.

4.3.6 Caecum

A. spinosissimus had a bean-shaped caecum (Figure 4.10 diagram A) with the ileo-caecal and caeco-colic openings positioned close to one another. Histologically, the caecum consisted of tube-like crypts, with tall columnar enterocytes and goblet cells in the surface epithelial layer and the walls of the crypts (Figure 4.10 diagram B). However, in the caecum of one specimen, transverse folds were observed macroscopically (Figure 4.10 diagram C) and histologically (Figure 4.10 diagram D). Macroscopically, it was observed that the latter folds were most prominent at the ileo-caecal and caeco-colic openings.

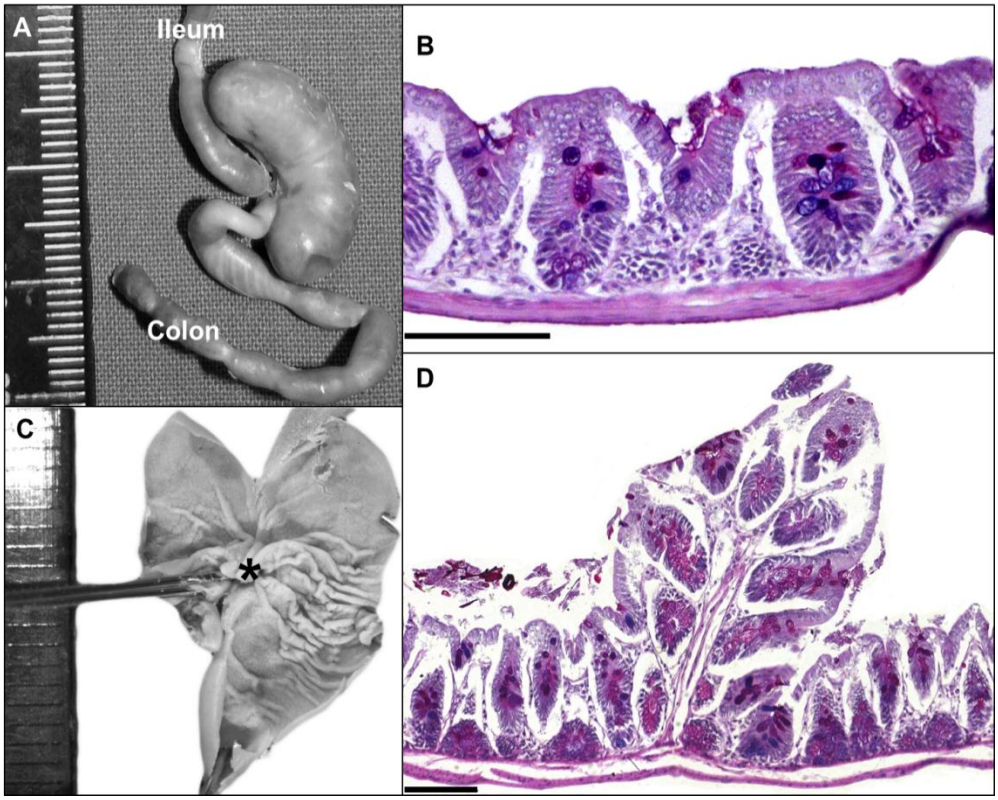

Figure 4.10: The macroscopic and microscopic images of the caecum in *A. spinosissimus*.

The microscopic images were stained with AB/PAS. The ruler in images A and C are measured in mm.

(A) The bean-shaped caecum with the ileo-caecal and caeco-colic openings positioned close to one another.

(B) Tube-like crypts in the caecum.

(C) The caecum was cut open on the anti-mesenteric border and photographed. This image illustrates the macroscopic view of the circularly arranged folds in the caecum. The asterisk indicates where the ileo-caecal and caeco-colic openings are.

(D) A composite image of the circularly arranged folds in the caecum. Bar = 100 µm.

4.3.7 Colon

The proximal colon of *A. spinosissimus* had a large lumen (Figure 4.11 diagram A) with tube-like crypts (Figure 4.11 diagram B) and curved plicae circulares (folds of the mucosa and underlying submucosa) (Figure 4.11 diagram C), which was also lined with crypts. Numerous goblet cells were present in the crypts, especially at the base. These curved submucosal folds were also seen macroscopically as part of V-shaped folds in the colon (Figure 4.12).

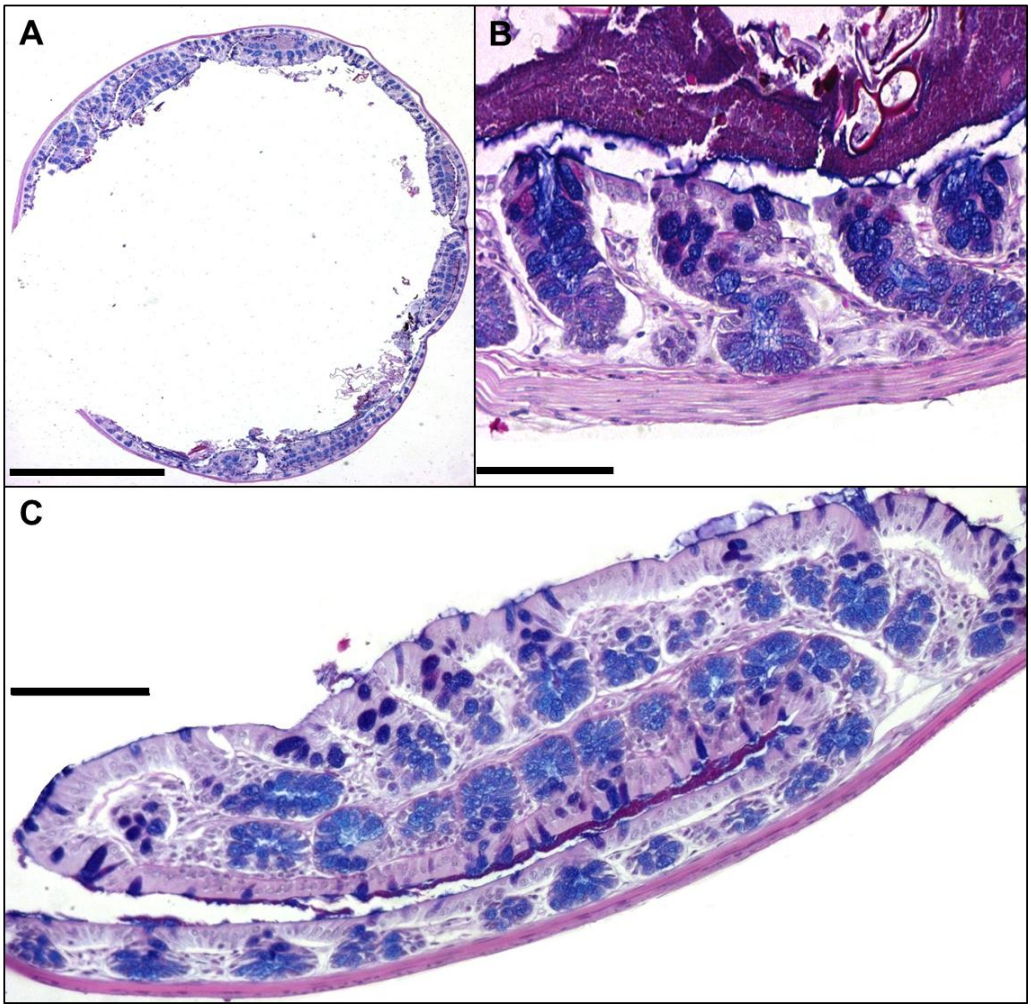

Figure 4.11: The colon of *A. spinosissimus* stained with AB/PAS.

(A) A cross section of the colon, Bar = 1000 µm.

(B) Tube-like crypts.

(C) A composite image of a transverse mucosal fold (plicae circulares) lined with crypts. Bar = 100 µm.

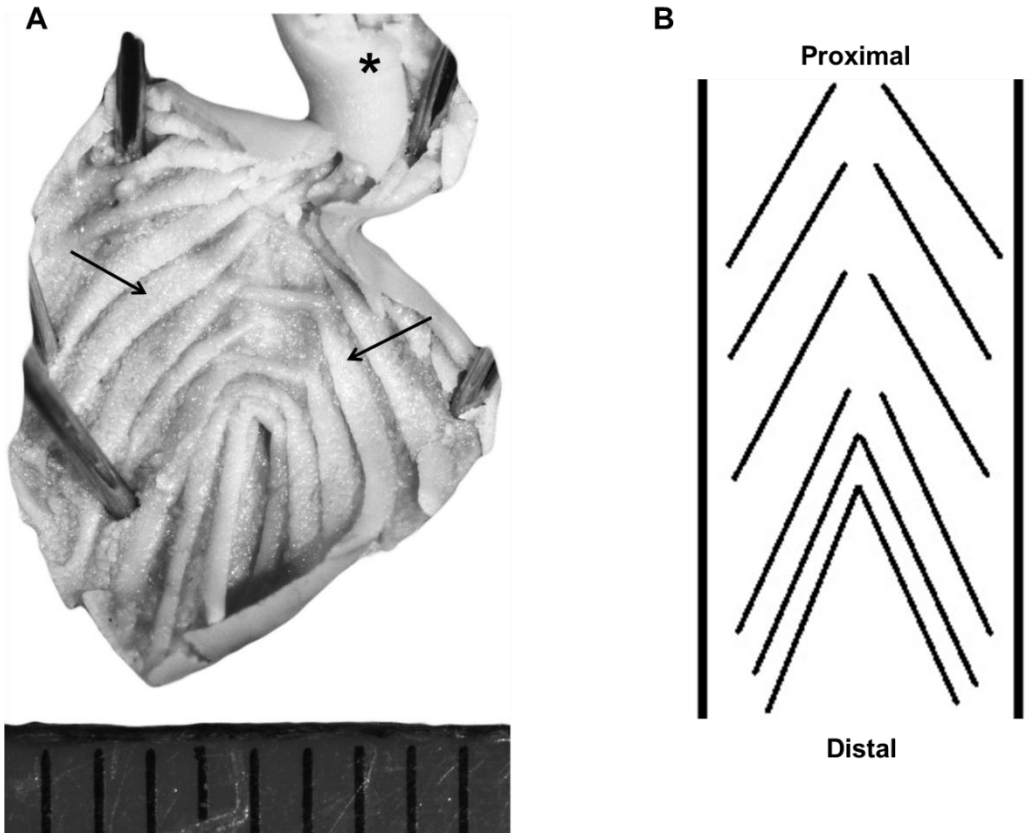

Figure 4.12: Macroscopic view of the V-shaped mucosal folds in the colon of *A. spinosissimus*.

The ruler in image A is measured in mm.

(A) The proximal region of the colon was cut longitudinally on the anti-mesenterial border and pinned open to observe the V-shaped folds (indicated with arrows). The asterisk indicates the proximal position of the colon.

(B) An illustration of the V-shaped folds in the proximal colon which appears V-shaped once the colon is open.

The colons of both *C. cyanea* (Figure 4.13 diagram A) and *A. hottentotus* (Figure 4.14 diagram A) contained prominent folds (plicae circulares). The plicae circulares in the colon of *A. hottentotus* consisted of tube-like crypts (Figure 4.14 diagram B), namely the crypts of Lieberkühn. Numerous goblet cells were present in the crypts. However, the colon of *C. cyanea* had villi and crypts on the extensively well-formed plicae circulares (Figure 4.13 diagrams B and C). The folds in the colon gave the region a narrow lumen compared to that of *A. spinosissimus*. In addition, both the inner circular and outer longitudinal muscle layers of the colon appeared to be thicker than the proximal regions of the GIT. In both *C. cyanea* (Figure 4.13 diagram D) and *A. hottentotus* (Figure 4.14 diagram C) the folds in the colon were seen macroscopically as part of longitudinal elevations. The longitudinal elevations in *C. cyanea* and *A. hottentotus* were observed roughly for 2 cm and 6 cm respectively in the distal regions of their GITs.

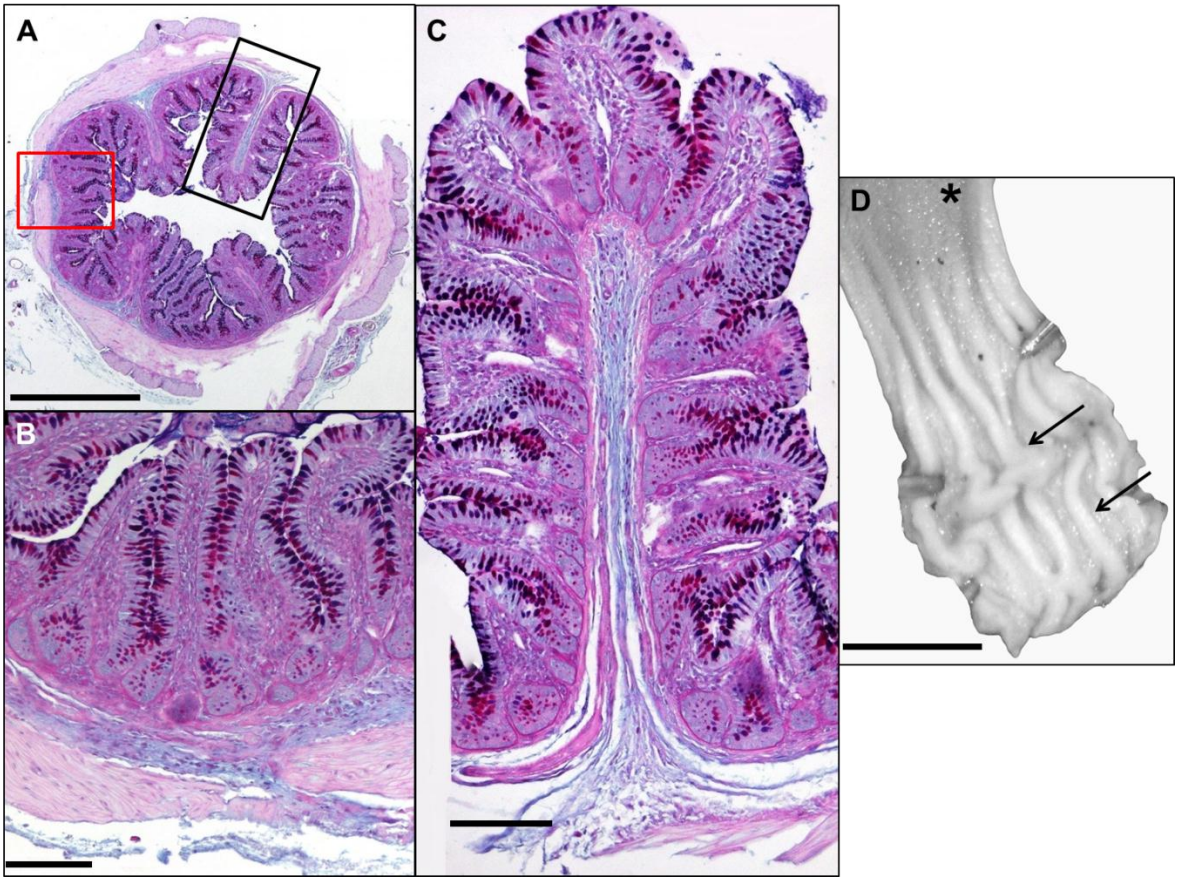

Figure 4.13: Microscopic and macroscopic images of the colon of *C. cyanea*.

The microscopic images were stained with the AB/PAS technique.

(A) A cross section of the colon, indicating the villi, plicae circulares and narrow lumen, Bar = 1000 µm. The red box is enlarged in image B and the black box is enlarged in image C.

(B) Broad finger-like villi with numerous goblet cells in the crypt and surface epithelial areas, Bar = 100 µm.

(C) A composite image that shows the mucosa is thrown into a longitudinal fold, plicae circulares, which is covered with villi, Bar = 100 µm.

(D) The distal region of the colon was cut longitudinally on the anti-mesenterial border and pinned open to observe the longitudinal elevations/folds (arrows). The asterisk indicates the proximal position of the colon. Bar = 4 mm.

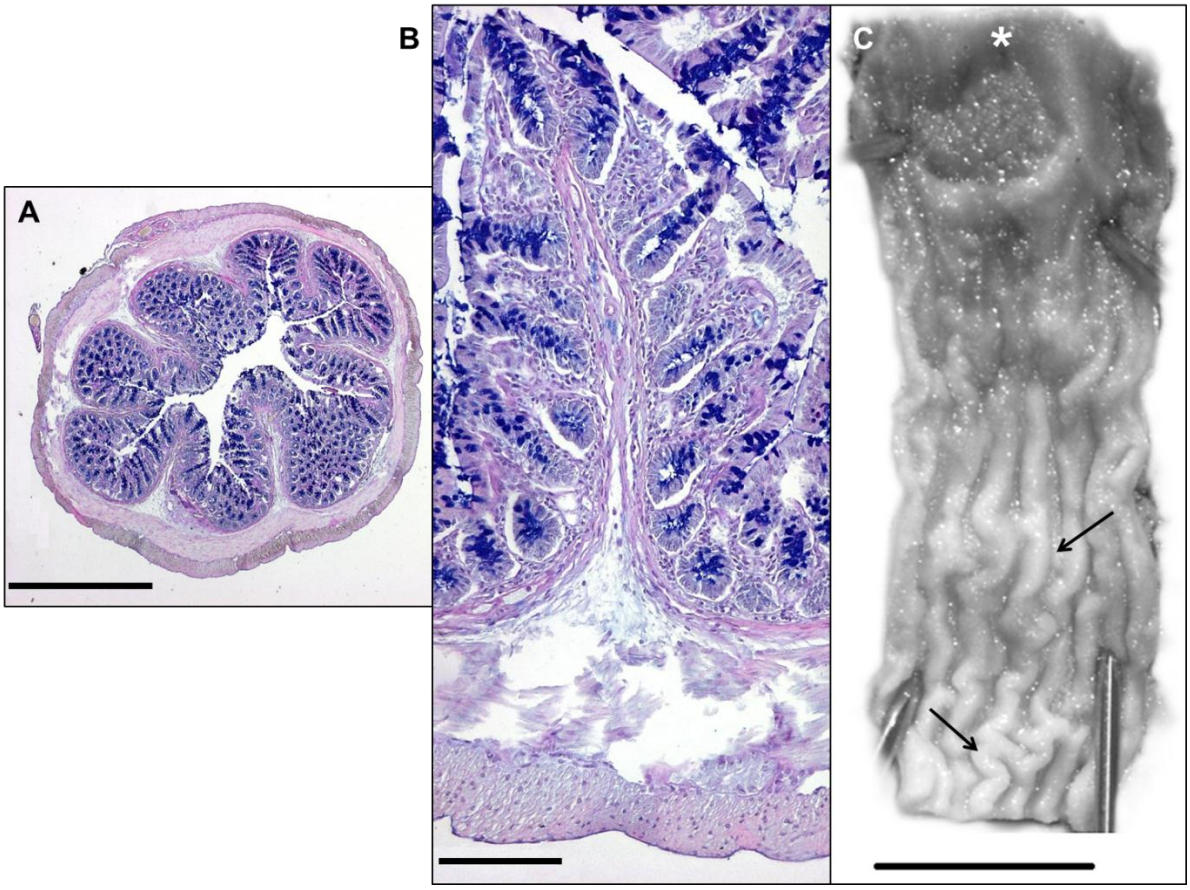

Figure 4.14: Microscopic and macroscopic images of the colon of *A. hottentotus*.

The microscopic images were stained with the AB/PAS technique.

(A) A cross section of the colon, indicating the plicae circulares and narrow lumen, Bar = 1000 µm.

(B) A composite image that shows the mucosa is thrown into a longitudinal fold, plicae circulares, which is covered with crypts, Bar = 100 µm.

(C) The distal region of the colon was cut longitudinally on the anti-mesenterial border and pinned open to observe the longitudinal elevations/folds (arrows). The asterisk indicates the proximal position of the colon. Bar = 5 mm.

4.4 The statistical interpretation of the macroscopic gastrointestinal data

The p-values for the graphs in the following section have been calculated by the F-, Mann-Whitney U and Kruskal Wallis tests (section 3.14, p. 55). The p-value calculated by the F-test is the only p-value that will be considered, as recommended by the statistician, as it is more accurate than the p-values calculated by the Mann-Whitney U and Kruskal Wallis tests. The F-test is less sensitive for big fluctuations in the data. In addition, on each of the line graphs there are vertical bars which indicate a 95% confidence interval. The confidence interval is used to indicate the reliability of an estimate (Keller, 2005). This is an observed interval calculated from the observations that frequently includes the parameter of interest, if the experiment should be repeated. In the following section the macroscopic results of all three insectivorous species, *A. spinosissimus*, *C. cyanea* and *A. hottentotus*, will be interpreted and compared.

4.4.1 The macroscopic gastrointestinal results of the three insectivorous species

For each species, the length and surface areas of the different gastrointestinal regions were expressed as a proportion of the total gastrointestinal length and/or surface area (Table 4.2).

Table 4.2: The mean proportions (%) and Std. Dev (±) of the total GIT surface areas and lengths of the anatomically distinct regions of the GITs of *A. spinosissimus*, *C. cyanea* and *A. hottentotus*.

	A. spinosissimus	***C. cyanea***	***A. hottentotus***
Proportional Surface Area (%)			
Stomach	26 (±5.2)	24.8 (±13)	20 (±3.8)
Small Intestine	43.3 (±5.2)	-	-
Small + Large Intestine	73.8 (±5.2)	75.2 (±13)	80 (±3.8)
Caecum	16.5 (±2.2)	-	-
Caecum + Colon	30.5 (±0.8)	-	-
Colon	14.0 (±2.6)	-	-
Ave total GIT surface area (mm^2)	6259.7(±339.2)	1789.5 (±332.9)	6269.4 (±521.7)
Proportional Length (%)			
Stomach	13.9 (±2.7)	18.5 (±5.8)*	11.1 (±2.1)*
Small Intestine	56.2 (±3.9)	-	-
Small + Large Intestine	86.06 (±2.7)	81.5 (5.8)*	88.9 (2.1)*
Caecum	11.7 (±1.5)	-	-
Caecum + Colon	29.8 (±2.3)	-	-
Colon	18.1 (±1.5)	-	-
Ave total GIT length (mm)	335.4 (±22.9)	132 (±7.8)	404.3 (±37)

*Statistically significant ($p < 0.05$) difference between species.

No statistically significant differences (p = 0.55) were observed between the surface areas of the stomach (Figure 4.15) and the combined surface area of the small intestine plus large intestine (further referred to as SI+LI) (Figure 4.16) *of A. spinosissimus*, *C. cyanea* and *A. hottentotus*. Despite these results, *A. spinosissimus* had the largest stomach surface area and *A. hottentotus* had the largest surface area of the SI+LI.

Statistically significant differences (p = 0.05) were observed between the lengths of the stomach (Figure 4.17) and the SI+LI (Figure 4.18) of *C. cyanea* and *A. hottentotus*. *C. cyanea* had the longest stomach and *A. hottentotus* the longest SI+LI. *A. spinosissimus* did not differ significantly from *C. cyanea* and *A. hottentotus*.

A comparison of the gastrointestinal weights (Figure 4.19) of the three insectivorous species studied here, indicated that *A. spinosissimus* had a significantly larger gastrointestinal weight than *C. cyanea* and *A. hottentotus* (p = 0.002 and p = 0.0003).

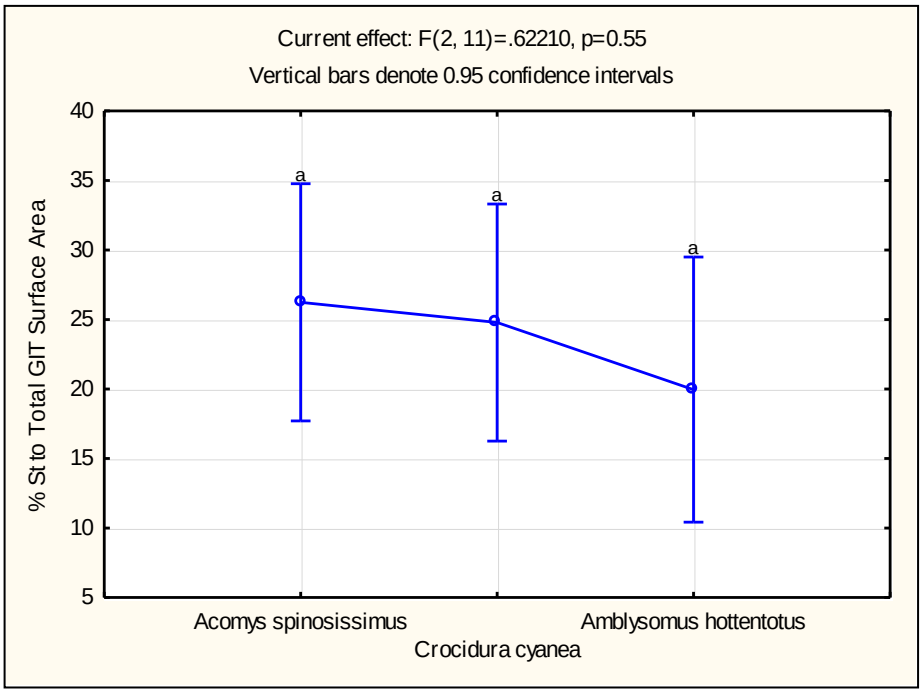

Figure 4.15: The proportional surface areas of the stomachs of *A. spinosissimus*, *C. cyanea*, and *A. hottentotus*.

The mean surface area of the stomach (St.) was expressed as a percentage of the total gastrointestinal surface area.

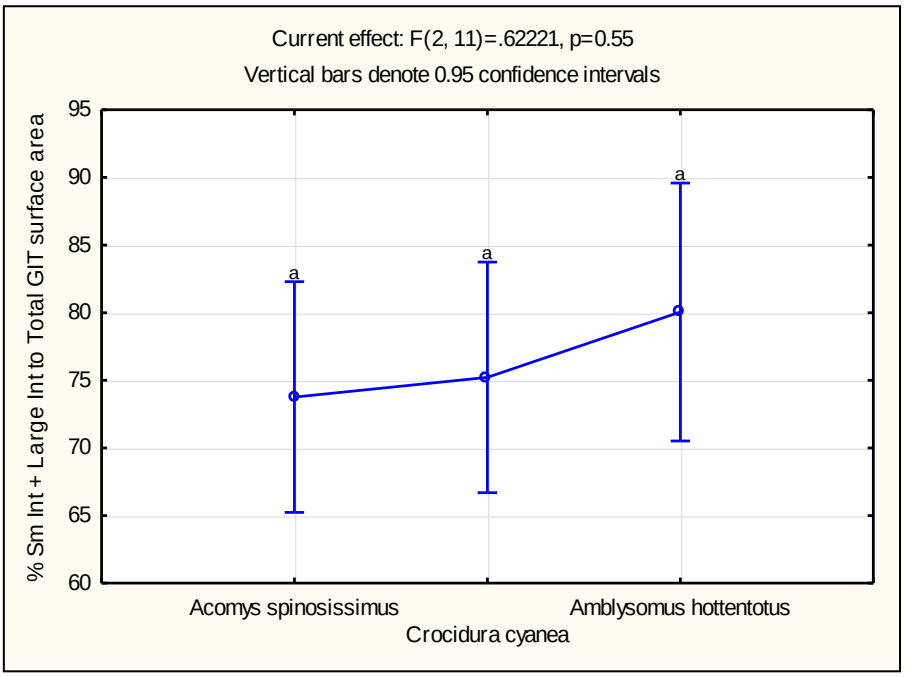

Figure 4.16: The proportional surface areas of the small intestines plus the large intestines of *A. spinosissimus*, *C. cyanea* and *A. hottentotus*.

The mean surface area of the combined SI+LI was expressed as a percentage of the total gastrointestinal surface area. Sm Int, Small intestine; Int, intestine.

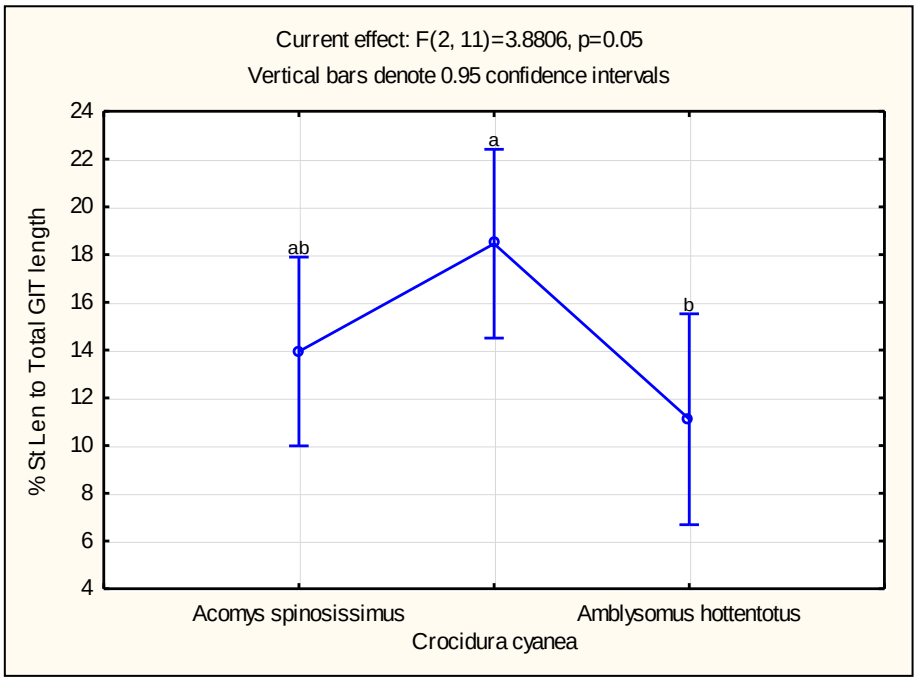

Figure 4.17: The proportional length of the stomach of the *A. spinosissimus*, *C. cyanea* and *A. hottentotus*.

The mean stomach length (St. Len.) was expressed as a percentage of the total gastrointestinal length.

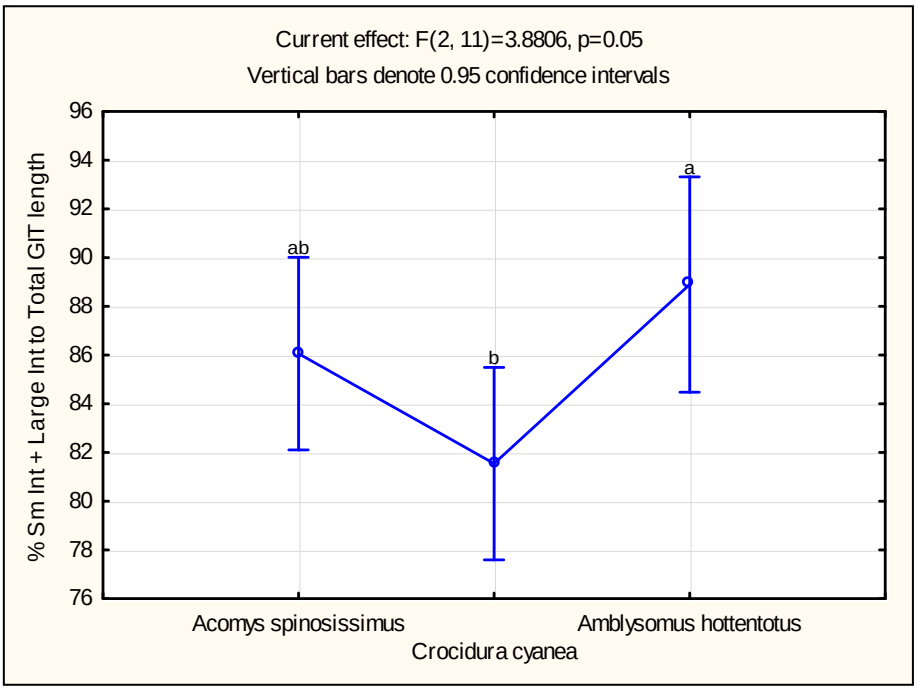

Figure 4.18: The proportional length of the small intestines plus the large intestines of *A. spinosissimus*, *C. cyanea* and *A. hottentotus*.

The mean length of the small intestine (Sm. Int.) plus the large intestine was expressed as a percentage of the total gastrointestinal length.

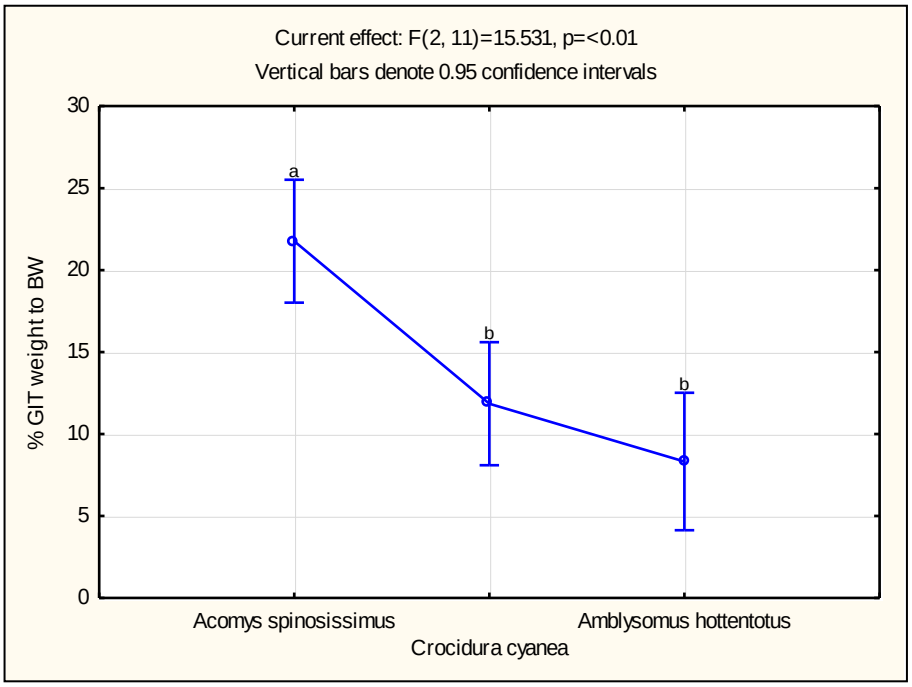

Figure 4.19: The proportion of the gastrointestinal weight of the *A. spinosissimus*, *C. cyanea* and *A. hottentotus*.

The mean gastrointestinal weight was expressed as a percentage of the body weight (BW).

A biplot was used to compare two different variables of *A. spinosissimus*, *C. cyanea* and *A. hottentotus* with one another. These variables were the surface areas (mm^2) of the gastrointestinal regions and the proportions (%) of these regions which were plotted on a biplot to determine whether they were related (Figure 4.20). Although it was observed in Table 4.2 that the proportions of the gastrointestinal regions of *C. cyanea* and *A. hottentotus* were significantly different ($p < 0.05$) from one another, the full extend thereof could not be observed. The proportions of the gastrointestinal regions of *A. spinosissimus* did not differ significantly from the latter species, but with the biplot, all of these measurements can be observed as a whole.

A biplot is a type of exploratory graph, and a generalisation of the simple two-variable scatterplot. The red (*A. spinosissimus*), black (*A. hottentotus*) and blue (*C. cyanea*) dots represent each animal within a species, and the vectors represent the variables. The dots on the biplot can be interpreted in a similar way as dots on a scatterplot. The dots close to one another correlate. *A. spinosissimus* (red) and *A. hottentotus* (blue) appear to be closely related. *C. cyanea* (blue dots) differ substantially from the latter species. The *C. cyanea* specimens were separated into two groups and correlation was evident within each grouping. The two specimens on the upper right quadrant correlated with one another and were larger than the three specimens on the lower left quadrant of the graph.

Vectors that pointed in the same direction correlate with each other, as illustrated by their direction representing the surface areas of the GI regions (Figure 4.20). As the length of the vector increased, so did its value. The graph indicated that the surface areas for *A. spinosissimus* (red dots) and *A. hottentotus* (black dots) were both larger than that of *C. cyanea* (blue dots). The percentage proportions of the regions of the GIT were opposites from one another, as the vectors pointed in opposite directions. The two proportional surface area vectors (%) showed no correlation with the non-proportional surface areas of the GIT, as all the vectors were not pointing in the same direction and intersected one another perpendicularly. As observed in the former graphs, there were differences between the proportional gastrointestinal measurements of the three insectivorous species studied in this thesis.

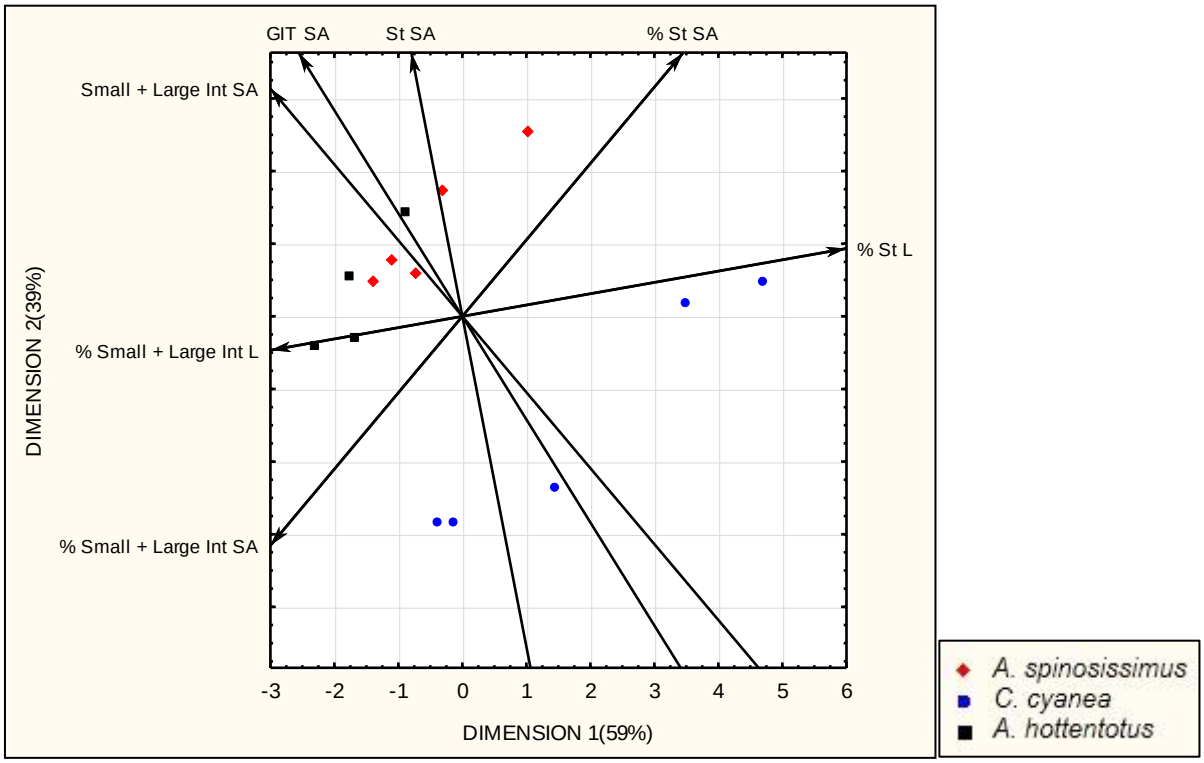

Figure 4.20: A biplot illustrating two different variables of *A. spinosissimus, C. cyanea* and *A. hottentotus*..

The variables are displayed as vectors and each specimen of each species are displayed by dots. SA, Surface area; St, Stomach; Int, Intestine; L, Length.

4.5 The statistical interpretation of the gastrointestinal mucin histochemistry data

In the section below, mean values of mucin secreting goblet cells per surface area are presented graphically for comparison of the different GI regions with one another. Log transformed values were used to construct the graphs. The respective GI regions of *C. cyanea* and *A. hottentotus* were the duodenum, the middle of the small intestine, distal small intestine and colon, for *A. spinosissimus* it was the duodenum, middle of the small intestine, distal ileum, caecum and proximal colon. The mucous cells of the stomach were not counted and were described for each species in section 4.3 on pages 59-64.

The p-values of the graphs in the following section were calculated by the F-test. The p-value is a collective value for the different regions of the GIT. For example: if the p-value was equal to, or smaller than 0.05 for a graph, it does not necessarily mean that the regions of the GIT in that graph were statistically significantly different from one another. P-values of a graph were a combination of the p-values of each GI region. The p-values for each graph and between each GI region, has been tabulated in appendices 9-48 (pp. 157-197). The statistical significance between the different regions of the GIT was

indicated on each graph by letters of the alphabet. When letters positioned above a specific region were the same as any of the letters positioned above another region, it indicated no statistical significance. Letters differing from one another indicates statistical significance. The vertical bars on each graph represent a 95% confidence interval, as described in section 4.4 on page 74.

4.5.1 Gastrointestinal mucin histochemistry results of *A. spinosissimus*

In this section and the next, the results obtained from the AB/PAS technique are interpreted separately from the HID/AB and AF/AB techniques. The results of the latter two stains will be interpreted in combination as these stains are similar.

The AB/PAS technique was used to distinguish between neutral and acid mucin secreting goblet cells. The neutral mucins stained magenta, acid mucins blue and a mixture of the two mucins purple. A goblet cell that contained both acid and neutral mucin granules situated in separate compartments within the cell can be classified as partitioned. Very little to no partitioned cells were observed throughout the GITs of any of the three insectivorous species.

The HID/AB and AF/AB techniques was used to identify different types of acid mucin secreting goblet cells (sulfated and sialomucins). The HID/AB technique stained the sulfated mucins black/brown, the sialomucins blue, and a mixture of the two mucins blue/green or black/blue. The AF/AB stain was able to distinguish between strongly sulfated and weakly sulfated mucins, which stained deep and light purple, respectively. The sialomucins stained blue and the mixed mucins blue/purple.

The result for each of the insectivorous species used in this study will be described as follows: an overview will be given of the total number of mucin secreting goblet cells per total measured area (surface epithelial area + crypt area in mm^2), and the total number of mucin cells in the respective surface epithelial and crypt areas will be expressed per measured area for each gastrointestinal (GI) region. The number of different mucin secreting goblet cells per measured area (mm^2) will also be interpreted for each GI region. These results provide a comprehensive representation of the distribution of the different types of mucin secreting goblet cells throughout the GIT. The surface epithelial and crypt areas will be compared with one another and will be described if there is a noticeable difference between the two regions. From here on statistically significant results will be referred to as significant.

4.5.1.1 The results of the AB/PAS technique in *A. spinosissimus*

The total number of goblet cells per total area (mm^2) (Figure 4.21 diagram A) illustrates the overall distribution of the mucin secreting goblet cells throughout the GIT. Both the surface epithelial (Figure 4.21 diagram B) and crypt areas (Figure 4.21 diagram C) revealed similar trends than observed in figure 4.21 diagram A. The latter areas showed a steady increase in the number of AB/PAS positive cells from the duodenum to the ileum, a decrease in the caecum and a substantial increase of cells in the colon. Despite these similarities, marked

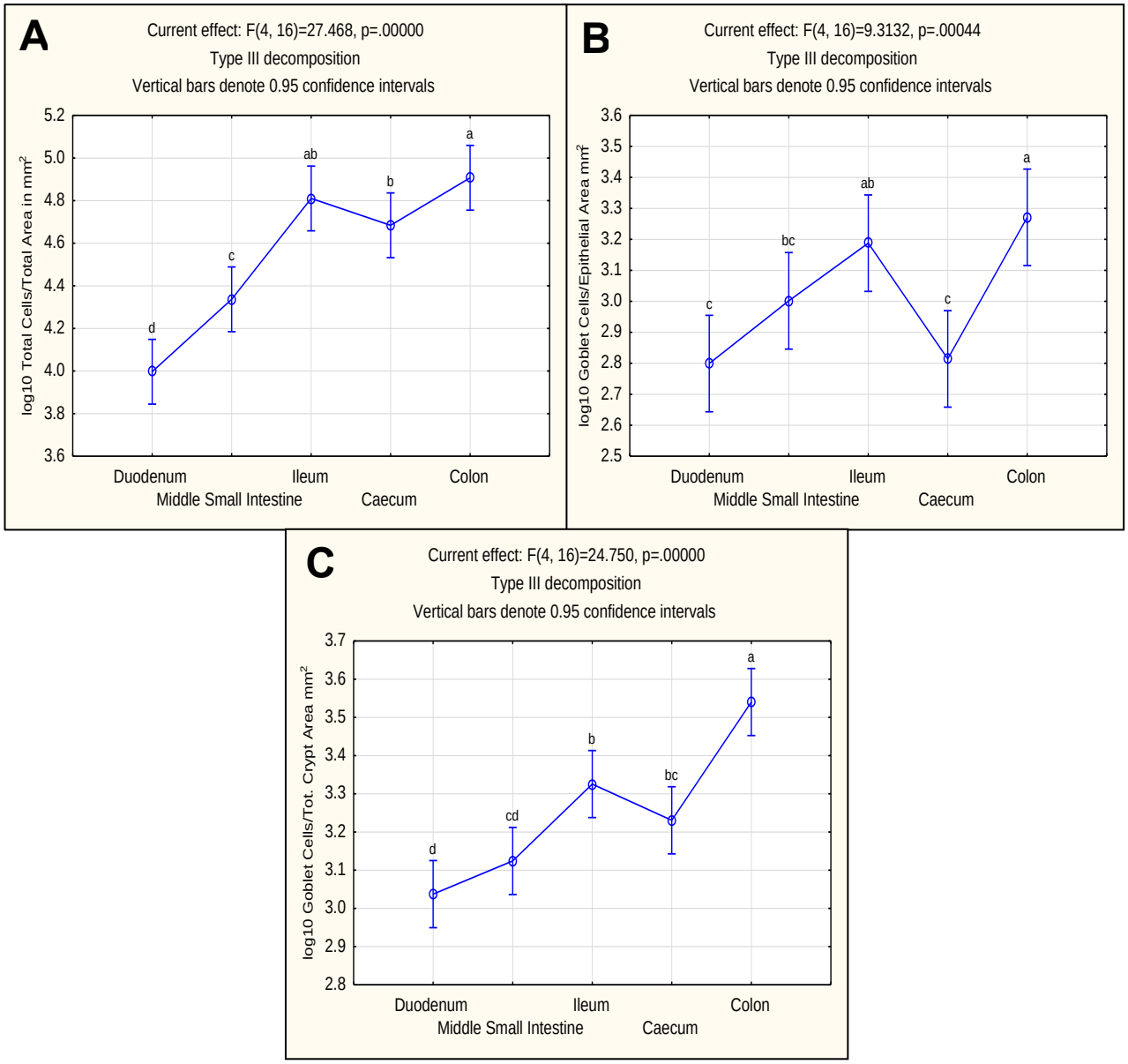

Figure 4.21: The distribution of the total number of mucin secreting goblet cells throughout the GIT of *A. spinosissimus*.

(A) Total number of goblet cells per total area (mm^2).

(B) Goblet cells per surface epithelial area (mm^2).

(C) Goblet cells per crypt area (mm^2).

differences were observed in the number of goblet cells present in the GI regions of the surface epithelial and crypt areas. The number of cells in the crypt area made the largest contribution to the overall distribution trend seen in figure 4.21 diagram A.

The number of acid mucin secreting goblet cells (Figure 4.22 diagram A) was observed to steadily increase from the duodenum to the colon. The distal part of the GIT had considerably more acid goblet cells than the proximal regions. This trend was not observed in the distribution of the cells in the surface epithelial area (Figure 4.22 diagram B), but it correlated with the trend in the crypt area (Figure 4.22 diagram C). A smaller

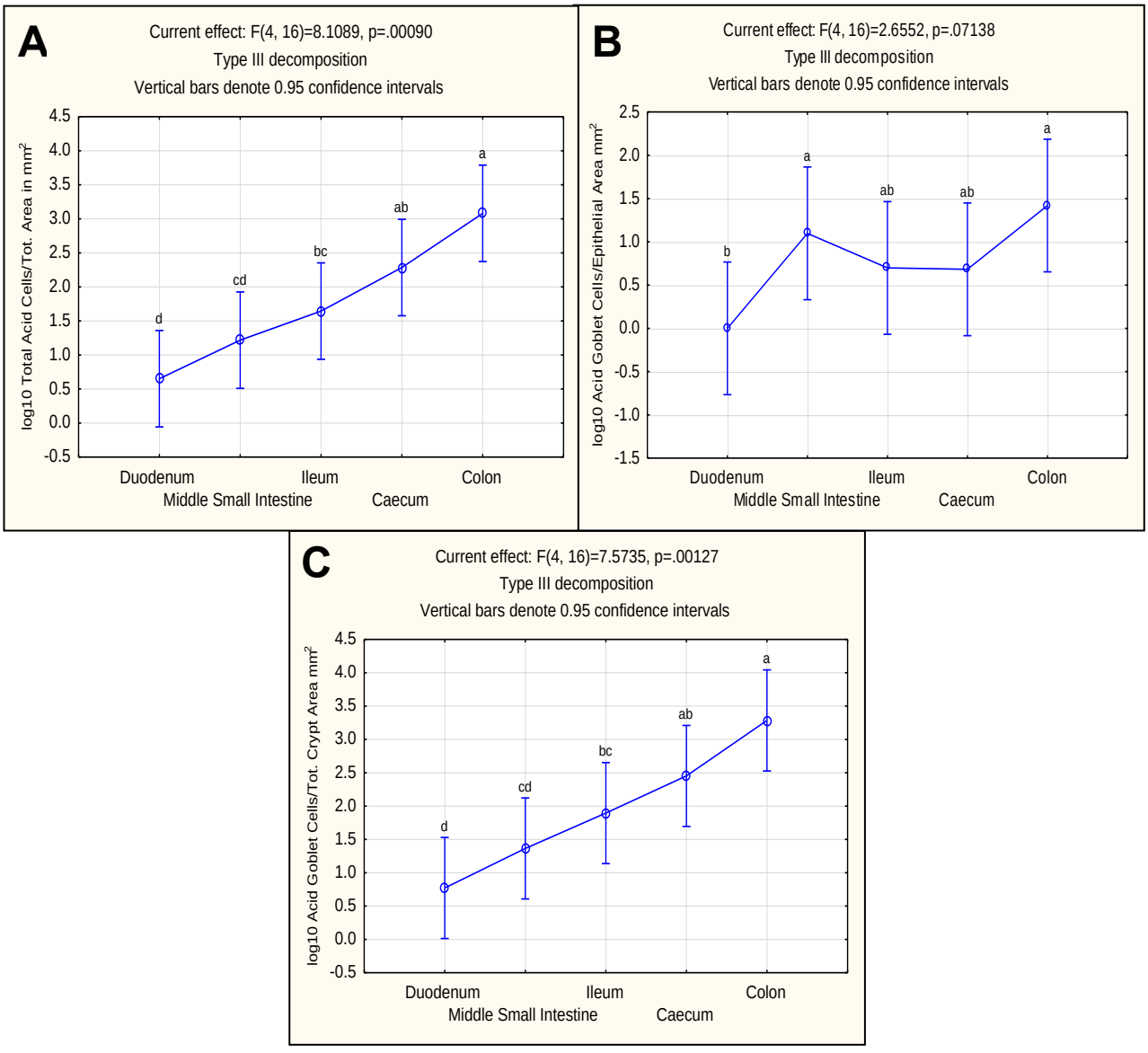

Figure 4.22: The distribution of the total number of acid mucin secreting goblet cells throughout the GIT of *A. spinosissimus*.

(A) Total number of acid goblet cells per total area (mm^2).

(B) Acid goblet cells per epithelial surface area (mm^2).

(C) Acid goblet cells per crypt area (mm^2).

number of acid mucin secreting goblet cells were present in the surface epithelial area than in the crypt area. Therefore, the number of acid goblet cells in the crypt area made the largest contribution to the total number of acid mucin secreting goblet cells (Figure 4.22 diagram A).

The total number of neutral goblet cells (Figure 4.23 diagram A) was considerably higher in the ileum, caecum and colon than in the duodenum and middle small intestine, with a significant difference (p = 0.02) between the middle small intestine and ileum. The distribution of the number of neutral goblet cells in the surface epithelial (Figure 4.23

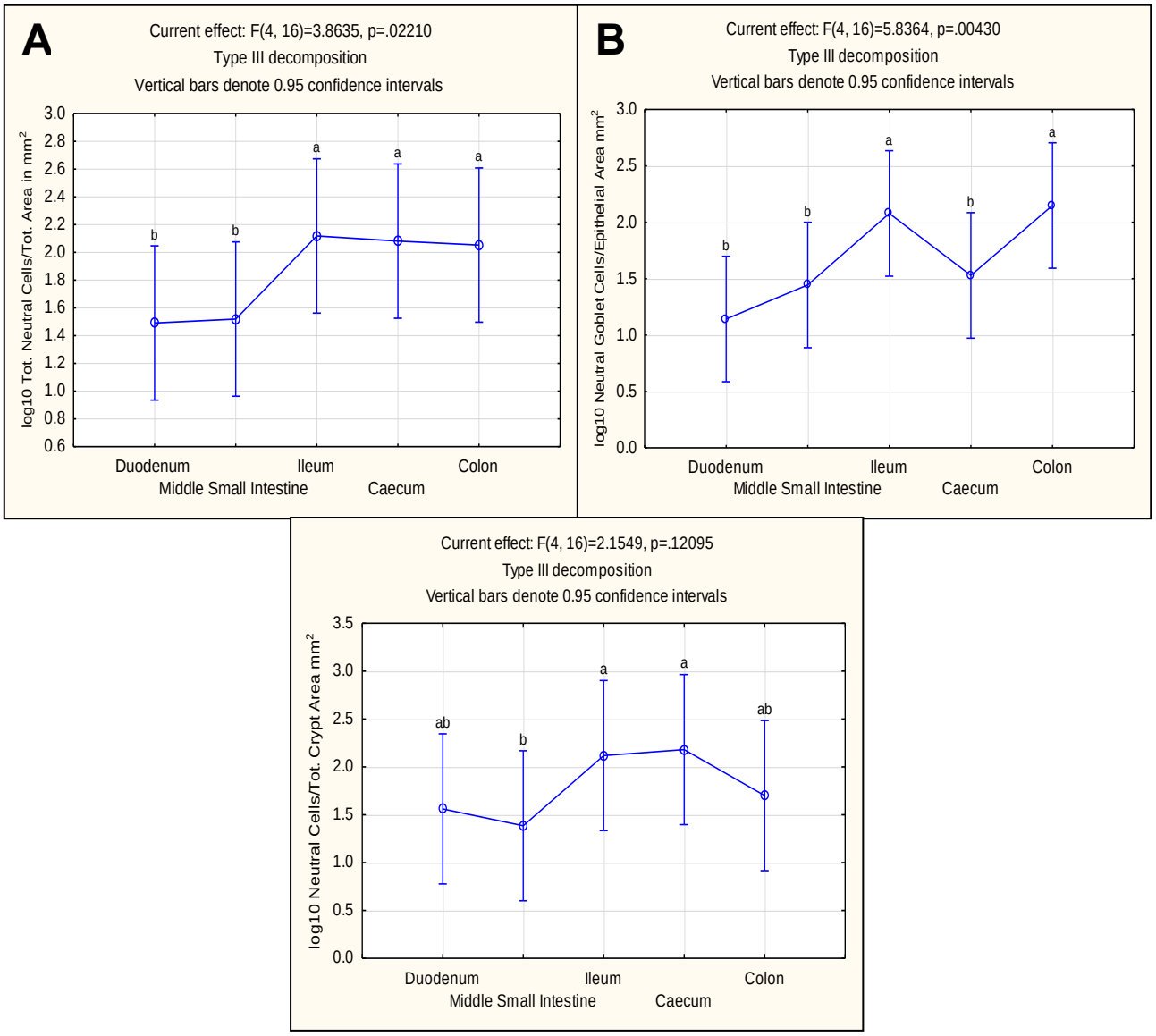

Figure 4.23: The distribution of the total number of neutral mucin secreting goblet cells throughout the GIT of *A. spinosissimus*.

(A) Total number of neutral goblet cells per total area (mm^2).

(B) Neutral goblet cells per epithelial surface area (mm^2).

(C) Neutral goblet cells per crypt area (mm^2).

diagram B) and crypt areas (Figure 4.23 diagram C) appeared different from the trend in figure 4.23 diagram A.

In the surface epithelial area an increase in the number of neutral cells was observed from the duodenum to the ileum, followed by a decrease in the caecum. In the crypt area (Figure 4.23 diagram C), the number of neutral goblet cells in the ileum and caecum were considerably more than in the middle small intestine. Relatively equal numbers of neutral goblet cells were present in both the surface epithelial and crypt areas.

Trends similar to the total number of mixed goblet cells in the total measured area (Figure 4.24 diagram A) were observed in both the surface epithelial (Figure 4.24 diagram B) and

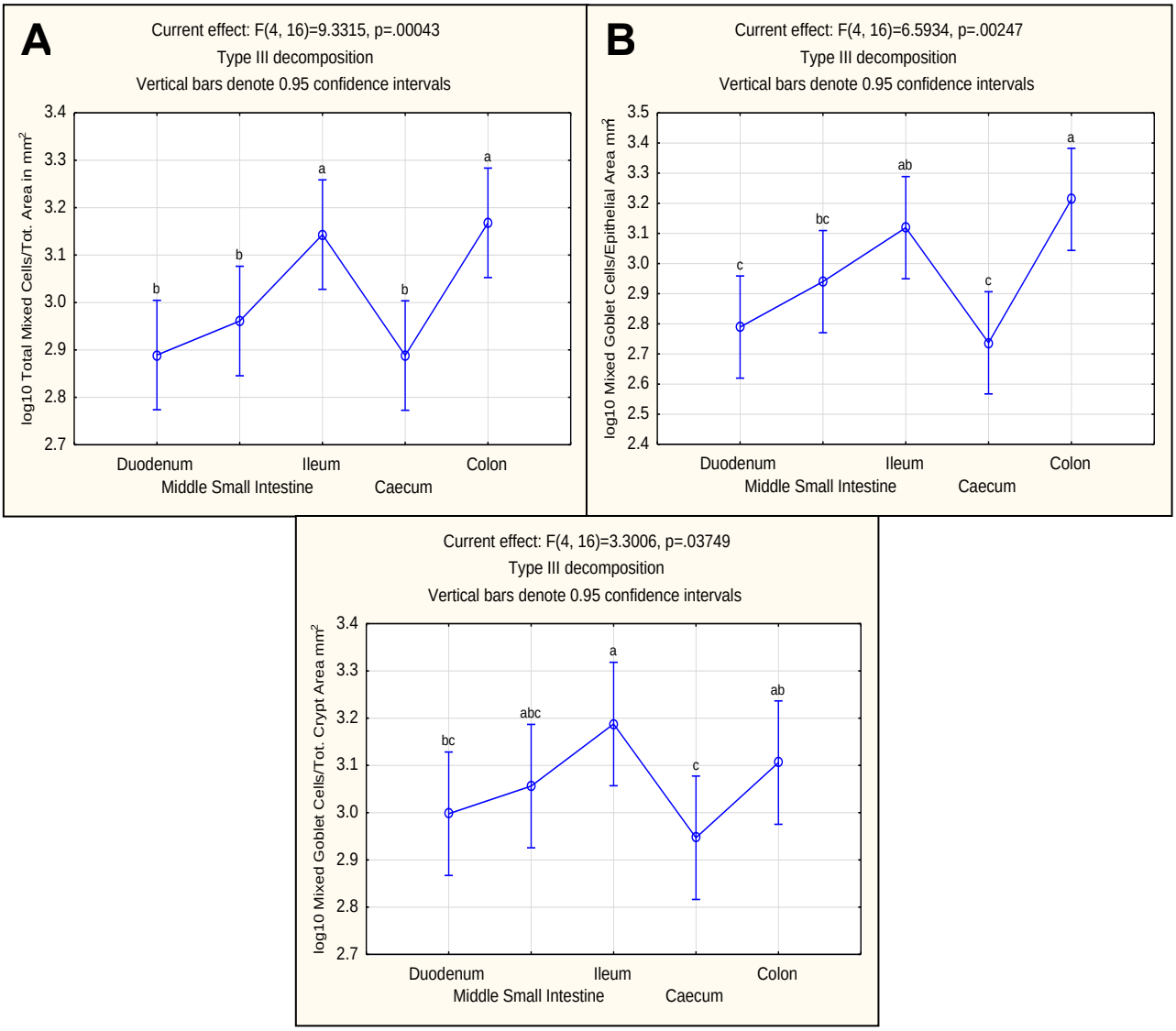

Figure 4.24: The distribution of the total number of mixed mucin secreting goblet cells throughout the GIT of *A. spinosissimus*.

(A) Total number of mixed goblet cells per total area (mm^2).

(B) Mixed goblet cells per epithelial surface area (mm^2).

(C) Mixed goblet cells per crypt area (mm^2).

crypt areas (Figure 4.24 diagram C). The ileum and colon had considerably more mixed goblet cells than the rest of the GI regions, except in the crypt area. All of the graphs (Figure 4.24 diagrams A, B and C) indicated a significant decrease ($p < 0.05$) in the number of cells from the middle small intestine to the caecum. Overall, the crypt areas of each GI region contained more mixed goblet cells than the surface epithelial areas, except in the colon.

4.5.1.1.1 Summary of the results of the AB/PAS technique in *A. spinosissimus*

To summarise the results of the AB/PAS technique:

- The total number of goblet cells per total area (mm^2) measured (Figure 4.21 diagram A) showed a steady increase of cells from the duodenum to the colon. The number of cells per area for each GI region showed a significant increase ($p < 0.05$) in cells, except between the ileum and caecum. Similar observations were made for both the surface epithelial (Figure 4.21 diagram B) and crypt (Figure 4.21 diagram C) areas. In both regions the colon had the largest number of cells in the GIT. Throughout the GIT, the largest number of goblet cells was present in the crypt areas.
- Acid mucin secreting goblet cells (Figure 4.22) increased substantially in number towards the colon. Less acid mucins were present in the surface epithelial areas than in the crypts.
- Neutral mucin secreting goblet cells (Figure 4.23) decreased towards the colon, with the largest number of cells present in the ileum. The surface epithelial areas in the colon contained larger numbers of cells than in the crypts.
- The mixed mucin secreting goblet cells (Figure 4.24) were the most abundant type of goblet cells throughout the GIT. The neutral mucin secreting goblet cells (Figure 4.23) were less than the mixed goblet cells, followed by even fewer acid mucin secreting cells (Figure 4.22) in the GIT. Partitioned goblet cells rarely occurred throughout any of the GI regions.
- The number of acid and mixed mucin secreting goblet cells was higher in the crypts than in the surface epithelial area, whereas the number of neutral goblet cells in both the crypts and epithelial areas were similar.

4.5.1.2 The results of the HID/AB and AF/AB techniques in *A. spinosissimus*

The same trend observed in the AB/PAS stain (Figure 4.21 diagram A) was noted for the total number of goblet cells per total area for the HID/AB stain (Figure 4.25 diagram A). The total number of acid goblet cells (Figure 4.25 diagram A) in the ileum, caecum and colon was considerably higher than in the proximal GI regions, with a significant difference ($p = 0.03$) between the distal regions. The surface epithelial (Figure 4.25 diagram B) and crypt (Figure 4.25 diagram C) areas displayed similar trends than figure 4.25 diagram A,

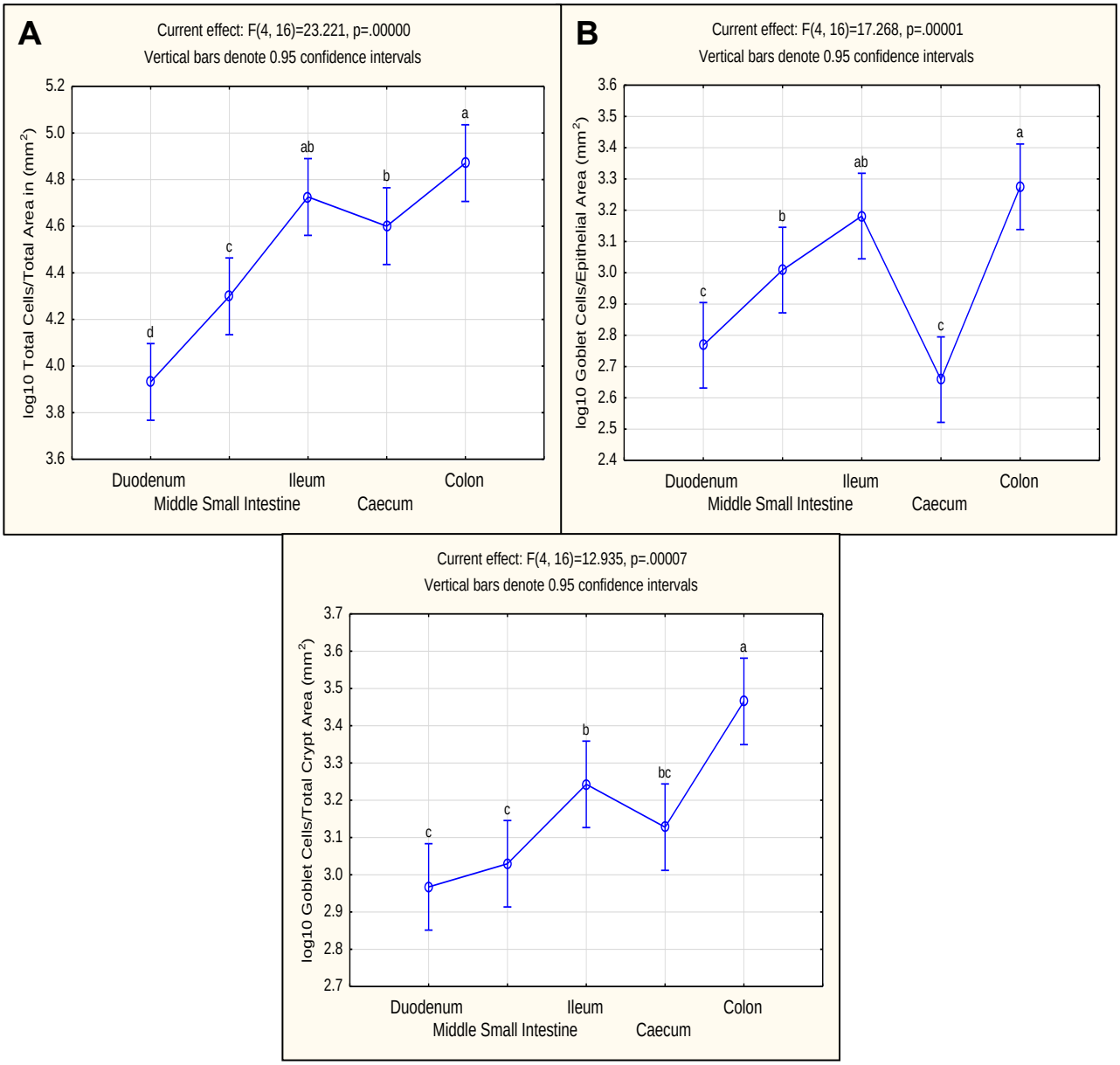

Figure 4.25: The distribution of the total number of acid mucin secreting goblet cells throughout the GIT of *A. spinosissimus*.

(A) Total number of goblet cells per total area (mm^2).

(B) Goblet cells per surface epithelial area (mm^2).

(C) Goblet cells per crypt area (mm^2).

which also indicated the decrease of cells in the caecum. A larger number of cells were present in the crypt areas, especially in the crypts of the caecum.

When distinguishing between the different types of acid mucin goblet cells it was observed that the total number of sulfated goblet cells in the colon was substantially higher than in the duodenum and caecum (Figure 4.26 diagram A). All three graphs, figure 4.26 diagrams A, B and C, displayed a similar trend, specifically referring to the decrease of cells from the middle small intestine to the caecum, followed by a significant increase ($p < 0.01$) in the number of cells in the colon. The number of cells in both the surface epithelial

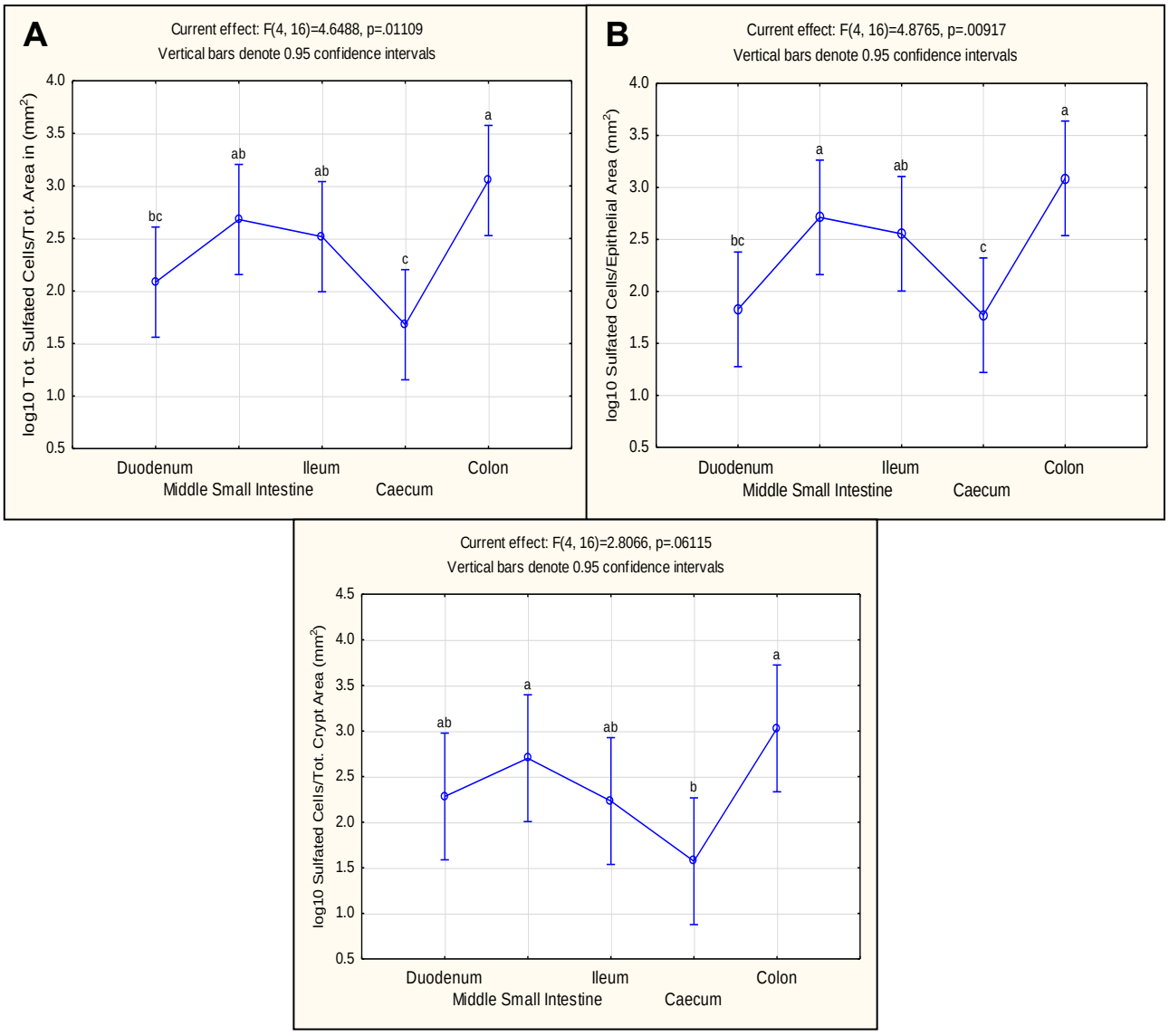

Figure 4.26: The distribution of the total number of sulfomucin secreting goblet cells throughout the GIT of *A. spinosissimus*.

(A) Total number of sulfated goblet cells per total area (mm^2).

(B) Sulfated goblet cells per epithelial surface area (mm^2).

(C) Sulfated goblet cells per crypt area (mm^2).

and crypt areas made a similar contribution to the total number of sulfated goblet cells.

The sulfomucin secreting goblet cells could be further classified as strongly sulfated (Figure 4.27) or weakly sulfated (Figure 4.28) mucin secreting goblet cells. The total number of strongly sulfated mucins (Figure 4.27 diagram A) in the colon was significantly higher ($p < 0.05$) than in the rest of the GI regions. A gradual increase in the number of cells from the duodenum to the colon was observed. These trends were similar to the distribution of the cells in both the surface epithelial (Figure 4.27 diagram B) and crypt

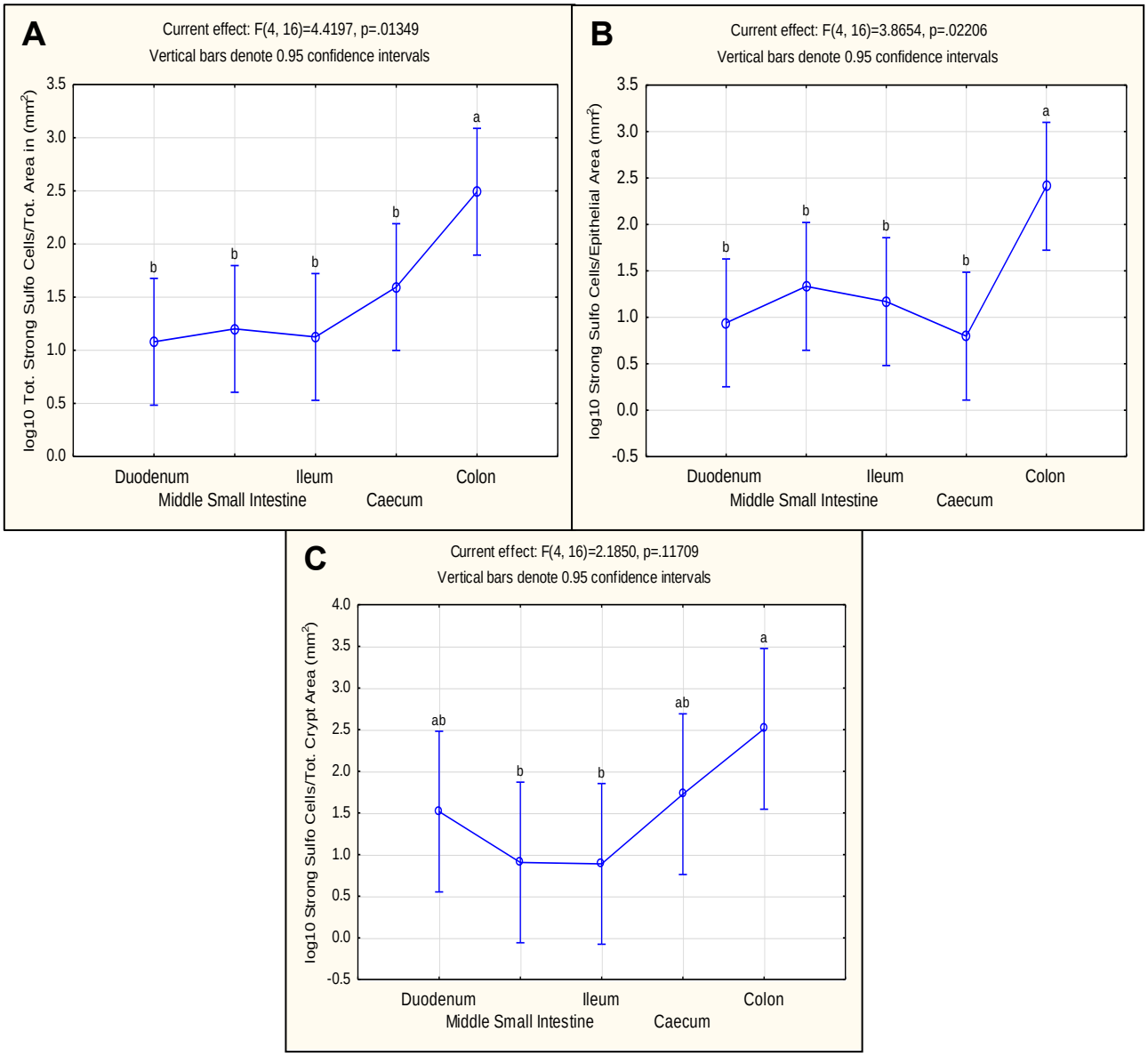

Figure 4.27: The distribution of the total number of strongly sulfated goblet cells throughout the GIT of *A. spinosissimus*.

(A) Total number of strongly sulfated goblet cells per total area (mm^2).

(B) Strongly sulfated goblet cells per epithelial surface area (mm^2).

(C) Strongly sulfated goblet cells per crypt area (mm^2).

areas (Figure 4.27 diagram C). The number of cells in the surface epithelial and crypt areas made a similar contribution to the total number of strongly sulfated goblet cells.

The distribution of the weakly sulfated goblet cells were somewhat similar in all three graphs of figure 4.28, namely graphs A, B, and C. In graphs A and C, the largest number of weakly sulfated goblet cells was present in the colon, whereas in the surface epithelial area (Figure 4.28 diagram B) it was present in the ileum. As a whole, the duodenum had

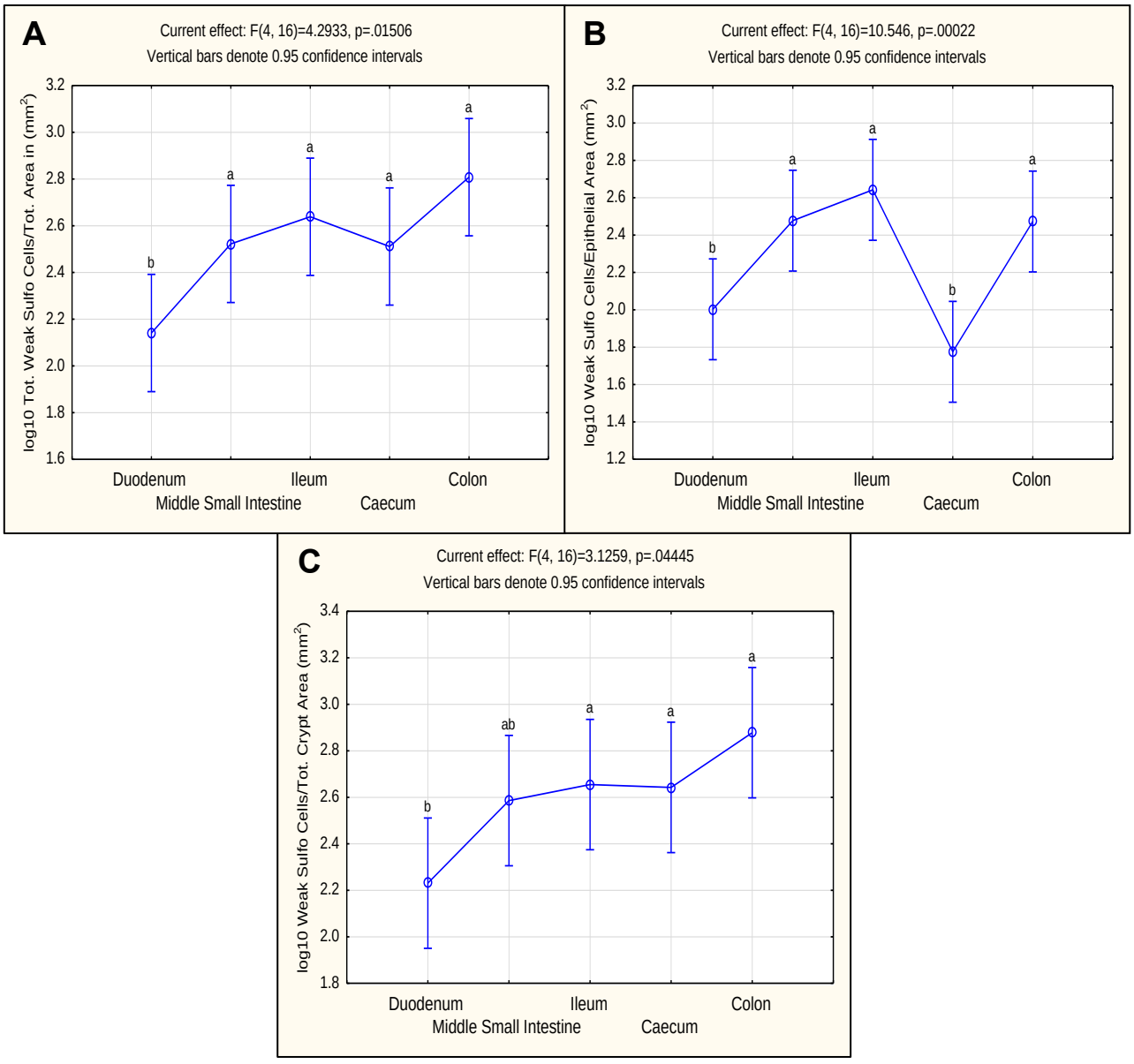

Figure 4.28: The distribution of the total number of weakly sulfated goblet cells throughout the GIT of *A. spinosissimus*.

(A) Total number of weakly sulfated goblet cells per total area (mm^2).

(B) Weakly sulfated goblet cells per epithelial surface area (mm^2).

(C) Weakly sulfated goblet cells per crypt area (mm^2).

substantially less goblet cells than the rest of the GI regions, as well as the surface epithelial area of the caecum. The number of weakly sulfated goblet cells in the crypt areas made a larger contribution to the total number of weakly sulfated goblet cells, than the cells in the surface epithelial area. In general, more weakly sulfated than strongly sulfated goblet cells were present in both the surface epithelial and crypt areas.

The distribution of the sialomucin secreting goblet cells was similar in graphs A, B and C of figure 4.29. From the duodenum to the caecum there were a consistent number of sialomucin goblet cells, without any substantial differences between the regions. However,

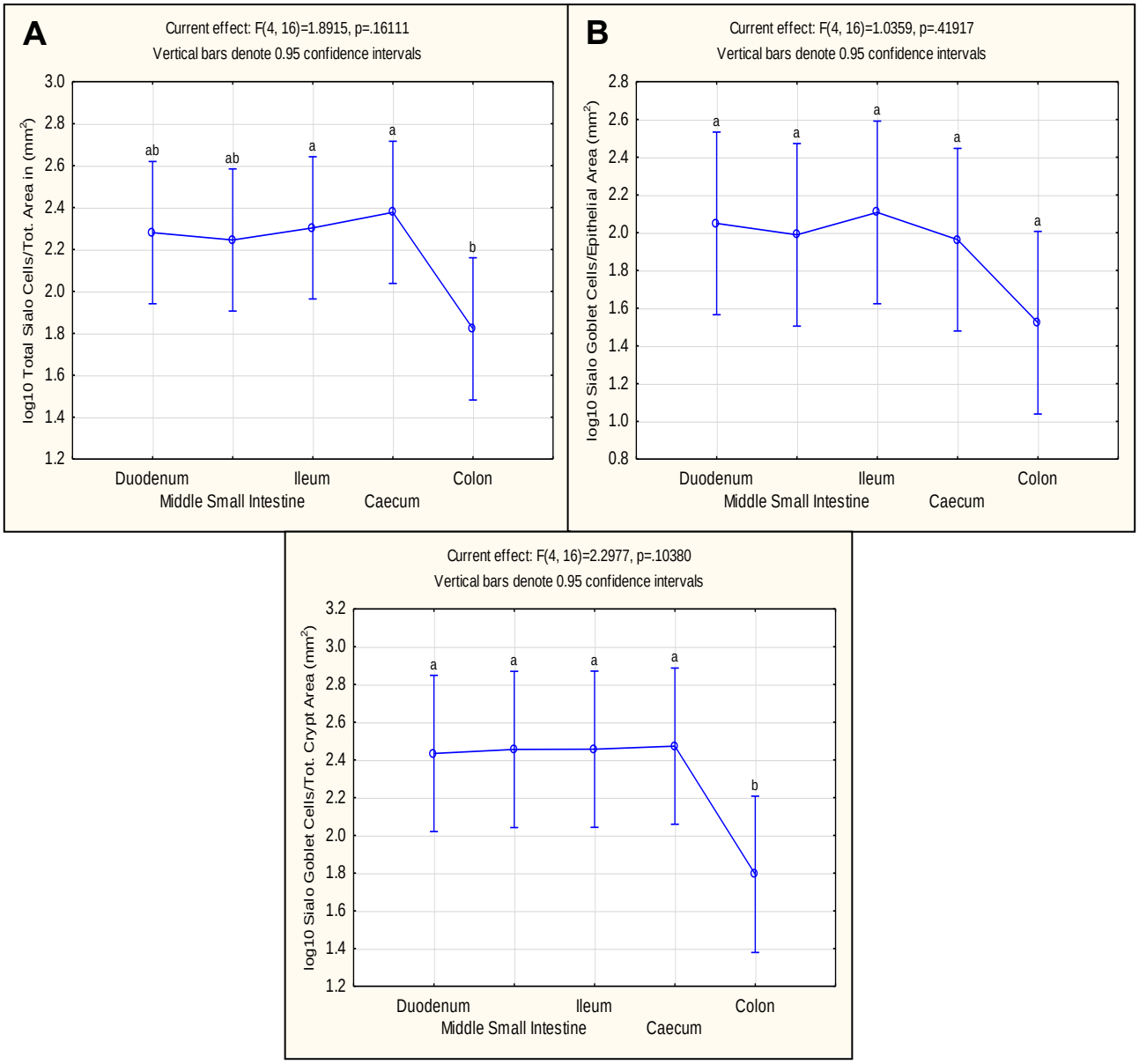

Figure 4.29: The distribution of the total number of sialomucin secreting goblet cells throughout the GIT of *A. spinosissimus*.

(A) Total number of sialo goblet cells per total area (mm^2).

(B) Sialo goblet cells per epithelial surface area (mm^2).

(C) Sialo goblet cells per crypt area (mm^2).

in the colon there was a substantial decrease in the number of sialomucin goblet cells. The largest number of sialomucin goblet cells was present in the crypt areas.

The mixed acid goblet cells were a combination of the sulfo- and sialomucin granules within a single mucin secreting goblet cell. The distribution trend of the total number of mixed acid goblet cells (Figure 4.30 diagram A) showed some similarities to figure 4.30 diagram B, but were more comparable with figure 4.30 diagram C. Diagrams A and C indicated that the colon and ileum had noticeably larger numbers of goblet cells than the

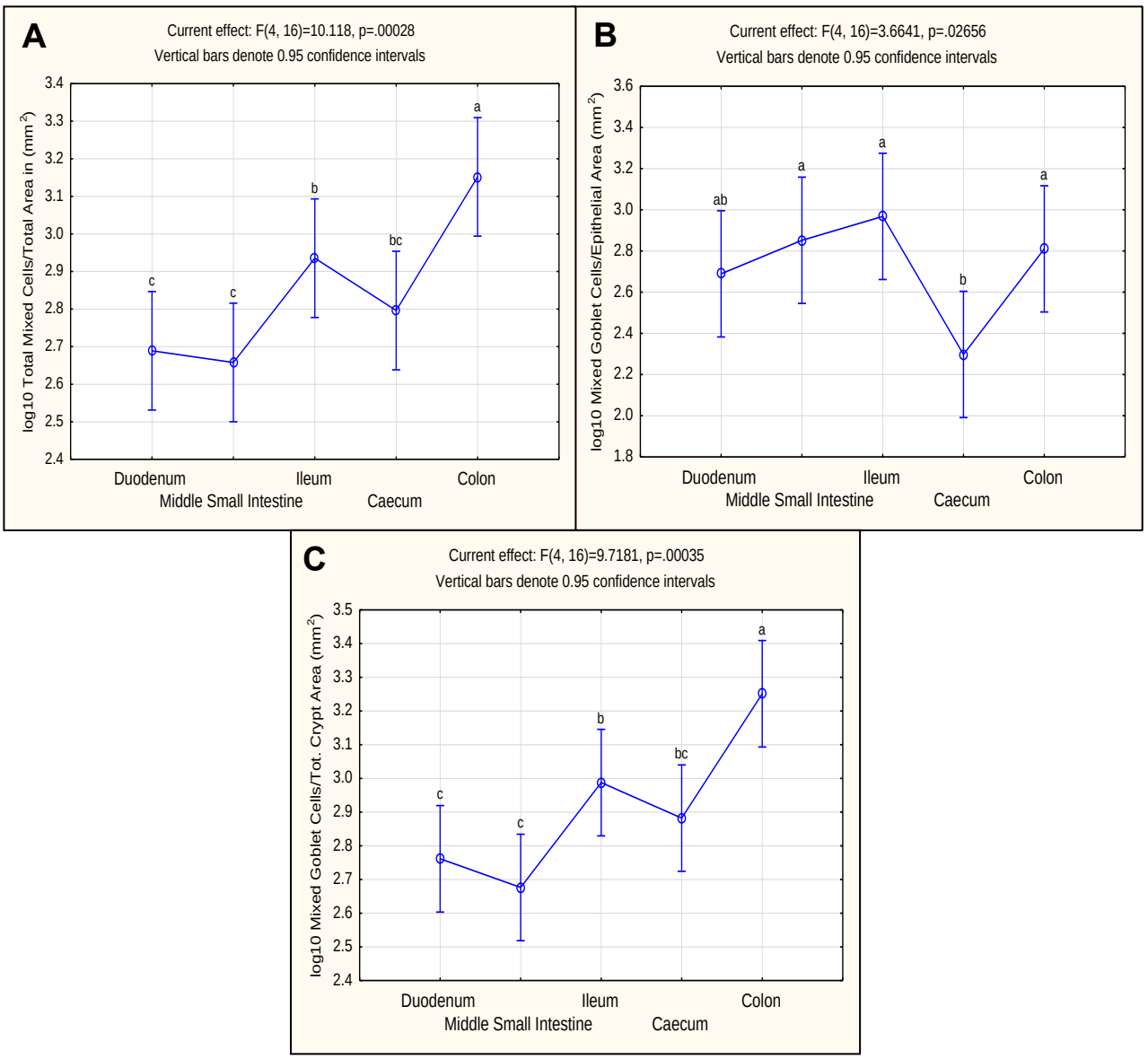

Figure 4.30: The distribution of the total number of mixed acid mucin secreting goblet cells throughout the GIT of *A. spinosissimus*.

(A) Total number of mixed goblet cells per total area (mm^2).

(B) Mixed goblet cells per epithelial surface area (mm^2).

(C) Mixed goblet cells per crypt area (mm^2).

proximal GI regions. However, in the surface epithelial area (Figure 4.30 diagram B), the highest number of mixed goblet cells were present in the ileum. All three graphs showed a decrease in the number of cells in the caecum, but it was most significantly observed in the surface epithelial area.

4.5.1.2.1 Summary of the results of the HID/AB and AF/AB techniques in *A. spinosissimus*

To summarise the results of the HID/AB and AF/AB techniques:

- The total number of mucin secreting goblet cells (Figure 4.25) showed a similar trend as observed in the AB/PAS technique shown in figure 4.21. The number of cells per area for each GI region showed a statistically significant increase ($p < 0.05$) in cells, except between the ileum and caecum. The colon had the largest number of cells in the GIT. Throughout the GIT, the largest number of goblet cells was present in the crypt areas.
- The number of sulfomucin secreting goblet cells in both the surface epithelial (Figure 4.26 diagram B) and crypt (Figure 4.26 diagram C) areas had a similar trend. There was a decrease in the number of cells from the middle small intestine to the caecum, followed by a statistically significant increase ($p < 0.01$) of cells in the colon.
- The sulfomucin secreting goblet cells were further divided into strongly (Figure 4.27) and weakly (Figure 4.28) sulfated goblet cells. The number of weakly sulfated goblet cells was more numerous in both the surface epithelial and crypt areas than the strongly sulfated goblet cells. The strongly sulfated goblet cells increased steadily from the duodenum to the caecum, followed by a statistically significant increase ($p < 0.05$) of cells in the colon. However, for the weakly sulfated goblet cells in the surface epithelial area (Figure 4.28 diagram B) there was a significant decrease ($p < 0.01$) of cells in the caecum, followed by a substantial increase of cells in the colon. The number of weakly sulfated cells in the crypt areas (Figure 4.28 diagram C) increased steadily throughout the GIT, with a noteworthy increase of cells between the duodenum and the colon.
- The distribution of the sialomucins (Figure 4.29) throughout the GIT was steady, with a substantial decrease of cells in the colon. Similar patterns were observed in both the surface epithelial (Figure 4.29 diagram B) and crypt (Figure 4.29 diagram C) areas. The largest number of sialomucin goblet cells was present in the crypts.

- Mixed acid mucin secreting goblet cells are a combination of the sulfo- and sialomucin granules found within a single goblet cell. The number of mixed acid mucins (Figure 4.30) represented a similar distribution trend as the total number of goblet cells as seen in figure 4.25. In the epithelial surface area (Figure 4.30 diagram B) there was a noteworthy decrease of cells in the caecum, followed by a substantial increase of cells in the colon. The largest number of goblet cells in the epithelial area was present in the ileum. In the crypt area (Figure 4.30 diagram C), the colon had significantly more cells than the other GI regions. There were considerable increases of mixed acid goblet cells between the middle small intestine and ileum, as well as between the caecum and the colon.
- It can be concluded from the results listed above that the mixed mucin secreting goblet cells were more abundant, followed by the weakly sulfated and sialomucin secreting goblet cells.

4.5.2 The gastrointestinal mucin histochemistry results of *C. cyanea* and *A. hottentotus*

4.5.2.1 The results of the AB/PAS technique in *C. cyanea* and *A. hottentotus*

The total number of goblet cells per total area measured (mm^2) (Figure 4.31 diagram A), reflected all of the accumulated data in its entirety which provided an overall distribution pattern of the mucin secreting goblet cells throughout the GIT. *C. cyanea* had statistically significantly more mucin secreting goblet cells in the surface epithelial (Figure 4.31 diagram B) and crypt (Figure 4.31 diagram C) areas than *A. hottentotus* (p = 0.0001 and p

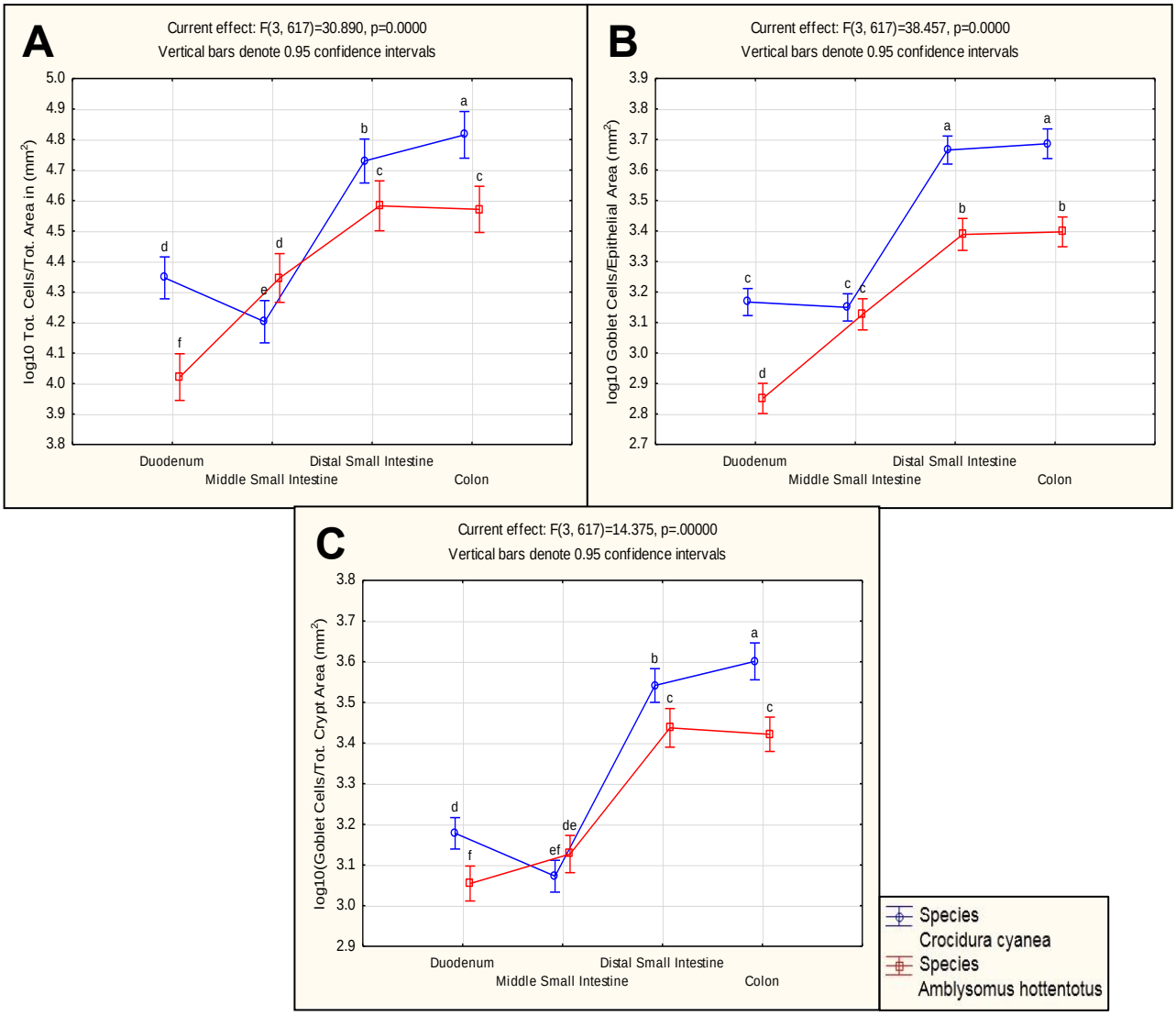

Figure 4.31: The distribution of the total number of mucin secreting goblet cells throughout the GITs of *C. cyanea* and *A. hottentotus*.

(A) Total number of goblet cells per total area (mm^2).

(B) Goblet cells per surface epithelial area (mm^2).

(C) Goblet cells per crypt area (mm^2).

= 0.004 respectively). The distribution of mucin secreting goblet cells in the surface epithelial and crypt areas showed similar trends, and also appeared similar to the overall trend in figure 4.31 diagram A. In both species (*A. hottentotus* & *C. cyanea*) the distal part of the GIT had considerably more mucin secreting goblet cells per area measured (mm^2) than the proximal GI regions.

The total number of goblet cells in both *C. cyanea* and *A. hottentotus* revealed similar distribution trends, but marked differences were observed in the number of cells per GI region. Overall, *C. cyanea* has a significantly larger ($p = 0.013$) number of goblet cells than *A. hottentotus*. When distinguishing between the distributions of the different types of mucin secreting goblet cells in each species, there were clear differences in both the number of cells and their distribution.

The total number of neutral mucin secreting goblet cells of *C. cyanea* was significantly more ($p = 0.0006$) than that of *A. hottentotus* (Figure 4.32 diagram A). In *C. cyanea* the distal small intestine had noticeably more neutral mucin secreting goblet cells than the rest of the GI regions. This was also observed in the surface epithelial (Figure 4.32 diagram B) and crypt (Figure 4.32 diagram C) areas. The distribution of the neutral mucin secreting goblet cells in *A. hottentotus* differed substantially from *C. cyanea*. The number of neutral goblet cells in *A. hottentotus* primarily increased towards the colon, except in the crypt areas. However, for *C. cyanea,* there was a decrease in the number of neutral goblet cells towards the colon.

In general, *A. hottentotus* had an extensively greater number of acid mucin secreting goblet cells than *C. cyanea* per measured area (mm^2) (Figure 4.33 diagram A). *C. cyanea* only had a few acid goblet cells in the surface epithelial (Figure 4.33 diagram B) area of the colon. The total number of acid mucin secreting goblet cells (Figure 4.33 diagram A) in *A. hottentotus* showed a gradual increase in the number of cells throughout the GIT with statistically significant increases ($p < 0.01$) between the GI regions. In addition, there was an increase in the number of acid goblet cells in the crypts of the distal GI regions, whereas the surface epithelial areas showed a decrease in the number of cells towards the colon.

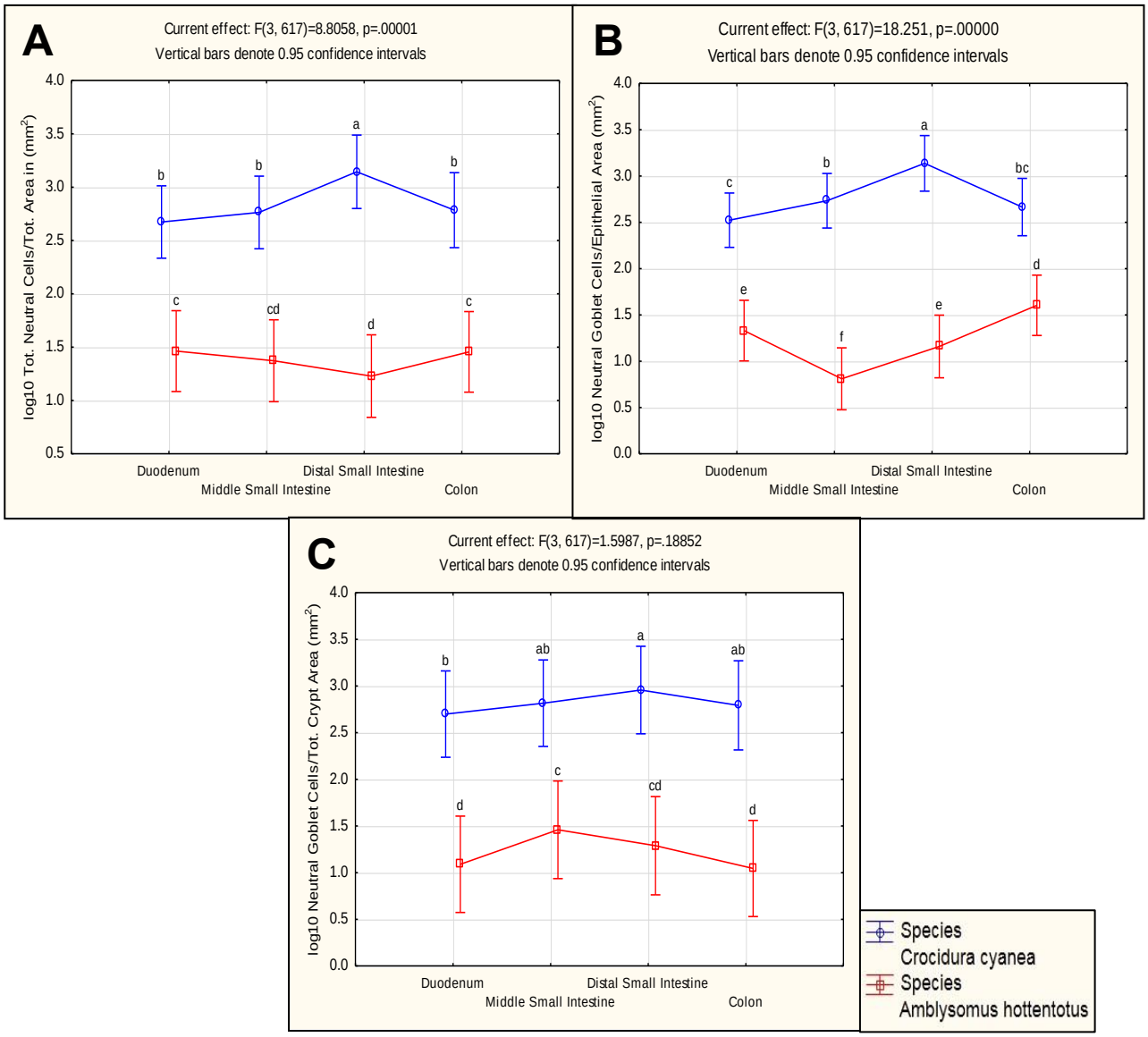

Figure 4.32: The distribution of the total number of neutral mucin secreting goblet cells throughout the GITs of *C. cyanea* and *A. hottentotus*.

(A) Total number of neutral goblet cells per total area (mm^2).

(B) Neutral goblet cells per epithelial surface area (mm^2).

(C) Neutral goblet cells per crypt area (mm^2).

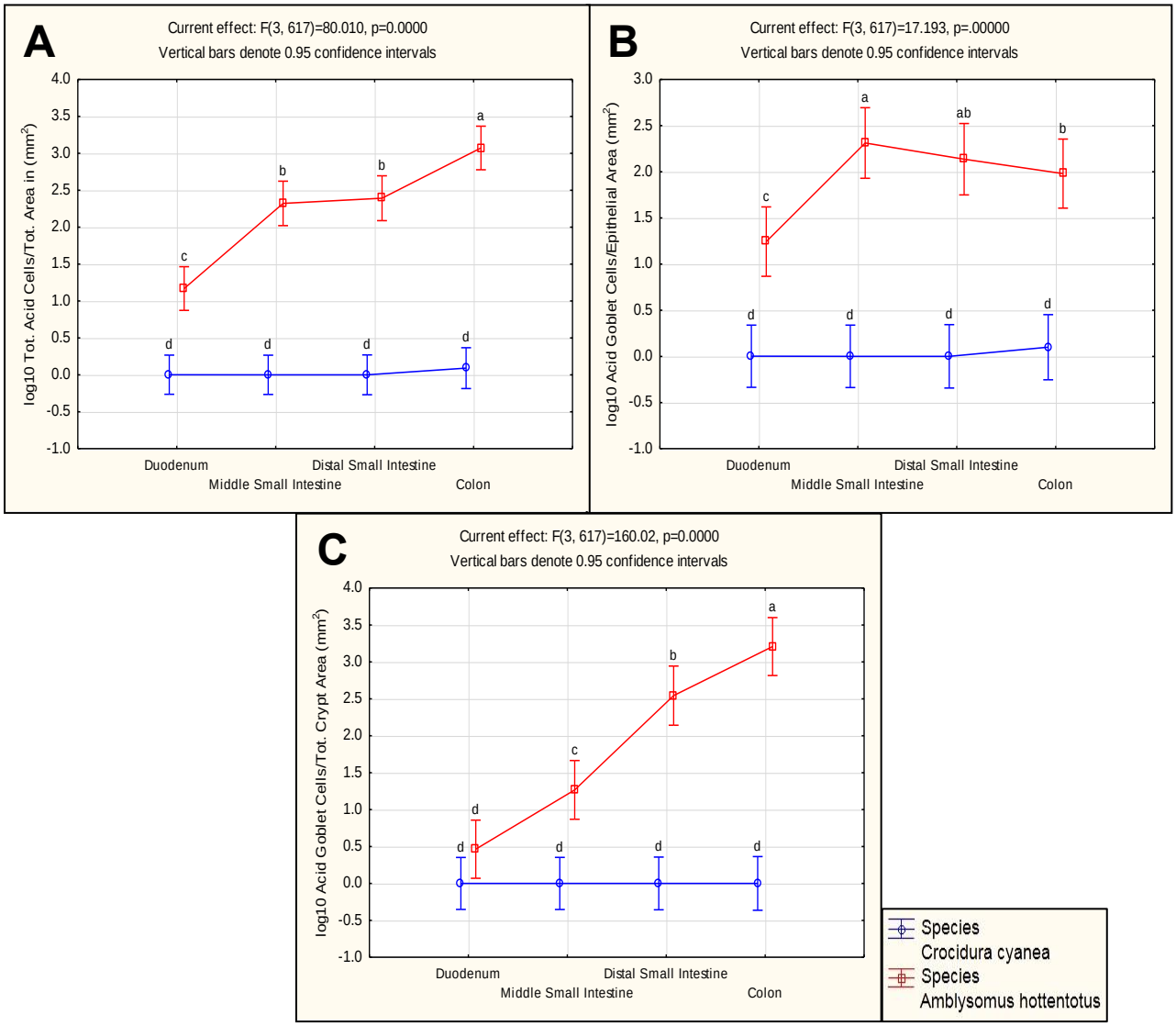

Figure 4.33: The distribution of the total number of acid mucin secreting goblet cells throughout the GIT of *C. cyanea* and *A. hottentotus*.

(A) Total number of acid goblet cells per total area (mm^2).

(B) Acid goblet cells per epithelial surface area (mm^2).

(C) Acid goblet cells per crypt area (mm^2).

The total number of mixed (acid & neutral) mucin (Figure 4.34 diagram A) secreting goblet cells per measured area (mm^2) of *C. cyanea* was significantly higher (p = 0.006) than in *A. hottentotus*. Both species indicated that the distal GI regions had considerably more mixed mucin secreting goblet cells than the proximal regions. Different from *C. cyanea*, *A. hottentotus* showed a decrease in the number of mixed mucin secreting goblet cells in the colon. Both the surface epithelial (Figure 4.34 diagram B) and crypt (Figure 4.34 diagram C) areas revealed similar trends than figure 4.34 diagram A. *C. cyanea* had significantly more (p = 0.0003) mixed mucin secreting goblet cells per area measured (mm^2) than *A. hottentotus* in the surface epithelial area but not in the crypt area.

The crypt areas (Figure 4.34 diagram C) of *A. hottentotus* differed from the trends in images A and C, and illustrated a substantial decrease of mixed mucin secreting goblet cells between the proximal GI regions.

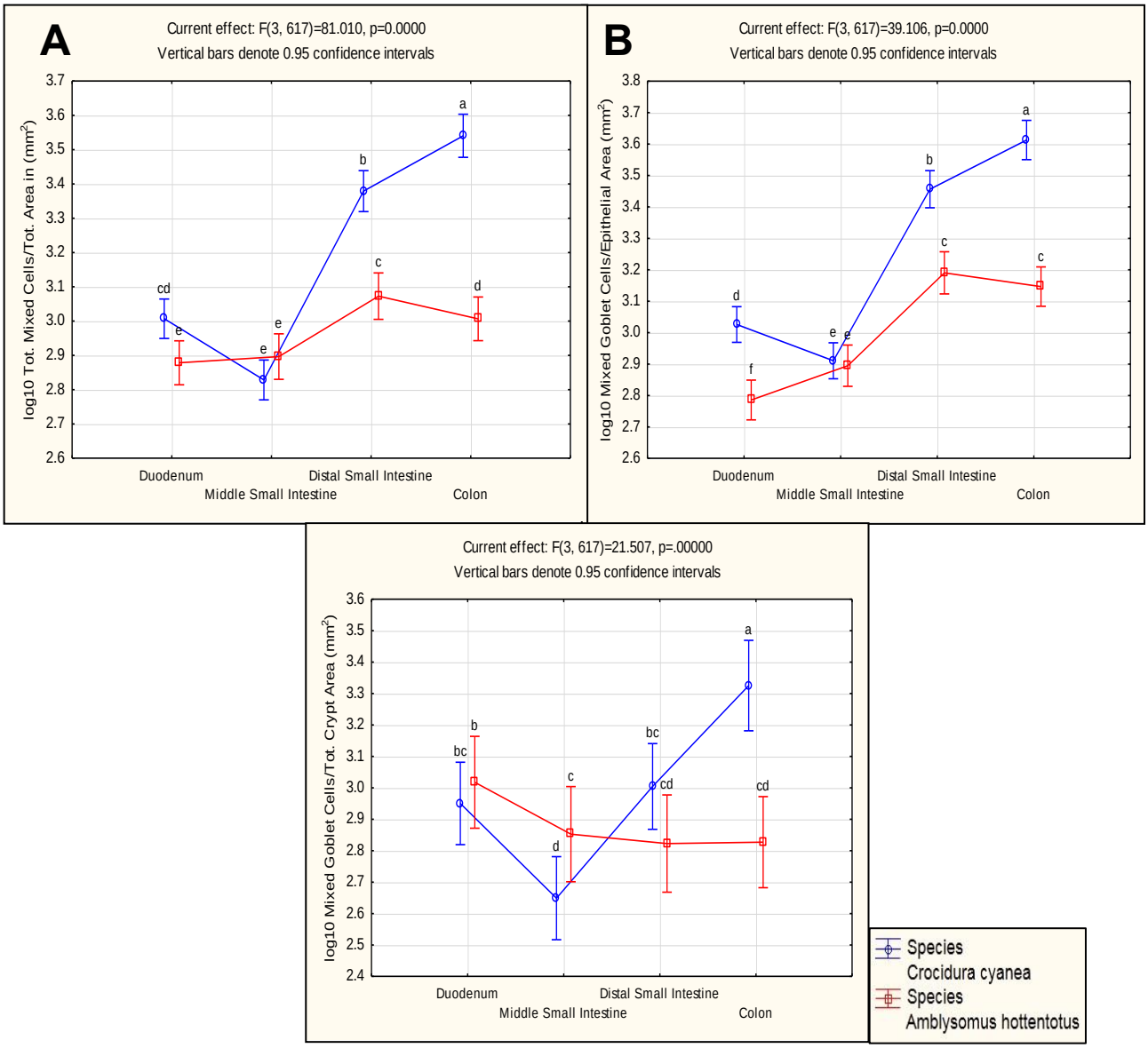

Figure 4.34: The distribution of the total number of mixed mucin secreting goblet cells throughout the GIT of *C. cyanea* and *A. hottentotus*.

(A) Total number of mixed goblet cells per total area (mm^2).

(B) Mixed goblet cells per epithelial surface area (mm^2)

(C) Mixed goblet cells per crypt area (mm^2).

4.5.2.2 The results of the HID/AB and AF/AB techniques in *C. cyanea* and *A. hottentotus*

Among *C. cyanea* and *A. hottentotus*, no statistically significant difference was observed in the total number of acid mucin secreting goblet cells measured per mm^2 (Figure 4.35 diagram A). However, *C. cyanea* had significantly more acid mucin secreting goblet cells than *A. hottentotus* in both the surface epithelial (Figure 4.35 diagram B) and crypt (Figure 4.35 diagram C) areas (p = 0.01 and p = 0.0001 respectively). The distribution of the acid

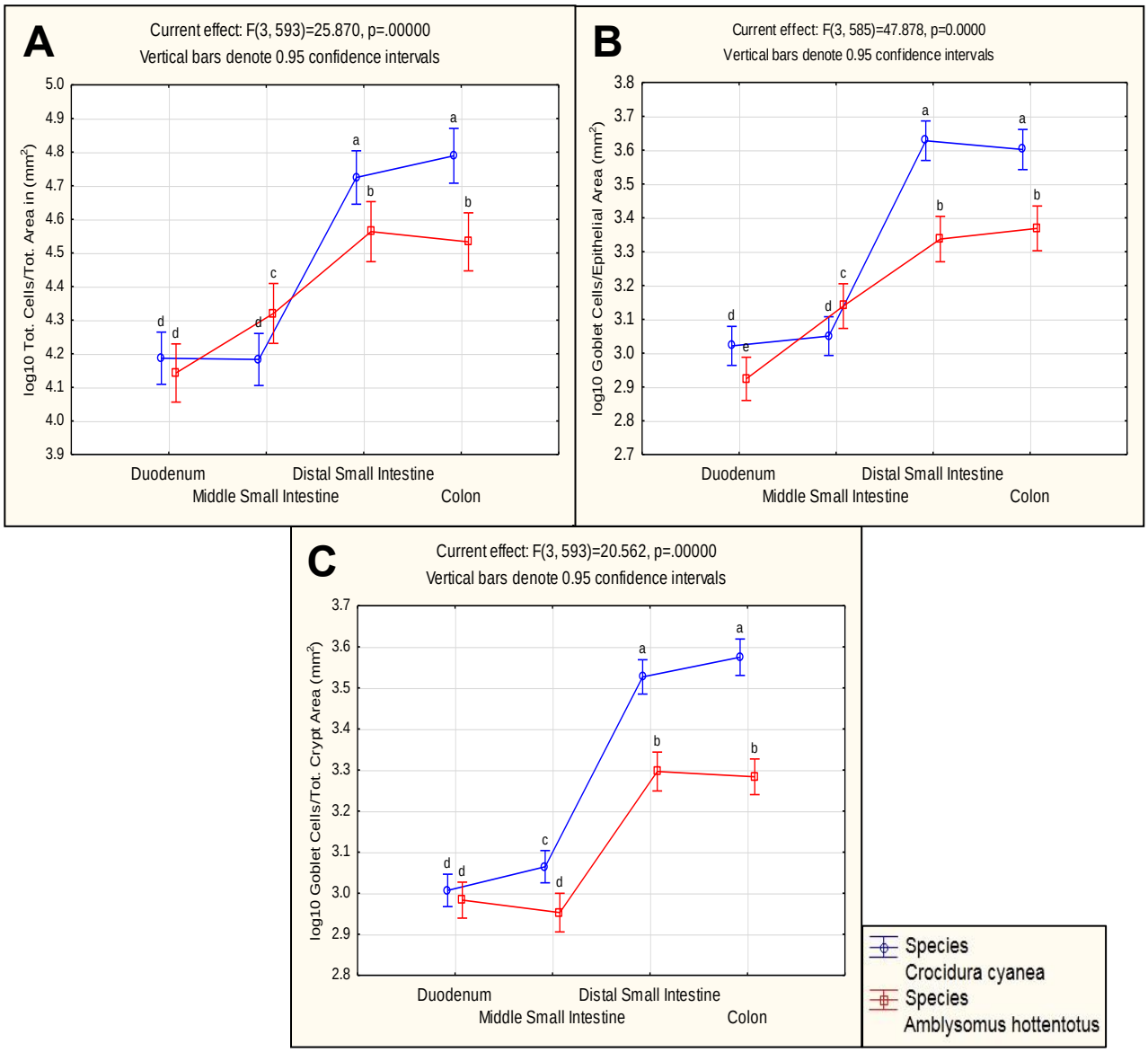

Figure 4.35: The distribution of the total number of acid (sulfo- and sialomucins) mucin secreting goblet cells throughout the GITs *of C. cyanea* and *A. hottentotus*.

(A) Total number of acid goblet cells per total area (mm^2).

(B) Acid goblet cells per epithelial surface area (mm^2).

(C) Acid goblet cells per crypt area (mm^2).

mucin secreting goblet cells in both the surface epithelial and crypt areas appeared similar, with both species indicating that the distal GI regions had a larger number of cells than the proximal regions. A comparable number of cells were present in both the surface epithelial and crypt areas.

Similar to the AB/PAS results of *C. cyanea* and *A. hottentotus*, clear differences were observed in the distribution and number of the different acid mucins in each species. The distribution trend of the total number of sulfomucin secreting goblet cells (Figure 4.36 diagram A) were similar to the trends in the surface epithelial (Figure 4.36 diagram B) and

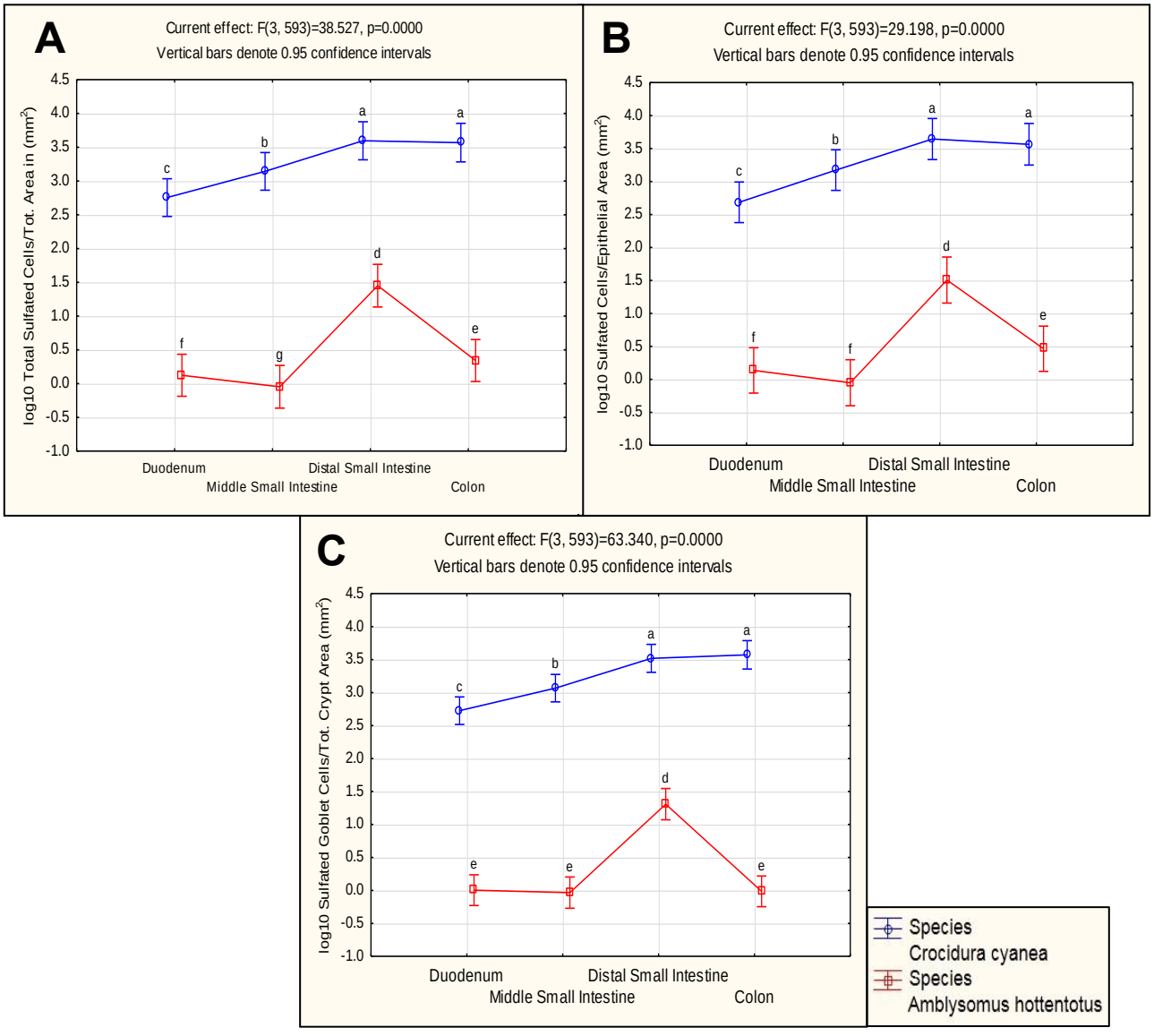

Figure 4.36: The distribution of the total number of sulfomucin secreting goblet cells throughout the GITs of *C. cyanea* and *A. hottentotus*.

(A) Total number of sulfated goblet cells per total area (mm^2).

(B) Sulfated goblet cells per epithelial surface area (mm^2).

(C) Sulfated goblet cells per crypt area (mm^2).

crypt areas (Figure 4.36 diagram C). Overall, *C. cyanea* had a significantly larger ($p < 0.01$) number of sulfomucin secreting goblet cells than *A. hottentotus*. In *C. cyanea*, the sulfomucin secreting goblet cells were more in the distal than the proximal GI regions. *A. hottentotus* had a small number of sulfomucin secreting goblet cells throughout the GIT, with the largest number of cells in the distal small intestine.

The sulfomucin secreting goblet cells could be further subdivided into strongly and weakly sulfated mucin secreting goblet cells, based on how intensely the cells were stained. *C. cyanea* had a significantly larger ($p < 0.01$) number of strongly sulfated goblet cells (Figure 4.37Figure 4.37) than *A. hottentotus*. The total number of strongly sulfated goblet cells (Figure 4.37 diagram A) in *C. cyanea*, increased extensively from the duodenum to the distal small intestine. However, A*. hottentotus* only contained strongly sulfated goblet cells in the distal GI regions. The distribution of the total number of strongly sulfated goblet cells (Figure 4.37 diagram A) had a similar trend as the surface epithelial (Figure 4.37 diagram B) and crypt (Figure 4.37 diagram C) areas of both *C. cyanea* and *A. hottentotus*. Compared to the colon surface epithelial area of *C. cyanea*, the crypt area showed an increase of cells. Overall, the largest number of strongly sulfated cells in both species was present in the surface epithelial areas.

The distribution trend of the weakly sulfated goblet cells in *C. cyanea and A. hottentotus* (Figure 4.38 diagram A), appeared similar than the trend of the strongly sulfated goblet cells in figure 4.37 diagram A. The total number of weakly sulfated goblet cells was significantly more ($p = 0.00002$) in *C. cyanea* than in *A. hottentotus*. In *A. hottentotus*, the proximal GI regions had little to no weakly sulfated goblet cells. Both of the surface epithelial (Figure 4.38 diagram B) and crypt (Figure 4.38 diagram C) areas also revealed similar trends than figure 4.37 diagram A. In both species, the number of weakly sulfated goblet cells was more abundant than the strongly sulfated goblet cells.

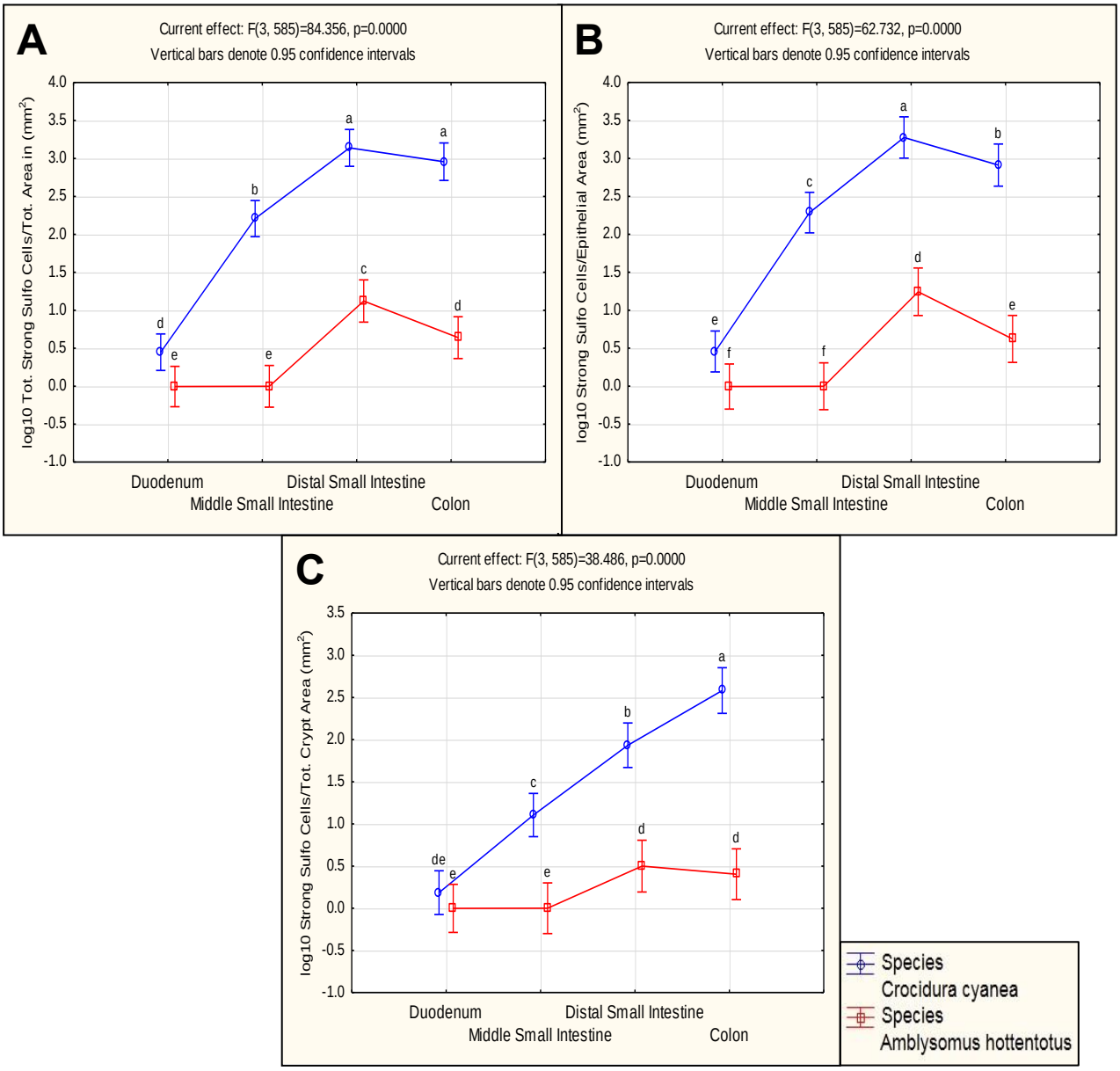

Figure 4.37: The distribution of the total number of strongly sulfated goblet cells throughout the GITs of *C. cyanea* and *A. hottentotus*.

(A) Total number of strong sulfomucin goblet cells per total area (mm^2).

(B) Strongly sulfated goblet cells per epithelial surface area (mm^2).

(C) Strongly sulfated goblet cells per crypt area (mm^2).

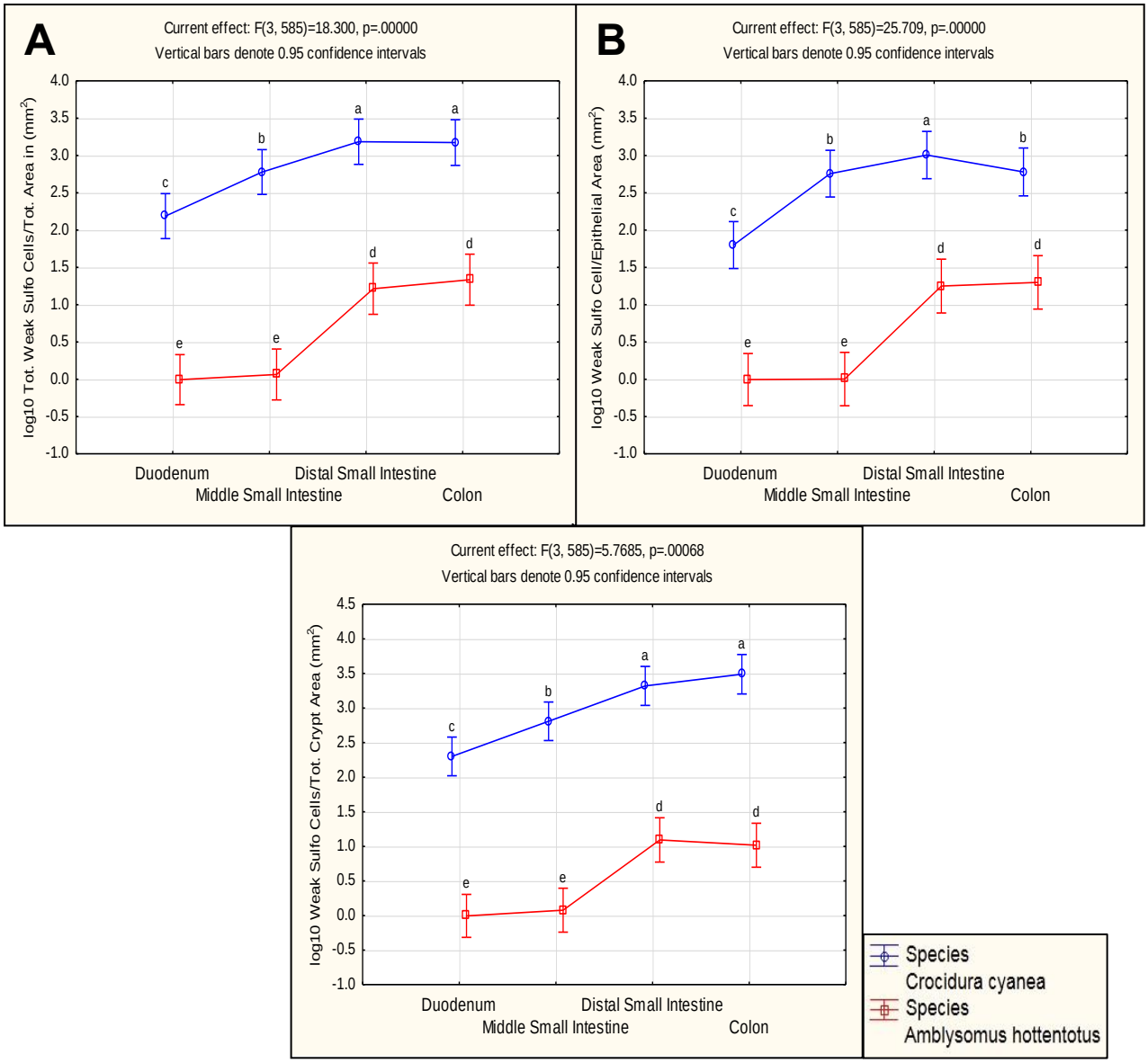

Figure 4.38: The distribution of the total number of weakly sulfated goblet cells throughout the GITs of *C. cyanea* and *A. hottentotus*.

(A) Total number of weak sulfomucin goblet cells per total area (mm^2).

(B) Weakly sulfated goblet cells per epithelial surface area (mm^2).

(C) Weakly sulfated goblet cells per crypt area (mm^2).

Sialomucin secreting goblet cells was found to be more abundant in *A. hottentotus* than any other type of acid mucin. *A. hottentotus* had significantly more ($p = 0.0006$) sialomucin secreting goblet cells than *C. cyanea* (Figure 4.39 diagram A). Throughout the GIT of *A. hottentotus* there was an increase of sialomucin goblet cells, except in the surface epithelial areas (Figure 4.39 diagram B) of the distal GI regions. In *C. cyanea* the duodenum had substantially more sialomucin secreting goblet cells than the other GI

regions. There was a statistically significant decrease ($p < 0.01$) in the number of sialomucin goblet cells from the duodenum to the middle small intestine.

Both the surface epithelial (Figure 4.39 diagram B) and crypt areas (Figure 4.39 diagram C) showed similar trends than figure 4.39 diagram A. The crypt areas (Figure 4.39 diagram C) of *C. cyanea* had little sialomucin goblet cells, and the duodenum was the only region with a large number of cells. *A. hottentotus* had a larger number of sialomucin goblet cells in the crypt areas of the distal GI regions than in the surface epithelial areas.

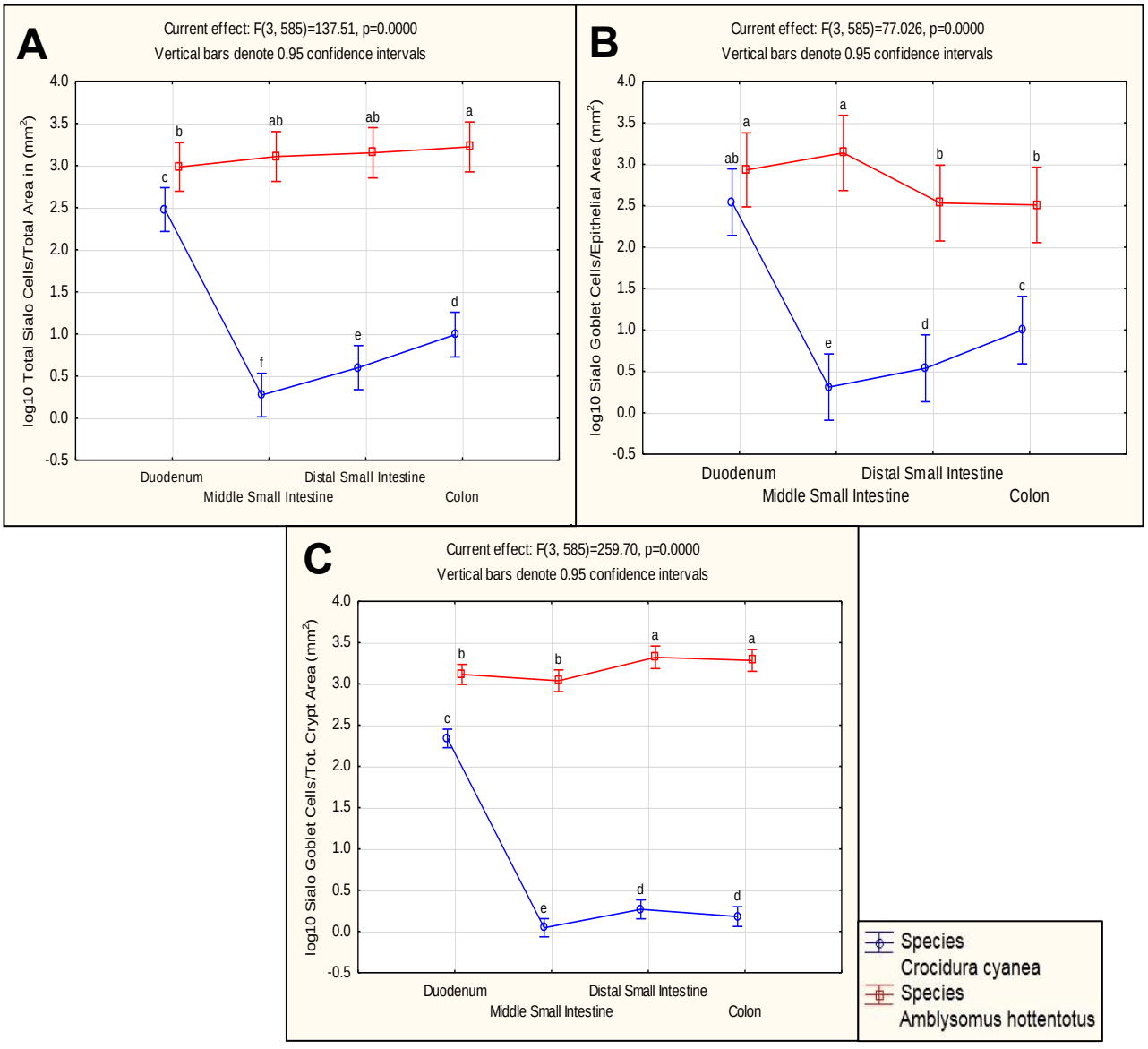

Figure 4.39: The distribution of the total number of sialomucin secreting goblet cells throughout the GITs of *C. cyanea* and *A. hottentotus*.

(A) Total number of sialomucin goblet cells per total area (mm^2).

(B) Sialomucin goblet cells per epithelial surface area (mm^2).

(C) Sialomucin goblet cells per crypt area (mm^2).

To conclude, *C. cyanea* had a larger number of mixed goblet cells than *A. hottentotus*, but it was not significant. In *C. cyanea* the total number of mixed goblet cells (Figure 4.40 diagram A), and the cells in the surface epithelial areas (Figure 4.40 diagram B), indicated that the distal GI regions had substantially higher numbers of cells than the proximal regions. However, in the duodenum crypt area (Figure 4.40 diagram C) of *C. cyanea* there was considerably more cells than in the other GI regions. *A. hottentotus* had little to no mixed goblet cells in the proximal GI regions (Figure 4.40 diagrams A, B, and C). Mixed

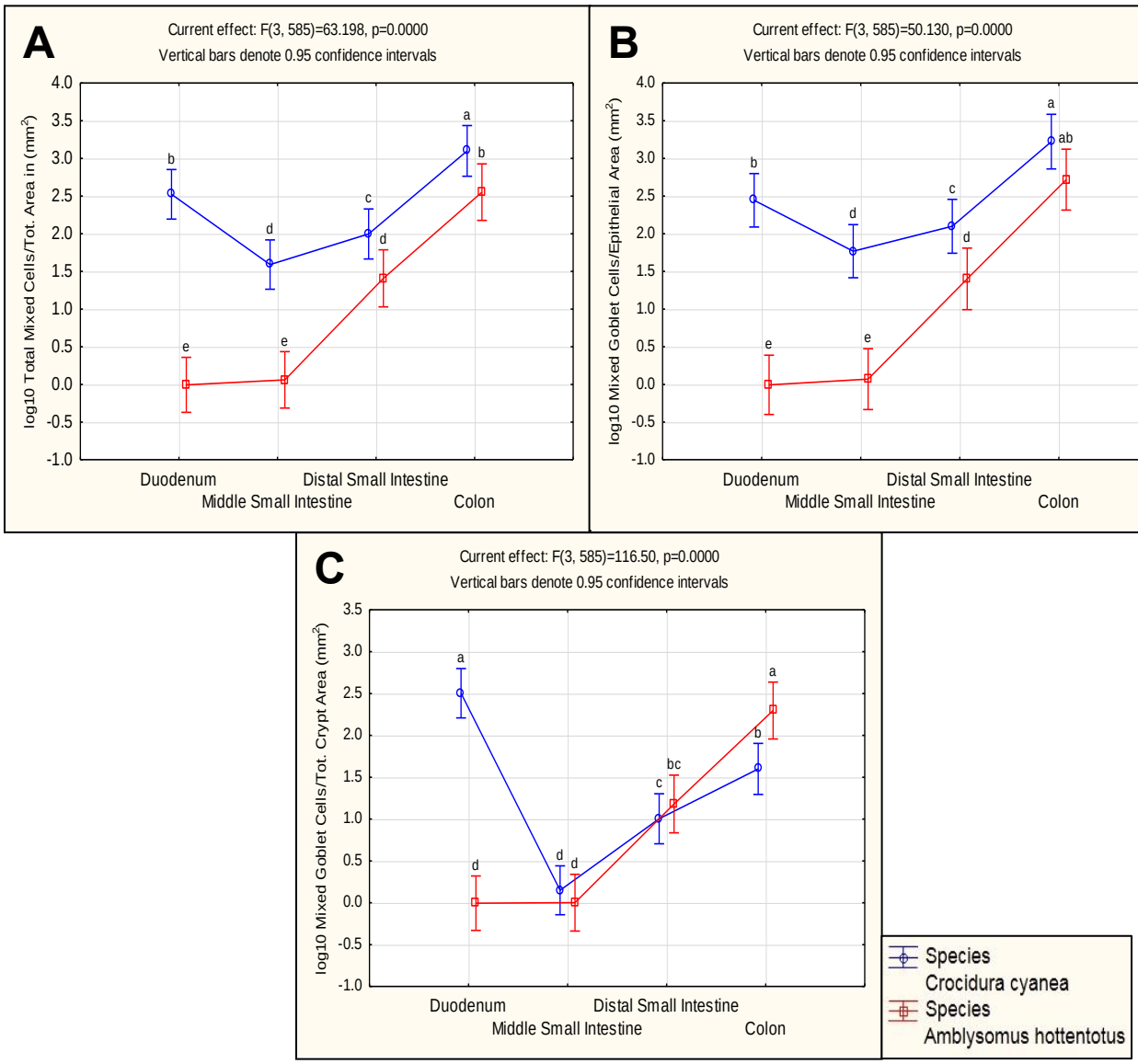

Figure 4.40: The distribution of the total number of mixed mucin secreting goblet cells throughout the GITs of *C. cyanea* and *A. hottentotus*.

(A) Total number of mixed mucin goblet cells per total area (mm^2).

(B) Mixed goblet cells per epithelial surface area (mm^2).

(C) Mixed goblet cells per crypt area (mm^2).

goblet cells were only observed in the distal GI regions of *A. hottentotus*. Overall, there was a larger number of mixed mucin secreting goblet cells present in the surface epithelial than crypt areas.

4.5.2.2.1 Summary of the results of the different types of mucin secreting goblet cells in *A. spinosissimus*, *C. cyanea* and *A. hottentotus*

- In *A. spinosissimus*, the largest number of mucin secreting goblet cells throughout the GIT, in both the surface epithelial and crypt areas, was mixed (neutral and acid) mucins. There was a uniform distribution of neutral and acid mucins throughout the GIT. Larger numbers of neutral mucin secreting goblet cells were present in the small intestine than acid mucins. Acid mucins were dominant in the large intestine.
- Both *C. cyanea* and *A. hottentotus* also had primarily mixed (neutral and acid) mucins throughout the GIT, similar *to A. spinosissimus*. In *C. cyanea*, the mixed mucins were dominant in both the surface epithelial and crypt areas. However, *A. hottentotus* had marginally more acid than neutral mucin secreting goblet cells in the crypts. *A. hottentotus* had larger numbers of acid mucin secreting goblet cells throughout the GIT, whereas *C. cyanea* contained mainly neutral mucins.
- In all three insectivorous species, weakly sulfated goblet cells were predominantly more than strongly sulfated goblet cells. In *A. spinosissimus*, the distribution of strongly sulfated goblet cells was consistent in the small intestine, with a notable increase in the colon. Weakly sulfated goblet cells were considerably more in the colon than in the rest of the GIT. In *A. hottentotus*, little to no sulfomucin secreting goblet cells was present in the small intestine, and sulfomucins were only observed in the distal small intestine and colon. *C. cyanea* had more weakly sulfated than strongly sulfated goblet cells, especially in the duodenum. The other GI regions of *C. cyanea* showed relatively similar numbers of both weakly and strongly sulfated goblet cells.
- Sialomucin secreting goblet cells in *A. spinosissimus* were uniform throughout the GIT, however, a significant decrease ($p < 0.05$) was observed in the colon. Large numbers of sialomucin secreting goblet cells were present in the crypts. The sialomucin goblet cells were the dominant acid mucin throughout the GIT of *A. hottentotus*. *C. cyanea* predominantly had sialomucin secreting goblet cells in the duodenum, and little in the rest of the GIT.

- Similar numbers of goblet cells were counted for *A. spinosissimus*, *C. cyanea* and *A. hottentotus*. Concluding from the total numbers of the different mucin goblet cells, it appeared as if *A. spinosissimus* had the smallest number of neutral mucin secreting goblet cells and *C. cyanea* the largest. In addition, *A. spinosissimus* had the largest number of mixed acid (sulfo- and sialomucins) mucins of the three insectivorous species. For the rest mucin goblet cells, *A. spinosissimus* mainly had intermediate numbers when compared to *C. cyanea* and *A. hottentotus*.

CHAPTER 5

DISCUSSION

5.1 Macroscopic morphology and histology of the gastrointestinal tracts

The observations made on the topographical arrangement of the GIT in *C. cyanea* could not be compared to the *A. spinosissimus* and *A. hottentotus*, because whole carcasses were not available for the latter two species. Two *C. cyanea* specimens were examined for the topographical arrangement of the intestinal tract, and both specimens differed from one another. Due to a small sample size and an absence of literature on the topographical studies in insectivores, the circumstances make it difficult to draw any conclusion. The basic pattern of the liver situated in the right cranial abdomen, the stomach situated in the left cranial abdomen, and loops of intestine lying in the caudal abdominal cavity was consistent with the literature described in a wide variety of mammals such as rodents (Behmann, 1973).

The shape and size of the GIT affects digestive efficiency and varies with diet (Sibly, 1981). According to Stevens and Hume (1995), structural and functional characteristics of the digestive system may result from the diet or evolutionary changes.

The GITs of *A. spinosissimus*, and particularly *C. cyanea* and *A. hottentotus*, showed primitive characteristics when compared to animals with other dietary preferences. Omnivores mostly have a simple stomach, a specialised caecum and colon which are often haustrated (Stevens & Hume, 1998). Herbivores, large or small, have either have a voluminous stomach, caecum or colon for the retention and microbial fermentation of plant material in the latter two structures (Stevens & Hume, 1998). All mammalian herbivores depend on bacterial fermentation of plant cell walls in the GIT (Clauss et al., 2003). Herbivores are either classified as foregut or hindgut fermenters depending on which region of the GIT is specialised. Foregut (stomach) fermenters have compartmentalised and complex stomachs, whereas hindgut (large intestine) fermenters have enlarged colons and well-developed caeca.

The morphological features of the GITs of the three insectivorous species in the present study were similar to that of carnivores in that they are relatively short and simple (Stevens & Hume, 1998). The stomachs are uncompartmentalised and are a bilateral dilation of the GIT. The hindgut is often difficult to identify in some carnivores, insectivores, bats, cetaceans and marsupials, with no valvular separation between the small and large intestines in some of the species. If the hindgut is present, it is short and rarely haustrated. A caecum may be present or absent.

In a study of 19 rodent species by Perrin and Curtis (1980), the authors describe the structure of the GIT of *A. spinosissimus* as primitive in its specialisation towards herbivory. Due to competition for habitats and food between the two rodent families, Cricetids (hamsters, voles, lemmings, new world rats and mice) and Murids (mice, rats, gerbils), diversity increased between the species. Muroids modified increasingly towards an herbivorous diet because of an expanding grassland ecosystem. Diets changed from mainly protein (insects and seeds) to a diet of plants with complex polysaccharides (Vorontsov, 1961; 1962).

A. spinosissimus (family Muridae) is classified as a granivorous-insectivore, and include seeds and insects in their diet (Kingdon, 1974b; Perrin & Curtis, 1980). *A. spinosissimus* is described as an opportunistic feeder and will eat coarse dry plants when other resources are scarce (Vesey-Fitzgerald, 1947; Kingdon, 1974b). According to Perrin and Curtis (1980), this species did not consume enough plant material to be classified as a herbivore, therefore the GIT is simple or unspecialised. Perrin and Curtis (1980) examined two *A. spinosissimus* specimens and found that they have a single-chambered stomach, a broad sac-like caecum without haustrations, and a simple colon. The results found from the five *A. spinosissimus* specimens examined in the present study mostly correlates with the observations of Perrin and Curtis (1980). The present study showed mucosal folds both macroscopically and microscopically on the internal aspect of the caecum and proximal colon, similar to the mucosal folds, named valves of Kerkering, observed in the colon of the grey-sided vole and muskrat (*Ondatra zibethicus*) by Behmann (1973).

The GITs of *C. cyanea* and *A. hottentotus* were even more primitive than that of *A. spinosissimus* because it lacked caeca. No clear macroscopic indication of a division between the small- and large intestines were found. This primitive morphological characteristic of the GIT, i.e., the presence of a single chambered stomach and lack of a caecum, is an indication of a proteinaceous (flesh-eating) diet (Kurohmaru et al., 1980; Perrin & Curtis, 1980). Hisaw (1923) reviewed various studies on the dietary preferences of different mole species and came to the conclusion that moles are carnivorous animals, and that they rarely and unintentionally eat plant material. *A. hottentotus* consumes about 45g of earthworms each day (excluding other insects) and is also classified as an insectivore/vermivore (Kingdon, 1974a).

Experimental studies conducted by Dickman (1995) found that shrews (*Crocidura cyanea*, *Crocidura fuscomurina*, *Crocidura hirta*) consumed primarily invertebrates and only small

numbers of leaf, seed or other plant material. Vertebrate remains were also present in the faeces of *C. cyanea*, such as the bones of small lizards and they showed a strong preference for Isoptera (termites) and Araneida (spiders). *C. fuscomurina* and *C. hirta* on the other hand preferred Chilopoda (centipedes), Coleoptera (beetles), Orthoptera (grasshoppers, crickets) and insect larvae. The insect taxa selected in the diets of the latter crocidurine species have a relatively high ratio of body water to energy content (Churchfield, 1990), which might be preferred in arid or water scarce environments. Heavily-chitinized beetles were avoided by *C. cyanea*, but were prominent in the diet of the other two crocidurine species (Dickman, 1995). Formicidae (ants) were avoided by all three shrew species, probably due to their low nutritional value. Even though these species consumed different ratios of varying insects, when comparing the GIT of *C. cyanea* with the musk shrew (*Suncus murinus*) and Watase's shrew (*Crocidura horsfieldi watasei*), similar primitive GI morphology could be seen (Kurohmaru et al., 1980, 1982; Hattori & Yamanouchi, 1984).

In a study done by Perrin and Curtis (1980) of 19 species of southern African rodents, they conclude that there was no convincing evidence that GI morphology and feeding habits could be related. Similar conclusions were also made by Gorgas (1967), who also performed a large comparative study on various rodent species. Neither Perrin and Curtis (1980) nor Gorgas (1967) measured the relative surface areas of the different GI regions. Perrin and Curtis (1980) realised the shortcomings of comparing GI length to diet and suggested that in future the gut surface area should be computed. In the present study, the proportional lengths of the stomach and the small and large intestines did not reflect the surface area of the respective GI regions. The proportional stomach length of *C. cyanea* was larger than that of *A. spinosissimus* and *A. hottentotus*, but *A. spinosissimus* had the largest proportional stomach surface area. In addition, the proportional length of the small and large intestines were larger in *A. hottentotus* and *A. spinosissimus* than in *C. cyanea*. However, *A. spinosissimus* had the smallest proportional surface area of the small and large intestines. Because of the mentioned differences between the proportional lengths and surface areas, the lengths alone of the GI regions could not be used to determine the influence of diet.

Mean circumference and length measurements were used to determine the surface areas of the different GI regions. The lengths and the surface areas of the GI regions were expressed as a percentage of the total GI lengths and surface areas. This approach might have shortcomings, but was successfully used to compare the GIT morphology of other

species such as mole-rats (Kotzé et al., 2010), and this method was chosen to compensate for the large variation in body weights between the species used in this study. Measurements of GIT morphology is, however, never exact as various factors play a role in causing variations such as tissue shrinkage and loss of pliability in fixed tissue. However, in the present study, all measurements were done on fixed intestinal tracts. In addition, because specimens were caught in the wild, there was no control over their diet and therefore the extent to which the intestines were filled with ingesta at the time of death. Consequently, the varying extent to which certain parts of the GIT were filled with intestinal content may have influenced the structure and measurements of the different GI regions.

According to Kurohmaru et al. (1980), the GITs of carnivorous animals were found to be shorter than that of herbivores, while omnivorous animals had an intermediate GIT length. Nickel et al. (1973) and Kurohmaru (1980) compared the rough ratios of the crown rump body lengths to the intestinal length of mammals of various dietary types. The mammals examined in the latter studies are: musk shrew, cat, dog, hamster, rat, mouse, human, horse, pig, ox, goat and sheep. Nickel et al. (1973) and Kurohmaru (1980) came to the conclusion that the ratios of the GIT length to body length in large species were larger than in small species. It appears that the length of GITs of a species might be related to size or body weight.

A study performed by Myrcha (1967) described a hypothetical curve, (constructed on the basis of data from the literature) which indicated that there was a correlation between the amount of food intake and the body weight of insectivores. According to this hypothetical curve, the number of food consumed in a day (24 hours) increased with the reduction in body size. Energy is the most vital requirement of the body, and therefore, one can almost undeniably assume that animals eat to meet their energy needs (Stevens & Hume, 1995). Energy is needed to maintain a constant body temperature. However, ambient temperatures influence both heat loss and heat gaining of the animal. A relatively large surface area (as with small animals) leads to a greater heat loss per unit mass of the animal (The Open University, 2008). In order to compensate for this enhanced heat loss, metabolic rate has to be sufficiently high to maintain its body temperature at a stable value of 36 °C or more. Thus, the larger an animal the lower their heat loss relative to their body size. Therefore large animals have reasonably lower metabolic rates than small animals. The diet of smaller animals are also more digestible and of a higher quality (protein diet

versus an herbivorous diet), because of their need to process energy at higher rates than larger animals (Stevens & Hume, 1995).

According to Mezhzherin (1964), in Soricidae there were correlations between their body weight, amount of food required and the ambient temperatures (cited in Myrcha, 1967). Cold ambient temperatures cause potential problems for small mammals, due to the reduced availability of food (Lacy et al., 1978). To be able to survive, these animals must either decrease their heat loss or increase heat production, without sustaining an excessively high energetic cost. Kingdon (1974a) found that shrews (Soricidae) may eat from three-quarters to more than three times their own weight of food per day. A mole is capable of eating two thirds of its body weight in eighteen hours. This is because per unit body weight, small mammals need higher amounts of energy for survival and growth than large mammals (Langer, 2002). Shrews adapt for survival in the winter by reducing their stomach and subsequently their body weight, so that they need less energy for survival (Myrcha, 1967). Whereas other small mammals, such as mice, reduce their energy needs by nest building, postural adjustment, huddling, increasing of subcutaneous fat and fur, decrease peripheral circulation and body temperature (Lacy et al., 1978).

Smaller mammal species might have larger and heavier stomachs in relation to their size and this is especially obvious in the species of the family Soricidae (shrews) (Myrcha, 1967). This correlates with the findings of the present study, where the proportional stomach length of *C. cyanea* is significantly longer than that of *A. hottentotus*, but not meaningfully longer than the stomach of *A. spinosissimus*. *C. cyanea* and *A. spinosissimus* have similar proportional surface areas, but not substantially larger than *A. hottentotus*.

Although the external appearance of the stomach varied between the species of this study, the stomach in all three species were unilocular (single compartment), similar to that observed in other rodents (Carleton, 1973; Perrin & Curtis, 1980), shrews and mole species (Myrcha, 1967). The internal surface of the stomach of *A. spinosissimus* differed from *C. cyanea* and *A. hottentotus*. *A. spinosissimus* had stratified squamous epithelium in the fundus and corpus regions, while in *C. cyanea* and *A. hottentotus*, the latter regions were lined with glandular epithelium. On the internal aspect of the stomach in *A. spinosissimus*, a line appeared to divide the fundus from the pyloric region of the stomach. This line crossed the lesser curvature at the angular incisure and the greater curvature at a point opposite the angular incisure and separated the stratified squamous epithelium of the

oesophagus and fundus from the glandular epithelium. These findings are similar to the observations made by Carleton (1973) in a study examining the stomachs of new world Cricetinae (hamsters), and he referred to the line that separates the different stomach regions as the bordering fold. The corpus region in the stomach of the hamsters was keratinized, while the pyloric region contained glandular epithelium. Perrin and Curtis (1980) observed stratified squamous and glandular epithelium in the stomach of *A. spinosissimus*, they did not specify in which regions the different epithelial types were observed. Based on the findings of Carleton (1973), one could assume that stratified squamous epithelium was present in the corpus. Thus, it appears as if the glandular epithelium found in the corpus of *A. spinosissimus* might really be part of the pyloric region. As *A. spinosissimus* inhabits arid regions (Kingdon, 1974b), the stratified squamous epithelium may be an adaptation to allow for temporary food storage. In addition, Carleton (1973) also suggested that due to the extensive area of stratified squamous epithelium (non-secretory) in the rat stomach, salivary amylase could remain active for longer, therefore enhanced digestion can take place.

The fundus and corpus regions in the stomach in *C. cyanea* and *A. hottentotus* were lined with glandular epithelium, which would typically be characterised by the presence of peptic and parietal cells (Myrcha,1967). Parietal cells were present in the gastric glands of all three insectivorous species of this study, but most abundant in *C. cyanea* and *A. hottentotus*, while peptic cells were not observed in either of the latter two species. Myrcha (1967) also did not observe peptic cells in 27 species of hedgehogs, moles and shrews. This study found a small area of cardiac glands in the stomach, bordering upon the oesophagus and observed that fundic glands covered the whole fundic area. This is consistent with the findings in the present study of *C. cyanea* and *A. hottentotus*. The distribution of gastric glands in the different stomach regions of *C. cyanea* as seen in the present study is similar to that observed in the Watase's shrew (*Crocidura horsfieldi watasei*) and musk shrew (*Suncus murinus*) (Hattori & Yamanouchi, 1984).

The elongation of the pyloric regions in *C. cyanea* and *A. hottentotus* was consistent with findings described by Myrcha (1967) in the Talpidae (moles) and Soricidae (shrews). As mentioned previously, Myrcha (1967) suggested that differences in stomach size between insectivorous species may be related to the quantitative differences in food requirements between these species. This is because insectivores consume large numbers of food during the day and this caused an increase in the digestive area of the mucous membrane of the stomach. According to Myrcha (1967), if the growth of the mucous membrane in the

stomach was insufficient, then the pyloric region underwent elongation. This was particularly well described in shrews, and to a lesser degree in moles. According to Skoczen (1966) the elongation of the stomach in *C. cyanea* and *A. hottentotus* is particularly important, because they fed on insects such as larvae which contain large numbers of fat. The elongation of the stomach allowed for better digestion of fat.

Brunner's glands (duodenal glands) are present in all mammals (Takehana et al., 2000). With this in mind, the present study found Brunner's glands in the submucosa of the duodenum in all three species examined. Other cells types such as endocrine and Paneth cells were found in *A. spinosissimus*. Paneth cells were not observed in *C. cyanea* and *A. hottentotus* in the present study. Paneth cells are typically located in the small intestine at the base of the crypts of Lieberkühn, and hold large secretory granules which contain the antibacterial enzyme, lysozyme (Gartner & Hiatt, 2000). Paneth cell secretions protect the luminal surface of the epithelium from pathogenic micro-organisms (Kierszenbaum, 2002; Young et al., 2006).

Kurohmaru et al. (1980, 1982) also did not observe any Paneth cells in the GITs of the musk shrew (*Suncus murinus*) and the Watase's shrew (*Crocidura horsfieldi watasei*) as was the case in this study. According to Satoh et al. (1986), Paneth cells are present in the intestinal crypts (crypts of Lieberkuhn) of many mammals except in carnivores. Satoh et al. (1990) observed Paneth cells under an electron microscope in humans, rhesus monkey, hare, guinea pig, rat, nude rat, mouse, golden hamster, and insect feeder bat. Sandow and Whitehead (1979) also reported that Paneth cells were absent in dogs and cats. It is, however, unclear whether the absence of Paneth cells is related to diet. Kurohmaru et al. (1980) reported from other studies that Paneth cells were absent in nutria (river rat), raccoons and pigs. Sandow & Whitehead (1979) suggested that there was a correlation between the Paneth cell numbers and the bacterial concentration in the small intestine.

According to Perrin and Curtis (1980), the rodent caecum could be classified as a blind, sac-like structure which might contain papillae and haustra leading into spiral loops of the colon. The structure of the caecum of *A. spinosissimus* had a broad sac-like appearance which was consistent with what Perrin and Curtis (1980) observed. In addition, folds were also observed macro- and microscopically in the caecum and proximal colon of *A. spinosissimus*. The folds in the proximal colon appear to be spiral-shaped, which might play a role in the transportation of food. Perrin and Curtis (1980) suggest that folds in the colon were adaptations to herbivory. According to Snipes and Kriete (1991) folds in the

caecum increased the surface area and therefore enhanced the contact of the intestinal wall with the luminal content which may improve the efficiency of the absorption of sodium, potassium and water (Lange & Staaland, 1970). Similar to the folds in the caecum, folds in the colon of *A. spinosissimus* may also be responsible for the increased absorption of salts and water. Compared to other rodents, the GIT of *A. spinosissimus* appears to have similarities with that of omnivorous rodents (Perrin & Curtis, 1980).

The GIT of *C. cyanea* and *A. hottentotus* both lacked a caecum making the demarcation between small and large intestine difficult to ascertain. Histologically, similar to the musk shrew (*Suncus murinus*), villi were observed throughout the GIT which may be due to the lack of a caecum (Kurohmaru et al., 1980). Villi were present in the small intestine as well as in the distal small intestine. Villi were also present in the part we called colon of *C. cyanea*, however in the colon of *A. hottentotus* no villi were observed. According to Kurohmaru et al. (1980) villi was also present in the rectum of shrews. However, in the present study, villi in the GIT gradually decreased in length from the duodenum to the colon, which was consistent with the pattern classically observed in other mammals (Hilton, 1902).

Circular folds lined with crypts were present in the colon of *A. hottentotus*. In addition, the circular folds (plicae circulares) with villi were well developed in the colon of *C. cyanea*, but according to studies done by Kurohmaru et al. (1980) and Hattori and Yamanouchi (1984), this region might represent the rectum. Nevertheless, during the early fetal period in mammals, villi were usually observed throughout the large intestine (Hilton, 1902). The villi normally disappeared gradually in the large intestine with the progression of fetal age (Hilton, 1902; Kurohmaru et al., 1980). Birds also had villi in the large intestine, even in adults, which was associated with a decreased GI length (Kurohmaru et al., 1980). In both birds and bats (McNab, 1973), the decreased GI length limits the capacity to store food because of flight constraints that did not allow sudden increases in the body weight.

Crocidurines are usually very active day and night (Meester, 1963; Pernetta, 1977; Genoud & Vogel, 1981; Baxter & Meester, 1982). Although some Crocidura species preferred a habitat at ground level, *C. cyanea* preferred a habitat in shrubs (35-95 cm above ground). Thus, the short GIT of *C. cyanea* may also be an adaptation to decrease the storage capacity of food to accommodate its climbing habits. The passage of food therefore, through the GIT must be fast with a high absorption rate (Keegan, 1977; Tedman & Hall, 1985). Villi in the large intestine may also be and adaptation to the

shortening of the GIT (Kurohmaru et al., 1980). Villi and circular folds in the large intestine would increase the absorption rates. Consequently, one could speculate that both the small and large intestines of *C. cyanea* have an absorptive function.

5.2 Mucin histochemistry and quantification of goblet cells in the gastrointestinal tract

The detection of mucins in both the clinical and research environment is of great importance, because it is necessary to determine the distribution, structure and function in health and disease (McGuckin & Thornton, 2000). In the present study, the primary focus was to determine the distribution of the different types of mucins (neutral, acid: sialo- and sulfomucin) with the use of histochemical detection methods.

The staining techniques used in the present study were the combined Alcian blue-Periodic Acid Schiff (AB/PAS), combined Alcian blue-High Iron Diamine (HID/AB) and the combined Alcian blue-Aldehyde Fuchsin (AF/AB) techniques. AB/PAS was used to distinguish between acid and neutral mucins, which stained blue and magenta respectively (Bancroft & Stevens, 1990). In addition, HID/AB and AF/AB techniques were used to distinguish between the different acid mucins, sulfo- and sialomucins, which stained black/brown and blue respectively.

The AB/PAS and HID/AB techniques, or the use of Alcian blue at varying pH levels, are the most commonly used techniques to identify the different types of mucins, as observed in several studies (Sheahan & Jervis, 1976; Sakata & von Engelhardt, 1981; Kotzé & Coetzee, 1994; Tibbetts, 1997; Scillitani et al., 2007; Cao & Wang, 2009). The AF/AB is not regularly used because it is similar to HID/AB. However, the AF/AB technique was used in the present study because it is sensitive for weak and strong sulfomucins (Bancroft & Gamble, 2008), whereas the HID/AB technique stains all sulfomucins, irrespective of whether it is weak or strong. In addition, the AF/AB technique was also used as a control for the HID/AB technique. It has been noted by Walsh and Jass (2000), that in the HID/AB technique there are ionic competition between HID and AB. Therefore, if the latter technique gives a brown/black reaction it does not necessarily indicate the absence of sialic acid mucins, nor does a blue reaction indicate the absence of sulfate mucins. Sheahan and Jervis (1976) made a similar observation and stated that when only intensely black stained sulfomucins were observed, there was a possibility that the sialomucins could be masked. However, despite the requirement for care during the interpretation of results and the carcinogenicity of the diamine compounds, the HID/AB technique is the

best method to stain acid mucins (Walsh & Jass, 2000). The structural information obtained from mucin histochemical methods are limited. For this information one must use lectin histochemistry and immunohistochemistry, which provides information of the composition of the mucin oligosaccharide chains.

With the aid of histochemical techniques, it was possible to observe the distribution patterns of mucin secreting goblet cells throughout the GITs of the three insectivorous species examined. In order to determine the relative proportions and distribution of the different types of mucins (neutral, acid: sulfo- and sialomucins), the mucin secreting goblet cells in each GI region had to be quantified.

Older histochemical studies done on the distribution of mucins used a scoring method to interpret the number and distribution of mucin secreting goblet cells (Sheahan & Jervis, 1976; Kotzé & Coetzee, 1994; Sharma et al., 1995; Tibbetts, 1997). However, relatively recent studies have also used the same scoring method (Fernandez et al., 2000; Scillitani et al., 2007). This suggests that the type of quantification method used depends on the reasons and preferred outcomes of the study. This scoring method makes use of either numbers (1-4) or symbols (++; +; +- ; -) to indicate the presence or absence of the different mucin types, as well as the intensity of the mucin staining.

The availability of ever-improving software has made it possible to explore other quantification methods. In the present study, mucin secreting goblet cells were counted in both the surface epithelial and crypt areas. The mucin secreting goblet cells for each GI region was expressed as the number of cells per mm^2. Similar quantification methods than in the present study, has been implemented in mucin histochemical studies with good results (Sharma & Schumacher, 1995; Ndou, 2007; Forder et al., 2007; Cao & Wang, 2009). The counting of mucin secreting goblet cells in allocated areas (for example: surface epithelium, villi, and crypts) gives a better representation of the number and distribution of the different types of mucin secreting goblet cells than the less specific scoring method. Consequently, more data are available for the distribution of the mucin secreting goblet cells, which provides sufficient results and better interpretations can be made.

In the present study, for all three insectivorous species, mucins were examined in the corpus (body) of the stomach. Neutral mucins were the dominant type in the surface mucous cells and mucous neck cells of the corpus in *A. spinosissimus* and *C. cyanea*. However, in the corpus stomach region of A. *hottentotus* there were mainly mixed (neutral

and acid) mucins in the surface mucous cells and mucous neck cells, whereas the neck mucous cells close to the base of the gastric glands contain mainly neutral mucins.

In all of the animals that Sheahan and Jervis (1976) examined, neutral mucins were the predominant type found on the entire gastric surface. Sheahan and Jervis (1976) examined the different types of mucins in three regions of the stomach (cardia, corpus and antrum), and found that there are less neutrally stained cells in the deep cardiac glands, mucous neck cells of the corpus and antral glands. In addition, neutral mucins were absent from the antral (antrum) glands of the rat. Compared to the present study, neutral mucins in the corpus mucous neck cells of *A. spinosissimus* stained weaker than the surface mucous cells. However, strongly stained neutral mucins were present in the mucous neck cells of *C. cyanea*. The proximal mucous neck cells of the gastric gland in *A. hottentotus* consisted of mixed mucins (neutral and acid), whereas the distal mucous neck cells were strongly neutral.

In an unpublished thesis by Ndou (2007) on three rodent species (*Bathyergus suillus*, *Georychus capensis*, and *Cryptomys hottentotus hottentotus*), sialomucins were the only acid mucin type present in the stomach. In the latter rodent species sialomucins were present in the cardia, pylorus and fundic regions, and in the latter region sialomucins were observed in surface epithelial cells and in the gastric pits. The staining of the sialomucins in *B. suillus* was more intense than in *G. capensis* and *C. h. hottentotus*, suggesting that less intensely stained sialomucins were present in the stomach of the latter two species. In *A. spinosissimus* (rodent), minimal numbers of sialomucins were present in the mucous neck cells of the corpus. Intensely stained sialomucins were present in the mucous cells of *A. hottentotus* (Afrosoricida, mole), and limited numbers of mixed sialo- and sulfomucins were present in the stomach. No acid mucins were observed in the stomach of *C. cyanea* (Eulipotyphla, shrew).

Sheahan and Jervis (1976) reported that sulfomucins were dominant in the stomachs of a number of rodent species (mouse, rat, hamster, gerbil and guinea pig). Of these rodent species, sialomucins were present in the stomach of the mouse, rat and guinea pig. The distribution of sialomucins in the mouse, rat and guinea pig, was different for each species. Sialomucins were present in the cardiac, corpus or antral regions and could be on the surface or in deep glandular regions. *A. spinosissimus*, *C. cyanea* and *A. hottentotus* belong to different orders (Rodentia, Afrosoricida and Eulipotyphla respectively) and even though these three species all have an insectivorous diet, the distribution of the different

mucin types in their stomach differed. Sheahan and Jervis (1976) observed some mucin similarities in rodents, but this was not consistent.

Emptying of the acidic stomach contents into the duodenum, along with gastric hydrochloric acid and proteases, creates a threat to the epithelial barrier of the duodenum (Moore et al., 2000). The duodenum protects itself from this threat by the secretion of mucin and bicarbonate into the lumen from specialised epithelial cells (goblet cells) and Brunner's glands in the submucosa. When the mucins come into contact with water it forms a viscoelastic gel. The viscoelastic gel is infiltrated with bicarbonate to form a physicochemical barrier which protects against hydrogen ions and proteolytic enzymes (Flemstrom & Kivilaakso, 1983).

Various histochemical studies on a variety of animals have shown that the duodenal glands consist mainly of neutral mucins (Sheahan & Jervis, 1976; Poddar & Jacob, 1979; Takehana et al., 2000). This is consistent with the observations in the Brunner's glands of *A. spinosissimus*, *C. cyanea* and *A. hottentotus*. Neutral mucins were the only type seen in Brunner's glands of *C. cyanea*. This was also observed in the Brunner's glands of the rat, cat, dog, marmoset, marsupial mouse, bandicoot, native cat of eastern Australia, horseshoe bat and man (Sheahan & Jervis, 1976; Poddar & Jacob, 1979; Scillitani et al., 2007).

Mixed mucins, which consist of neutral and weakly stained sialomucins, were present in the Brunner's gland ducts of *A. hottentotus* and in a few random mucous cells in *A. spinosissimus*. Sheahan and Jervis (1976) observed mixed (neutral and acid) mucins in the ducts of Brunner's glands of the mouse, containing either sulfo- or sialomucins. Ndou (2007) also observed mixed (neutral and acid) mucins in the Brunner's glands of *B. suillus*, *G. capensis* and *C. h. hottentotus*. Although both sulfo- and sialomucins were observed, sulfomucins appeared to be the prominent type in the Brunner's glands. Various other species (gerbil, hamster, rabbit, horse, baboon, rhesus monkey) also contained sulfo- and sialomucins, along with neutral mucins, in the Brunner's glands (Sheahan & Jervis, 1976; Takehana et al., 1989). Takehana et al., (2000) found that the Brunner's glands of the camel mainly contained acid mucins. This was also observed in the African elephant, which contained primarily sulfo- and sialomucins in the Brunner's glands (Kotzé & Coetzee, 1994).

Previous studies by Grossman (1988) have shown that the Brunner's glands, along with pancreatic, bile and goblet cell secretions in the small intestine, neutralised the gastric

hydrochloric acid. Both acid and neutral mucins increase the viscosity of the mucous gel that protects the epithelial surface (Bansil & Turner, 2006). The increased acid mucins secreted by the Brunner's glands may facilitate the protection against bacteria (Cao & Wang, 2009).

In the present study, mixed mucins (neutral and acid) appeared to be the predominant type present in the small and large intestines of all three insectivorous species. These findings are in agreement with a study carried out by Sheahan and Jervis (1976) on 11 mammals (mouse, rat, hamster, gerbil, guinea pig, rabbit, cat, dog, rhesus monkey, baboon and man). Despite the general trend of mixed mucin secreting goblet cells, there were marked differences between species in the qualitative expression of the mixed, neutral and acid mucin secreting goblet cells in each GI region.

Mixed (neutral and acid) mucins in the small intestine of *A. spinosissimus*, *C. cyanea* and *A. hottentotus*, were abundant in both the villi and crypts. Mole-rats studied by Ndou (2007) did not prove to be an exception, goblet cells in the villi and crypts also contained numerous mixed mucins. The overall similarity between the three insectivores in this study and other distantly related species such as primates and lagomorphs suggest that mixed mucin types are common as well as fundamental to the majority of mammals, irrespective of their diet or taxonomy.

Neutral mucin secreting goblet cells in the small intestines of *A. spinosissimus* and *C. cyanea* appeared to dominate the acid mucin secreting goblet cells. However, in *A. hottentotus*, the acid mucin secreting goblet cells were predominantly more in the small intestine. Havez et al. (1967, 1969) have reported important differences in the biological and physical properties of neutral and acid mucins. Havez et al. (1967, 1969) found that neutral mucins possess blood group activity, whereas acid mucins, specifically sialomucins are most important in gel formation. The neutral mucins with blood group activity possess blood group specific antigens on the terminal aspect of their oligosaccharide chain, which may protect against specific pathogens (Linden et al., 2008).

The small intestine of various animals (mouse, rat hamster, guinea pig, rabbit, cat) examined by Sheahan and Jervis (1976) revealed that goblet cells, exhibiting sulfomucins, were predominantly more than sialomucins. Ndou (2007) found almost exclusively sulfomucins in the small intestines of three mole-rat (rodents) species. In *A. spinosissimus*, like the other rodents, sulfomucins were more abundant in the small intestine than sialomucins. However, in the gerbil (rodent) sialomucins were the main acid mucin present

in the small intestine (Sheahan & Jervis, 1976). This correlates with findings in *A. hottentotus*, with large numbers of sialomucin secreting goblet cells in the duodenum and middle small intestine. Large numbers of sulfo- and sialomucins were present in the duodenum of *C. cyanea*. Sulfomucins were more abundant than sialomucins in the middle of the small intestine of the latter species. Abundant sulfo- and sialomucins were present in the small intestine of the dog (Sheahan & Jervis, 1976), and equal numbers of sulfo- and sialomucins were present in the African elephant and the horseshoe bat, the latter being an insectivorous species (Kotzé & Coetzee, 1994; Scillitani et al., 2007). The sulfomucins in the present study were largely weakly sulfated, in both the small and large intestines of all three insectivorous species. Some specific correlations have been observed between rodent species examined by Sheahan and Jervis (1976), in terms of the presence of sulfomucins in the small intestine. However, between the insectivorous species in this study, there were few similarities.

As in the small intestine, the predominant type of mucin in the large intestine of the species in this study, and in those examined by Sheahan and Jervis (1976), were mixed (acid and neutral). In the colon of *A. spinosissimus*, neutral mucins were abundant in the epithelial layer, whereas acid mucins were numerous in the crypts. The number of acid mucins in the colon of *A. hottentotus* was substantially more than the neutral mucins in both the surface epithelial and crypt areas. However, small numbers of “pure” acid mucins were present in the entire GIT of *C. cyanea*. Neutral and mixed (acid and neutral) mucins were predominant in both the small and large intestines. These findings correlate with studies carried out by Sheahan and Jervis (1976), and Kotzé and Coetzee (1994). The former authors observed that acid mucin secreting goblet cells were abundant in the intestinal epithelium, but most prominent in the large intestine, with a decrease in neutral mucins towards the large intestine. Since large bacterial colonies are found in the large intestine, especially the colon (Macfarlane & Dillon, 2007), the increase of acid mucins suggests that the mucus gel viscosity is increased to better protect the surface epithelial layer.

The caecum compared to the other GI regions in *A. spinosissimus* showed a constant decrease in the number of goblet cells. This decrease may be influenced by microflora present in the caecum (Sharma et al., 1995). Large numbers of mixed (acid and neutral), neutral and acid mucins were present in the caecum of *A. spinosissimus*. Relatively equal numbers of acid mucins, sulfo- and sialomucins were also observed. This correlates with the findings of Sheahan and Jervis (1976) in the rat. Both Ndou (2007) and Sheahan and

Jervis (1976) observed that sulfomucins were dominant in the caecum, with only small numbers of sialomucin cells.

Kotzé and Coetzee (1994) observed that there were slightly more sulfomucins than sialomucins in the large intestine of the African elephant. In addition, Sheahan and Jervis (1976) report that sulfomucins were the main type in all 11 species examined. In the present study, similar observations are made in *A. spinosissimus* and *C. cyanea*. However, *A. hottentotus* have substantially more sialomucins in the distal small intestine and colon.

Despite the few general similarities between the insectivorous species in this study, there were differences between the species in the qualitative expression of the different mucins in each GI region. A similar observation was made by Sheahan and Jervis (1976). It is therefore difficult to determine whether the distribution of mucins is related to diet. Sheahan and Jervis (1976) examined animals that were captured in the wild, and some were laboratory animals, for their mucin histochemical study. This study also used animals that were captured in the wild. Therefore, none of the animals that were studied were subjected to a controlled diet. Sheahan and Jervis (1976) suggested that a controlled diet in all of the latter species may represent different results in terms of the distribution and type of mucins in the GIT.

Studies performed by Sharma et al. (1993) and Sharma and Schumacher (1995) on germ-free and conventional rats indicated that the diet and microflora could influence both the secretory pattern of GI mucins and mucosal architecture. Neutral and sulfomucins of the GI epithelial cells showed changes in the jejunum and proximal colon with response to diet and/or microflora. However, some contradictory results have been reported by other authors on the mucin secretory activity of goblet cells. Studies done by Vahouny et al. (1985) and Schneeman et al. (1982) report that a wheat bran-containing diet increases the turnover of mucins and caused increased differentiation of goblet cells. In addition, Lundin et al. (1993) found that fibre supplementation to a low-fibre diet did not influence the quality of mucins in the goblet cells, but increases the number of goblet cells in the small intestine.

The mucins synthesised and secreted by specialised goblet cells were responsible for the protective characteristics of the mucus gel in the GIT (Sharma & Schumacher, 1995). Apart from the protective function, mucins were also responsible for the formation of the mucus gel due to the presence of numerous sulfate and/or sialic acid residues on the

oligosaccharide chains (Strous & Dekker, 1992). According to Forstner (1978) and Proust et al. (1984), mucins also act as a selective barrier for the absorption of nutrients.

5.3 Function of mucins

Mucins are high molecular weight, highly glycosylated glycoproteins (Devine & McKenzie, 1992) which form the principal viscous and gel-forming components of the mucus gel (Pearson & Brownlee, 2005). Mucins were not only present on the apical epithelial surfaces of the GITs of mammals, it is also present on the epithelial surfaces of the respiratory, reproductive and urinary tracts as well as on the surface of the eye (Rose & Voynow, 2006; Linden et al., 2008). These mucosal surfaces covered by mucus, was colonised by local microbial flora, which varied substantially in complexity and composition (Linden et al., 2008). From a microbiological view, the protecting, undisturbed mucus layer in the gut created a micro-environment for microflora, and is referred to as biofilm (Probert & Gibson, 2002). A biofilm describes enclosed bacterial populations that adhere to each other and to other surfaces (Costerton et al., 1995). The colonisation of microflora on the mucus layer prevents the colonisation by pathogens (Montagne, Piel, & Lallès, 2004).

As a result of the exposure of mucosal surfaces to the external environment, these surfaces were the primary focus point of attack by micro-organisms (Pearson & Brownlee, 2005). The mucus layer and biofilm provided a protective barrier against toxins and pathogens and also contributed to the innate defence system (Corfield & Shukla, 2004). In addition, the mucus layer also provided lubrication for the passage of objects, hydration of the epithelium and it functions as a permeable layer for the exchange of nutrients and gasses with the underlying epithelium (Allen, 1981; Neutra & Forstner, 1987).

The bacteria in the biofilm were associated with food particles in the lumen (indirectly supports the digestive processes by fermentation) (Montagne et al., 2004; Macfarlane & Dillon, 2007) and the protection of the host against microbial pathogens (Probert & Gibson, 2002).

The mucin oligosaccharides in the mucus gel represent a direct source of peptides, carbohydrates, and nutrients that allows for the colonisation of bacteria in the mucus layer (Deplancke & Gaskins, 2001). In that regard, it is not surprising that microbes and their microbial products in the biofilm can stimulate the epithelial cells to allow for the increased production of mucins (Linden et al., 2008). According to Linden et al. (2008), there was evidence that the attachment of probiotic bacteria up-regulates the expression of cell-

surface mucins *in vitro*, and therefore represents an important part of the protective mechanism by which probiotic bacteria can limit infections by pathogens and toxins.

The mucosal epithelial tissues have evolved several defensive mechanisms against microbial attack, such as the secretion of mucins, defensins, antibodies, and lysozyme, into the mucosal layer (Linden et al., 2008). These different compounds form a physical barrier with antimicrobial activity and the ability to opsonise (the rendering of bacteria and other foreign substances to phagocytosis) and remove micro-organisms (Linden et al., 2008). However, all of these roles can individually be fulfilled by mucin glycoproteins. The defensive mechanism of mucins lies in the capability to entrap microbes (Deplancke & Gaskins, 2001) and then clearing it from the gut through shedding of the mucus layer (Pearson & Brownlee, 2005; Linden et al., 2008). The state of GI protection against bacterial infection appears to be related to the degree of mucin maturation (Montagne, Piel, & Lallès, 2004). According to Van Leeuwen and Versantvoort (1999), mature mucins were primarily sulfated. The acidic mucins, sulfo- and sialomucins increases the ability of mucus to resist attack by bacteria and bacterial enzymes.

When the normal micro-flora, the mucus layer or the epithelial cells were disturbed by pathogens, antigens and other toxic substances from the gut lumen, defects in the mucosal barrier system becomes evident (Montagne et al., 2004; Pearson & Brownlee, 2005). As a result of most of these intestinal infections, goblet cells were stimulated to secrete and synthesize mucins (Kim & Ho, 2010). However, chronic infections caused the depletion of goblet cells (Kim & Ho, 2010). Consequently, the quantitative and qualitative alteration of the mucus layers occurred, because both the synthesis and secretion of mucins have been altered.

Mucins have been implicated in GI diseases (Shirazi et al., 2000; McGuckin et al., 2009), cancer (Forstner & Forstner, 1994; Varki et al., 1999), respiratory diseases (Brock, 1995; Fahy, 2002; Thornton et al., 2008), and ocular surface diseases (Gipson et al., 2004).

Mucins in inflammatory bowel disease (IBD) have undergone biochemical changes, such as glycosylation and sulfation (Shirazi et al., 2000). The oligosaccharide chain length of mucins in IBD has been reported to be half than the normal length (Clamp et al., 1981). Inflammatory bowel disease was also associated with increased sialylation (Parker et al., 1995) and decreased sulfation of mucins (Raouf, Tsai, Parker, & et al., 1992). Thus, the synthesis of increased sialomucins has been observed in IBD. These changes are likely to alter the properties of the viscous mucus gel and also influence the interactions of mucins

with micro-organisms, defensive proteins, and therefore reducing the protection abilities of the mucus layer. Sialylation and sulfation are important because they play a role in the prevention of bacterial degradation of mucins (Shirazi et al., 2000).

Mucins have become an important element in the study of GI physiology, pathology and even taxonomic problems (Scillitani et al., 2007; Cao & Wang, 2009). The different types of mucins (neutral, sulfo- and sulfomucins) have also been implicated in the colonisation of the biofilm in the GIT (Deplancke & Gaskins, 2001). It is therefore, important to determine the composition of the different types of mucins in the mucosal layer which affects the colonisation of microflora. It is essential to understand the normal microbiome of the GIT in various species to provide a better understanding of the role of normal gut flora which is important for the maintenance of a healthy GIT.

There are still many unanswered questions about the distribution, function and structure of mucins in health and disease. A better understanding of mucins in a variety of normal tissues is needed, because most mucin studies have been performed on diseased tissue or cell lines (Hattrup & Gendler, 2008).

CHAPTER 6

CONCLUSION

6.1 Limitations of the study

The GITs of the three insectivorous species of this study were removed at the University of Pretoria by other researchers not involved in the current study. This is a limitation because the present study had no control over the specimens. The GITs of the specimens were severed before entering the pelvic cavity, and unfortunately the rectum could not be included in this study. In addition, because specimens were caught in the wild, there was no control over their diet and therefore the extent to which the intestines were filled with ingesta at the time of death. Consequently, the varying extent to which certain parts of the GIT were filled with intestinal content may have influenced the structure and measurements of the different GI regions.

6.2 Concluding remarks and prospective research

In general, the GITs of *A. spinosissimus*, *C. cyanea* and *A. hottentotus* have primitive characteristics which might have been influenced by both evolution and diet. All three species had a single chambered (unilocular) stomach, and *C. cyanea* and *A. hottentotus* lacked caeca.

The histology of the GITs of the three insectivorous species was mainly consistent with what had been observed in the literature, with the exception of *A. spinosissimus* in which transverse and V-shaped mucosal folds had been observed in the caecum and proximal colon, respectively. *C. cyanea* and *A. hottentotus* have villi in the distal small intestine and prominent longitudinal folds (plicae circulares) within the colon. All of these structures have been observed both macro- and microscopically. In addition, parietal cells and Brunner's glands were present in all three species. For *C. cyanea* and *A. hottentotus* no peptic or paneth cells were observed.

Some similarities have been observed in the distribution of the different types of mucins in the GITs of the insectivores and other mammals discussed. However, noticeable differences in the number of mucins in each of the GI regions were present. The insectivorous species predominantly have neutral mucins in the mucous cells of the stomach, whereas *A. hottentotus* also had large numbers of sialomucins in the mucous cells. Mixed (neutral and acid) and mixed acid mucins (sulfo- and sialomucins) were the predominant mucin type in both the small- and large intestines of the species studied. *A. hottentotus* primarily has primarily sialomucins in the small- and large intestine. The large number of mixed acid mucins (sulfo- and sialomucins) in the GITs of the species studied,

suggested that the mucus gel had an increased viscosity for the protection against pathogens. The overall similarity between the three insectivores and other distantly related species, such as primates and lagomorphs, suggests that mixed mucin types were essential to the formation of the biofilm in the GITs of the majority of mammals, irrespective of their diet or taxonomy.

Mucins associated with disease have generally been malformed by pathogens. The secretion of the altered mucins influenced the viscosity of the protective mucus gel and also the colonisation of microflora, which protected against pathogens. The mucosal surface became susceptible to attack by various pathogens and toxins. Mucins have become an important element in the study of GI physiology, pathology and even taxonomic problems, and the different mucins have also been implicated in the colonisation of the mucus layer. However, there are still many unanswered questions about the distribution, function and structure of mucins in health and disease. A better understanding of mucins and biofilm in a variety of normal tissues is essential, as most mucin and biofilm studies have been performed on diseased tissue or cell lines.

The present study provides a baseline for further morphological and mucin histochemical studies. The detection of mucins with histochemical staining techniques did not provide structural information about the different oligosaccharide chains attached to the mucin molecule. Future studies using lectin histochemistry techniques would better describe the structural aspects of the mucins distributed throughout the biofilm of the GIT.

LIST OF REFERENCES

Allen, A. (1981). Structure and function of gastrointestinal mucus. In L. Johnson (Ed.), *Physiology of the gastroenterology tract.* (1st ed., pp. 617-639). New York: Raven Press.

Allen, A., & Pearson, J. (1993). Mucus glycoproteins of the normal gastrointestinal tract. *European Journal of Gastroenterology and Hepatology*(5), 193-199.

Asher, R. J., Bennett, N., & Lehmann, T. (2009). The new framework for understanding placental mammal evolution. *BioEssays, 31*, 853-864.

Bancroft, J., & Gamble, M. (Eds.). (2008). *Theory and practice of histological techniques.* Edinburg, London: Churchill Livingston Elsevier Limited.

Bancroft, J., & Stevens, A. (Eds.). (1990). *Theory and Practice of Histological Techniques* (3rd ed.). Edinburg, London: Churchill Livingstone.

Bansil, R., & Turner, B. (2006). Mucin structure, aggregation, physiological functions and biomedical applications. *Current Opinion in Colloid & Interface Science 11*, 164-170.

Baxter, R., & Meester, J. (1982). The captive behaviour of the red musk shrew, *Crocidura f. flavescens* (I. Geoffroy, 1827) (Soricidae: Crocidurinae). *Mammalia, 46*, 10-27.

Beck, R. M., Bininda-Emonds, O. R., Cardillo, M., Lui, F.-G. R., & Purvis, A. (2006). A higher-level MRP supertree of placental mammals. *BMC Evolutionary Biology, 6*(93).

Behmann, H. (1973). Vergleichend- und funktionell-anatomische Untersuchungen am Caecum und Colon myomorpher Nagetiere. *Zeitschrift für wissenschaftliche Zoologie, 186*, 173-294.

Björnhag, G. (1994). Adaptations in the large intestine allowing small animals to eat fibrous food. In D. Chivers, & P. Langer (Eds.), *The Digestive System in Mammals: Food, Form and Function* (pp. 287-312). Cambridge: Cambridge University Press.

Bowdich, T. (1821). *An analysis or the natural classifications of mammalia for the use of students and travellers.* Paris: J. Smith.

Brock, C. (1995). An evaluation of mucus glycoproteins in the larynges of victims of sudden infant death syndrome. *The Journal of Laryngology and Otology, 109*, 403-409.

Brockhausen, I., Schachter, H., & Stanley, P. (2009). O-GalNAc Glycans. In A. Varki, R. Cummings, J. Esko, H. Freeze, P. Stanley, C. Bertozzi, et al. (Eds.), *Essentials of Glycobiology* (2nd ed., pp. 115-127). New York: Cold Spring Harbor Laboratory Press.

Bronner, G. (1995). *Systematic revision of the golden mole genera Amblysomus, Chlorotalpa and Calcochloris (Insectivora: Chrysochloromorpha, Chrysochloridae).* Unpublished PhD Thesis, University of Natal, Durban.

Broom, R. (1915). On the organ of Jacobson and its relations in the Insectivora. *Proceedings of the Zoological society of London*, 157-162, 347-354.

Broom, R. (1916). On the structure of the skull in Chrysochloris. *Proceedings of the Zoological society of London, 126*, 453-481.

Butler, P. (1956). The skull of Ictops and the classification of the Insectivora. *Proceedings of the Zoological Society of London, 126*, 453-481.

Butler, P. (1972). The problem of insectivore classification. In K. Joysey, & T. Kemp (Eds.), *Studies in Vertebrate Evolution* (pp. 253-265). Edinburgh: Oliver & Boyd.

Cao, X., & Wang, W. (2009). Histology and mucin histochemistry of the digestive tract of yellow catfish, *Pelteobagrus fulvidraco*. *Anatomia Histologia Embryologia, 38*, 254-261.

Carleton, M. (1973). *A survey of gross stomach morphology in New world Cricetinae (Rodentia, Muroidea), with comments on functional interpretations* (Vol. 146). Ann Arbor, Michigan: Miscellaneous Publications.

Cheng, H., Bjerknes, M., & Amar, J. (1984). Methods for the determination of epithelial cell kinetic parameters of human colonic epithelium isolated from surgical and biopsy specimens. *Gastroenterology, 86*, 78-85.

Chivers, D., & Hladik, C. (1980). Morphology of the gastrointestinal tract in Primates: Comparisons with other mammals in relation to diet. *Journal of Morphology, 166*, 337-386.

Churchfield, S. (1990). *The natural history of shrews* (Illustrated ed.). (E. Neal, Ed.) United Kindom: Comstock Publishing Associates.

Cizek, D., & Myers, P. (2000). *http://animaldiversity.org*. Retrieved March 20, 2010, from Animal Diversity Web: http://animaldiversity.ummz.umich.edu/site/accounts/information/Chrysochloridae.html.

Clamp, J., Fraser, G., & Read, A. (1981). Study of the carbohydrat content of mucus glycoproteins from normal and diseased colons. *Clinical Science, 61*, 229-234.

Clauss, M., Frey, R., Kiefer, B., Lechner-Doll, M., Loehlein, W., Polster, C., et al. (2003). The maximum attainable body size of herbivorous mammals: morphophysiological constraints on foregut, and adaptations of hindgut fermenters. *Oecologia, 136*, 14-27.

Corfield, A., & Shukla, A. (2004). Mucins: vital components of the mucosal defensive barrier. *Genomic/Proteomic Technology, 3*, 20-22.

Costerton, J., Lewandowski, Z., Caldwell, D., Korber, D., & Lappin-Scott, H. (1995). Microbial biofilms. *Ann. Revi. Microbiol., 49*, 711-745.

Crawley, S., Gum, J., Hicks, J., Pratt, W., Aubert, J., Swallow, D., et al. (1999). Genomic organization and structure of the 3' region of human MUC3: alternative splicing predicts membrane-bound and soluble forms of the mucin. *Biochemical and Biophysical Research Communications, 263*, 728-736.

De Blainville, H. (1816). Prodrome d'une nouvelle distribution systématique du régne animal. *Journal de Physique, Chimie et Histoire Naturelle, 83*, 244-267.

Dekker, J., Rossen, J., Buller, H., & Einerhand, A. (2002). The MUC family; and obituary. *Trends in Biochemical Sciences, 27*, 126-131.

Deplancke, B., & Gaskins, H. (2001). Microbial modulation of innate defense: goblet cells and the intestinal mucus layer. *The America Journal of Clinical Nutrition, 71(suppl)*, 1131S-1141S.

Derting, T., & Noakes, E. (1995). Seasonal changes in gut capacity in the white-footed mouse (*Peromyscus leucopus*) and meadow vole (*Microtus pennsylvanicus*). *Canadian Journal of Zoology, 73*, 243-252.

Devine, P., & McKenzie, F. (1992). Mucins: Structure, Function, and Associations with Malignancy. *BioEssays, 14*(9), 619-625.

Dickman, C. (1995). Diets and habitat preferences of three species of crocidurine shrews in arid southern Africa. *Journal of Zoology, London, 237*, 499-514.

Douady, C., & Douzery, E. (2009). Hedgehogs, shrews, moles and solenodons (Eulipotyphla). In S. Hedges, & S. Kumar (Eds.), *The Timetree of Life* (pp. 495-498). New York: Oxford University Press.

Enss, M., Muller, H., Schmidt-Wittig, U., Kownatzki, R., Coenen, M., & Hendrich, H. (1996). Effects of perorally applied endotoxin on colonic mucins of germfree rats. *Scandinavian Journal of Gastroenterology, 31*, 868-874.

Fahy, J. (2002). Goblet cell and mucin gene abnormalities in asthma. *Chest, 122*, 320S-326S.

Fernandez, F., Sharma, R., Hinton, M., & Bedford, M. (2000). Diet influences the colonisation of *Campylobacter jejuni* and distribution of mucin carbohydrates in the chick intestinal tract. *Cellular and Molecular Life Sciences, 57*, 1793-1801.

Filipe, M. (1979). Mucins in the human gastrointestinal epithelium: A review. *Investigative Cell Pathology, 2*, 195-216.

Flemstrom, G., & Kivilaakso, E. (1983). Demonstration of a pH-gradient at the luminal surface of rat duodenum and its dependence on mucosal alkaline secretion. *Gastroenterology, 84*, 787-794.

Flower, W. (1872, Des. 24). Lectures on the comparative anatomy of the organs of digestion of the mammalia. *Medical Times and Gazette, Feb., 14*.

Forder, R., Howarth, G., Tivey, D., & Hughes, R. (2007). Bacterial modulation of small intestinal goblet cells and mucin composition during early posthatch development of poultry. *Poultry Science, 86*, 2396-2403.

Forstner, J. (1978). Intestinal Mucins in Health and Disease. *Digestion (International Journal of Gastroenterology), 17*(3), 234-263.

Forstner, J., & Forstner, G. (1994). Gastrointestinal Mucus. In L. Johnson (Ed.), *Physiology of the Gastrointestinal Tract* (3rd ed., Vol. 2, pp. 1255-1283). New York, United States of America: Raven Press, Ltd.

Freeman, J. (1966, January). Goblet cell fine structure. *The Anatomical Record, 154*, 121-148.

Gallagher, J., & Corfield, A. (1978). Mucin-type glycoproteins - new perspectives on their structure and synthesis. *Trends in Biochemical Sciences, 3*(1), 38-41.

Gartner, L., & Hiat, J. (2000). *Color atlas of histology* (3rd ed.). United States of America: Lippincott Williams & Wilkins.

Genoud, M., & Vogel, P. (1981). The activity of *Crocidura russula* (Insectivora, Soricidae) in the field and in captivity. *Zeitschrift für Säugetierkunde, 46*, 222-232.

Gill, T. (1872). *Arrangement of the families of mammals with analytical tables* (Vol. 11). Washington: Smithsonian Miscellaneous Collections.

Gipson, I., Hori, Y., & Argueso, P. (2004). Character of ocular surface mucins and their alteration in dry eye disease. *The Ocular Surfae, 2*(2), 131-148.

Goralski, A., Sawicki, W., & Blaton, O. (1975). Nonrandom distribution of goblet cells around the circumference of colonic crypts. *Cell Tissue Research, 160*, 551-556.

Gorgas, M. (1967). Vergleichend-anatomische Untersuchungen am Magen-Darm-Kanal der Scuiromorpha, Hystricomorpha und Caviomorpha (Rodentia). *Zeitschrift für wissenschaftliche Zoologie, 175*, 237-404.

Gregory, W. (1910). The orders of mammals. *Bulletin of the American Museum of Natural History, 27*, 1-524.

Grossman, M. (1958). The glands of Brunner. *Pysiological Reviews, 38*(4), 675-690.

Haeckel, E. (1866). Systematische Einleitung in die allgemeine entwicklungsgesgichte. In *Generelle morphologie der organismen Bd 2* (pp. 17-160). Berlin: Georg Reimer.

Hattori, S., & Yamanouchi, K. (1984). Gross Anatomy of Watase's Shrew, *Crocidura horsfieldi watasei*. *Jikken dobutsu. Experimental animals, 33*(4), 519-524.

Hattrup, C., & Gendler, S. (2008). Structure and function of the cell surface (tethered) mucins. *The Annual Review of Physiology, 70*, 431-57.

Havez, R., Regand, P., Randoux, A., & Biserte, G. (1969). In H. Peeters (Ed.), *Protides of the biological fluids* (pp. 343-360). London: Pergamon Press.

Havez, R., Roussel, P., Degand, P., & Biserte, G. (1967, September). Study of carboxylic and sulfated glycoproteins in human bronchial mucus. *Clinica Chimica Acta, 17*(3), 463-477.

Hecht, G. (1999). Innate mechanisms of epithelial host defense: spotlight on intestine. *Am. J. Physiol. Ser., C277*, C351-C358.

Hilton, W. (1902). The morphology and development of intestinal folds and villi in vertebrates. *Am. J. Anat., 1*, 459-504.

Hisaw, F. (1923). Feeding habits of moles. *Journal of Mammology, 4*(1), 9-20.

Hotchkiss, R. (1948). A microchemical reaction resulting in the staining of polysaccharide structures in fixed tissue preparations. *Archives of Biochemistry, 16*, 131-141.

Illiger, J. (1811). *Prodromus systematis mammalium et avium: Additis terminis zoographicis utruisque classiss, eorumque versione germanica.* Berlin: Salfeld.

Kawakubo, M., & et al. (2004). Natural antibiotic function of a human gastric mucin against Helicobacter pylori infection. *Science, 305*, 1003-1006.

Keegan, D. (1977). Aspects of the assimilation of sugars by Rousettus aegypticus. Comparative biochemistry and physiology. Part A. *Physiology, 58*, 349-352.

Keller, G. (2005). *Statistics: For management and economics* (7th ed.). Belmont, USA: Duxbury, Thomson Brooks/Cole.

Kierszenbaum, A. (2002). *Histology and Cell Biology: An Introduction to Pathology.* St. Louis, Missouri, United states of America: Mosby Inc.

Kim, Y., & Ho, S. (2010). Intestinal goblet cells and mucins in health and disease: Recent insights and progress. *Current Gastroenterology Reports, 12*, 319-330.

Kingdon, J. (1974a). *East African Mammals, An Atlas of Evolution in Africa, Volume II Part A (Insectivores and Bats).* London: Academic Press.

Kingdon, J. (1974b). *East African Mammals, An Atlas of Evolution in Africa, Volume II Part B (Hares and Rodents).* London: Academic Press Inc. (London) LTD.

Kotzé, S., & Coetzee, H. (1994). A histocytochemical study of mucus glycoproteins or mucins in the intestinal tract of the African elephant (*Loxodonta africana*). *Onderstepoort Journal of Veterinary Research, 61*, 177-181.

Kotzé, S., Van der Merwe, E., Bennett, N., & O'Rian, M. (2010). The comparative anatomy of the abdominal gastrointestinal tract of six species of African mole-rats. *Journal of Morphology, 271*, 50-60.

Kurohmaru, M., Nishida, T., & Mochizuki, K. (1980). Morphological study on the intestine of the Musk Shrew, *Suncus murinus*. *Japanese Journal of Veterinary Science, 42*, 61-71.

Kurohmaru, M., Nishida, T., Mochizuki, K., Hayashi, Y., & Hattori, S. (1982). Morphology of the intestine of the Watase's Shrew, *Crocidura horsfieldi watasei*. *Japanese Journal of Veterinary Science, 44*, 795-799.

Kuyper, M. (1985). The Ecology of the Golden Mole, *Amblysomus hottentotus*. *Mammal Review, 15*(1), 3-11.

Lacy, R., Lynch, C., & Lynch, G. (1978). Developmental and adult acclimation effects of ambient temperature on temperature regulation of mice selected for high and low levels of nest-building. *Journal of Comparative Physiology, 123*, 185-192.

Lange, R., & Staaland, H. (1970). Adaptations of the caecum-colon structure of rodents. *Comparative Biochemistry and Physiology, 35*, 905-919.

Langer, P. (1988). *The mammalian herbivore stomach: Comparative anatomy, function and evolution.* New York: Gustav Fischer Verlag.

Langer, P. (1991). Evolution of the digestive tract in mammals. *Verhandlungen der Deutschen Zoologischen Gesellschaft, 84*, 169-193.

Langer, P. (2002). The digestive tract and life history of small mammals. *Mammal Review, 32*(2), 107-131.

Laux, D., Cohen, P., & Conway, T. (2005). Role of mucus layer in bacterial colonization of the intestine. In J. Nataro, P. Cohen, H. Mobley, & J. Weiser (Eds.), *Colonization of Mucosal Surfaces* (pp. 199-212). Washington, D. C.: ASM Press.

Leche, W. (1885). Über die Säugethiergattung Galeopithecus. *Kongliga Svenska Vetenskap-Akademiens Handlingar, 21*, 1-92.

Levene, H. (1960). *Contributions to probability and statistics: Essays in Honor of Harold Hotelling.* (I. e. Olkin, Ed.) Stanford: Stanford University Press.

Linden, S., Sutton, P., Karlsson, N., Korolik, V., & McGuckin, M. (2008, May). Mucins in the mucosal barrier to infection. *Mucosal Immunology, 1*(3), 183-197.

Linnaeus, C. (1758). *Systema Naturae per Regna Tria Naturae* (Vol. 10th). Stockholm: Laurentii Salvii.

Lundin, E., Zhang, J.-X., Huang, C.-B., Reuterving, C.-O., Hallmans, F., Nygren, C., et al. (1993). Oat bran, rye bran, and soybean hull increase goblet cell volume density in the small intestine of the golden hamster. A histochemical and stereological light microscopic study. *Scandinavian Journal of Gastroenterology, 28*, 15-22.

Macfarlane, S., & Dillon, J. (2007). Microbial biofilms in the human gastrointestinal tract. *Journal of Applied Microbiology, 102*, 1187-1196.

Mack, D., Ahrne, S., Hyde, L., Wei, S., & Hollingsworth, M. (2003). Extracellular MUC3 mucin secretion follows adherence of Lactobacillus strains to intestinal epithelial cells in vitro. *Gut, 52*, 827-833.

MacPhee, R., & Novacek, M. (1993). Definition and relationships of Lipotyphla. In F. Szalay, M. Novacek, & M. McKenna (Eds.), *Mammal Phylogeny* (Vol. II, pp. 13-31). New York: Springer.

Madsen, O., Scally, M., Douady, C., Kao, D., Debry, R., Adkins, R., et al. (2001). Parallel adaptive radiations in two major clades of placental mammals. *Nature, 409*, 610-614.

Mason, M. (2003). Morphology of the middle ear of golden moles (Chrysocholoridae). *Journal of Zoology*(260), 391-403.

McAuley, J., Linden, S., Png, C., King, R., Pennington, H., Gendler, S., et al. (2007). MUC1 cell surface mucin is a critical element of the mucosal barrier to infection. *Journal of Clinical Investigation, 117*, 2313-2324.

McGuckin, M., & Thornton, D. (2000). Detection and Quantitation of Mucins Using Chemical, Lectin, and Antibody Methods. In A. Corfiel (Ed.), *Glycoprotein methods and protocols: The Mucins* (Vol. 125, pp. 45-47). Totowa, New Jersy: Humana Press Inc.

McGuckin, M., Eri, R., Simms, L., Florin, T., & Radford-Smith, G. (2009). Intestinal barrier dysfunction in inflammatory bowel diseases. *Inflammatory Bowel Diseases, 15*(1), 100-110.

McGuckin, M., Every, A., Skene, C., Linden, S., Chionh, Y., Swierczak, A., et al. (2007). Muc1 mucin limits both Helicobacter pylori colonization of the murine gastric mucosa and associated gastritis. *Gastroenterology, 133*, 1210-1218.

McNab, B. (1973). Energetics and distribution of vampires. *Journal of Mammalogy, 54*, 131-144.

Meester, J. (1963). A systematic revision of the shrew genus Crocidura in southern Africa. *Transvaal Museum Memoir, 13*(13), 1-127.

Milinkovitch, M., Guillermo, O., & Meyer, A. (1993). Revised phylogeny of whales suggested by mitochondrial DNA sequences. *Nature, 361*, 346-348.

Mills, G., & Hes, L. (1997). *The Complete Book of Southern African Mammals.* Cape Town: Struik Winchester Publishers.

Montagne, L., Piel, C., & Lallès, J. (2004, March). Effect of diet on mucin kinetics and composition: Nutrition and health implications. *Nutrition Reviews, 62*(3), 105-114.

Moore, B., Morris, G., & Vanner, S. (2000). A novel in vitro model of Brunner's gland secretion in the guinea pid duodenum. *American Journal of Physiology: Gastrointestinal and Liver Physiology, 278*, G477-G485.

Mowry, R. (1956). Alcian blue technics for the histochemical study of acidic carbohydrates. *Journal of Histochemistry and Cytochemistry, 4*, 407.

Myrcha, A. (1967). Comparative studies on the morphology of the stomach in the Insectivora. *Acta Theriologica, 12*(14), 223-244.

Ndou, R. (2007). *The histology of the gastrointestinal tract of mole-rats B. suillus, G. capensis and C. h. hottentotus: A morphological and mucin histochemical study.* Unpublished Thesis, University of Cape Town, Department of Human Biology, Cape Town.

Neutra, M., & Forstner, J. (1987). Gastrointestinal Mucus: Synthesis, secretion, and function. In L. Johnson (Ed.), *Physiology of the Gastrointestinal Tract* (2nd ed., pp. 975-1009). New York: Raven Press.

Nickel, R., Schummor, A., & Seiferle, E. (1973). The viscera of the domestic mammals. Berlin and Hamburg: Verlag Paul Parey.

Parker, N., Tsai, H., Ryder, S., & et al. (1995). Increased rate of sialylation of colonic mucin by cultured ulcerative colitis mucosal explants. *Digestion, 56*, 52-56.

Paulus, U., Loeffler, M., Zeidler, J., Owen, G., & Potten, C. (1993). The differentiation and lineage development of goblet cells in the murine small intestinal crypt: experimental and modelling studies. *Journal of Cell Sciense, 106*, 473-484.

Pavelka, M., & Roth, J. (2010). *Functional Ultrastructure: Atlas of Tissue Biology and Pathology* (2nd ed.). Austria: Springer-Verlag/Wien.

Pearce, A. (1968). *Histochemistry: Theoretical and Applied* (3rd ed., Vol. 1). Gloucester Place, London: J. & A. Churchill Ltd.

Pearson, J., & Brownlee, I. (2005). Structure and Function of Mucosal Surfaces. In J. Nataro, P. Cohen, H. Mobley, & J. Weiser (Eds.), *Colonization of Mucosal Surfaces* (pp. 3-16). Washington, D.C.: ASM Press.

Pearson, J., Brownlee, I., & Taylor, C. (2004). Mucin genes in the GI tract. In P. Williams, & G. Phillips (Eds.), *Gums and Stabilisers for the Food Industry* (pp. 517-524). Cambridge, United Kingdom: Royal Society of Chemistry.

Perez-Villar, J., & Hill, R. (1999). The structure and assembly of secreted mucins. *The Journal of Biological Chemistry, 274*(45), 31751-31754.

Pernetta, J. (1977). Activity and behaviour of captive *Crocidura suaveolens cassiteridum* (Hinton, 1924). *Acta Theriologica, 22*, 387-389.

Perrin, M., & Curtis, B. (1980). Comparative morphology of the digestive system of 19 species of Southern African myomorph rodents in relation to diet and evolution. *South African Journal of Zoology, 15*(1), 22-33.

Peters, W. (1864). *Über die Säugethier-Gattung Solenodon. Abhandlüngen der Königlichen Akademie der Wissenschäften zu Berlin (für 1893). p. 22.*

Poddar, S., & Jacob, S. (1979). Mucosubstance histochemistry of Brunner's glands, pyloric glands and duodenal goblet cells in the ferret. *Histochemistry, 65*, 67-81.

Probert, H., & Gibson, G. (2002). Bacterial biofilms in the human gastrointestinal tract. *Current Issues in Intestinal Microbiology, 3*, 23-27.

Proust, J., Tchaliovska, S., & Ter Minassioan Sar, L. (1984). Mucin thin-film as a model of the tear film rupture. *Science, 98*, 319.

Pullan, R., Thomas, G., Rhodes, M., Newcombe, R., Williams, G., Allen, A., et al. (1994). Thickness of adherent mucus gel on colonic mucosa in humans and its relevance to colitis. *Gut, 35*(3), 353-359.

Radwan, K., Oliver, M., & Specian, R. (1990). Cytoarchitectural reorganization of rabbit colonic goblet cells during baseline secretion. *Americal Journal of Anatomy, 189*, 365-376.

Raouf, A., Tsai, H., Parker, N., & et al. (1992). Sulphation of colonic mucin in ulcerative colitis and Crohn's disease. *Clinical Science, 83*, 623-626.

Rhodes, J. (1997). Mucins and inflammatory bowel disease. *QJM: An International Journal of Medicine, 90*, 79-82.

Rose, M., & Voynow, J. (2006). Respiratory tract mucin genes and mucin glycoproteins in health and diseas. *Physiological Reviews, 80*, 245-278.

Ruselervanembden, J., Vanlieshout, L., Gosselink, M., & Marteau, P. (1995). Inability of *Lactobacillus casei* strain Gg, *L. acidophilus*, and *Bifidobacterium bifidum* to degrade intestinal mucus glycoproteins. *Scandinavian Journal of Gastroenterology, 30*, 675-680.

Sakata, T., & Von Engelhardt, W. (1981). Luminal mucin in the large intestine of mice, rats and guinea pigs. *Cell and Tissue Research, 219*, 629-635.

Sandow, M., & Whitehead, R. (1979). The Paneth cell: Progress Report. *Gut, 20*, 420-431.

Satoh, Y., Ishikawa, K., Ono, K., & Vollrath, L. (1986). Quantitative light microscopic observations on Paneth cells of germ-free and ex-germ-free Wistar rats. *Digestion, 34*, 115-121.

Satoh, Y., Yamano, M., Matsuda, M., & Ono, K. (1990). Ultrastructure of Paneth cells in the intestine of various mammals. *Journal of Electron Microscopy Technique, 16*(1), 69-80.

Schneeman, B., Richter, B., & Jacobs, L. (1982). Response to dietary wheat bran in the exocrine pancreas and intestine of rats. *Journal of Nutrition, 112*, 283-286.

Scillitani, G., Zizza, S., Liquori, G., & Ferri, D. (2007). Lectin histochemistry of gastrointestinal glycoconjugates in the greater horseshoe bat, *Rhinolophus ferrumequinum* (Schreber, 1774). *Acta histochemica, 109*, 347-357.

Sharma, R., & Schumacher, U. (1995, December). Morphometric analysis of intestinal mucins under different dietary conditions and gut flora in rats. *Digestive Diseases and Sciences, 40*(12), 2532-2539.

Sharma, R., Schumacher, U., Ronaasen, V., & Coates, M. (1993). The effects of diet and human microbial flora on the morphology and carbohydrate composition of rat intestine. In A. Pusztai, M. Hinton, & R. Mulder (Eds.), *Prevention and control of potentially pathogenic organisms in poultry and poultry meat processing* (pp. 109-116). Netherlands: Het Spelderholt.

Sharma, R., Schumacher, U., Ronaasen, V., & Coates, M. (1995). Rat intestinal mucosal responses to a microbial flora and different diets. *Gut, 36*, 209-214.

Sheahan, D., & Jervis, H. (1976). Comparative histochemistry of gastrointestinal mucosubstances. *American Journal of Anatomy, 146*, 103-132.

Shirazi, T., Longman, R., Corfield, A., & Probert, C. (2000). Mucins and inflammatory bowel disease. *Postgraduate Medical Journal, 76*, 473-478.

Sibly, R. (1981). Strategies of digestion and defecation. In C. Townsend, & P. Callow (Eds.), *Physiological ecology* (pp. 109-114). Sunderland: Sinauer Associates Inc.

Simpson, G. G. (1945). The Principles of Classification and a Classification of Mammals. (R. Tyler, Ed.) *Bulletin of the American Museum of Natural History, 85*, 1-350.

Skinner, J., & Chimimba, C. (2005). *The mammals of the southern African subregion* (3rd, illustrated, revised ed.). (J. Skinner, & C. Chimimba, Eds.) Cape Town: Cambridge University Press.

Skinner, J., & Smithers, R. (1990). *The Mammals of the Southern African Subregion.* Pretoria: University of Pretoria.

Skoczen, S. (1966). Stomach contents of the mole, Talpa europaea Linnaeus, 1758 from Southern Poland. *Acta theriologica, 11*(28), 551-577.

Snipes, R., & Kriete, A. (1991). Quantative investigation of the area and volume in different compartments of the intestine of 18 mammalian species. *Zeitschrift für Säugetierkunde, 56*, 225-244.

Southgate, H. (1927). Note on preparing mucicarmine. *Journal of Pathology and Bacteriology, 30*, 729.

Spicer, S. (1965). Diamine methods for differentiating mucosubstances histochemically. *The Journal of Histochemistry and Cytochemistry, 13*(3), 211-233.

Spicer, S., & Meyer, D. (1960). Histochemical differentiation of acid mucopolysaccharides by means of combined aldehyde fuchsin-alcian blue stain. *American Journal of Clinical Pathology, 33*, 453-460.

Spinks, A., Bennett, N., & Jarvis, J. (2000). A comparison of the ecology of two populations of the common mole-rat, *Cryptomys hottentotus hottentotus*: the effect of aridity on food, foraging and body mass. *Oecologia, 125*, 341-349.

Springer, M. S., & Murphy, W. J. (2007). Mammalian evolution and biomedicine: new view from phylogeny. *Biological Reviews, 82*, 375-392.

Springer, M., & De Jong, W. (2001, March 2). Phylogenetics. Which mammalian supertree to bark up? *Science, 291*(5509), 1709-11.

Springer, M., Cleven, G., Madsen, O., De Jong, W., Waddell, V., Amrine, H., et al. (1997). Endemic African mammals shake the phylogenetic tree. *Nature, 388*, 61-64.

Springer, M., Murphy, W., Eizirik, E., & O'Brien, S. (2005). Molecular evidence for major placental clades. In K. Rose, & J. Archibald (Eds.), *The Rise of Placental Mammals: Origin, Timing, and Relationships of the Major Extant Clades* (pp. 37-49). Baltimore: The John Hopkins University Press.

Springer, M., Stanhope, M., Madsen, O., & de Jong, W. (2004). Molecules consolidate the placental mammal tree. *Trends in Ecology and Evolution, 19*, 430-438.

St. Geoffroy, H., & Cuvier, G. (1795). Mémoire sur une nouvelle division des mammiferes, et sur les principes quie doivent servir de base dans cette sorte de travail. *Magasin Encyclopédique, 1*, 164-190.

Stanhope, M., Waddell, V., Madsen, O., De Jong , W., Hedges, S., Cleven, G., et al. (1998). Molecular evidence for multiple origins of Insectivora and for a new order of endemic African insectivore mammals. *Proceedings of the National Academy of Sciences USA, 95*, 9967-9972.

Statsoft, I. (2011). *[Online] Electronic Statistics Textbook.* Tulsa, Oklahoma.

Stevens, C., & Hume, I. (1995). *Comparative Physiology of the Vertebrate Digestive System* (2nd ed.). Cambridge: Cambridge University Press.

Stevens, C., & Hume, I. (1998). Contributions of microbes in vertebrate gastrointestinal tract to production and conservation of nutrients. *Physiological Reviews, 78*(2), 393-427.

Strous, G., & Dekker, J. (1992). Mucin-type glycoproteins. *Critical Reviews in Biochemistry and Molecular Biology, 27*, 57-92.

Strugala, V., Allen, A., Dettmar, P., & Pearson, J. (2003). Colonic mucin: methods of measuring mucus thickness. *The Proceedings of the Nutrition Society, 62*, 237-243.

Stuart, C., & Stuart, M. (2001). *Field Guide to Mammels of Southern Africa.* Cape Town: Struik Publishers.

Symonds, M. R. (2005). Phylogeny and life histories of the 'Insectivora': controversies and consequences. *Biological Reviews, 80*, 93-128.

Takehana, K., Abe, M., Iwasa, K., & Hiraga, T. (1989). Histochemistry of complex carbohydrates in the horse duodenal gland. *Nihon juigaku zasshi. The Japanese Journal of Veterinary Science, 51*, 909-915.

Takehana, K., Eerdunchaoluo, Ueda, H., Kobayashi, A., Iwasa, K., & Sou, K. (2000). A histochemical study of the Camel (*Camelus bactrianus*) duodenal glands. *The Journal of Veterinary Medical Science/ The Japanese Society of Veterinary Science, 62*(4), 449-452.

Taylor, C., Allen, A., Dettmar, P., & Pearson, J. (2003). The gel matrix of gastric mucus is maintained by a complex interplay of transient and nontransient associateions. *Biomacromolecules, 4*(4), 922-927.

Tedman, R., & Hall, L. (1985). The morphology of the gastrointestinal tract and food transit time in the fruit bats *Pteropus alecto* and *P. poliocephalus* (Megachiroptera). *Australian Journal of Zoology*.

The Free Dictionary: Glycosylation, 3.0. (2004). (Farlex, Inc.) Retrieved August 3, 2011, from http://medical-dictionary.thefreedictionary.com/glycosylation

The Open University. (2008, October 20). Retrieved 02 28, 2012, from Studying mammals: The insect hunters: http://openlearn.open.ac.uk/mod/oucontent/view.php?id=398740&section=5.3

Thornton, D., Rousseau, K., & McGuckin, M. (2008). Structure and function of the polymeric mucins in airways mucus. *Annu. Rev. Physio., 70*, 459-86.

Tibbetts, I. (1997). The distribution and function of mucous cells and their secretions in the alimentary tract of *Arrhamphus sclerolepis kre tii*. *Journal of Fish Biology, 50*, 809-820.

Trier, J. (1968). Morphology of the epithelium of the small intestine. In C. Code, *Handbook of physiology. Section 6: Alimentary canal, Vol. III: Intestinal absorption.* (pp. 1125-1175). American Physiological Society.

Vahouny, G., Le, T., Ifrim, I., Satchithanandam, S., & Cassidy, M. (1985). Stimulation of intestinal cytokinetics and mucin turnover in rats fed wheat bran and cellulose. *The American Journal of Clinical Nutrition, 41*, 895-900.

Van Klinken, J., Dekker, J., Büller, H., & Einerhand, A. (1995). Mucin gene structure and expression: protection vs. adhesion. *269*(5 Pt 1), G613-627.

Van Leeuwen, P., & Versantvoort, C. (1999). Functional histology of the small intestinal mucosa in livestock production animals. In A. Jansman, & J. Huisman (Eds.), *Nutrition and Gastrointestinal Physiology - Today and Tomorrow* (pp. 9-21). Wageningen: TNO.

Varki, A., & Sharon, N. (2009). Historical Background and Overview. In A. Varki, R. D. Cummings, J. D. Esko, H. H. Freeze, P. Stanley, C. R. Bertozzi, et al. (Eds.), *Essentials of Glycobiology* (2nd ed., pp. 1-22). New York: Cold Spring Harbor Laboratory Press.

Varki, A., Kannagi, R., & Toole, B. (1999). Glycosylation changes in cancer. In A. Varki, R. Cummings, J. Esko, H. Freeze, G. Hart, & J. Marth (Eds.), *Essentials of Glycobiology* (pp. 617-632). Cold Spring Harbor (NY): Cold Spring Harbor Laboratory Press.

Vaughan, T., Ryan, J., & Czaplewski, N. (2000). *Mammalogy* (4th revised ed.). University of Michigan: Saunders College Pub.

Vesey-Fitzgerald, B. (1947, January). The senses of bats. *Endeavour, 6*(21), 36-41.

Vesey-Fitzgerald, D. (1966). The habits and habitats of small rodents in the Congo River catchment region of Zambia and Tanzania. *Zoologica Africana, 2*, 111-122.

Vorontsov, N. (1961). Variation in the transformation rates of organs of the digestive systems in rodents and the principle of functional compensation. *Doklady Akademii Nauk. SSSR., 136*, 1494-1497.

Vorontsov, N. (1962). The ways of food specialization and the evolution of the alimentary system in Muroidea. In J. Kratochvil, & J. Pelikan (Eds.), *Symposium Theriologicum* (pp. 360-377). Praha: Czechoslavak Academy of Science.

Waddell, P., Okada, N., & Hasegawa, M. (1999). Towards resolving the interordinal relationships of placental mammals. *Systematic Biology, 48*, 1-5.

Wagner, J. (1855). *Die Säugethiere in Abbildungen nach der Natur.* Weigner, Leipzig.

Walsh, M., & Jass, J. (2000). Histologically based methods for detection of mucin. In A. Corfield (Ed.), *Glycoprotein Methods and Protocols: The Mucins* (Vol. 125, pp. 29-44). Totowa, New Jersey: Humana Press Inc.

Wang, D., Pei, Y., Yang, J., & Wang, Z. (2003). Digestive tract morphology and food habits in six species of rodents. *Folia Zoologica, 52*(1), 51-55.

White, J. (2007). *Modes of feeding in mammals.* Retrieved March 17, 2010, from Arkansas Forest Resources Center: http://www.afrc.uamont.edu/whited/WLF%203413%20pdf%20files/WLF%203413%20Feeding%20modes.pdf

Wilson, D., & Reeder, D. (2005). *Mammals Species of the World. A Taxonomic and Geographic Reference.* (3rd ed.). (D. Wilson, & D. Reeder, Eds.) Baltimore: Johns Hopkins University Press.

Young, B., Lowe, J., Stevens, A., & Heath, J. (2006). *Wheater's Functional Histology: A Text and Colour Atlas* (5th ed.). China: Churchill Livingstone Elsevier.

APPENDICES

Appendix 1

Processed (grey highlighted areas) and raw data of all the gastrointestinal measurements of *A. spinosissimus*

***A. spinosissimus* specimen no.:**	**1**	**2**	**3**	**4**	**5**
Sex	**Female**	**Female**	**Female**	**Female**	**Female**
Bodyweight (g)	24.00	24.00	21.30	10.90	25.30
Total gastrointestinal weight (g)	5.18	4.84	4.11	3.32	4.39
GIT weight expressed as a proportion (%) of the bodyweight	21.60	20.15	19.30	30.42	17.34
Stomach length (mm)	50.00	57.00	41.00	42.00	42.00
Stomach circumference (mm)	37.50	38.50	32.00	35.00	33.00
Stomach surface area (mm^2)	1875.00	2194.50	1312.00	1470.00	1386.00
Small intestine length (mm)	210.00	155.00	189.00	216.00	176.00
Small Intestine circumference (mm)	12.70	15.00	17.00	13.00	14.30
Small intestine surface area (mm^2)	2667.00	2325.00	3213.00	2808.00	2516.80
Caecum length (mm)	33.00	40.00	38.00	43.00	42.00
Caecum circumference (mm)	30.50	32.50	27.00	24.50	19.00
Caecum surface area (mm^2)	1006.50	1300.00	1026.00	1053.50	798.00
Colon length (mm)	65.00	55.00	57.00	59.00	67.00
Colon circumference (mm)	14.00	12.70	16.30	13.30	15.30
Colon surface area (mm^2)	910.00	698.50	929.10	784.70	1025.10
Caecum + Colon surface area (mm^2)	1916.50	1998.50	1955.10	1838.20	1823.10
Total GIT surface area (mm^2)	6458.50	6518.00	6480.10	6116.20	5725.90
Total GIT length (mm)	358.00	307.00	325.00	360.00	327.00
Proportional surface area of the:					
Stomach (%)	29.03	33.67	20.25	24.03	24.21
Small intestine (%)	41.29	35.67	49.58	45.91	43.95
Caecum (%)	15.58	19.94	15.83	17.22	13.94
Colon (%)	14.09	10.72	14.34	12.83	17.90
Caecum + Colon (%)	29.67	30.66	30.17	30.05	31.84
Proportional length of the:					
Stomach (%)	13.97	18.57	12.62	11.67	12.84
Small intestine (%)	58.66	50.49	58.15	60.00	53.82
Caecum (%)	9.22	13.03	11.69	11.94	12.84
Colon (%)	18.16	17.92	17.54	16.39	20.49
Caecum + Colon (%)	27.37	30.94	29.23	28.33	33.33

Appendix 2

Processed (grey highlighted areas) and raw data of all the gastrointestinal measurements of *C. cyanea*

***C. cyanea* specimen no.:**	**1**	**2**	**3**	**4**	**5**
Sex	**Male**	**Female**	**Male**	**Male**	**Male**
Bodyweight (g)	17.00	10.77	20.00	11.41	15.43
Total gastrointestinal weight (g)	2.27	1.74	2.03	1.17	1.45
GIT weight expressed as a proportion (%) of the bodyweight	13.37	16.12	10.13	10.21	9.42
Stomach length (mm)	34.00	17.00	31.00	21.00	18.00
Stomach circumference (mm)	24.50	14.00	23.50	12.50	13.50
Stomach surface area (mm^2)	833.00	238.00	728.50	262.50	243.00
Small intestine + colon length (mm)	115.00	110.00	91.00	92.00	131.00
Small Intestine + colon circumference (mm)	13.00	13.50	11.25	12.50	11.25
Small intestine + colon surface area (mm^2)	1495.00	1485.00	1023.75	1150.00	1473.75
Total GIT surface area (mm^2)	2328.00	1723.00	1752.25	1412.50	1716.75
Total GIT length (mm)	149.00	127.00	122.00	113.00	149.00
Proportional surface area of the:					
% Stomach	35.78	13.81	41.58	18.58	14.15
% Small intestine + colon	64.22	86.19	58.42	81.42	85.85
Proportional length of the:					
% Stomach	22.82	13.39	25.41	18.58	12.08
% Small intestine + colon	77.18	86.61	74.59	81.42	87.92

Appendix 3

Processed (grey highlighted areas) and raw data of all the gastrointestinal measurements of *A. hottentotus*

***A. hottentotus* specimen no.:**	**1**	**2**	**3**	**4**
Sex	**Male**	**Male**	**Female**	**Male**
Bodyweight (g)	72.00	65.00	54.00	51.00
Total gastrointestinal weight (g)	3.06	6.21	5.83	4.44
GIT weight expressed as a proportion (%) of the bodyweight	4.25	9.55	10.80	8.71
Stomach length (mm)	40.00	58.00	42.00	39.00
Stomach circumference (mm)	24.25	29.50	32.50	26.00
Stomach surface area (mm^2)	970.00	1711.00	1365.00	1014.00
Small intestine + colon length (mm)	402.00	354.00	367.00	315.00
Small Intestine + colon circumference (mm)	12.50	14.75	13.75	15.00
Small intestine + colon surface area (mm^2)	5025.00	5221.50	5046.25	4725.00
Total GIT surface area (mm^2)	5995.00	6932.50	6411.25	5739.00
Total GIT length (mm)	442.00	412.00	409.00	354.00
Proportional surface area of the:				
Stomach (%)	16.18	24.68	21.29	17.67
Small intestine + colon (%)	83.82	75.32	78.71	82.33
Proportional length of the:				
Stomach (%)	9.05	14.08	10.27	11.02
Small intestine + colon (%)	90.95	85.92	89.73	88.98

Appendix 4

Tissue Processing Schedule

Solution	Duration	Purpose
Formaldehyde	12-24 hours	Fixation
Alcohol 70 %	2.0 hours	Dehydration
Alcohol 96 %	1.5 hours	Dehydration
Alcohol 96 %	1.5 hours	Dehydration
Alcohol 100 %	1.5 hours	Dehydration
Alcohol 100 %	1.5 hours	Dehydration
Alcohol 100 %	1.5 hours	Dehydration
Xylene	1.5 hours	Clearing
Xylene	1.0 hours	Clearing
Paraffin Wax	2.0 hours (at 60 °C)	Processing
Paraffin Wax	2.0 hours (at 60 °C)	Processing

Appendix 5

HAEMATOXYLIN AND EOSIN STAIN

Method:

- Incubation:

  Incubate at 60 °C in an incubator (M53c Incubator), for at least 60 minutes.
- Hydration:
  1. Immerse in Xylene for 2 minutes x 2.
  2. Immerse in absolute (100%) alcohol for 1 minute x 2.
  3. Immerse in 96% alcohol for 1 minute x 2.
  4. Immerse in 70% alcohol for 1 minute.
  5. Wash in tap water for 2 minutes.
- Staining:
  1. Stain in Haematoxylin for 4 minutes.
  2. Wash in running tap water for 3 minutes.
  3. Stain in Eosin for 2.30 seconds.
  4. Wash in running tap water for 2 minutes.
- Dehydration and mounting:
  1. Immerse in 70% alcohol for 0.20 seconds.
  2. Immerse in 96% alcohol for 0.15 seconds x 2.
  3. Immerse in absolute (100%) alcohol for 0.15 seconds x 2.
  4. Immerse in Xylene for 0.30 seconds.
  5. Immerse for a second time in Xylene for 1 minute.
  6. Mount the slides with DPX mounting medium and a cover slide.

Results:

Nuclei	Blue
Cytoplasm	Pink
Red blood cells, eosinophilic granules, other tissue elements	Varying shades of pink

Appendix 6

ALCAIN BLUE/PERIODIC ACID SCHIFF (AB/PAS)

Reagents:

1. Haematoxylin (Mayer's)
2. 1% Periodic Acid Solution
3. Schiff's Reagent
4. Alcian Blue pH 2.5 (8GX, C.I. 74240)
    a. Alcian Blue 1 g
    b. 3% Acetic Acid 100 ml

Method:

- Deparaffinize and hydrate slides to distilled water.
- Stain with Alcian Blue for 15 minutes.
- Rinse well in running tap water for 2 minutes.
- Rinse in distilled water.
- Oxidize in 1% Periodic Acid solution for 10 minutes.
- Rinse in distilled water.
- Place in Schiff's reagent for 15 minutes (Sections become a light pink color during this step).
- Wash in lukewarm tap water for 8 minutes (Immediately sections turn dark pink color).
- Counterstain in Mayer's Haematoxylin solution for 1 minute.
- Wash in tap water for 3 minutes.
- Dehydrate and clear as usual.
- Mount in DPX.

Results:

Acid mucosubstances	Blue
Neutral polysaccharides	Magenta
Mixture of above	Blue/Purple
Nuclei	Blue/Black

Appendix 7

ALDEHYDE FUCHSIN/ALCIAN BLUE (Spicer & Meyer, 1960)

Reagents:

Aldehyde Fuchsin:

*Pararosaniline	1 g
** Paraldehyde (Paracetaldehyde)	2 ml
Concentrated HCL	1 ml
Ethanol	60 ml
Distilled water	40 ml

Dissolve the pararosaniline in the alcohol and distilled water mix. Add the HCL and the paraldehyde. Allow to ripen for 2-7 days at room temperature, and then filter. Store at 4 °C. A fresh preparation should be made every 3-6 months.

* The color index number of pararosaniline is C.I. 42500. This should be a finely powdered pure form.

** Must be within date. Old stock may not work correctly.

Method:

Use a positive control section

- Dewax sections, rinse in water.
- Rinse in 70% alcohol.
- Stain in Aldehyde Fuchsin – 20 minutes
- Rinse well in 70% alcohol.
- Rinse in tap water.
- Stain with Alcian Blue (1% Alcian Blue, 3% Acetic Acid) – 5 minutes.
- Rinse in tap water.
- Dehydrate, clear and mount

Results:

Sulfated mucins	Purple
Carboxylated mucins	Blue

Appendix 8

HIGH IRON DIAMINE/ALCIAN BLUE

Sections:

8 µm paraffin wax sections

Solutions:

1) High Iron Diamine:

a.	N, N-dimethyl-meta-phenylenediamine dihydrochloride	120mg
b.	N, N-dimethyl-para-phenylenediamine dihydrochloride	20mg
c.	Distilled Water	50ml
d.	Ferric Chloride (60% BDH solution)	1.4ml

Dissolve the two diamine salts simultaneously in the distilled water and then add to the ferric chloride solution and mix.

2) 1% Alcian Blue in 3% Acetic Acid

3) 0.5% Aqueous Neutral Red

Method:

- Take positive control and the test sections to distilled water.
- Place sections in the High Iron Diamine solution for 18 hours at room temperature.
- Wash well in running water.
- Stain with the Alcian Blue solution for 10 minutes.
- Wash in water, stain nuclei with Neutral Red solution for 1 min 30 sec.
- Wash in water. Dehydrate, clear.
- Mount sections in DPX.

Results:

Sulfated mucins	Black/Brown
Carboxylated mucins	Blue
Nuclei	Red

Notes for High Iron Diamine Staining

- *If the times of incubation are exceeded the non-sulfated mucins become stained and the method loses specificity.*
- *Ferric chloride is used as a 60% stock solution which should be no older than 2 weeks.*
- *A heavy background staining is evidence of a deteriorated ferric chloride solution or diamine. The shelf-life of diamine salt (dry) is about a year.*
- *Store solutions in a dark area, very light sensitive.*

Appendices 9-48

The interpretation of the following tables was done in Statistica. The p-values in the tables represent the statistical significance between each gastrointestinal region. Statistical significance was indicated on the graphs in sections 4.5.1 and 4.5.2 (pp. 81-107) via alphabetical letters. All of the p-values were grouped together in the same way the graphs were grouped together in the results section. A corresponding figure legend is included with each table of p-values so that it is clear which of the p-values belongs to which graph.

Each gastrointestinal region has been assigned a number and compared with one another: Gastrointestinal regions for *A. spinosissimus*: duodenum (1), middle small intestine (2), ileum (3), caecum (4) and colon (5).

Gastrointestinal regions for:

C. cyanea: duodenum (1), middle small intestine (2), distal small intestine (3), colon (4)

A. hottentotus: duodenum (5), middle small intestine (6), distal small intestine (7), colon (8)

The first column in the table indicates which gastrointestinal regions are compared with one another for example: {1}-{2} compares the duodenum and middle small intestine, {1}-{3} compares the duodenum and ileum and so forth.

All statistically significant p-values are indicated in red. P-values that appear to be zero (0.000) are smaller than 0.01.

Appendix 9

AB/PAS result: **P-values for the graphs of figure 4.21: The distribution of the total number of mucin secreting goblet cells throughout the GIT of *A. spinosissimus*.**

Figure 4.21A: Total number of goblet cells per total area (mm^2).				
Comparison of the Gastrointestinal Regions	1st	2nd	Standard Error	p-value
{1}-{2}	Duodenum	Middle Small Intestine	0.101	0.004
{1}-{3}	Duodenum	Ileum	0.101	0.000
{1}-{4}	Duodenum	Caecum	0.101	0.000
{1}-{5}	Duodenum	Colon	0.101	0.000
{2}-{3}	Middle Small Intestine	Ileum	0.101	0.000
{2}-{4}	Middle Small Intestine	Caecum	0.101	0.003
{2}-{5}	Middle Small Intestine	Colon	0.101	0.000
{3}-{4}	Ileum	Caecum	0.101	0.231
{3}-{5}	Ileum	Colon	0.101	0.354
{4}-{5}	Caecum	Colon	0.101	0.043
Figure 4.21B: Goblet cells per surface epithelial area (mm^2).				
Comparison of the Gastrointestinal Regions	1st	2nd	Standard Error	p-value
{1}-{2}	Duodenum	Middle Small Intestine	0.099	0.058
{1}-{3}	Duodenum	Ileum	0.099	0.001
{1}-{4}	Duodenum	Caecum	0.099	0.882
{1}-{5}	Duodenum	Colon	0.099	0.000
{2}-{3}	Middle Small Intestine	Ileum	0.099	0.078
{2}-{4}	Middle Small Intestine	Caecum	0.099	0.077
{2}-{5}	Middle Small Intestine	Colon	0.099	0.015
{3}-{4}	Ileum	Caecum	0.099	0.002
{3}-{5}	Ileum	Colon	0.099	0.412
{4}-{5}	Caecum	Colon	0.099	0.000
Figure 4.21C: Goblet cells per crypt area (mm^2).				
Comparison of the Gastrointestinal Regions	1st	2nd	Standard Error	p-value
{1}-{2}	Duodenum	Middle Small Intestine	0.055	0.136
{1}-{3}	Duodenum	Ileum	0.055	0.000
{1}-{4}	Duodenum	Caecum	0.055	0.003
{1}-{5}	Duodenum	Colon	0.055	0.000
{2}-{3}	Middle Small Intestine	Ileum	0.055	0.002
{2}-{4}	Middle Small Intestine	Caecum	0.055	0.072
{2}-{5}	Middle Small Intestine	Colon	0.055	0.000
{3}-{4}	Ileum	Caecum	0.055	0.106
{3}-{5}	Ileum	Colon	0.055	0.001
{4}-{5}	Caecum	Colon	0.055	0.000

Appendix 10

AB/PAS result: **P-values for the graphs of figure 4.22: The distribution of the total number of acid mucin secreting goblet cells throughout the GIT of *A. spinosissimus*.**

Figure 4.22A: Total number of acid goblet cells per total area (mm^2).				
Comparison of the Gastrointestinal Regions	1st	2nd	Standard Error	p-value
{1}-{2}	Duodenum	Middle Small Intestine	0.468	0.243
{1}-{3}	Duodenum	Ileum	0.468	0.050
{1}-{4}	Duodenum	Caecum	0.468	0.003
{1}-{5}	Duodenum	Colon	0.468	0.000
{2}-{3}	Middle Small Intestine	Ileum	0.468	0.376
{2}-{4}	Middle Small Intestine	Caecum	0.468	0.037
{2}-{5}	Middle Small Intestine	Colon	0.468	0.001
{3}-{4}	Ileum	Caecum	0.468	0.190
{3}-{5}	Ileum	Colon	0.468	0.007
{4}-{5}	Caecum	Colon	0.468	0.109
Figure 4.22B: Acid goblet cells per surface epithelial area (mm^2).				
Comparison of the Gastrointestinal Regions	1st	2nd	Standard Error	p-value
{1}-{2}	Duodenum	Middle Small Intestine	0.462	0.030
{1}-{3}	Duodenum	Ileum	0.462	0.150
{1}-{4}	Duodenum	Caecum	0.462	0.159
{1}-{5}	Duodenum	Colon	0.462	0.007
{2}-{3}	Middle Small Intestine	Ileum	0.462	0.400
{2}-{4}	Middle Small Intestine	Caecum	0.462	0.382
{2}-{5}	Middle Small Intestine	Colon	0.462	0.497
{3}-{4}	Ileum	Caecum	0.462	0.973
{3}-{5}	Ileum	Colon	0.462	0.138
{4}-{5}	Caecum	Colon	0.462	0.130
Figure 4.22C: Acid goblet cells per crypt area (mm^2).				
Comparison of the Gastrointestinal Regions	1st	2nd	Standard Error	p-value
{1}-{2}	Duodenum	Middle Small Intestine	0.499	0.252
{1}-{3}	Duodenum	Ileum	0.499	0.039
{1}-{4}	Duodenum	Caecum	0.499	0.004
{1}-{5}	Duodenum	Colon	0.499	0.000
{2}-{3}	Middle Small Intestine	Ileum	0.499	0.303
{2}-{4}	Middle Small Intestine	Caecum	0.499	0.044
{2}-{5}	Middle Small Intestine	Colon	0.499	0.001
{3}-{4}	Ileum	Caecum	0.499	0.280
{3}-{5}	Ileum	Colon	0.499	0.013
{4}-{5}	Caecum	Colon	0.499	0.114

Appendix 11

AB/PAS result: **P-values for the graphs of figure 4.23: The distribution of the total number of neutral mucin secreting goblet cells throughout the GIT of *A. spinosissimus*.**

Figure 4.23A: Total number of neutral goblet cells pet total area (mm^2).				
Comparison of the Gastrointestinal Regions	1st	2nd	Standard Error	p-value
{1}-{2}	Duodenum	Middle Small Intestine	0.229	0.903
{1}-{3}	Duodenum	Ileum	0.229	0.014
{1}-{4}	Duodenum	Caecum	0.229	0.020
{1}-{5}	Duodenum	Colon	0.229	0.026
{2}-{3}	Middle Small Intestine	Ileum	0.229	0.019
{2}-{4}	Middle Small Intestine	Caecum	0.229	0.026
{2}-{5}	Middle Small Intestine	Colon	0.229	0.033
{3}-{4}	Ileum	Caecum	0.229	0.873
{3}-{5}	Ileum	Colon	0.229	0.778
{4}-{5}	Caecum	Colon	0.229	0.903
Figure 4.23B: Neutral goblet cells per epithelial surface area (mm^2).				
Comparison of the Gastrointestinal Regions	1st	2nd	Standard Error	p-value
{1}-{2}	Duodenum	Middle Small Intestine	0.253	0.250
{1}-{3}	Duodenum	Ileum	0.253	0.002
{1}-{4}	Duodenum	Caecum	0.253	0.146
{1}-{5}	Duodenum	Colon	0.253	0.001
{2}-{3}	Middle Small Intestine	Ileum	0.253	0.023
{2}-{4}	Middle Small Intestine	Caecum	0.253	0.741
{2}-{5}	Middle Small Intestine	Colon	0.253	0.013
{3}-{4}	Ileum	Caecum	0.253	0.045
{3}-{5}	Ileum	Colon	0.253	0.783
{4}-{5}	Caecum	Colon	0.253	0.026
Figure 4.23C: Neutral goblet cells per crypt area (mm^2).				
Comparison of the Gastrointestinal Regions	1st	2nd	Standard Error	p-value
{1}-{2}	Duodenum	Middle Small Intestine	0.335	0.607
{1}-{3}	Duodenum	Ileum	0.335	0.116
{1}-{4}	Duodenum	Caecum	0.335	0.083
{1}-{5}	Duodenum	Colon	0.335	0.684
{2}-{3}	Middle Small Intestine	Ileum	0.335	0.044
{2}-{4}	Middle Small Intestine	Caecum	0.335	0.031
{2}-{5}	Middle Small Intestine	Colon	0.335	0.361
{3}-{4}	Ileum	Caecum	0.335	0.854
{3}-{5}	Ileum	Colon	0.335	0.231
{4}-{5}	Caecum	Colon	0.335	0.171

Appendix 12

AB/PAS result: **P-values for the graphs of figure 4.24: The distribution of the total number of mixed mucin secreting goblet cells throughout the GIT of *A. spinosissimus*.**

Figure 4.24A: Total number of mixed goblet cells per total area (mm^2).				
Comparison of the Gastrointestinal Regions	1st	2nd	Standard Error	p-value
{1}-{2}	Duodenum	Middle Small Intestine	0.063	0.273
{1}-{3}	Duodenum	Ileum	0.063	0.001
{1}-{4}	Duodenum	Caecum	0.063	0.987
{1}-{5}	Duodenum	Colon	0.063	0.000
{2}-{3}	Middle Small Intestine	Ileum	0.063	0.011
{2}-{4}	Middle Small Intestine	Caecum	0.063	0.267
{2}-{5}	Middle Small Intestine	Colon	0.063	0.005
{3}-{4}	Ileum	Caecum	0.063	0.001
{3}-{5}	Ileum	Colon	0.063	0.700
{4}-{5}	Caecum	Colon	0.063	0.000
Figure 4.24B: Mixed goblet cells per epithelial surface area (mm^2).				
Comparison of the Gastrointestinal Regions	1st	2nd	Standard Error	p-value
{1}-{2}	Duodenum	Middle Small Intestine	0.113	0.201
{1}-{3}	Duodenum	Ileum	0.113	0.010
{1}-{4}	Duodenum	Caecum	0.113	0.650
{1}-{5}	Duodenum	Colon	0.113	0.002
{2}-{3}	Middle Small Intestine	Ileum	0.113	0.133
{2}-{4}	Middle Small Intestine	Caecum	0.113	0.091
{2}-{5}	Middle Small Intestine	Colon	0.113	0.028
{3}-{4}	Ileum	Caecum	0.113	0.004
{3}-{5}	Ileum	Colon	0.113	0.418
{4}-{5}	Caecum	Colon	0.113	0.001
Figure 4.24C: Mixed goblet cells per crypt area (mm^2).				
Comparison of the Gastrointestinal Regions	1st	2nd	Standard Error	p-value
{1}-{2}	Duodenum	Middle Small Intestine	0.073	0.435
{1}-{3}	Duodenum	Ileum	0.073	0.019
{1}-{4}	Duodenum	Caecum	0.073	0.495
{1}-{5}	Duodenum	Colon	0.073	0.157
{2}-{3}	Middle Small Intestine	Ileum	0.073	0.090
{2}-{4}	Middle Small Intestine	Caecum	0.073	0.153
{2}-{5}	Middle Small Intestine	Colon	0.073	0.504
{3}-{4}	Ileum	Caecum	0.073	0.004
{3}-{5}	Ileum	Colon	0.073	0.279
{4}-{5}	Caecum	Colon	0.073	0.044

Appendix 13

HID/AB and AF/AB result: **P-values for the graphs of figure 4.25: The distribution of the total number of acid mucin secreting goblet cells throughout the GIT of *A. spinosissimus*.**

Figure 4.25A: Total number of acid goblet cells per total area (mm^2).				
Comparison of the Gastrointestinal Regions	1st	2nd	Standard Error	p-value
{1}-{2}	Duodenum	Middle Small Intestine	0.110	0.004
{1}-{3}	Duodenum	Ileum	0.110	0.000
{1}-{4}	Duodenum	Caecum	0.110	0.000
{1}-{5}	Duodenum	Colon	0.110	0.000
{2}-{3}	Middle Small Intestine	Ileum	0.110	0.001
{2}-{4}	Middle Small Intestine	Caecum	0.110	0.015
{2}-{5}	Middle Small Intestine	Colon	0.110	0.000
{3}-{4}	Ileum	Caecum	0.110	0.271
{3}-{5}	Ileum	Colon	0.110	0.205
{4}-{5}	Caecum	Colon	0.110	0.026
Figure 4.25B: Acid goblet cells per surface epithelial area (mm^2).				
Comparison of the Gastrointestinal Regions	1st	2nd	Standard Error	p-value
{1}-{2}	Duodenum	Middle Small Intestine	0.090	0.016
{1}-{3}	Duodenum	Ileum	0.090	0.000
{1}-{4}	Duodenum	Caecum	0.090	0.238
{1}-{5}	Duodenum	Colon	0.090	0.000
{2}-{3}	Middle Small Intestine	Ileum	0.090	0.072
{2}-{4}	Middle Small Intestine	Caecum	0.090	0.001
{2}-{5}	Middle Small Intestine	Colon	0.090	0.009
{3}-{4}	Ileum	Caecum	0.090	0.000
{3}-{5}	Ileum	Colon	0.090	0.311
{4}-{5}	Caecum	Colon	0.090	0.000
Figure 4.25C: Acid goblet cells per crypt area (mm^2).				
Comparison of the Gastrointestinal Regions	1st	2nd	Standard Error	p-value
{1}-{2}	Duodenum	Middle Small Intestine	0.077	0.434
{1}-{3}	Duodenum	Ileum	0.077	0.003
{1}-{4}	Duodenum	Caecum	0.077	0.055
{1}-{5}	Duodenum	Colon	0.077	0.000
{2}-{3}	Middle Small Intestine	Ileum	0.077	0.014
{2}-{4}	Middle Small Intestine	Caecum	0.077	0.223
{2}-{5}	Middle Small Intestine	Colon	0.077	0.000
{3}-{4}	Ileum	Caecum	0.077	0.157
{3}-{5}	Ileum	Colon	0.077	0.011
{4}-{5}	Caecum	Colon	0.077	0.000

Appendix 14

HID/AB and AF/AB result: **P-values for the graphs of figure 4.26: The distribution of the total number of sulfomucin secreting goblet cells throughout the GIT of *A. spinosissimus*.**

Figure 4.26A: Total number of sulfated goblet cells per total area (mm^2).				
Comparison of the Gastrointestinal Regions	1st	2nd	Standard Error	p-value
{1}-{2}	Duodenum	Middle Small Intestine	0.350	0.107
{1}-{3}	Duodenum	Ileum	0.350	0.234
{1}-{4}	Duodenum	Caecum	0.350	0.264
{1}-{5}	Duodenum	Colon	0.350	0.014
{2}-{3}	Middle Small Intestine	Ileum	0.350	0.646
{2}-{4}	Middle Small Intestine	Caecum	0.350	0.011
{2}-{5}	Middle Small Intestine	Colon	0.350	0.304
{3}-{4}	Ileum	Caecum	0.350	0.029
{3}-{5}	Ileum	Colon	0.350	0.146
{4}-{5}	Caecum	Colon	0.350	0.001
Figure 4.26B: Sulfated goblet cells per surface epithelial area (mm^2).				
Comparison of the Gastrointestinal Regions	1st	2nd	Standard Error	p-value
{1}-{2}	Duodenum	Middle Small Intestine	0.367	0.029
{1}-{3}	Duodenum	Ileum	0.367	0.065
{1}-{4}	Duodenum	Caecum	0.367	0.880
{1}-{5}	Duodenum	Colon	0.367	0.003
{2}-{3}	Middle Small Intestine	Ileum	0.367	0.673
{2}-{4}	Middle Small Intestine	Caecum	0.367	0.021
{2}-{5}	Middle Small Intestine	Colon	0.367	0.322
{3}-{4}	Ileum	Caecum	0.367	0.049
{3}-{5}	Ileum	Colon	0.367	0.166
{4}-{5}	Caecum	Colon	0.367	0.002
Figure 4.26C: Sulfated goblet cells per crypt area (mm^2).				
Comparison of the Gastrointestinal Regions	1st	2nd	Standard Error	p-value
{1}-{2}	Duodenum	Middle Small Intestine	0.464	0.379
{1}-{3}	Duodenum	Ileum	0.464	0.915
{1}-{4}	Duodenum	Caecum	0.464	0.145
{1}-{5}	Duodenum	Colon	0.464	0.127
{2}-{3}	Middle Small Intestine	Ileum	0.464	0.326
{2}-{4}	Middle Small Intestine	Caecum	0.464	0.027
{2}-{5}	Middle Small Intestine	Colon	0.464	0.491
{3}-{4}	Ileum	Caecum	0.464	0.174
{3}-{5}	Ileum	Colon	0.464	0.105
{4}-{5}	Caecum	Colon	0.464	0.006

Appendix 15

HID/AB and AF/AB result: **P-values for the graphs of figure 4.27: The distribution of the total number of strongly sulfated goblet cells throughout the GIT of *A. spinosissimus*.**

Figure 4.27A: Total number of strongly sulfated goblet cells per total area (mm^2).				
Comparison of the Gastrointestinal Regions	1st	2nd	Standard Error	p-value
{1}-{2}	Duodenum	Middle Small Intestine	0.398	0.764
{1}-{3}	Duodenum	Ileum	0.398	0.909
{1}-{4}	Duodenum	Caecum	0.398	0.214
{1}-{5}	Duodenum	Colon	0.398	0.003
{2}-{3}	Middle Small Intestine	Ileum	0.398	0.852
{2}-{4}	Middle Small Intestine	Caecum	0.398	0.337
{2}-{5}	Middle Small Intestine	Colon	0.398	0.005
{3}-{4}	Ileum	Caecum	0.398	0.256
{3}-{5}	Ileum	Colon	0.398	0.003
{4}-{5}	Caecum	Colon	0.398	0.038
Figure 4.27B: Strongly sulfated goblet cells per surface epithelial area (mm^2).				
Comparison of the Gastrointestinal Regions	1st	2nd	Standard Error	p-value
{1}-{2}	Duodenum	Middle Small Intestine	0.459	0.405
{1}-{3}	Duodenum	Ileum	0.459	0.625
{1}-{4}	Duodenum	Caecum	0.459	0.759
{1}-{5}	Duodenum	Colon	0.459	0.006
{2}-{3}	Middle Small Intestine	Ileum	0.459	0.726
{2}-{4}	Middle Small Intestine	Caecum	0.459	0.260
{2}-{5}	Middle Small Intestine	Colon	0.459	0.032
{3}-{4}	Ileum	Caecum	0.459	0.430
{3}-{5}	Ileum	Colon	0.459	0.016
{4}-{5}	Caecum	Colon	0.459	0.003
Figure 4.27C: Strongly sulfated goblet cells per crypt area (mm^2).				
Comparison of the Gastrointestinal Regions	1st	2nd	Standard Error	p-value
{1}-{2}	Duodenum	Middle Small Intestine	0.641	0.355
{1}-{3}	Duodenum	Ileum	0.641	0.342
{1}-{4}	Duodenum	Caecum	0.641	0.749
{1}-{5}	Duodenum	Colon	0.641	0.141
{2}-{3}	Middle Small Intestine	Ileum	0.641	0.979
{2}-{4}	Middle Small Intestine	Caecum	0.641	0.220
{2}-{5}	Middle Small Intestine	Colon	0.641	0.024
{3}-{4}	Ileum	Caecum	0.641	0.211
{3}-{5}	Ileum	Colon	0.641	0.022
{4}-{5}	Caecum	Colon	0.641	0.239

Appendix 16

HID/AB and AF/AB result: **P-values for the graphs of figure 4.28: The distribution of the total number of weakly sulfated goblet cells throughout the GIT of *A. spinosissimus*.**

Figure 4.28A: Total number of weakly sulfated goblet cells per total area (mm^2).				
Comparison of the Gastrointestinal Regions	1st	2nd	Standard Error	p-value
{1}-{2}	Duodenum	Middle Small Intestine	0.167	0.037
{1}-{3}	Duodenum	Ileum	0.167	0.009
{1}-{4}	Duodenum	Caecum	0.167	0.042
{1}-{5}	Duodenum	Colon	0.167	0.001
{2}-{3}	Middle Small Intestine	Ileum	0.167	0.497
{2}-{4}	Middle Small Intestine	Caecum	0.167	0.948
{2}-{5}	Middle Small Intestine	Colon	0.167	0.107
{3}-{4}	Ileum	Caecum	0.167	0.458
{3}-{5}	Ileum	Colon	0.167	0.327
{4}-{5}	Caecum	Colon	0.167	0.095
Figure 4.28B: Weakly sulfated goblet cells per surface epithelial area (mm^2).				
Comparison of the Gastrointestinal Regions	1st	2nd	Standard Error	p-value
{1}-{2}	Duodenum	Middle Small Intestine	0.160	0.009
{1}-{3}	Duodenum	Ileum	0.160	0.001
{1}-{4}	Duodenum	Caecum	0.160	0.174
{1}-{5}	Duodenum	Colon	0.160	0.010
{2}-{3}	Middle Small Intestine	Ileum	0.160	0.318
{2}-{4}	Middle Small Intestine	Caecum	0.160	0.000
{2}-{5}	Middle Small Intestine	Colon	0.160	0.977
{3}-{4}	Ileum	Caecum	0.160	0.000
{3}-{5}	Ileum	Colon	0.160	0.305
{4}-{5}	Caecum	Colon	0.160	0.000
Figure 4.28C: Weakly sulfated goblet cells per crypt area (mm^2).				
Comparison of the Gastrointestinal Regions	1st	2nd	Standard Error	p-value
{1}-{2}	Duodenum	Middle Small Intestine	0.187	0.076
{1}-{3}	Duodenum	Ileum	0.187	0.038
{1}-{4}	Duodenum	Caecum	0.187	0.043
{1}-{5}	Duodenum	Colon	0.187	0.003
{2}-{3}	Middle Small Intestine	Ileum	0.187	0.718
{2}-{4}	Middle Small Intestine	Caecum	0.187	0.766
{2}-{5}	Middle Small Intestine	Colon	0.187	0.138
{3}-{4}	Ileum	Caecum	0.187	0.949
{3}-{5}	Ileum	Colon	0.187	0.250
{4}-{5}	Caecum	Colon	0.187	0.226

Appendix 17

HID/AB and AF/AB result: **P-values for the graphs of figure 4.29: The distribution of the total number of sialomucin secreting goblet cells throughout the GIT of *A. spinosissimus*.**

Figure 4.29A: Total number of sialylated goblet cells per total area (mm^2).				
Comparison of the Gastrointestinal Regions	1st	2nd	Standard Error	p-value
{1}-{2}	Duodenum	Middle Small Intestine	0.226	0.879
{1}-{3}	Duodenum	Ileum	0.226	0.921
{1}-{4}	Duodenum	Caecum	0.226	0.675
{1}-{5}	Duodenum	Colon	0.226	0.060
{2}-{3}	Middle Small Intestine	Ileum	0.226	0.801
{2}-{4}	Middle Small Intestine	Caecum	0.226	0.568
{2}-{5}	Middle Small Intestine	Colon	0.226	0.079
{3}-{4}	Ileum	Caecum	0.226	0.748
{3}-{5}	Ileum	Colon	0.226	0.049
{4}-{5}	Caecum	Colon	0.226	0.026
Figure 4.29B: Sialylated goblet cells per surface epithelial area (mm^2).				
Comparison of the Gastrointestinal Regions	1st	2nd	Standard Error	p-value
{1}-{2}	Duodenum	Middle Small Intestine	0.323	0.853
{1}-{3}	Duodenum	Ileum	0.323	0.859
{1}-{4}	Duodenum	Caecum	0.323	0.792
{1}-{5}	Duodenum	Colon	0.323	0.122
{2}-{3}	Middle Small Intestine	Ileum	0.323	0.717
{2}-{4}	Middle Small Intestine	Caecum	0.323	0.937
{2}-{5}	Middle Small Intestine	Colon	0.323	0.168
{3}-{4}	Ileum	Caecum	0.323	0.660
{3}-{5}	Ileum	Colon	0.323	0.089
{4}-{5}	Caecum	Colon	0.323	0.192
Figure 4.29C: Sialylated goblet cells per crypt area (mm^2).				
Comparison of the Gastrointestinal Regions	1st	2nd	Standard Error	p-value
{1}-{2}	Duodenum	Middle Small Intestine	0.276	0.939
{1}-{3}	Duodenum	Ileum	0.276	0.936
{1}-{4}	Duodenum	Caecum	0.276	0.890
{1}-{5}	Duodenum	Colon	0.276	0.034
{2}-{3}	Middle Small Intestine	Ileum	0.276	0.997
{2}-{4}	Middle Small Intestine	Caecum	0.276	0.951
{2}-{5}	Middle Small Intestine	Colon	0.276	0.029
{3}-{4}	Ileum	Caecum	0.276	0.954
{3}-{5}	Ileum	Colon	0.276	0.029
{4}-{5}	Caecum	Colon	0.276	0.026

Appendix 18

HID/AB and AF/AB result: **P-values for the graphs of figure 4.30: The distribution of the total number of mixed acid mucin secreting goblet cells throughout the GIT of *A. spinosissimus*.**

Figure 4.30A: Total number of mixed acid goblet cells per total area (mm^2).				
Comparison of the Gastrointestinal Regions	1st	2nd	Standard Error	p-value
{1}-{2}	Duodenum	Middle Small Intestine	0.090	0.735
{1}-{3}	Duodenum	Ileum	0.090	0.015
{1}-{4}	Duodenum	Caecum	0.090	0.251
{1}-{5}	Duodenum	Colon	0.090	0.000
{2}-{3}	Middle Small Intestine	Ileum	0.090	0.007
{2}-{4}	Middle Small Intestine	Caecum	0.090	0.144
{2}-{5}	Middle Small Intestine	Colon	0.090	0.000
{3}-{4}	Ileum	Caecum	0.090	0.141
{3}-{5}	Ileum	Colon	0.090	0.029
{4}-{5}	Caecum	Colon	0.090	0.001
Figure 4.30B: Mixed acid goblet cells per surface epithalial area (mm^2).				
Comparison of the Gastrointestinal Regions	1st	2nd	Standard Error	p-value
{1}-{2}	Duodenum	Middle Small Intestine	0.191	0.406
{1}-{3}	Duodenum	Ileum	0.191	0.163
{1}-{4}	Duodenum	Caecum	0.191	0.057
{1}-{5}	Duodenum	Colon	0.191	0.533
{2}-{3}	Middle Small Intestine	Ileum	0.191	0.551
{2}-{4}	Middle Small Intestine	Caecum	0.191	0.010
{2}-{5}	Middle Small Intestine	Colon	0.191	0.831
{3}-{4}	Ileum	Caecum	0.191	0.003
{3}-{5}	Ileum	Colon	0.191	0.421
{4}-{5}	Caecum	Colon	0.191	0.016
Figure 4.30C: Mixed acid goblet cells per total crypt area (mm^2).				
Comparison of the Gastrointestinal Regions	1st	2nd	Standard Error	p-value
{1}-{2}	Duodenum	Middle Small Intestine	0.101	0.414
{1}-{3}	Duodenum	Ileum	0.101	0.040
{1}-{4}	Duodenum	Caecum	0.101	0.251
{1}-{5}	Duodenum	Colon	0.101	0.000
{2}-{3}	Middle Small Intestine	Ileum	0.101	0.007
{2}-{4}	Middle Small Intestine	Caecum	0.101	0.059
{2}-{5}	Middle Small Intestine	Colon	0.101	0.000
{3}-{4}	Ileum	Caecum	0.101	0.314
{3}-{5}	Ileum	Colon	0.101	0.019
{4}-{5}	Caecum	Colon	0.101	0.002

Appendix 19

AB/PAS results

P-values for the graph of figure 4.31A: The distribution of the total number of mucin secreting goblet cells throughout the GIT of *C. cyanea* and *A. hottentotus*.

Figure 4.31A: Total number of goblet cells per total area (mm^2)				
Comparison of the Gastrointestinal Regions	1st	2nd	Standard Error	p-value
{1}-{2}	(C.c)*Duodenum	(C.c)*Middle Small Int.	0.034	0.000
{1}-{3}	(C.c)*Duodenum	(C.c)*Distal Small Int.	0.035	0.000
{1}-{4}	(C.c)*Duodenum	(C.c)*Colon	0.038	0.000
{1}-{5}	(C.c)*Duodenum	(A. h)*Duodenum	0.052	0.000
{1}-{6}	(C.c)*Duodenum	(A. h)*Middle Small Int.	0.054	0.993
{1}-{7}	(C.c)*Duodenum	(A. h)*Distal Small Int.	0.054	0.000
{1}-{8}	(C.c)*Duodenum	(A. h)*Colon	0.052	0.000
{2}-{3}	(C.c)*Middle Small Int.	(C.c)*Distal Small Int.	0.035	0.000
{2}-{4}	(C.c)*Middle Small Int.	(C.c)*Colon	0.038	0.000
{2}-{5}	(C.c)*Middle Small Int.	(A. h)*Duodenum	0.053	0.001
{2}-{6}	(C.c)*Middle Small Int.	(A. h)*Middle Small Int.	0.054	0.008
{2}-{7}	(C.c)*Middle Small Int.	(A. h)*Distal Small Int.	0.055	0.000
{2}-{8}	(C.c)*Middle Small Int.	(A. h)*Colon	0.052	0.000
{3}-{4}	(C.c)*Distal Small Int.	(C.c)*Colon	0.039	0.028
{3}-{5}	(C.c)*Distal Small Int.	(A. h)*Duodenum	0.054	0.000
{3}-{6}	(C.c)*Distal Small Int.	(A. h)*Middle Small Int.	0.055	0.000
{3}-{7}	(C.c)*Distal Small Int.	(A. h)*Distal Small Int.	0.056	0.008
{3}-{8}	(C.c)*Distal Small Int.	(A. h)*Colon	0.053	0.003
{4}-{5}	(C.c)*Colon	(A. h)*Duodenum	0.055	0.000
{4}-{6}	(C.c)*Colon	(A. h)*Middle Small Int.	0.056	0.000
{4}-{7}	(C.c)*Colon	(A. h)*Distal Small Int.	0.057	0.000
{4}-{8}	(C.c)*Colon	(A. h)*Colon	0.055	0.000
{5}-{6}	(A. h)*Duodenum	(A. h)*Middle Small Int.	0.039	0.000
{5}-{7}	(A. h)*Duodenum	(A. h)*Distal Small Int.	0.040	0.000
{5}-{8}	(A. h)*Duodenum	(A. h)*Colon	0.036	0.000
{6}-{7}	(A. h)*Middle Small Int.	(A. h)*Distal Small Int.	0.041	0.000
{6}-{8}	(A. h)*Middle Small Int.	(A. h)*Colon	0.038	0.000
{7}-{8}	(A. h)*Distal Small Int.	(A. h)*Colon	0.039	0.770

C.c: *Crocicura cyanea*

A.h: *Amblysomus hottentotus*

Appendix 20

AB/PAS results

P-values for the graph of figure 4.31B: The distribution of the total number of mucin secreting goblet cells throughout the GI surface epithelial areas of *C. cyanea* and *A. hottentotus*.

Figure 4.31B: Goblet cells per surface epithelial area (mm^2)				
Comparison of the Gastrointestinal Regions	1st	2nd	Standard Error	p- value
{1}-{2}	(C.c)*Duodenum	(C.c)*Middle Small Int.	0.020	0.377
{1}-{3}	(C.c)*Duodenum	(C.c)*Distal Small Int.	0.021	0.000
{1}-{4}	(C.c)*Duodenum	(C.c)*Colon	0.022	0.000
{1}-{5}	(C.c)*Duodenum	(A. h)*Duodenum	0.034	0.000
{1}-{6}	(C.c)*Duodenum	(A. h)*Middle Small Int.	0.034	0.242
{1}-{7}	(C.c)*Duodenum	(A. h)*Distal Small Int.	0.035	0.000
{1}-{8}	(C.c)*Duodenum	(A. h)*Colon	0.034	0.000
{2}-{3}	(C.c)*Middle Small Int.	(C.c)*Distal Small Int.	0.021	0.000
{2}-{4}	(C.c)*Middle Small Int.	(C.c)*Colon	0.022	0.000
{2}-{5}	(C.c)*Middle Small Int.	(A. h)*Duodenum	0.034	0.000
{2}-{6}	(C.c)*Middle Small Int.	(A. h)*Middle Small Int.	0.035	0.511
{2}-{7}	(C.c)*Middle Small Int.	(A. h)*Distal Small Int.	0.035	0.000
{2}-{8}	(C.c)*Middle Small Int.	(A. h)*Colon	0.034	0.000
{3}-{4}	(C.c)*Distal Small Int.	(C.c)*Colon	0.023	0.368
{3}-{5}	(C.c)*Distal Small Int.	(A. h)*Duodenum	0.034	0.000
{3}-{6}	(C.c)*Distal Small Int.	(A. h)*Middle Small Int.	0.035	0.000
{3}-{7}	(C.c)*Distal Small Int.	(A. h)*Distal Small Int.	0.035	0.000
{3}-{8}	(C.c)*Distal Small Int.	(A. h)*Colon	0.034	0.000
{4}-{5}	(C.c)*Colon	(A. h)*Duodenum	0.035	0.000
{4}-{6}	(C.c)*Colon	(A. h)*Middle Small Int.	0.036	0.000
{4}-{7}	(C.c)*Colon	(A. h)*Distal Small Int.	0.036	0.000
{4}-{8}	(C.c)*Colon	(A. h)*Colon	0.035	0.000
{5}-{6}	(A. h)*Duodenum	(A. h)*Middle Small Int.	0.023	0.000
{5}-{7}	(A. h)*Duodenum	(A. h)*Distal Small Int.	0.024	0.000
{5}-{8}	(A. h)*Duodenum	(A. h)*Colon	0.022	0.000
{6}-{7}	(A. h)*Middle Small Int.	(A. h)*Distal Small Int.	0.025	0.000
{6}-{8}	(A. h)*Middle Small Int.	(A. h)*Colon	0.023	0.000
{7}-{8}	(A. h)*Distal Small Int.	(A. h)*Colon	0.023	0.719

C.c: *Crocicura cyanea*

A.h: *Amblysomus hottentotus*

Appendix 21

AB/PAS results

P-values for the graph of figure 4.31C: The distribution of the total number of mucin secreting goblet cells throughout the GI crypt areas of *C. cyanea* and *A. hottentotus*.

Figure 4.31C: Goblet cells per crypt area (mm^2)				
Comparison of the Gastrointestinal Regions	1st	2nd	Standard Error	p- value
{1}-{2}	(C.c)*Duodenum	(C.c)*Middle Small Int.	0.024	0.000
{1}-{3}	(C.c)*Duodenum	(C.c)*Distal Small Int.	0.025	0.000
{1}-{4}	(C.c)*Duodenum	(C.c)*Colon	0.026	0.000
{1}-{5}	(C.c)*Duodenum	(A. h)*Duodenum	0.029	0.000
{1}-{6}	(C.c)*Duodenum	(A. h)*Middle Small Int.	0.031	0.095
{1}-{7}	(C.c)*Duodenum	(A. h)*Distal Small Int.	0.031	0.000
{1}-{8}	(C.c)*Duodenum	(A. h)*Colon	0.029	0.000
{2}-{3}	(C.c)*Middle Small Int.	(C.c)*Distal Small Int.	0.025	0.000
{2}-{4}	(C.c)*Middle Small Int.	(C.c)*Colon	0.027	0.000
{2}-{5}	(C.c)*Middle Small Int.	(A. h)*Duodenum	0.030	0.541
{2}-{6}	(C.c)*Middle Small Int.	(A. h)*Middle Small Int.	0.031	0.077
{2}-{7}	(C.c)*Middle Small Int.	(A. h)*Distal Small Int.	0.031	0.000
{2}-{8}	(C.c)*Middle Small Int.	(A. h)*Colon	0.029	0.000
{3}-{4}	(C.c)*Distal Small Int.	(C.c)*Colon	0.027	0.031
{3}-{5}	(C.c)*Distal Small Int.	(A. h)*Duodenum	0.030	0.000
{3}-{6}	(C.c)*Distal Small Int.	(A. h)*Middle Small Int.	0.031	0.000
{3}-{7}	(C.c)*Distal Small Int.	(A. h)*Distal Small Int.	0.032	0.001
{3}-{8}	(C.c)*Distal Small Int.	(A. h)*Colon	0.030	0.000
{4}-{5}	(C.c)*Colon	(A. h)*Duodenum	0.032	0.000
{4}-{6}	(C.c)*Colon	(A. h)*Middle Small Int.	0.033	0.000
{4}-{7}	(C.c)*Colon	(A. h)*Distal Small Int.	0.033	0.000
{4}-{8}	(C.c)*Colon	(A. h)*Colon	0.032	0.000
{5}-{6}	(A. h)*Duodenum	(A. h)*Middle Small Int.	0.027	0.008
{5}-{7}	(A. h)*Duodenum	(A. h)*Distal Small Int.	0.028	0.000
{5}-{8}	(A. h)*Duodenum	(A. h)*Colon	0.026	0.000
{6}-{7}	(A. h)*Middle Small Int.	(A. h)*Distal Small Int.	0.029	0.000
{6}-{8}	(A. h)*Middle Small Int.	(A. h)*Colon	0.027	0.000
{7}-{8}	(A. h)*Distal Small Int.	(A. h)*Colon	0.028	0.571

C.c: *Crocicura cyanea*

A.h: *Amblysomus hottentotus*

Appendix 22

AB/PAS results

P-values for the graph of figure 4.32A: The distribution of the total number of neutral mucin secreting goblet cells throughout the GIT of *C. cyanea* and *A. hottentotus*.

Figure 4.32A: Total number of neutral goblet cells per total area (mm^2)				
Comparison of the Gastrointestinal Regions	1st	2nd	Standard Error	p- value
{1}-{2}	(C.c)*Duodenum	(C.c)*Middle Small Int.	0.092	0.328
{1}-{3}	(C.c)*Duodenum	(C.c)*Distal Small Int.	0.096	0.000
{1}-{4}	(C.c)*Duodenum	(C.c)*Colon	0.102	0.278
{1}-{5}	(C.c)*Duodenum	(A. h)*Duodenum	0.259	0.000
{1}-{6}	(C.c)*Duodenum	(A. h)*Middle Small Int.	0.261	0.000
{1}-{7}	(C.c)*Duodenum	(A. h)*Distal Small Int.	0.262	0.000
{1}-{8}	(C.c)*Duodenum	(A. h)*Colon	0.259	0.000
{2}-{3}	(C.c)*Middle Small Int.	(C.c)*Distal Small Int.	0.096	0.000
{2}-{4}	(C.c)*Middle Small Int.	(C.c)*Colon	0.103	0.836
{2}-{5}	(C.c)*Middle Small Int.	(A. h)*Duodenum	0.259	0.000
{2}-{6}	(C.c)*Middle Small Int.	(A. h)*Middle Small Int.	0.261	0.000
{2}-{7}	(C.c)*Middle Small Int.	(A. h)*Distal Small Int.	0.263	0.000
{2}-{8}	(C.c)*Middle Small Int.	(A. h)*Colon	0.259	0.000
{3}-{4}	(C.c)*Distal Small Int.	(C.c)*Colon	0.106	0.001
{3}-{5}	(C.c)*Distal Small Int.	(A. h)*Duodenum	0.261	0.000
{3}-{6}	(C.c)*Distal Small Int.	(A. h)*Middle Small Int.	0.263	0.000
{3}-{7}	(C.c)*Distal Small Int.	(A. h)*Distal Small Int.	0.264	0.000
{3}-{8}	(C.c)*Distal Small Int.	(A. h)*Colon	0.260	0.000
{4}-{5}	(C.c)*Colon	(A. h)*Duodenum	0.263	0.000
{4}-{6}	(C.c)*Colon	(A. h)*Middle Small Int.	0.265	0.000
{4}-{7}	(C.c)*Colon	(A. h)*Distal Small Int.	0.266	0.000
{4}-{8}	(C.c)*Colon	(A. h)*Colon	0.263	0.000
{5}-{6}	(A. h)*Duodenum	(A. h)*Middle Small Int.	0.105	0.392
{5}-{7}	(A. h)*Duodenum	(A. h)*Distal Small Int.	0.108	0.031
{5}-{8}	(A. h)*Duodenum	(A. h)*Colon	0.099	0.942
{6}-{7}	(A. h)*Middle Small Int.	(A. h)*Distal Small Int.	0.113	0.202
{6}-{8}	(A. h)*Middle Small Int.	(A. h)*Colon	0.105	0.428
{7}-{8}	(A. h)*Distal Small Int.	(A. h)*Colon	0.108	0.035

C.c: *Crocicura cyanea*

A.h: *Amblysomus hottentotus*

Appendix 23

AB/PAS results

P-values for the graph of figure 4.32B: The distribution of the total number of neutral mucin secreting goblet cells throughout the GI surface epithelial areas of *C. cyanea* and *A. hottentotus*.

Figure 4.32B: Neutral goblet cells per surface epithelial area (mm^2)				
Comparison of the Gastrointestinal Regions	1st	2nd	Standard Error	p- value
{1}-{2}	(C.c)*Duodenum	(C.c)*Middle Small Int.	0.099	0.035
{1}-{3}	(C.c)*Duodenum	(C.c)*Distal Small Int.	0.103	0.000
{1}-{4}	(C.c)*Duodenum	(C.c)*Colon	0.111	0.201
{1}-{5}	(C.c)*Duodenum	(A. h)*Duodenum	0.224	0.000
{1}-{6}	(C.c)*Duodenum	(A. h)*Middle Small Int.	0.227	0.000
{1}-{7}	(C.c)*Duodenum	(A. h)*Distal Small Int.	0.228	0.000
{1}-{8}	(C.c)*Duodenum	(A. h)*Colon	0.223	0.000
{2}-{3}	(C.c)*Middle Small Int.	(C.c)*Distal Small Int.	0.104	0.000
{2}-{4}	(C.c)*Middle Small Int.	(C.c)*Colon	0.111	0.538
{2}-{5}	(C.c)*Middle Small Int.	(A. h)*Duodenum	0.224	0.000
{2}-{6}	(C.c)*Middle Small Int.	(A. h)*Middle Small Int.	0.227	0.000
{2}-{7}	(C.c)*Middle Small Int.	(A. h)*Distal Small Int.	0.229	0.000
{2}-{8}	(C.c)*Middle Small Int.	(A. h)*Colon	0.224	0.000
{3}-{4}	(C.c)*Distal Small Int.	(C.c)*Colon	0.115	0.000
{3}-{5}	(C.c)*Distal Small Int.	(A. h)*Duodenum	0.226	0.000
{3}-{6}	(C.c)*Distal Small Int.	(A. h)*Middle Small Int.	0.229	0.000
{3}-{7}	(C.c)*Distal Small Int.	(A. h)*Distal Small Int.	0.230	0.000
{3}-{8}	(C.c)*Distal Small Int.	(A. h)*Colon	0.226	0.000
{4}-{5}	(C.c)*Colon	(A. h)*Duodenum	0.230	0.000
{4}-{6}	(C.c)*Colon	(A. h)*Middle Small Int.	0.232	0.000
{4}-{7}	(C.c)*Colon	(A. h)*Distal Small Int.	0.234	0.000
{4}-{8}	(C.c)*Colon	(A. h)*Colon	0.229	0.000
{5}-{6}	(A. h)*Duodenum	(A. h)*Middle Small Int.	0.114	0.000
{5}-{7}	(A. h)*Duodenum	(A. h)*Distal Small Int.	0.117	0.145
{5}-{8}	(A. h)*Duodenum	(A. h)*Colon	0.107	0.011
{6}-{7}	(A. h)*Middle Small Int.	(A. h)*Distal Small Int.	0.122	0.004
{6}-{8}	(A. h)*Middle Small Int.	(A. h)*Colon	0.113	0.000
{7}-{8}	(A. h)*Distal Small Int.	(A. h)*Colon	0.116	0.000

C.c: *Crocicura cyanea*

A.h: *Amblysomus hottentotus*

Appendix 24

AB/PAS results

P-values for the graph of figure 4.32C: The distribution of the total number of neutral mucin secreting goblet cells throughout the GI crypt areas of *C. cyanea* and *A. hottentotus*.

Figure 4.32C: Neutral goblet cells per crypt area (mm^2)				
Comparison of the Gastrointestinal Regions	1st	2nd	Standard Error	p- value
{1}-{2}	(C.c)*Duodenum	(C.c)*Middle Small Int.	0.119	0.326
{1}-{3}	(C.c)*Duodenum	(C.c)*Distal Small Int.	0.124	0.038
{1}-{4}	(C.c)*Duodenum	(C.c)*Colon	0.133	0.479
{1}-{5}	(C.c)*Duodenum	(A. h)*Duodenum	0.353	0.000
{1}-{6}	(C.c)*Duodenum	(A. h)*Middle Small Int.	0.355	0.001
{1}-{7}	(C.c)*Duodenum	(A. h)*Distal Small Int.	0.357	0.000
{1}-{8}	(C.c)*Duodenum	(A. h)*Colon	0.353	0.000
{2}-{3}	(C.c)*Middle Small Int.	(C.c)*Distal Small Int.	0.125	0.259
{2}-{4}	(C.c)*Middle Small Int.	(C.c)*Colon	0.133	0.863
{2}-{5}	(C.c)*Middle Small Int.	(A. h)*Duodenum	0.353	0.000
{2}-{6}	(C.c)*Middle Small Int.	(A. h)*Middle Small Int.	0.356	0.000
{2}-{7}	(C.c)*Middle Small Int.	(A. h)*Distal Small Int.	0.357	0.000
{2}-{8}	(C.c)*Middle Small Int.	(A. h)*Colon	0.353	0.000
{3}-{4}	(C.c)*Distal Small Int.	(C.c)*Colon	0.138	0.235
{3}-{5}	(C.c)*Distal Small Int.	(A. h)*Duodenum	0.355	0.000
{3}-{6}	(C.c)*Distal Small Int.	(A. h)*Middle Small Int.	0.358	0.000
{3}-{7}	(C.c)*Distal Small Int.	(A. h)*Distal Small Int.	0.359	0.000
{3}-{8}	(C.c)*Distal Small Int.	(A. h)*Colon	0.355	0.000
{4}-{5}	(C.c)*Colon	(A. h)*Duodenum	0.358	0.000
{4}-{6}	(C.c)*Colon	(A. h)*Middle Small Int.	0.361	0.000
{4}-{7}	(C.c)*Colon	(A. h)*Distal Small Int.	0.362	0.000
{4}-{8}	(C.c)*Colon	(A. h)*Colon	0.358	0.000
{5}-{6}	(A. h)*Duodenum	(A. h)*Middle Small Int.	0.137	0.007
{5}-{7}	(A. h)*Duodenum	(A. h)*Distal Small Int.	0.140	0.156
{5}-{8}	(A. h)*Duodenum	(A. h)*Colon	0.129	0.731
{6}-{7}	(A. h)*Middle Small Int.	(A. h)*Distal Small Int.	0.147	0.245
{6}-{8}	(A. h)*Middle Small Int.	(A. h)*Colon	0.136	0.002
{7}-{8}	(A. h)*Distal Small Int.	(A. h)*Colon	0.140	0.081

C.c: *Crocicura cyanea*

A.h: *Amblysomus hottentotus*

Appendix 25

AB/PAS results

P-values for the graph of figure 4.33A: The distribution of the total number of acid mucin secreting goblet cells throughout the GIT of *C. cyanea* and *A. hottentotus*.

Figure 4.33A: Total number of acid goblet cells per total area (mm^2)				
Comparison of the Gastrointestinal Regions	1st	2nd	Standard Error	p- value
{1}-{2}	(C.c)*Duodenum	(C.c)*Middle Small Int.	0.078	0.985
{1}-{3}	(C.c)*Duodenum	(C.c)*Distal Small Int.	0.082	0.988
{1}-{4}	(C.c)*Duodenum	(C.c)*Colon	0.087	0.308
{1}-{5}	(C.c)*Duodenum	(A. h)*Duodenum	0.202	0.000
{1}-{6}	(C.c)*Duodenum	(A. h)*Middle Small Int.	0.204	0.000
{1}-{7}	(C.c)*Duodenum	(A. h)*Distal Small Int.	0.205	0.000
{1}-{8}	(C.c)*Duodenum	(A. h)*Colon	0.202	0.000
{2}-{3}	(C.c)*Middle Small Int.	(C.c)*Distal Small Int.	0.082	0.998
{2}-{4}	(C.c)*Middle Small Int.	(C.c)*Colon	0.088	0.303
{2}-{5}	(C.c)*Middle Small Int.	(A. h)*Duodenum	0.203	0.000
{2}-{6}	(C.c)*Middle Small Int.	(A. h)*Middle Small Int.	0.204	0.000
{2}-{7}	(C.c)*Middle Small Int.	(A. h)*Distal Small Int.	0.206	0.000
{2}-{8}	(C.c)*Middle Small Int.	(A. h)*Colon	0.202	0.000
{3}-{4}	(C.c)*Distal Small Int.	(C.c)*Colon	0.091	0.320
{3}-{5}	(C.c)*Distal Small Int.	(A. h)*Duodenum	0.204	0.000
{3}-{6}	(C.c)*Distal Small Int.	(A. h)*Middle Small Int.	0.206	0.000
{3}-{7}	(C.c)*Distal Small Int.	(A. h)*Distal Small Int.	0.207	0.000
{3}-{8}	(C.c)*Distal Small Int.	(A. h)*Colon	0.204	0.000
{4}-{5}	(C.c)*Colon	(A. h)*Duodenum	0.206	0.000
{4}-{6}	(C.c)*Colon	(A. h)*Middle Small Int.	0.208	0.000
{4}-{7}	(C.c)*Colon	(A. h)*Distal Small Int.	0.209	0.000
{4}-{8}	(C.c)*Colon	(A. h)*Colon	0.206	0.000
{5}-{6}	(A. h)*Duodenum	(A. h)*Middle Small Int.	0.090	0.000
{5}-{7}	(A. h)*Duodenum	(A. h)*Distal Small Int.	0.093	0.000
{5}-{8}	(A. h)*Duodenum	(A. h)*Colon	0.085	0.000
{6}-{7}	(A. h)*Middle Small Int.	(A. h)*Distal Small Int.	0.097	0.469
{6}-{8}	(A. h)*Middle Small Int.	(A. h)*Colon	0.089	0.000
{7}-{8}	(A. h)*Distal Small Int.	(A. h)*Colon	0.092	0.000

C.c: *Crocicura cyanea*

A.h: *Amblysomus hottentotus*

Appendix 26

AB/PAS results

P-values for the graph of figure 4.33B: The distribution of the total number of acid mucin secreting goblet cells throughout the GI surface epithelial areas of *C. cyanea* and *A. hottentotus*.

Figure 4.33B: Acid goblet cells per surface epithelial area (mm^2)				
Comparison of the Gastrointestinal Regions	1st	2nd	Standard Error	p- value
{1}-{2}	(C.c)*Duodenum	(C.c)*Middle Small Int.	0.105	0.988
{1}-{3}	(C.c)*Duodenum	(C.c)*Distal Small Int.	0.110	0.990
{1}-{4}	(C.c)*Duodenum	(C.c)*Colon	0.117	0.405
{1}-{5}	(C.c)*Duodenum	(A. h)*Duodenum	0.257	0.000
{1}-{6}	(C.c)*Duodenum	(A. h)*Middle Small Int.	0.260	0.000
{1}-{7}	(C.c)*Duodenum	(A. h)*Distal Small Int.	0.261	0.000
{1}-{8}	(C.c)*Duodenum	(A. h)*Colon	0.256	0.000
{2}-{3}	(C.c)*Middle Small Int.	(C.c)*Distal Small Int.	0.110	0.998
{2}-{4}	(C.c)*Middle Small Int.	(C.c)*Colon	0.118	0.401
{2}-{5}	(C.c)*Middle Small Int.	(A. h)*Duodenum	0.257	0.000
{2}-{6}	(C.c)*Middle Small Int.	(A. h)*Middle Small Int.	0.260	0.000
{2}-{7}	(C.c)*Middle Small Int.	(A. h)*Distal Small Int.	0.262	0.000
{2}-{8}	(C.c)*Middle Small Int.	(A. h)*Colon	0.257	0.000
{3}-{4}	(C.c)*Distal Small Int.	(C.c)*Colon	0.122	0.417
{3}-{5}	(C.c)*Distal Small Int.	(A. h)*Duodenum	0.259	0.000
{3}-{6}	(C.c)*Distal Small Int.	(A. h)*Middle Small Int.	0.262	0.000
{3}-{7}	(C.c)*Distal Small Int.	(A. h)*Distal Small Int.	0.263	0.000
{3}-{8}	(C.c)*Distal Small Int.	(A. h)*Colon	0.259	0.000
{4}-{5}	(C.c)*Colon	(A. h)*Duodenum	0.263	0.000
{4}-{6}	(C.c)*Colon	(A. h)*Middle Small Int.	0.265	0.000
{4}-{7}	(C.c)*Colon	(A. h)*Distal Small Int.	0.267	0.000
{4}-{8}	(C.c)*Colon	(A. h)*Colon	0.262	0.000
{5}-{6}	(A. h)*Duodenum	(A. h)*Middle Small Int.	0.121	0.000
{5}-{7}	(A. h)*Duodenum	(A. h)*Distal Small Int.	0.124	0.000
{5}-{8}	(A. h)*Duodenum	(A. h)*Colon	0.114	0.000
{6}-{7}	(A. h)*Middle Small Int.	(A. h)*Distal Small Int.	0.130	0.177
{6}-{8}	(A. h)*Middle Small Int.	(A. h)*Colon	0.120	0.006
{7}-{8}	(A. h)*Distal Small Int.	(A. h)*Colon	0.124	0.207

C.c: *Crocicura cyanea*

A.h: *Amblysomus hottentotus*

Appendix 27

AB/PAS results

P-values for the graph of figure 4.33C: The distribution of the total number of acid mucin secreting goblet cells throughout the GI crypt areas of *C. cyanea* and *A. hottentotus*.

Figure 4.33C: Acid goblet cells per crypt area (mm^2)				
Comparison of the Gastrointestinal Regions	1st	2nd	Standard Error	p- value
{1}-{2}	(C.c)*Duodenum	(C.c)*Middle Small Int.	0.089	1.000
{1}-{3}	(C.c)*Duodenum	(C.c)*Distal Small Int.	0.092	1.000
{1}-{4}	(C.c)*Duodenum	(C.c)*Colon	0.099	1.000
{1}-{5}	(C.c)*Duodenum	(A. h)*Duodenum	0.269	0.085
{1}-{6}	(C.c)*Duodenum	(A. h)*Middle Small Int.	0.271	0.000
{1}-{7}	(C.c)*Duodenum	(A. h)*Distal Small Int.	0.272	0.000
{1}-{8}	(C.c)*Duodenum	(A. h)*Colon	0.269	0.000
{2}-{3}	(C.c)*Middle Small Int.	(C.c)*Distal Small Int.	0.093	1.000
{2}-{4}	(C.c)*Middle Small Int.	(C.c)*Colon	0.099	1.000
{2}-{5}	(C.c)*Middle Small Int.	(A. h)*Duodenum	0.269	0.086
{2}-{6}	(C.c)*Middle Small Int.	(A. h)*Middle Small Int.	0.271	0.000
{2}-{7}	(C.c)*Middle Small Int.	(A. h)*Distal Small Int.	0.272	0.000
{2}-{8}	(C.c)*Middle Small Int.	(A. h)*Colon	0.269	0.000
{3}-{4}	(C.c)*Distal Small Int.	(C.c)*Colon	0.103	1.000
{3}-{5}	(C.c)*Distal Small Int.	(A. h)*Duodenum	0.270	0.087
{3}-{6}	(C.c)*Distal Small Int.	(A. h)*Middle Small Int.	0.272	0.000
{3}-{7}	(C.c)*Distal Small Int.	(A. h)*Distal Small Int.	0.273	0.000
{3}-{8}	(C.c)*Distal Small Int.	(A. h)*Colon	0.270	0.000
{4}-{5}	(C.c)*Colon	(A. h)*Duodenum	0.273	0.090
{4}-{6}	(C.c)*Colon	(A. h)*Middle Small Int.	0.274	0.000
{4}-{7}	(C.c)*Colon	(A. h)*Distal Small Int.	0.275	0.000
{4}-{8}	(C.c)*Colon	(A. h)*Colon	0.272	0.000
{5}-{6}	(A. h)*Duodenum	(A. h)*Middle Small Int.	0.102	0.000
{5}-{7}	(A. h)*Duodenum	(A. h)*Distal Small Int.	0.105	0.000
{5}-{8}	(A. h)*Duodenum	(A. h)*Colon	0.096	0.000
{6}-{7}	(A. h)*Middle Small Int.	(A. h)*Distal Small Int.	0.109	0.000
{6}-{8}	(A. h)*Middle Small Int.	(A. h)*Colon	0.101	0.000
{7}-{8}	(A. h)*Distal Small Int.	(A. h)*Colon	0.104	0.000

C.c: *Crocicura cyanea*

A.h: *Amblysomus hottentotus*

Appendix 28

AB/PAS results

P-values for the graph of figure 4.34A: The distribution of the total number of mixed mucin secreting goblet cells throughout the GIT of *C. cyanea* and *A. hottentotus*.

Figure 4.34A: Total number of mixed goblet cells per total area (mm^2)				
Comparison of the Gastrointestinal Regions	1st	2nd	Standard Error	p- value
{1}-{2}	(C.c)*Duodenum	(C.c)*Middle Small Int.	0.025	0.000
{1}-{3}	(C.c)*Duodenum	(C.c)*Distal Small Int.	0.026	0.000
{1}-{4}	(C.c)*Duodenum	(C.c)*Colon	0.028	0.000
{1}-{5}	(C.c)*Duodenum	(A. h)*Duodenum	0.044	0.004
{1}-{6}	(C.c)*Duodenum	(A. h)*Middle Small Int.	0.045	0.014
{1}-{7}	(C.c)*Duodenum	(A. h)*Distal Small Int.	0.045	0.146
{1}-{8}	(C.c)*Duodenum	(A. h)*Colon	0.044	0.992
{2}-{3}	(C.c)*Middle Small Int.	(C.c)*Distal Small Int.	0.026	0.000
{2}-{4}	(C.c)*Middle Small Int.	(C.c)*Colon	0.028	0.000
{2}-{5}	(C.c)*Middle Small Int.	(A. h)*Duodenum	0.044	0.256
{2}-{6}	(C.c)*Middle Small Int.	(A. h)*Middle Small Int.	0.045	0.130
{2}-{7}	(C.c)*Middle Small Int.	(A. h)*Distal Small Int.	0.045	0.000
{2}-{8}	(C.c)*Middle Small Int.	(A. h)*Colon	0.044	0.000
{3}-{4}	(C.c)*Distal Small Int.	(C.c)*Colon	0.029	0.000
{3}-{5}	(C.c)*Distal Small Int.	(A. h)*Duodenum	0.045	0.000
{3}-{6}	(C.c)*Distal Small Int.	(A. h)*Middle Small Int.	0.045	0.000
{3}-{7}	(C.c)*Distal Small Int.	(A. h)*Distal Small Int.	0.046	0.000
{3}-{8}	(C.c)*Distal Small Int.	(A. h)*Colon	0.044	0.000
{4}-{5}	(C.c)*Colon	(A. h)*Duodenum	0.046	0.000
{4}-{6}	(C.c)*Colon	(A. h)*Middle Small Int.	0.047	0.000
{4}-{7}	(C.c)*Colon	(A. h)*Distal Small Int.	0.047	0.000
{4}-{8}	(C.c)*Colon	(A. h)*Colon	0.046	0.000
{5}-{6}	(A. h)*Duodenum	(A. h)*Middle Small Int.	0.029	0.535
{5}-{7}	(A. h)*Duodenum	(A. h)*Distal Small Int.	0.030	0.000
{5}-{8}	(A. h)*Duodenum	(A. h)*Colon	0.027	0.000
{6}-{7}	(A. h)*Middle Small Int.	(A. h)*Distal Small Int.	0.031	0.000
{6}-{8}	(A. h)*Middle Small Int.	(A. h)*Colon	0.029	0.000
{7}-{8}	(A. h)*Distal Small Int.	(A. h)*Colon	0.030	0.025

C.c: *Crocicura cyanea*

A.h: *Amblysomus hottentotus*

Appendix 29

AB/PAS results

P-values for the graph of figure 4.34B: The distribution of the total number of mixed mucin secreting goblet cells throughout the GI surface epithelial areas of *C. cyanea* and *A. hottentotus*.

Figure 4.34B: Mixed goblet cells per surface epithelial area (mm^2)				
Comparison of the Gastrointestinal Regions	1st	2nd	Standard Error	p- value
{1}-{2}	(C.c)*Duodenum	(C.c)*Middle Small Int.	0.026	0.000
{1}-{3}	(C.c)*Duodenum	(C.c)*Distal Small Int.	0.027	0.000
{1}-{4}	(C.c)*Duodenum	(C.c)*Colon	0.029	0.000
{1}-{5}	(C.c)*Duodenum	(A. h)*Duodenum	0.043	0.000
{1}-{6}	(C.c)*Duodenum	(A. h)*Middle Small Int.	0.044	0.003
{1}-{7}	(C.c)*Duodenum	(A. h)*Distal Small Int.	0.045	0.000
{1}-{8}	(C.c)*Duodenum	(A. h)*Colon	0.043	0.005
{2}-{3}	(C.c)*Middle Small Int.	(C.c)*Distal Small Int.	0.027	0.000
{2}-{4}	(C.c)*Middle Small Int.	(C.c)*Colon	0.029	0.000
{2}-{5}	(C.c)*Middle Small Int.	(A. h)*Duodenum	0.043	0.004
{2}-{6}	(C.c)*Middle Small Int.	(A. h)*Middle Small Int.	0.044	0.725
{2}-{7}	(C.c)*Middle Small Int.	(A. h)*Distal Small Int.	0.045	0.000
{2}-{8}	(C.c)*Middle Small Int.	(A. h)*Colon	0.043	0.000
{3}-{4}	(C.c)*Distal Small Int.	(C.c)*Colon	0.030	0.000
{3}-{5}	(C.c)*Distal Small Int.	(A. h)*Duodenum	0.044	0.000
{3}-{6}	(C.c)*Distal Small Int.	(A. h)*Middle Small Int.	0.045	0.000
{3}-{7}	(C.c)*Distal Small Int.	(A. h)*Distal Small Int.	0.046	0.000
{3}-{8}	(C.c)*Distal Small Int.	(A. h)*Colon	0.044	0.000
{4}-{5}	(C.c)*Colon	(A. h)*Duodenum	0.045	0.000
{4}-{6}	(C.c)*Colon	(A. h)*Middle Small Int.	0.046	0.000
{4}-{7}	(C.c)*Colon	(A. h)*Distal Small Int.	0.047	0.000
{4}-{8}	(C.c)*Colon	(A. h)*Colon	0.045	0.000
{5}-{6}	(A. h)*Duodenum	(A. h)*Middle Small Int.	0.030	0.000
{5}-{7}	(A. h)*Duodenum	(A. h)*Distal Small Int.	0.031	0.000
{5}-{8}	(A. h)*Duodenum	(A. h)*Colon	0.028	0.000
{6}-{7}	(A. h)*Middle Small Int.	(A. h)*Distal Small Int.	0.032	0.000
{6}-{8}	(A. h)*Middle Small Int.	(A. h)*Colon	0.030	0.000
{7}-{8}	(A. h)*Distal Small Int.	(A. h)*Colon	0.031	0.154

C.c: *Crocicura cyanea*

A.h: *Amblysomus hottentotus*

Appendix 30

AB/PAS results

P-values for the graph of figure 4.34C: The distribution of the total number of mixed mucin secreting goblet cells throughout the GI crypt areas of *C. cyanea* and *A. hottentotus*.

Figure 4.34C: Mixed goblet cells per crypt area (mm^2)				
Comparison of the Gastrointestinal Regions	1st	2nd	Standard Error	p- value
{1}-{2}	(C.c)*Duodenum	(C.c)*Middle Small Int.	0.059	0.000
{1}-{3}	(C.c)*Duodenum	(C.c)*Distal Small Int.	0.062	0.379
{1}-{4}	(C.c)*Duodenum	(C.c)*Colon	0.066	0.000
{1}-{5}	(C.c)*Duodenum	(A. h)*Duodenum	0.100	0.500
{1}-{6}	(C.c)*Duodenum	(A. h)*Middle Small Int.	0.102	0.339
{1}-{7}	(C.c)*Duodenum	(A. h)*Distal Small Int.	0.103	0.217
{1}-{8}	(C.c)*Duodenum	(A. h)*Colon	0.100	0.216
{2}-{3}	(C.c)*Middle Small Int.	(C.c)*Distal Small Int.	0.062	0.000
{2}-{4}	(C.c)*Middle Small Int.	(C.c)*Colon	0.066	0.000
{2}-{5}	(C.c)*Middle Small Int.	(A. h)*Duodenum	0.100	0.000
{2}-{6}	(C.c)*Middle Small Int.	(A. h)*Middle Small Int.	0.102	0.047
{2}-{7}	(C.c)*Middle Small Int.	(A. h)*Distal Small Int.	0.104	0.094
{2}-{8}	(C.c)*Middle Small Int.	(A. h)*Colon	0.100	0.075
{3}-{4}	(C.c)*Distal Small Int.	(C.c)*Colon	0.068	0.000
{3}-{5}	(C.c)*Distal Small Int.	(A. h)*Duodenum	0.102	0.896
{3}-{6}	(C.c)*Distal Small Int.	(A. h)*Middle Small Int.	0.104	0.144
{3}-{7}	(C.c)*Distal Small Int.	(A. h)*Distal Small Int.	0.105	0.084
{3}-{8}	(C.c)*Distal Small Int.	(A. h)*Colon	0.101	0.080
{4}-{5}	(C.c)*Colon	(A. h)*Duodenum	0.104	0.003
{4}-{6}	(C.c)*Colon	(A. h)*Middle Small Int.	0.106	0.000
{4}-{7}	(C.c)*Colon	(A. h)*Distal Small Int.	0.108	0.000
{4}-{8}	(C.c)*Colon	(A. h)*Colon	0.104	0.000
{5}-{6}	(A. h)*Duodenum	(A. h)*Middle Small Int.	0.068	0.015
{5}-{7}	(A. h)*Duodenum	(A. h)*Distal Small Int.	0.070	0.005
{5}-{8}	(A. h)*Duodenum	(A. h)*Colon	0.064	0.003
{6}-{7}	(A. h)*Middle Small Int.	(A. h)*Distal Small Int.	0.073	0.680
{6}-{8}	(A. h)*Middle Small Int.	(A. h)*Colon	0.067	0.703
{7}-{8}	(A. h)*Distal Small Int.	(A. h)*Colon	0.069	0.950

C.c: *Crocicura cyanea*

A.h: *Amblysomus hottentotus*

Appendix 31

HID/AB and AF/AB results

P-values for the graph of figure 4.35A: The distribution of the total number of acid (sulfo- and sialomucins) mucin secreting goblet cells throughout the GIT of *C. cyanea* and *A. hottentotus*.

Figure 4.35A: Total number of acid goblet cells per total area (mm^2)				
Comparison of the Gastrointestinal Regions	1st	2nd	Standard Error	p- value
{1}-{2}	(C.c)*Duodenum	(C.c)*Middle Small Int.	0.030	0.899
{1}-{3}	(C.c)*Duodenum	(C.c)*Distal Small Int.	0.031	0.000
{1}-{4}	(C.c)*Duodenum	(C.c)*Colon	0.032	0.000
{1}-{5}	(C.c)*Duodenum	(A. h)*Duodenum	0.059	0.459
{1}-{6}	(C.c)*Duodenum	(A. h)*Middle Small Int.	0.060	0.027
{1}-{7}	(C.c)*Duodenum	(A. h)*Distal Small Int.	0.060	0.000
{1}-{8}	(C.c)*Duodenum	(A. h)*Colon	0.059	0.000
{2}-{3}	(C.c)*Middle Small Int.	(C.c)*Distal Small Int.	0.031	0.000
{2}-{4}	(C.c)*Middle Small Int.	(C.c)*Colon	0.032	0.000
{2}-{5}	(C.c)*Middle Small Int.	(A. h)*Duodenum	0.059	0.497
{2}-{6}	(C.c)*Middle Small Int.	(A. h)*Middle Small Int.	0.060	0.023
{2}-{7}	(C.c)*Middle Small Int.	(A. h)*Distal Small Int.	0.060	0.000
{2}-{8}	(C.c)*Middle Small Int.	(A. h)*Colon	0.059	0.000
{3}-{4}	(C.c)*Distal Small Int.	(C.c)*Colon	0.033	0.054
{3}-{5}	(C.c)*Distal Small Int.	(A. h)*Duodenum	0.060	0.000
{3}-{6}	(C.c)*Distal Small Int.	(A. h)*Middle Small Int.	0.061	0.000
{3}-{7}	(C.c)*Distal Small Int.	(A. h)*Distal Small Int.	0.061	0.008
{3}-{8}	(C.c)*Distal Small Int.	(A. h)*Colon	0.060	0.001
{4}-{5}	(C.c)*Colon	(A. h)*Duodenum	0.061	0.000
{4}-{6}	(C.c)*Colon	(A. h)*Middle Small Int.	0.062	0.000
{4}-{7}	(C.c)*Colon	(A. h)*Distal Small Int.	0.062	0.000
{4}-{8}	(C.c)*Colon	(A. h)*Colon	0.061	0.000
{5}-{6}	(A. h)*Duodenum	(A. h)*Middle Small Int.	0.035	0.000
{5}-{7}	(A. h)*Duodenum	(A. h)*Distal Small Int.	0.035	0.000
{5}-{8}	(A. h)*Duodenum	(A. h)*Colon	0.033	0.000
{6}-{7}	(A. h)*Middle Small Int.	(A. h)*Distal Small Int.	0.036	0.000
{6}-{8}	(A. h)*Middle Small Int.	(A. h)*Colon	0.034	0.000
{7}-{8}	(A. h)*Distal Small Int.	(A. h)*Colon	0.035	0.380

C.c: *Crocicura cyanea*

A.h: *Amblysomus hottentotus*

Appendix 32

HID/AB and AF/AB results

P-values for the graph of figure 4.35B: The distribution of the total number of acid (sulfo- and sialomucins) mucin secreting goblet cells throughout the GI surface epithelial areas of *C. cyanea* and *A. hottentotus*.

Figure 4.35B: Acid goblet cells per surface epithelial area (mm^2)				
Comparison of the Gastrointestinal Regions	1st	2nd	Standard Error	p- value
{1}-{2}	(C.c)*Duodenum	(C.c)*Middle Small Int.	0.021	0.177
{1}-{3}	(C.c)*Duodenum	(C.c)*Distal Small Int.	0.022	0.000
{1}-{4}	(C.c)*Duodenum	(C.c)*Colon	0.023	0.000
{1}-{5}	(C.c)*Duodenum	(A. h)*Duodenum	0.044	0.027
{1}-{6}	(C.c)*Duodenum	(A. h)*Middle Small Int.	0.045	0.009
{1}-{7}	(C.c)*Duodenum	(A. h)*Distal Small Int.	0.045	0.000
{1}-{8}	(C.c)*Duodenum	(A. h)*Colon	0.045	0.000
{2}-{3}	(C.c)*Middle Small Int.	(C.c)*Distal Small Int.	0.022	0.000
{2}-{4}	(C.c)*Middle Small Int.	(C.c)*Colon	0.023	0.000
{2}-{5}	(C.c)*Middle Small Int.	(A. h)*Duodenum	0.044	0.004
{2}-{6}	(C.c)*Middle Small Int.	(A. h)*Middle Small Int.	0.045	0.047
{2}-{7}	(C.c)*Middle Small Int.	(A. h)*Distal Small Int.	0.045	0.000
{2}-{8}	(C.c)*Middle Small Int.	(A. h)*Colon	0.045	0.000
{3}-{4}	(C.c)*Distal Small Int.	(C.c)*Colon	0.023	0.265
{3}-{5}	(C.c)*Distal Small Int.	(A. h)*Duodenum	0.044	0.000
{3}-{6}	(C.c)*Distal Small Int.	(A. h)*Middle Small Int.	0.045	0.000
{3}-{7}	(C.c)*Distal Small Int.	(A. h)*Distal Small Int.	0.045	0.000
{3}-{8}	(C.c)*Distal Small Int.	(A. h)*Colon	0.045	0.000
{4}-{5}	(C.c)*Colon	(A. h)*Duodenum	0.044	0.000
{4}-{6}	(C.c)*Colon	(A. h)*Middle Small Int.	0.045	0.000
{4}-{7}	(C.c)*Colon	(A. h)*Distal Small Int.	0.046	0.000
{4}-{8}	(C.c)*Colon	(A. h)*Colon	0.045	0.000
{5}-{6}	(A. h)*Duodenum	(A. h)*Middle Small Int.	0.025	0.000
{5}-{7}	(A. h)*Duodenum	(A. h)*Distal Small Int.	0.025	0.000
{5}-{8}	(A. h)*Duodenum	(A. h)*Colon	0.025	0.000
{6}-{7}	(A. h)*Middle Small Int.	(A. h)*Distal Small Int.	0.027	0.000
{6}-{8}	(A. h)*Middle Small Int.	(A. h)*Colon	0.026	0.000
{7}-{8}	(A. h)*Distal Small Int.	(A. h)*Colon	0.027	0.242

C.c: *Crocicura cyanea*

A.h: *Amblysomus hottentotus*

Appendix 33

HID/AB and AF/AB results

P-values for the graph of figure 4.35C: The distribution of the total number of acid (sulfo- and sialomucins) mucin secreting goblet cells throughout the GI crypt areas of *C. cyanea* and *A. hottentotus*.

Figure 4.35C: Acid goblet cells per crypt area (mm^2)				
Comparison of the Gastrointestinal Regions	1st	2nd	Standard Error	p- value
{1}-{2}	(C.c)*Duodenum	(C.c)*Middle Small Int.	0.024	0.016
{1}-{3}	(C.c)*Duodenum	(C.c)*Distal Small Int.	0.025	0.000
{1}-{4}	(C.c)*Duodenum	(C.c)*Colon	0.026	0.000
{1}-{5}	(C.c)*Duodenum	(A. h)*Duodenum	0.030	0.431
{1}-{6}	(C.c)*Duodenum	(A. h)*Middle Small Int.	0.031	0.084
{1}-{7}	(C.c)*Duodenum	(A. h)*Distal Small Int.	0.031	0.000
{1}-{8}	(C.c)*Duodenum	(A. h)*Colon	0.030	0.000
{2}-{3}	(C.c)*Middle Small Int.	(C.c)*Distal Small Int.	0.025	0.000
{2}-{4}	(C.c)*Middle Small Int.	(C.c)*Colon	0.026	0.000
{2}-{5}	(C.c)*Middle Small Int.	(A. h)*Duodenum	0.030	0.007
{2}-{6}	(C.c)*Middle Small Int.	(A. h)*Middle Small Int.	0.031	0.000
{2}-{7}	(C.c)*Middle Small Int.	(A. h)*Distal Small Int.	0.031	0.000
{2}-{8}	(C.c)*Middle Small Int.	(A. h)*Colon	0.030	0.000
{3}-{4}	(C.c)*Distal Small Int.	(C.c)*Colon	0.027	0.077
{3}-{5}	(C.c)*Distal Small Int.	(A. h)*Duodenum	0.031	0.000
{3}-{6}	(C.c)*Distal Small Int.	(A. h)*Middle Small Int.	0.032	0.000
{3}-{7}	(C.c)*Distal Small Int.	(A. h)*Distal Small Int.	0.032	0.000
{3}-{8}	(C.c)*Distal Small Int.	(A. h)*Colon	0.031	0.000
{4}-{5}	(C.c)*Colon	(A. h)*Duodenum	0.032	0.000
{4}-{6}	(C.c)*Colon	(A. h)*Middle Small Int.	0.033	0.000
{4}-{7}	(C.c)*Colon	(A. h)*Distal Small Int.	0.033	0.000
{4}-{8}	(C.c)*Colon	(A. h)*Colon	0.032	0.000
{5}-{6}	(A. h)*Duodenum	(A. h)*Middle Small Int.	0.028	0.278
{5}-{7}	(A. h)*Duodenum	(A. h)*Distal Small Int.	0.028	0.000
{5}-{8}	(A. h)*Duodenum	(A. h)*Colon	0.026	0.000
{6}-{7}	(A. h)*Middle Small Int.	(A. h)*Distal Small Int.	0.029	0.000
{6}-{8}	(A. h)*Middle Small Int.	(A. h)*Colon	0.028	0.000
{7}-{8}	(A. h)*Distal Small Int.	(A. h)*Colon	0.028	0.646

C.c: *Crocicura cyanea*

A.h: *Amblysomus hottentotus*

Appendix 34

HID/AB and AF/AB results

P-values for the graph of figure 4.36A: The distribution of the total number of sulfomucin secreting goblet cells throughout the GIT of *C. cyanea* and *A. hottentotus*.

Figure 4.36A: Total number of sulfated goblet cells per total area (mm^2)				
Comparison of the Gastrointestinal Regions	1st	2nd	Standard Error	p- value
{1}-{2}	(C.c)*Duodenum	(C.c)*Middle Small Int.	0.073	0.000
{1}-{3}	(C.c)*Duodenum	(C.c)*Distal Small Int.	0.076	0.000
{1}-{4}	(C.c)*Duodenum	(C.c)*Colon	0.080	0.000
{1}-{5}	(C.c)*Duodenum	(A. h)*Duodenum	0.213	0.000
{1}-{6}	(C.c)*Duodenum	(A. h)*Middle Small Int.	0.214	0.000
{1}-{7}	(C.c)*Duodenum	(A. h)*Distal Small Int.	0.215	0.000
{1}-{8}	(C.c)*Duodenum	(A. h)*Colon	0.213	0.000
{2}-{3}	(C.c)*Middle Small Int.	(C.c)*Distal Small Int.	0.076	0.000
{2}-{4}	(C.c)*Middle Small Int.	(C.c)*Colon	0.079	0.000
{2}-{5}	(C.c)*Middle Small Int.	(A. h)*Duodenum	0.213	0.000
{2}-{6}	(C.c)*Middle Small Int.	(A. h)*Middle Small Int.	0.214	0.000
{2}-{7}	(C.c)*Middle Small Int.	(A. h)*Distal Small Int.	0.214	0.000
{2}-{8}	(C.c)*Middle Small Int.	(A. h)*Colon	0.212	0.000
{3}-{4}	(C.c)*Distal Small Int.	(C.c)*Colon	0.082	0.739
{3}-{5}	(C.c)*Distal Small Int.	(A. h)*Duodenum	0.214	0.000
{3}-{6}	(C.c)*Distal Small Int.	(A. h)*Middle Small Int.	0.215	0.000
{3}-{7}	(C.c)*Distal Small Int.	(A. h)*Distal Small Int.	0.216	0.000
{3}-{8}	(C.c)*Distal Small Int.	(A. h)*Colon	0.214	0.000
{4}-{5}	(C.c)*Colon	(A. h)*Duodenum	0.215	0.000
{4}-{6}	(C.c)*Colon	(A. h)*Middle Small Int.	0.217	0.000
{4}-{7}	(C.c)*Colon	(A. h)*Distal Small Int.	0.217	0.000
{4}-{8}	(C.c)*Colon	(A. h)*Colon	0.215	0.000
{5}-{6}	(A. h)*Duodenum	(A. h)*Middle Small Int.	0.085	0.045
{5}-{7}	(A. h)*Duodenum	(A. h)*Distal Small Int.	0.085	0.000
{5}-{8}	(A. h)*Duodenum	(A. h)*Colon	0.080	0.007
{6}-{7}	(A. h)*Middle Small Int.	(A. h)*Distal Small Int.	0.089	0.000
{6}-{8}	(A. h)*Middle Small Int.	(A. h)*Colon	0.084	0.000
{7}-{8}	(A. h)*Distal Small Int.	(A. h)*Colon	0.085	0.000

C.c: *Crocicura cyanea*

A.h: *Amblysomus hottentotus*

Appendix 35

HID/AB and AF/AB results

P-values for the graph of figure 4.36B: The distribution of the total number of sulfomucin secreting goblet cells throughout the GI surface epithelial areas of *C. cyanea* and *A. hottentotus*.

Figure 4.36B: Sulfated goblet cells per surface epithelial area (mm^2)				
Comparison of the Gastrointestinal Regions	1st	2nd	Standard Error	p- value
{1}-{2}	(C.c)*Duodenum	(C.c)*Middle Small Int.	0.082	0.000
{1}-{3}	(C.c)*Duodenum	(C.c)*Distal Small Int.	0.086	0.000
{1}-{4}	(C.c)*Duodenum	(C.c)*Colon	0.090	0.000
{1}-{5}	(C.c)*Duodenum	(A. h)*Duodenum	0.235	0.000
{1}-{6}	(C.c)*Duodenum	(A. h)*Middle Small Int.	0.237	0.000
{1}-{7}	(C.c)*Duodenum	(A. h)*Distal Small Int.	0.237	0.000
{1}-{8}	(C.c)*Duodenum	(A. h)*Colon	0.235	0.000
{2}-{3}	(C.c)*Middle Small Int.	(C.c)*Distal Small Int.	0.085	0.000
{2}-{4}	(C.c)*Middle Small Int.	(C.c)*Colon	0.089	0.000
{2}-{5}	(C.c)*Middle Small Int.	(A. h)*Duodenum	0.235	0.000
{2}-{6}	(C.c)*Middle Small Int.	(A. h)*Middle Small Int.	0.237	0.000
{2}-{7}	(C.c)*Middle Small Int.	(A. h)*Distal Small Int.	0.237	0.000
{2}-{8}	(C.c)*Middle Small Int.	(A. h)*Colon	0.235	0.000
{3}-{4}	(C.c)*Distal Small Int.	(C.c)*Colon	0.093	0.393
{3}-{5}	(C.c)*Distal Small Int.	(A. h)*Duodenum	0.236	0.000
{3}-{6}	(C.c)*Distal Small Int.	(A. h)*Middle Small Int.	0.238	0.000
{3}-{7}	(C.c)*Distal Small Int.	(A. h)*Distal Small Int.	0.238	0.000
{3}-{8}	(C.c)*Distal Small Int.	(A. h)*Colon	0.236	0.000
{4}-{5}	(C.c)*Colon	(A. h)*Duodenum	0.238	0.000
{4}-{6}	(C.c)*Colon	(A. h)*Middle Small Int.	0.240	0.000
{4}-{7}	(C.c)*Colon	(A. h)*Distal Small Int.	0.240	0.000
{4}-{8}	(C.c)*Colon	(A. h)*Colon	0.238	0.000
{5}-{6}	(A. h)*Duodenum	(A. h)*Middle Small Int.	0.096	0.052
{5}-{7}	(A. h)*Duodenum	(A. h)*Distal Small Int.	0.096	0.000
{5}-{8}	(A. h)*Duodenum	(A. h)*Colon	0.091	0.000
{6}-{7}	(A. h)*Middle Small Int.	(A. h)*Distal Small Int.	0.101	0.000
{6}-{8}	(A. h)*Middle Small Int.	(A. h)*Colon	0.096	0.000
{7}-{8}	(A. h)*Distal Small Int.	(A. h)*Colon	0.096	0.000

C.c: *Crocicura cyanea*

A.h: *Amblysomus hottentotus*

Appendix 36

HID/AB and AF/AB results

P-values for the graph of figure 4.36C: The distribution of the total number of sulfomucin secreting goblet cells throughout the GI crypt areas of *C. cyanea* and *A. hottentotus*.

Figure 4.36C: Sulfated goblet cells per crypt area (mm^2)				
Comparison of the Gastrointestinal Regions	1st	2nd	Standard Error	p- value
{1}-{2}	(C.c)*Duodenum	(C.c)*Middle Small Int.	0.064	0.000
{1}-{3}	(C.c)*Duodenum	(C.c)*Distal Small Int.	0.067	0.000
{1}-{4}	(C.c)*Duodenum	(C.c)*Colon	0.070	0.000
{1}-{5}	(C.c)*Duodenum	(A. h)*Duodenum	0.159	0.000
{1}-{6}	(C.c)*Duodenum	(A. h)*Middle Small Int.	0.161	0.000
{1}-{7}	(C.c)*Duodenum	(A. h)*Distal Small Int.	0.161	0.000
{1}-{8}	(C.c)*Duodenum	(A. h)*Colon	0.159	0.000
{2}-{3}	(C.c)*Middle Small Int.	(C.c)*Distal Small Int.	0.067	0.000
{2}-{4}	(C.c)*Middle Small Int.	(C.c)*Colon	0.070	0.000
{2}-{5}	(C.c)*Middle Small Int.	(A. h)*Duodenum	0.159	0.000
{2}-{6}	(C.c)*Middle Small Int.	(A. h)*Middle Small Int.	0.161	0.000
{2}-{7}	(C.c)*Middle Small Int.	(A. h)*Distal Small Int.	0.161	0.000
{2}-{8}	(C.c)*Middle Small Int.	(A. h)*Colon	0.159	0.000
{3}-{4}	(C.c)*Distal Small Int.	(C.c)*Colon	0.072	0.464
{3}-{5}	(C.c)*Distal Small Int.	(A. h)*Duodenum	0.160	0.000
{3}-{6}	(C.c)*Distal Small Int.	(A. h)*Middle Small Int.	0.162	0.000
{3}-{7}	(C.c)*Distal Small Int.	(A. h)*Distal Small Int.	0.162	0.000
{3}-{8}	(C.c)*Distal Small Int.	(A. h)*Colon	0.160	0.000
{4}-{5}	(C.c)*Colon	(A. h)*Duodenum	0.162	0.000
{4}-{6}	(C.c)*Colon	(A. h)*Middle Small Int.	0.163	0.000
{4}-{7}	(C.c)*Colon	(A. h)*Distal Small Int.	0.163	0.000
{4}-{8}	(C.c)*Colon	(A. h)*Colon	0.161	0.000
{5}-{6}	(A. h)*Duodenum	(A. h)*Middle Small Int.	0.075	0.619
{5}-{7}	(A. h)*Duodenum	(A. h)*Distal Small Int.	0.075	0.000
{5}-{8}	(A. h)*Duodenum	(A. h)*Colon	0.071	0.804
{6}-{7}	(A. h)*Middle Small Int.	(A. h)*Distal Small Int.	0.078	0.000
{6}-{8}	(A. h)*Middle Small Int.	(A. h)*Colon	0.075	0.792
{7}-{8}	(A. h)*Distal Small Int.	(A. h)*Colon	0.075	0.000

C.c: *Crocicura cyanea*

A.h: *Amblysomus hottentotus*

Appendix 37

HID/AB and AF/AB results

P-values for the graph of figure 4.37A: The distribution of the total number of strongly sulfated goblet cells throughout the GIT of *C. cyanea* and *A. hottentotus*.

Figure 4.37A: Total number of strongly sulfated goblet cells per total area (mm^2)				
Comparison of the Gastrointestinal Regions	1st	2nd	Standard Error	p- value
{1}-{2}	(C.c)*Duodenum	(C.c)*Middle Small Int.	0.088	0.000
{1}-{3}	(C.c)*Duodenum	(C.c)*Distal Small Int.	0.091	0.000
{1}-{4}	(C.c)*Duodenum	(C.c)*Colon	0.094	0.000
{1}-{5}	(C.c)*Duodenum	(A. h)*Duodenum	0.182	0.013
{1}-{6}	(C.c)*Duodenum	(A. h)*Middle Small Int.	0.186	0.016
{1}-{7}	(C.c)*Duodenum	(A. h)*Distal Small Int.	0.187	0.000
{1}-{8}	(C.c)*Duodenum	(A. h)*Colon	0.186	0.304
{2}-{3}	(C.c)*Middle Small Int.	(C.c)*Distal Small Int.	0.090	0.000
{2}-{4}	(C.c)*Middle Small Int.	(C.c)*Colon	0.093	0.000
{2}-{5}	(C.c)*Middle Small Int.	(A. h)*Duodenum	0.182	0.000
{2}-{6}	(C.c)*Middle Small Int.	(A. h)*Middle Small Int.	0.185	0.000
{2}-{7}	(C.c)*Middle Small Int.	(A. h)*Distal Small Int.	0.187	0.000
{2}-{8}	(C.c)*Middle Small Int.	(A. h)*Colon	0.185	0.000
{3}-{4}	(C.c)*Distal Small Int.	(C.c)*Colon	0.096	0.056
{3}-{5}	(C.c)*Distal Small Int.	(A. h)*Duodenum	0.183	0.000
{3}-{6}	(C.c)*Distal Small Int.	(A. h)*Middle Small Int.	0.187	0.000
{3}-{7}	(C.c)*Distal Small Int.	(A. h)*Distal Small Int.	0.188	0.000
{3}-{8}	(C.c)*Distal Small Int.	(A. h)*Colon	0.187	0.000
{4}-{5}	(C.c)*Colon	(A. h)*Duodenum	0.185	0.000
{4}-{6}	(C.c)*Colon	(A. h)*Middle Small Int.	0.188	0.000
{4}-{7}	(C.c)*Colon	(A. h)*Distal Small Int.	0.190	0.000
{4}-{8}	(C.c)*Colon	(A. h)*Colon	0.188	0.000
{5}-{6}	(A. h)*Duodenum	(A. h)*Middle Small Int.	0.102	0.977
{5}-{7}	(A. h)*Duodenum	(A. h)*Distal Small Int.	0.105	0.000
{5}-{8}	(A. h)*Duodenum	(A. h)*Colon	0.102	0.000
{6}-{7}	(A. h)*Middle Small Int.	(A. h)*Distal Small Int.	0.111	0.000
{6}-{8}	(A. h)*Middle Small Int.	(A. h)*Colon	0.109	0.000
{7}-{8}	(A. h)*Distal Small Int.	(A. h)*Colon	0.111	0.000

C.c: *Crocicura cyanea*

A.h: *Amblysomus hottentotus*

Appendix 38

HID/AB and AF/AB results

P-values for the graph of figure 4.37B: The distribution of the total number of strongly sulfated goblet cells throughout the GI surface epithelial areas of *C. cyanea* and *A. hottentotus*.

Figure 4.37B: Strongly sulfated goblet cells per surface epithelial area (mm^2)				
Comparison of the Gastrointestinal Regions	1st	2nd	Standard Error	p- value
{1}-{2}	(C.c)*Duodenum	(C.c)*Middle Small Int.	0.103	0.000
{1}-{3}	(C.c)*Duodenum	(C.c)*Distal Small Int.	0.107	0.000
{1}-{4}	(C.c)*Duodenum	(C.c)*Colon	0.110	0.000
{1}-{5}	(C.c)*Duodenum	(A. h)*Duodenum	0.204	0.024
{1}-{6}	(C.c)*Duodenum	(A. h)*Middle Small Int.	0.208	0.028
{1}-{7}	(C.c)*Duodenum	(A. h)*Distal Small Int.	0.210	0.000
{1}-{8}	(C.c)*Duodenum	(A. h)*Colon	0.209	0.429
{2}-{3}	(C.c)*Middle Small Int.	(C.c)*Distal Small Int.	0.105	0.000
{2}-{4}	(C.c)*Middle Small Int.	(C.c)*Colon	0.109	0.000
{2}-{5}	(C.c)*Middle Small Int.	(A. h)*Duodenum	0.203	0.000
{2}-{6}	(C.c)*Middle Small Int.	(A. h)*Middle Small Int.	0.208	0.000
{2}-{7}	(C.c)*Middle Small Int.	(A. h)*Distal Small Int.	0.209	0.000
{2}-{8}	(C.c)*Middle Small Int.	(A. h)*Colon	0.208	0.000
{3}-{4}	(C.c)*Distal Small Int.	(C.c)*Colon	0.112	0.001
{3}-{5}	(C.c)*Distal Small Int.	(A. h)*Duodenum	0.205	0.000
{3}-{6}	(C.c)*Distal Small Int.	(A. h)*Middle Small Int.	0.209	0.000
{3}-{7}	(C.c)*Distal Small Int.	(A. h)*Distal Small Int.	0.211	0.000
{3}-{8}	(C.c)*Distal Small Int.	(A. h)*Colon	0.210	0.000
{4}-{5}	(C.c)*Colon	(A. h)*Duodenum	0.207	0.000
{4}-{6}	(C.c)*Colon	(A. h)*Middle Small Int.	0.211	0.000
{4}-{7}	(C.c)*Colon	(A. h)*Distal Small Int.	0.213	0.000
{4}-{8}	(C.c)*Colon	(A. h)*Colon	0.211	0.000
{5}-{6}	(A. h)*Duodenum	(A. h)*Middle Small Int.	0.119	0.979
{5}-{7}	(A. h)*Duodenum	(A. h)*Distal Small Int.	0.122	0.000
{5}-{8}	(A. h)*Duodenum	(A. h)*Colon	0.120	0.000
{6}-{7}	(A. h)*Middle Small Int.	(A. h)*Distal Small Int.	0.129	0.000
{6}-{8}	(A. h)*Middle Small Int.	(A. h)*Colon	0.127	0.000
{7}-{8}	(A. h)*Distal Small Int.	(A. h)*Colon	0.130	0.000

C.c: *Crocicura cyanea*

A.h: *Amblysomus hottentotus*

Appendix 39

HID/AB and AF/AB results

P-values for the graph of figure 4.37C: The distribution of the total number of strongly sulfated goblet cells throughout the GI crypt areas of *C. cyanea* and *A. hottentotus*.

Figure 4.37C: Strongly sulfated goblet cells per crypt area (mm^2)				
Comparison of the Gastrointestinal Regions	1st	2nd	Standard Error	p- value
{1}-{2}	(C.c)*Duodenum	(C.c)*Middle Small Int.	0.120	0.000
{1}-{3}	(C.c)*Duodenum	(C.c)*Distal Small Int.	0.124	0.000
{1}-{4}	(C.c)*Duodenum	(C.c)*Colon	0.128	0.000
{1}-{5}	(C.c)*Duodenum	(A. h)*Duodenum	0.196	0.342
{1}-{6}	(C.c)*Duodenum	(A. h)*Middle Small Int.	0.202	0.361
{1}-{7}	(C.c)*Duodenum	(A. h)*Distal Small Int.	0.205	0.124
{1}-{8}	(C.c)*Duodenum	(A. h)*Colon	0.202	0.280
{2}-{3}	(C.c)*Middle Small Int.	(C.c)*Distal Small Int.	0.122	0.000
{2}-{4}	(C.c)*Middle Small Int.	(C.c)*Colon	0.126	0.000
{2}-{5}	(C.c)*Middle Small Int.	(A. h)*Duodenum	0.195	0.000
{2}-{6}	(C.c)*Middle Small Int.	(A. h)*Middle Small Int.	0.201	0.000
{2}-{7}	(C.c)*Middle Small Int.	(A. h)*Distal Small Int.	0.204	0.003
{2}-{8}	(C.c)*Middle Small Int.	(A. h)*Colon	0.201	0.001
{3}-{4}	(C.c)*Distal Small Int.	(C.c)*Colon	0.130	0.000
{3}-{5}	(C.c)*Distal Small Int.	(A. h)*Duodenum	0.198	0.000
{3}-{6}	(C.c)*Distal Small Int.	(A. h)*Middle Small Int.	0.204	0.000
{3}-{7}	(C.c)*Distal Small Int.	(A. h)*Distal Small Int.	0.206	0.000
{3}-{8}	(C.c)*Distal Small Int.	(A. h)*Colon	0.204	0.000
{4}-{5}	(C.c)*Colon	(A. h)*Duodenum	0.200	0.000
{4}-{6}	(C.c)*Colon	(A. h)*Middle Small Int.	0.206	0.000
{4}-{7}	(C.c)*Colon	(A. h)*Distal Small Int.	0.208	0.000
{4}-{8}	(C.c)*Colon	(A. h)*Colon	0.206	0.000
{5}-{6}	(A. h)*Duodenum	(A. h)*Middle Small Int.	0.139	0.990
{5}-{7}	(A. h)*Duodenum	(A. h)*Distal Small Int.	0.143	0.000
{5}-{8}	(A. h)*Duodenum	(A. h)*Colon	0.139	0.004
{6}-{7}	(A. h)*Middle Small Int.	(A. h)*Distal Small Int.	0.151	0.001
{6}-{8}	(A. h)*Middle Small Int.	(A. h)*Colon	0.148	0.006
{7}-{8}	(A. h)*Distal Small Int.	(A. h)*Colon	0.151	0.523

C.c: *Crocicura cyanea*

A.h: *Amblysomus hottentotus*

Appendix 40

HID/AB and AF/AB results

P-values for the graph of figure 4.38A: The distribution of the total number of weakly sulfated goblet cells throughout the GIT of *C. cyanea* and *A. hottentotus*.

Figure 4.38A: Total number of weakly sulfated goblet cells per total area (mm^2)				
Comparison of the Gastrointestinal Regions	1st	2nd	Standard Error	p- value
{1}-{2}	(C.c)*Duodenum	(C.c)*Middle Small Int.	0.079	0.000
{1}-{3}	(C.c)*Duodenum	(C.c)*Distal Small Int.	0.082	0.000
{1}-{4}	(C.c)*Duodenum	(C.c)*Colon	0.085	0.000
{1}-{5}	(C.c)*Duodenum	(A. h)*Duodenum	0.230	0.000
{1}-{6}	(C.c)*Duodenum	(A. h)*Middle Small Int.	0.232	0.000
{1}-{7}	(C.c)*Duodenum	(A. h)*Distal Small Int.	0.233	0.000
{1}-{8}	(C.c)*Duodenum	(A. h)*Colon	0.232	0.000
{2}-{3}	(C.c)*Middle Small Int.	(C.c)*Distal Small Int.	0.081	0.000
{2}-{4}	(C.c)*Middle Small Int.	(C.c)*Colon	0.084	0.000
{2}-{5}	(C.c)*Middle Small Int.	(A. h)*Duodenum	0.229	0.000
{2}-{6}	(C.c)*Middle Small Int.	(A. h)*Middle Small Int.	0.232	0.000
{2}-{7}	(C.c)*Middle Small Int.	(A. h)*Distal Small Int.	0.232	0.000
{2}-{8}	(C.c)*Middle Small Int.	(A. h)*Colon	0.232	0.000
{3}-{4}	(C.c)*Distal Small Int.	(C.c)*Colon	0.086	0.899
{3}-{5}	(C.c)*Distal Small Int.	(A. h)*Duodenum	0.230	0.000
{3}-{6}	(C.c)*Distal Small Int.	(A. h)*Middle Small Int.	0.233	0.000
{3}-{7}	(C.c)*Distal Small Int.	(A. h)*Distal Small Int.	0.233	0.000
{3}-{8}	(C.c)*Distal Small Int.	(A. h)*Colon	0.233	0.000
{4}-{5}	(C.c)*Colon	(A. h)*Duodenum	0.231	0.000
{4}-{6}	(C.c)*Colon	(A. h)*Middle Small Int.	0.233	0.000
{4}-{7}	(C.c)*Colon	(A. h)*Distal Small Int.	0.234	0.000
{4}-{8}	(C.c)*Colon	(A. h)*Colon	0.234	0.000
{5}-{6}	(A. h)*Duodenum	(A. h)*Middle Small Int.	0.092	0.451
{5}-{7}	(A. h)*Duodenum	(A. h)*Distal Small Int.	0.094	0.000
{5}-{8}	(A. h)*Duodenum	(A. h)*Colon	0.092	0.000
{6}-{7}	(A. h)*Middle Small Int.	(A. h)*Distal Small Int.	0.100	0.000
{6}-{8}	(A. h)*Middle Small Int.	(A. h)*Colon	0.098	0.000
{7}-{8}	(A. h)*Distal Small Int.	(A. h)*Colon	0.100	0.228

C.c: *Crocicura cyanea*

A.h: *Amblysomus hottentotus*

Appendix 41

HID/AB and AF/AB results

P-values for the graph of figure 4.38B: The distribution of the total number of weakly sulfated goblet cells throughout the GI surface epithelial areas of *C. cyanea* and *A. hottentotus*.

Figure 4.38B: Weakly sulfated goblet cells per surface epithelial area (mm^2)				
Comparison of the Gastrointestinal Regions	1st	2nd	Standard Error	p- value
{1}-{2}	(C.c)*Duodenum	(C.c)*Middle Small Int.	0.097	0.000
{1}-{3}	(C.c)*Duodenum	(C.c)*Distal Small Int.	0.100	0.000
{1}-{4}	(C.c)*Duodenum	(C.c)*Colon	0.104	0.000
{1}-{5}	(C.c)*Duodenum	(A. h)*Duodenum	0.239	0.000
{1}-{6}	(C.c)*Duodenum	(A. h)*Middle Small Int.	0.242	0.000
{1}-{7}	(C.c)*Duodenum	(A. h)*Distal Small Int.	0.244	0.024
{1}-{8}	(C.c)*Duodenum	(A. h)*Colon	0.243	0.040
{2}-{3}	(C.c)*Middle Small Int.	(C.c)*Distal Small Int.	0.099	0.012
{2}-{4}	(C.c)*Middle Small Int.	(C.c)*Colon	0.102	0.823
{2}-{5}	(C.c)*Middle Small Int.	(A. h)*Duodenum	0.239	0.000
{2}-{6}	(C.c)*Middle Small Int.	(A. h)*Middle Small Int.	0.242	0.000
{2}-{7}	(C.c)*Middle Small Int.	(A. h)*Distal Small Int.	0.243	0.000
{2}-{8}	(C.c)*Middle Small Int.	(A. h)*Colon	0.242	0.000
{3}-{4}	(C.c)*Distal Small Int.	(C.c)*Colon	0.105	0.032
{3}-{5}	(C.c)*Distal Small Int.	(A. h)*Duodenum	0.240	0.000
{3}-{6}	(C.c)*Distal Small Int.	(A. h)*Middle Small Int.	0.243	0.000
{3}-{7}	(C.c)*Distal Small Int.	(A. h)*Distal Small Int.	0.245	0.000
{3}-{8}	(C.c)*Distal Small Int.	(A. h)*Colon	0.244	0.000
{4}-{5}	(C.c)*Colon	(A. h)*Duodenum	0.241	0.000
{4}-{6}	(C.c)*Colon	(A. h)*Middle Small Int.	0.245	0.000
{4}-{7}	(C.c)*Colon	(A. h)*Distal Small Int.	0.246	0.000
{4}-{8}	(C.c)*Colon	(A. h)*Colon	0.245	0.000
{5}-{6}	(A. h)*Duodenum	(A. h)*Middle Small Int.	0.112	0.953
{5}-{7}	(A. h)*Duodenum	(A. h)*Distal Small Int.	0.115	0.000
{5}-{8}	(A. h)*Duodenum	(A. h)*Colon	0.113	0.000
{6}-{7}	(A. h)*Middle Small Int.	(A. h)*Distal Small Int.	0.122	0.000
{6}-{8}	(A. h)*Middle Small Int.	(A. h)*Colon	0.120	0.000
{7}-{8}	(A. h)*Distal Small Int.	(A. h)*Colon	0.122	0.683

C.c: *Crocicura cyanea*

A.h: *Amblysomus hottentotus*

Appendix 42

HID/AB and AF/AB results

P-values for the graph of figure 4.38C: The distribution of the total number of weakly sulfated goblet cells throughout the GI crypt areas of *C. cyanea* and *A. hottentotus*.

Figure 4.38C: Weakly sulfated goblet cells per crypt area (mm^2)				
Comparison of the Gastrointestinal Regions	1st	2nd	Standard Error	p- value
{1}-{2}	(C.c)*Duodenum	(C.c)*Middle Small Int.	0.083	0.000
{1}-{3}	(C.c)*Duodenum	(C.c)*Distal Small Int.	0.086	0.000
{1}-{4}	(C.c)*Duodenum	(C.c)*Colon	0.089	0.000
{1}-{5}	(C.c)*Duodenum	(A. h)*Duodenum	0.213	0.000
{1}-{6}	(C.c)*Duodenum	(A. h)*Middle Small Int.	0.216	0.000
{1}-{7}	(C.c)*Duodenum	(A. h)*Distal Small Int.	0.217	0.000
{1}-{8}	(C.c)*Duodenum	(A. h)*Colon	0.216	0.000
{2}-{3}	(C.c)*Middle Small Int.	(C.c)*Distal Small Int.	0.084	0.000
{2}-{4}	(C.c)*Middle Small Int.	(C.c)*Colon	0.087	0.000
{2}-{5}	(C.c)*Middle Small Int.	(A. h)*Duodenum	0.212	0.000
{2}-{6}	(C.c)*Middle Small Int.	(A. h)*Middle Small Int.	0.215	0.000
{2}-{7}	(C.c)*Middle Small Int.	(A. h)*Distal Small Int.	0.216	0.000
{2}-{8}	(C.c)*Middle Small Int.	(A. h)*Colon	0.215	0.000
{3}-{4}	(C.c)*Distal Small Int.	(C.c)*Colon	0.090	0.062
{3}-{5}	(C.c)*Distal Small Int.	(A. h)*Duodenum	0.214	0.000
{3}-{6}	(C.c)*Distal Small Int.	(A. h)*Middle Small Int.	0.216	0.000
{3}-{7}	(C.c)*Distal Small Int.	(A. h)*Distal Small Int.	0.217	0.000
{3}-{8}	(C.c)*Distal Small Int.	(A. h)*Colon	0.216	0.000
{4}-{5}	(C.c)*Colon	(A. h)*Duodenum	0.215	0.000
{4}-{6}	(C.c)*Colon	(A. h)*Middle Small Int.	0.217	0.000
{4}-{7}	(C.c)*Colon	(A. h)*Distal Small Int.	0.218	0.000
{4}-{8}	(C.c)*Colon	(A. h)*Colon	0.217	0.000
{5}-{6}	(A. h)*Duodenum	(A. h)*Middle Small Int.	0.096	0.390
{5}-{7}	(A. h)*Duodenum	(A. h)*Distal Small Int.	0.098	0.000
{5}-{8}	(A. h)*Duodenum	(A. h)*Colon	0.096	0.000
{6}-{7}	(A. h)*Middle Small Int.	(A. h)*Distal Small Int.	0.104	0.000
{6}-{8}	(A. h)*Middle Small Int.	(A. h)*Colon	0.102	0.000
{7}-{8}	(A. h)*Distal Small Int.	(A. h)*Colon	0.104	0.462

C.c: *Crocicura cyanea*

A.h: *Amblysomus hottentotus*

Appendix 43

HID/AB and AF/AB results

P-values for the graph of figure 4.39A: The distribution of the total number of sialomucin secreting goblet cells throughout the GIT of *C. cyanea* and *A. hottentotus*.

Figure 4.39A: Total number of sialylated goblet cells per total area (mm^2)				
Comparison of the Gastrointestinal Regions	1st	2nd	Standard Error	p- value
{1}-{2}	(C.c)*Duodenum	(C.c)*Middle Small Int.	0.083	0.000
{1}-{3}	(C.c)*Duodenum	(C.c)*Distal Small Int.	0.086	0.000
{1}-{4}	(C.c)*Duodenum	(C.c)*Colon	0.089	0.000
{1}-{5}	(C.c)*Duodenum	(A. h)*Duodenum	0.198	0.011
{1}-{6}	(C.c)*Duodenum	(A. h)*Middle Small Int.	0.201	0.002
{1}-{7}	(C.c)*Duodenum	(A. h)*Distal Small Int.	0.202	0.001
{1}-{8}	(C.c)*Duodenum	(A. h)*Colon	0.201	0.000
{2}-{3}	(C.c)*Middle Small Int.	(C.c)*Distal Small Int.	0.085	0.000
{2}-{4}	(C.c)*Middle Small Int.	(C.c)*Colon	0.087	0.000
{2}-{5}	(C.c)*Middle Small Int.	(A. h)*Duodenum	0.197	0.000
{2}-{6}	(C.c)*Middle Small Int.	(A. h)*Middle Small Int.	0.200	0.000
{2}-{7}	(C.c)*Middle Small Int.	(A. h)*Distal Small Int.	0.201	0.000
{2}-{8}	(C.c)*Middle Small Int.	(A. h)*Colon	0.200	0.000
{3}-{4}	(C.c)*Distal Small Int.	(C.c)*Colon	0.090	0.000
{3}-{5}	(C.c)*Distal Small Int.	(A. h)*Duodenum	0.199	0.000
{3}-{6}	(C.c)*Distal Small Int.	(A. h)*Middle Small Int.	0.201	0.000
{3}-{7}	(C.c)*Distal Small Int.	(A. h)*Distal Small Int.	0.203	0.000
{3}-{8}	(C.c)*Distal Small Int.	(A. h)*Colon	0.202	0.000
{4}-{5}	(C.c)*Colon	(A. h)*Duodenum	0.200	0.000
{4}-{6}	(C.c)*Colon	(A. h)*Middle Small Int.	0.203	0.000
{4}-{7}	(C.c)*Colon	(A. h)*Distal Small Int.	0.204	0.000
{4}-{8}	(C.c)*Colon	(A. h)*Colon	0.203	0.000
{5}-{6}	(A. h)*Duodenum	(A. h)*Middle Small Int.	0.096	0.196
{5}-{7}	(A. h)*Duodenum	(A. h)*Distal Small Int.	0.098	0.089
{5}-{8}	(A. h)*Duodenum	(A. h)*Colon	0.096	0.014
{6}-{7}	(A. h)*Middle Small Int.	(A. h)*Distal Small Int.	0.104	0.674
{6}-{8}	(A. h)*Middle Small Int.	(A. h)*Colon	0.102	0.266
{7}-{8}	(A. h)*Distal Small Int.	(A. h)*Colon	0.104	0.503

C.c: *Crocicura cyanea*

A.h: *Amblysomus hottentotus*

Appendix 44

HID/AB and AF/AB results

P-values for the graph of figure 4.39B: The distribution of the total number of sialomucin secreting goblet cells throughout the GI surface epithelial areas of *C. cyanea* and *A. hottentotus*.

Figure 4.39B: Sialylated goblet cells per surface epithelial area (mm^2)				
Comparison of the Gastrointestinal Regions	1st	2nd	Standard Error	p- value
{1}-{2}	(C.c)*Duodenum	(C.c)*Middle Small Int.	0.107	0.000
{1}-{3}	(C.c)*Duodenum	(C.c)*Distal Small Int.	0.111	0.000
{1}-{4}	(C.c)*Duodenum	(C.c)*Colon	0.115	0.000
{1}-{5}	(C.c)*Duodenum	(A. h)*Duodenum	0.306	0.204
{1}-{6}	(C.c)*Duodenum	(A. h)*Middle Small Int.	0.309	0.055
{1}-{7}	(C.c)*Duodenum	(A. h)*Distal Small Int.	0.310	0.971
{1}-{8}	(C.c)*Duodenum	(A. h)*Colon	0.309	0.915
{2}-{3}	(C.c)*Middle Small Int.	(C.c)*Distal Small Int.	0.109	0.038
{2}-{4}	(C.c)*Middle Small Int.	(C.c)*Colon	0.113	0.000
{2}-{5}	(C.c)*Middle Small Int.	(A. h)*Duodenum	0.305	0.000
{2}-{6}	(C.c)*Middle Small Int.	(A. h)*Middle Small Int.	0.308	0.000
{2}-{7}	(C.c)*Middle Small Int.	(A. h)*Distal Small Int.	0.310	0.000
{2}-{8}	(C.c)*Middle Small Int.	(A. h)*Colon	0.308	0.000
{3}-{4}	(C.c)*Distal Small Int.	(C.c)*Colon	0.116	0.000
{3}-{5}	(C.c)*Distal Small Int.	(A. h)*Duodenum	0.306	0.000
{3}-{6}	(C.c)*Distal Small Int.	(A. h)*Middle Small Int.	0.310	0.000
{3}-{7}	(C.c)*Distal Small Int.	(A. h)*Distal Small Int.	0.311	0.000
{3}-{8}	(C.c)*Distal Small Int.	(A. h)*Colon	0.310	0.000
{4}-{5}	(C.c)*Colon	(A. h)*Duodenum	0.308	0.000
{4}-{6}	(C.c)*Colon	(A. h)*Middle Small Int.	0.311	0.000
{4}-{7}	(C.c)*Colon	(A. h)*Distal Small Int.	0.312	0.000
{4}-{8}	(C.c)*Colon	(A. h)*Colon	0.311	0.000
{5}-{6}	(A. h)*Duodenum	(A. h)*Middle Small Int.	0.124	0.099
{5}-{7}	(A. h)*Duodenum	(A. h)*Distal Small Int.	0.127	0.002
{5}-{8}	(A. h)*Duodenum	(A. h)*Colon	0.125	0.001
{6}-{7}	(A. h)*Middle Small Int.	(A. h)*Distal Small Int.	0.135	0.000
{6}-{8}	(A. h)*Middle Small Int.	(A. h)*Colon	0.132	0.000
{7}-{8}	(A. h)*Distal Small Int.	(A. h)*Colon	0.135	0.872

C.c: *Crocicura cyanea*

A.h: *Amblysomus hottentotus*

Appendix 45

HID/AB and AF/AB results

P-values for the graph of figure 4.39C: The distribution of the total number of sialomucin secreting goblet cells throughout the GI crypt areas of *C. cyanea* and *A. hottentotus*.

Figure 4.39C: Sialylated goblet cells per crypt area (mm^2)				
Comparison of the Gastrointestinal Regions	1st	2nd	Standard Error	p- value
{1}-{2}	(C.c)*Duodenum	(C.c)*Middle Small Int.	0.065	0.000
{1}-{3}	(C.c)*Duodenum	(C.c)*Distal Small Int.	0.068	0.000
{1}-{4}	(C.c)*Duodenum	(C.c)*Colon	0.070	0.000
{1}-{5}	(C.c)*Duodenum	(A. h)*Duodenum	0.084	0.000
{1}-{6}	(C.c)*Duodenum	(A. h)*Middle Small Int.	0.088	0.000
{1}-{7}	(C.c)*Duodenum	(A. h)*Distal Small Int.	0.090	0.000
{1}-{8}	(C.c)*Duodenum	(A. h)*Colon	0.088	0.000
{2}-{3}	(C.c)*Middle Small Int.	(C.c)*Distal Small Int.	0.067	0.001
{2}-{4}	(C.c)*Middle Small Int.	(C.c)*Colon	0.069	0.050
{2}-{5}	(C.c)*Middle Small Int.	(A. h)*Duodenum	0.083	0.000
{2}-{6}	(C.c)*Middle Small Int.	(A. h)*Middle Small Int.	0.088	0.000
{2}-{7}	(C.c)*Middle Small Int.	(A. h)*Distal Small Int.	0.089	0.000
{2}-{8}	(C.c)*Middle Small Int.	(A. h)*Colon	0.088	0.000
{3}-{4}	(C.c)*Distal Small Int.	(C.c)*Colon	0.071	0.219
{3}-{5}	(C.c)*Distal Small Int.	(A. h)*Duodenum	0.085	0.000
{3}-{6}	(C.c)*Distal Small Int.	(A. h)*Middle Small Int.	0.089	0.000
{3}-{7}	(C.c)*Distal Small Int.	(A. h)*Distal Small Int.	0.091	0.000
{3}-{8}	(C.c)*Distal Small Int.	(A. h)*Colon	0.089	0.000
{4}-{5}	(C.c)*Colon	(A. h)*Duodenum	0.087	0.000
{4}-{6}	(C.c)*Colon	(A. h)*Middle Small Int.	0.091	0.000
{4}-{7}	(C.c)*Colon	(A. h)*Distal Small Int.	0.092	0.000
{4}-{8}	(C.c)*Colon	(A. h)*Colon	0.091	0.000
{5}-{6}	(A. h)*Duodenum	(A. h)*Middle Small Int.	0.076	0.309
{5}-{7}	(A. h)*Duodenum	(A. h)*Distal Small Int.	0.078	0.008
{5}-{8}	(A. h)*Duodenum	(A. h)*Colon	0.076	0.026
{6}-{7}	(A. h)*Middle Small Int.	(A. h)*Distal Small Int.	0.082	0.001
{6}-{8}	(A. h)*Middle Small Int.	(A. h)*Colon	0.080	0.002
{7}-{8}	(A. h)*Distal Small Int.	(A. h)*Colon	0.082	0.645

C.c: *Crocicura cyanea*

A.h: *Amblysomus hottentotus*

Appendix 46

HID/AB and AF/AB results

P-values for the graph of figure 4.40A: The distribution of the total number of mixed acid secreting goblet cells throughout the GIT of *C. cyanea* and *A. hottentotus*.

Figure 4.40A: Total number of mixed acid goblet cells per total area (mm^2)				
Comparison of the Gastrointestinal Regions	1st	2nd	Standard Error	p- value
{1}-{2}	(C.c)*Duodenum	(C.c)*Middle Small Int.	0.107	0.000
{1}-{3}	(C.c)*Duodenum	(C.c)*Distal Small Int.	0.111	0.000
{1}-{4}	(C.c)*Duodenum	(C.c)*Colon	0.114	0.000
{1}-{5}	(C.c)*Duodenum	(A. h)*Duodenum	0.250	0.000
{1}-{6}	(C.c)*Duodenum	(A. h)*Middle Small Int.	0.254	0.000
{1}-{7}	(C.c)*Duodenum	(A. h)*Distal Small Int.	0.255	0.000
{1}-{8}	(C.c)*Duodenum	(A. h)*Colon	0.254	0.909
{2}-{3}	(C.c)*Middle Small Int.	(C.c)*Distal Small Int.	0.109	0.000
{2}-{4}	(C.c)*Middle Small Int.	(C.c)*Colon	0.113	0.000
{2}-{5}	(C.c)*Middle Small Int.	(A. h)*Duodenum	0.250	0.000
{2}-{6}	(C.c)*Middle Small Int.	(A. h)*Middle Small Int.	0.253	0.000
{2}-{7}	(C.c)*Middle Small Int.	(A. h)*Distal Small Int.	0.255	0.472
{2}-{8}	(C.c)*Middle Small Int.	(A. h)*Colon	0.253	0.000
{3}-{4}	(C.c)*Distal Small Int.	(C.c)*Colon	0.116	0.000
{3}-{5}	(C.c)*Distal Small Int.	(A. h)*Duodenum	0.251	0.000
{3}-{6}	(C.c)*Distal Small Int.	(A. h)*Middle Small Int.	0.255	0.000
{3}-{7}	(C.c)*Distal Small Int.	(A. h)*Distal Small Int.	0.256	0.022
{3}-{8}	(C.c)*Distal Small Int.	(A. h)*Colon	0.255	0.030
{4}-{5}	(C.c)*Colon	(A. h)*Duodenum	0.253	0.000
{4}-{6}	(C.c)*Colon	(A. h)*Middle Small Int.	0.256	0.000
{4}-{7}	(C.c)*Colon	(A. h)*Distal Small Int.	0.258	0.000
{4}-{8}	(C.c)*Colon	(A. h)*Colon	0.257	0.033
{5}-{6}	(A. h)*Duodenum	(A. h)*Middle Small Int.	0.124	0.590
{5}-{7}	(A. h)*Duodenum	(A. h)*Distal Small Int.	0.127	0.000
{5}-{8}	(A. h)*Duodenum	(A. h)*Colon	0.124	0.000
{6}-{7}	(A. h)*Middle Small Int.	(A. h)*Distal Small Int.	0.134	0.000
{6}-{8}	(A. h)*Middle Small Int.	(A. h)*Colon	0.132	0.000
{7}-{8}	(A. h)*Distal Small Int.	(A. h)*Colon	0.134	0.000

C.c: *Crocicura cyanea*

A.h: *Amblysomus hottentotus*

Appendix 47

HID/AB and AF/AB results

P-values for the graph of figure 4.40B: The distribution of the total number of mixed acid secreting goblet cells throughout the GI surface epithelial areas of *C. cyanea* and *A. hottentotus*.

Figure 4.40B: Mixed acid goblet cells per surface epithelial area (mm^2)				
Comparison of the Gastrointestinal Regions	1st	2nd	Standard Error	p- value
{1}-{2}	(C.c)*Duodenum	(C.c)*Middle Small Int.	0.115	0.000
{1}-{3}	(C.c)*Duodenum	(C.c)*Distal Small Int.	0.119	0.004
{1}-{4}	(C.c)*Duodenum	(C.c)*Colon	0.123	0.000
{1}-{5}	(C.c)*Duodenum	(A. h)*Duodenum	0.270	0.000
{1}-{6}	(C.c)*Duodenum	(A. h)*Middle Small Int.	0.274	0.000
{1}-{7}	(C.c)*Duodenum	(A. h)*Distal Small Int.	0.275	0.000
{1}-{8}	(C.c)*Duodenum	(A. h)*Colon	0.274	0.317
{2}-{3}	(C.c)*Middle Small Int.	(C.c)*Distal Small Int.	0.118	0.005
{2}-{4}	(C.c)*Middle Small Int.	(C.c)*Colon	0.122	0.000
{2}-{5}	(C.c)*Middle Small Int.	(A. h)*Duodenum	0.269	0.000
{2}-{6}	(C.c)*Middle Small Int.	(A. h)*Middle Small Int.	0.273	0.000
{2}-{7}	(C.c)*Middle Small Int.	(A. h)*Distal Small Int.	0.275	0.182
{2}-{8}	(C.c)*Middle Small Int.	(A. h)*Colon	0.273	0.001
{3}-{4}	(C.c)*Distal Small Int.	(C.c)*Colon	0.125	0.000
{3}-{5}	(C.c)*Distal Small Int.	(A. h)*Duodenum	0.271	0.000
{3}-{6}	(C.c)*Distal Small Int.	(A. h)*Middle Small Int.	0.275	0.000
{3}-{7}	(C.c)*Distal Small Int.	(A. h)*Distal Small Int.	0.276	0.012
{3}-{8}	(C.c)*Distal Small Int.	(A. h)*Colon	0.275	0.025
{4}-{5}	(C.c)*Colon	(A. h)*Duodenum	0.272	0.000
{4}-{6}	(C.c)*Colon	(A. h)*Middle Small Int.	0.276	0.000
{4}-{7}	(C.c)*Colon	(A. h)*Distal Small Int.	0.278	0.000
{4}-{8}	(C.c)*Colon	(A. h)*Colon	0.277	0.069
{5}-{6}	(A. h)*Duodenum	(A. h)*Middle Small Int.	0.134	0.571
{5}-{7}	(A. h)*Duodenum	(A. h)*Distal Small Int.	0.137	0.000
{5}-{8}	(A. h)*Duodenum	(A. h)*Colon	0.134	0.000
{6}-{7}	(A. h)*Middle Small Int.	(A. h)*Distal Small Int.	0.145	0.000
{6}-{8}	(A. h)*Middle Small Int.	(A. h)*Colon	0.142	0.000
{7}-{8}	(A. h)*Distal Small Int.	(A. h)*Colon	0.145	0.000

C.c: *Crocicura cyanea*

A.h: *Amblysomus hottentotus*

Appendix 48

HID/AB and AF/AB results

P-values for the graph of figure 4.40C: The distribution of the total number of mixed acid secreting goblet cells throughout the GI crypt areas of *C. cyanea* and *A. hottentotus*.

Figure 4.40C: Mixed acid goblet cells per crypt area (mm^2)				
Comparison of the Gastrointestinal Regions	1st	2nd	Standard Error	p- value
{1}-{2}	(C.c)*Duodenum	(C.c)*Middle Small Int.	0.121	0.000
{1}-{3}	(C.c)*Duodenum	(C.c)*Distal Small Int.	0.125	0.000
{1}-{4}	(C.c)*Duodenum	(C.c)*Colon	0.129	0.000
{1}-{5}	(C.c)*Duodenum	(A. h)*Duodenum	0.223	0.000
{1}-{6}	(C.c)*Duodenum	(A. h)*Middle Small Int.	0.229	0.000
{1}-{7}	(C.c)*Duodenum	(A. h)*Distal Small Int.	0.231	0.000
{1}-{8}	(C.c)*Duodenum	(A. h)*Colon	0.229	0.367
{2}-{3}	(C.c)*Middle Small Int.	(C.c)*Distal Small Int.	0.123	0.000
{2}-{4}	(C.c)*Middle Small Int.	(C.c)*Colon	0.127	0.000
{2}-{5}	(C.c)*Middle Small Int.	(A. h)*Duodenum	0.222	0.490
{2}-{6}	(C.c)*Middle Small Int.	(A. h)*Middle Small Int.	0.228	0.517
{2}-{7}	(C.c)*Middle Small Int.	(A. h)*Distal Small Int.	0.230	0.000
{2}-{8}	(C.c)*Middle Small Int.	(A. h)*Colon	0.228	0.000
{3}-{4}	(C.c)*Distal Small Int.	(C.c)*Colon	0.131	0.000
{3}-{5}	(C.c)*Distal Small Int.	(A. h)*Duodenum	0.225	0.000
{3}-{6}	(C.c)*Distal Small Int.	(A. h)*Middle Small Int.	0.230	0.000
{3}-{7}	(C.c)*Distal Small Int.	(A. h)*Distal Small Int.	0.232	0.447
{3}-{8}	(C.c)*Distal Small Int.	(A. h)*Colon	0.230	0.000
{4}-{5}	(C.c)*Colon	(A. h)*Duodenum	0.227	0.000
{4}-{6}	(C.c)*Colon	(A. h)*Middle Small Int.	0.232	0.000
{4}-{7}	(C.c)*Colon	(A. h)*Distal Small Int.	0.234	0.074
{4}-{8}	(C.c)*Colon	(A. h)*Colon	0.232	0.003
{5}-{6}	(A. h)*Duodenum	(A. h)*Middle Small Int.	0.140	0.966
{5}-{7}	(A. h)*Duodenum	(A. h)*Distal Small Int.	0.144	0.000
{5}-{8}	(A. h)*Duodenum	(A. h)*Colon	0.140	0.000
{6}-{7}	(A. h)*Middle Small Int.	(A. h)*Distal Small Int.	0.152	0.000
{6}-{8}	(A. h)*Middle Small Int.	(A. h)*Colon	0.149	0.000
{7}-{8}	(A. h)*Distal Small Int.	(A. h)*Colon	0.152	0.000

C.c: *Crocicura cyanea*

A.h: *Amblysomus hottentotus*